Sur les systèmes à commutation à deux échelles de temps : une application au contrôle de guidage de bande dans un laminoir à chaud

Ivan Malloci

Nancy-Université INPL

École doctorale IAEM Lorraine
DFD Automatique et Production Automatisée
Institut National Polytechnique de Lorraine

Sur les systèmes à commutation à deux échelles de temps: Une application au contrôle de guidage de bande dans un laminoir à chaud

THÈSE

présentée et soutenue publiquement le 13 Novembre 2009

pour l'obtention du

Doctorat de l'Institut National Polytechnique de Lorraine

Spécialité Automatique et Traitement du signal

par

Ivan Malloci

Composition du jury

Président :	Alessandro Giua	Prof., DIEE, Università di Cagliari
Rapporteurs :	Germain Garcia	Prof., LAAS-CNRS, Toulouse
	Jean Lévine	Prof., École de Mines de Paris
Examinateurs :	Jamal Daafouz	Prof., INPL, Nancy Université (directeur de thèse)
	Claude Iung	Prof., INPL, Nancy Université (co-directeur de thèse)
	Christian Moretto	Ingénieur, ArcelorMittal R&D, Maizières-lès-Metz

CRAN

Centre de Recherche en Automatique de Nancy
UMR 7039 Nancy-Université – CNRS
2, avenue de la forêt de Haye 54516 Vandœuvre-lès-Nancy
Tél.+33 (0)3 83 59 59 59 Fax +33 (0)3 83 59 56 44

Mis en page avec la classe thloria.

Acknowledgments

Cette thèse a été réalisée en collaboration entre le CRAN, Unité Mixte de Recherche 7039 Nancy Université - INPL - CNRS, et ArcelorMittal R&D. Je remercie la Région Lorraine et ArcelorMittal, pour avoir financé ce travail. Merci à mes directeurs de thèse, Jamal Daafouz et Claude Iung, professeurs à l'INPL-Nancy Université, et à Christian Moretto, ingénieur ArcelorMittal, pour me conseiller et m'aider dans ces dernières trois années.

Je tiens à remercier Alessandro Giua, professeur à l'Università di Cagliari, pour présider mon jury ainsi que Germain Garcia, professeur au LAAS de Toulouse, et Jean Lévine, professeur à l'École de Mines de Paris, pour avoir accepté le rôle de rapporteurs de ma thèse.

Merci aux chercheurs du CRAN Marc Jungers, Pierre Riedinger, Radu Ranta, Benoît Marx, Samia Maza et Nicolae Brinzei pour les discussions, scientifiques et non, toujours intéressantes. Merci à Patrick Szczepanski, Rémi Bonidal, Alain Mouchette et Bertrand Bèle, ingénieurs ArcelorMittal, pour la disponibilité et le professionalisme. Je remercie Céline Morville, Christine Pierson et Carole Courrier pour m'aider dans les interminables problèmes bureaucratiques typiques d'une thèse. Merci à tous les doctorants, stagiaires et étudiants que j'ai connu dans les couloirs du CRAN. Vous êtes trop nombreux pour faire une liste exhaustive et donc je ne vais pas la faire... cependant, je dois au moins citer Émilie, Laurentiu, Sophie et Diego. Quand j'ai commencé ma thèse, je n'avais pas "quelques" questions comme tout le monde. J'avais millions de questions. De comme dire "pomme" en roumain jusqu'à où aller pour acheter un vélo (que je n'ai jamais acheté...). C'était surtout à vous de me supporter... merci!

Durante mi Erasmus y mi doctorado acà en France, tuve la suerte de conocer muchas personas interesantes, de culturas e idiomas diferentes. Básicamente una torre de babel. Como tengo que elegir un idioma para agradecer a todo el mundo, quiero hacerlo en español que, probablemente, es el idioma que mejor representa los años que pasé en Nancy. La vida a veces te da sorpresas, como dice esa canción... Entonces gracias, por la simpatía, la amistad y, sobre todo, la buena onda /′

Emigrare non é mai facile. Se poi sei nato in Sardegna, é ancora piú difficile. Grazie ai miei amici e a mia sorella, per supportarmi e sopportarmi, sempre. Infine, grazie a mia madre, per avermi donato un pò della sua straordinaria, salgariana fantasia, e a mio padre, che non ha bisogno di un Dottorato di Ricerca per battermi ancora a scacchi.

Ai miei genitori, Tore e Anna Clara

Contents

Notations

- $X \succ 0 \, (X \succeq 0)$ - positive (no negative) definite matrix,
- $X \prec 0 \, (X \preceq 0)$ - negative (no positive) definite matrix,
- I_n - identity matrix $\in \mathbb{R}^{n \times n}$,
- $Tr(X)$ - trace of the matrix X,
- $\|X\|$ - induced euclidean norm of the matrix X,
- $\lambda_{max}(X)$ and $\lambda_{min}(X)$ - the maximum and the minimum eigenvalue of the symmetric matrix X,
- $\xi\{X\}$ - spectrum of the matrix X,
- X^{-1} - inverse of the non-singular matrix X,
- X' - transpose of the matrix X,
- $X = \begin{bmatrix} A & B \\ (\star)' & C \end{bmatrix}$ - symmetric matrix X where $(\star)'$ means B',
- X is Hurwitz - all the eigenvalues of the matrix X have negative real parts,
- X is Schur - all the eigenvalues of the matrix X have modulus smaller than one,

- $Re\{x\}$ - real part of the vector x,
- $\|x\|$ - induced euclidean norm of the vector x,
- $O(\cdot)$ - order of magnitude.

General introduction

This Ph.D. thesis was conducted as part of a joint research collaboration between the *CRAN* and *ArcelorMittal R&D*. The objective is to provide a solution to a certain number of problems arising in practical implementation of regulators for nonlinear systems [Kha02], [FLMR95]: sudden modifications on the system dynamics, multi time scale phenomena, large discontinuities on the control signal due to controller switchings, the need of design a limited number of controllers in spite of a wide variation on the physical parameters. In order to illustrate the validity of the obtained results, we will resort to a real problem concerning the steel production framework, the robust steering control of a hot strip finishing mill.

The interest of the control scientific community for multi time scale systems dates back to the sixties. Examples of systems operating in different time scales may be found in the electric power framework, aerospace systems, robotics, chemical and biological systems [KKO86], [Nai02]. Last two decades have witnessed an increase of attention to switched systems, which combine continuous dynamics with discrete logic. This structure allows modeling a large class of systems, as event driven systems, network control systems, adaptive control or biologic networks. In order to study their main properties (e.g. stability, controllability, observability), a wide number of tools have been developed [Lib03], [SWM+07]. Even though modern control techniques often have to deal with multi time scale switched systems, there exist very few contributions in this area. Motivated by the hot strip mill control design, we are interested in studying the behavior of multi time scale switched systems to establish stability conditions and design a stabilizing control law when arbitrary switchings arise.

Switching among different controllers implies undesired transient behaviors due to control signal jumps [Han88], [EP98]. This phenomenon may affect the system performances and, in the worst case, destabilizes the closed loop system. Therefore, another purpose of this work is to find a solution to this problem in the discrete time switched systems framework.

The practical contribution of this thesis, the robust steering control of a hot strip mill, exploits some of the previous theoretical results. The goal is to guarantee asymptotic stability of the system and improve the quality of the strips treated during the rolling process. The influence of the uncertain parameters,

due to the difference among the physical parameters of the rolled products, is also taken into account. Although all the presented experimental results concern the Eisenhüttenstadt ArcelorMittal hot strip mill (Germany), this study aims at obtaining a control design adaptable to any mill. Thus, the last task of this work is the realization of a dedicated software that implements the algorithms necessary for extending the robust steering control design to other mills.

Structure

This thesis is organized in five chapters that are structured as follows:

The first chapter is concerned with the switched system modeling of a hot strip mill system for steering control purposes. Two time scale phenomena and parametric uncertainties in the polytopic form are considered.

The second chapter presents a LMI (linear matrix inequalities) based solution for the linear quadratic optimal control design of two time scale systems in discrete time. This approach is particularly adequate to the case of high dimensional systems. Fast and slow sampling state feedback control design problems are studied. An extension to polytopic uncertain systems is also presented.

In chapter 3, stability of two time scale switched systems is investigated. First, we show that, when no assumption on the minimal dwell time is made, stability of the fast and slow switched subsystems under an arbitrary switching rule is not sufficient for assessing stability of the original two time scale switched system, even if the singular perturbation parameter tends to zero. We propose LMI based conditions, independent of the singular perturbation parameter, which guarantee the asymptotic stability of a two time scale switched linear system, in the continuous and discrete time frameworks. These conditions express the fact that the coupling between the fast and slow dynamics has to be considered, when the switching rule is arbitrary. The proposed conditions are then extended to state feedback control design.

In chapter 4, a bumpless transfer method for discrete time switched linear systems is proposed. To this aim, an additional controller is activated at the switching time for reducing the control signal discontinuities. The bumpless transfer regulation is based on the finite horizon solution of a linear quadratic optimization problem. We resort to dwell time conditions for establishing asymptotical stability of the closed loop switched system.

In the last chapter, a new robust steering control design of hot strip finishing mill is presented. The objective is to guarantee asymptotic stability of a hot strip mill system and minimize the lateral displacement of the strip for the whole set of treated products. First, a method for reducing the number of uncertainties by exploiting the physical relations among the different products parameters

is introduced. Thus, since the system involves a two time scale dynamics and the fast dynamics is stable and impossible to control due to the limitation on the actuators rate, a robust reduced controller is designed for each subsystem separately. The asymptotic stability of the tail end switched system is verified through a dwell time criterion. The whole database is partitioned into different families, with respect to the physical parameters of the products. Improved performances are obtained by designing a specific controller for each family. Finally, simulations and experimental results concerning the Eisenhüttenstadt hot strip mill are shown.

Personal publications

The research exposed in this thesis can be found in the following publications:

International Journals

1. **I. Malloci**, J. Daafouz, C. Iung, R. Bonidal, P. Szczepanski, Switched system modeling and robust steering control of the tail end phase in a hot strip mill, *Nonlinear Analysis: Hybrid Systems*, 3(3):239-250, 2009.

2. **I. Malloci**, J. Daafouz, C. Iung, R. Bonidal, P. Szczepanski, Robust steering control of hot strip mill, *IEEE Transactions on Control Systems Technology, Digital Object Identifier 10.1109/TCST.2009.2031146.*

3. **I. Malloci**, J. Daafouz, C. Iung, Stability and stabilization of two-time scale switched linear systems in discrete time, *IEEE Transactions on Automatic Control*, **In revision**.

4. **I. Malloci**, L. Hetel, J. Daafouz, C. Iung, P. Szczepanski, Bumpless transfer for discrete-time switched systems, *Systems & Control Letters*, **In revision**.

International Conferences

5. **I. Malloci**, J. Daafouz, C. Iung, Stabilization of continuous-time singularly perturbed switched systems, *IEEE Conference on Decision and Control*, December, 2009, Shanghai, China.

6. **I. Malloci**, J. Daafouz, C. Iung, P. Szczepanski, Switched system modeling and robust steering control of the tail end phase in a hot strip mill, *IFAC Conference on Analysis and Design of Hybrid Systems*, September, 2009, Zaragoza, Spain.

7. **I. Malloci**, J. Daafouz, C. Iung, R. Bonidal, A LMI solution to the LQ problem for discrete-time singularly perturbed systems, *European Control Conference*, August, 2009, Budapest, Hungary.

8. **I. Malloci**, J. Daafouz, C. Iung, R. Bonidal, P. Szczepanski, Robust steering control of hot strip mill, *European Control Conference*, August, 2009, Budapest, Hungary.

9. **I. Malloci**, L. Hetel, J. Daafouz, C. Iung, R. Bonidal, Bumpless transfer for discrete-time switched systems, *American Control Conference*, June 2009, Saint Louis, U.S.A.

10. **I. Malloci**, L. Hetel, J. Daafouz, C. Iung, R. Bonidal, Une approche pour maîtriser les discontinuités de la commande pour les systèmes linéaires à commutation en temps discret, *Conférence International Francophone d'Automatique*, September 2008, Bucarest, Rumanie.

National Conferences

11. **I. Malloci**, J. Daafouz, C. Iung, R. Bonidal, P. Szczepanski, Contrôle robuste d'un laminoir à chaud, *Journées Doctorales et Nationales du GDR MACS*, March 2009, Angers, France.

Résumé en français

Introduction générale

Dans cette thèse, on s'est attaché à résoudre un certain nombre de problèmes qui apparaissent lorsqu'on traite des problèmes concrets de contrôle: phénomènes à plusieurs échelles de temps, discontinuités de la commande lors du basculement d'un correcteur à un autre, nécessité de concevoir un nombre limité de correcteurs différents malgré une gamme très importante de produits traités. Pour illustrer concrètement les résultats obtenus, nous nous sommes appuyés sur un exemple industriel concret, le contrôle de guidage de bande durant le processus de laminage dans un laminoir à chaud. D'abord, nous proposons une solution au problème de commande optimale linéaire quadratique pour les systèmes linéaires à deux échelles de temps en temps discret. Nous montrons que cette solution peut être étendue directement aux systèmes avec des incertitudes polytopiques. De plus, nous établissons des conditions suffisantes, formulées sous la forme d'inégalités matricielles linéaires, qui permettent de vérifier la stabilité d'un système à commutation à deux échelles de temps et de synthétiser des correcteurs stabilisants. Nous proposons aussi dans ce travail une méthode pour minimiser les discontinuités sur la commande dans le cadre des systèmes à commutation.

Dans le contexte du contrôle de guidage de bande pour un laminoir à chaud, nous ne pouvons pas négliger l'influence des paramètres incertains, qui sont dus principalement au fait que ce genre de système traite une gamme de produits très large. Donc, dans la synthèse du correcteur, nous avons pris en compte ces variations en divisant l'ensemble des produits en plusieurs familles et en synthétisant un correcteur différent pour chaque famille de produits. Cette stratégie permet d'atteindre le même niveau de performances pour la majorité des produits laminés. Afin d'obtenir une procédure simple et systématique qui permet d'étendre le contrôle de guidage de bande dans plusieurs usines, nous avons développé une boite à outils Matlab, appelée RSCT. Les résultats expérimentaux effectués dans le laminoir à chaud ArcelorMittal d'Eisenhüttenstadt (Allemagne) prouvent l'efficacité de notre approche.

Ce chapitre représente un résumé du mémoire de thèse, qui a été rédigé en anglais, et il est organisé en trois sections qui se présentent comme suit:

Dans la première section, nous proposons un correcteur robuste capable de

garantir la stabilité d'un laminoir à chaud et d'améliorer ses performances. L'objectif principal du processus de laminage est d'obtenir des tôles métalliques avec l'épaisseur désirée. Le décentrement de la tôle par rapport à l'axe de laminage peut dégrader la qualité du produit voire endommager le système de production. L'objectif est de réduire ce décentrement. Comme un laminoir travaille avec des produits qui peuvent avoir des caractéristiques très différentes, nous avons créé une base de données qui décrit l'ensemble des produits traités et nous l'avons divisée en plusieurs familles de produits. Nous décrivons une méthode pour réduire la complexité du problème en exploitant les relations physiques entre les paramètres. Cette méthode permet de formuler le problème de stabilisation comme un problème convexe et, par conséquent, de synthétiser un correcteur H_2 différent pour chaque famille de produits. Nous présentons aussi les résultats expérimentaux obtenus sur le laminoir d'ArcelorMittal situé à Eisenhüttenstadt.

Dans la deuxième section, nous adressons la stabilité des systèmes à commutation à deux échelles de temps dans le temps continu. Nous montrons que la stabilité des sous systèmes à commutation lents et rapides ne représente pas une condition suffisante pour la stabilité du système à commutation à deux échelles de temps lorsque la loi de commutation est arbitraire. Ensuite, nous proposons des conditions suffisantes, formulées sous la forme d'inégalités matricielles linéaires, qui permettent de synthétiser des correcteurs stabilisants pour cette classe de systèmes.

Dans la dernière section, nous présentons une méthode pour maîtriser les discontinuités de commande dans le cadre des systèmes à commutation en temps discret. Le correcteur qui permet de minimiser les discontinuités sur la commande sera synthétisé en utilisant une méthode d'optimisation LQ. L'idée est de forcer le signal de contrôle à suivre un profil désiré. Une minimisation de la distance entre la sortie réelle et la sortie désirée est également proposée.

1 Contrôle robuste d'un laminoir à chaud

1.1 Introduction

Le laminage de produits plats à chaud est une des étapes d'élaboration des tôles. Le procédé consiste à réduire la section d'un produit métallique en l'entraînant par frottement entre deux cylindres en rotation afin d'obtenir une tôle (ou bande) avec l'épaisseur désirée. De plus, il faut garantir un produit avec les caractéristiques géométriques, métalliques et mécaniques présentes dans le cahier des charges. Un laminoir est l'association de plusieurs cages, où chaque cage est constituée par un ensemble de cylindres. Au cours du laminage, si la tôle ne suit pas une trajectoire rectiligne, elle risque de se déchirer ou de se replier sur elle-même. Outre le fait que cette tôle devient inutilisable, un incident de laminage de ce type peut engendrer de sérieux défauts sur les cylindres de travail. Le déplacement latéral du produit par rapport à un axe de référence, appelé décentrement de bande, est la conséquence des dissymétries de laminage liées à la cage et/ou au produit, et

il doit être réduit si on veut améliorer la fiabilité du processus.

Dans le contexte du contrôle de déport de bande, les contributions les plus importantes sont basées sur la mesure du différentiel de force [FFT92], [MIYS01], [OH97], [SP98]. Normalement, les industriels supposent que le différentiel de force est l'image du décentrement de bande. Dans ce cas, le différentiel de serrage est fixé proportionnel au décentrement de bande et un correcteur de type PID peut être utilisé. En revanche, [Oka03] a développé une méthode de régulation non-linéaire en utilisant la théorie des modes glissantes [Utk92]. Néanmoins, la loi qui lie le différentiel de force et le décentrement de bande est non-linéaire. Ces contraintes ont été considérées dans [DBI+08], où un correcteur linéaire quadratique (LQ) a été synthétisé dans un cadre nominal [AM89]. Cependant, plusieurs types de produits avec des caractéristiques très différentes transitent dans un laminoir. Cette stratégie ne peut pas garantir le même niveau de performances pour l'ensemble des produits, malgré les propriétés de robustesse des correcteurs LQ. Dans ce travail, nous proposons un correcteur robuste H_2 en temps discret capable de garantir la stabilité d'un laminoir et de minimiser le décentrement de bande pour la totalité des produits laminés [MDI+ar], [MDI+09d], [MDI+09c], [MDI+09e], [MDIS09]. Dans la synthèse du correcteur, nous avons pris en compte la variation des paramètres physiques en divisant l'ensemble des produits en plusieurs familles et en synthétisant un correcteur différent pour chaque famille de produits. Nous avons aussi utilisé une approche polytopique afin de décrire le système comme un problème convexe, ce qui permet de synthétiser les correcteurs en utilisant des techniques LMI [BGFB94].

1.2 Description du système

1.2.1 Description physique du système

Un laminoir (Fig. 1 et 2) est composé de n cages, où chaque cage contient un ensemble de cylindres (composé par deux cylindres de travail et deux cylindres de soutien). Dans les laminoirs d'ArcelorMittal $n \in \{5, 6, 7\}$. Nous ne considérerons que le cas $n = 5$ car la généralisation ne présente pas de difficultés théoriques. Le modèle non-linéaire est obtenu à partir des relations qui gouvernent le comportement du système.

Pour chaque cage $g \in \mathcal{G} = \{1, ..., n\}$, les paramètres physiques principaux sont la largeur de la tôle w_g, l'épaisseur de la tôle h_g, la tension amont à la cage T_g^{am}, la tension aval à la cage T_g^{av}, la longueur entraxe des vis l_g^v, la distance entre deux cages l_g^0, la longueur des cylindres de travail b_g, la vitesse des cylindres de travail s_g et le module de Young E_g. Les constantes c_g^{fh}, $c_g^{fT_{am}}$, $c_g^{fT_{av}}$, c_g^{gh}, $c_g^{gT_{am}}$, $c_g^{gT_{av}}$, K_g^h, K_g^f, K_g^l, P_g et g_g représentent le gradient des paramètres de la tôle. Elles peuvent être évaluées en utilisant des algorithmes numériques spécifiques, développés par les ingénieurs d'ArcelorMittal. Les asymétries principales sont le décentrement de bande $Z_g(t)$, le différentiel d'épaisseur en sortie de cage $\Delta h_g(t)$, le différentiel de serrage $\Delta S_g(t)$ et le différentiel de cédage $\Delta K_g(t)$. Les équations principales qui gouvernent le comportement du système sont:

Figure 1: Laminoir ArcelorMittal d'Eisenhüttenstadt

– L'équation qui détermine le différentiel de force de laminage

$$\Delta P_g(t) = c_{g-1}^{fh}\Delta h_{g-1}(t) + c_g^{fh}\Delta h_g(t) + c_g^{fT_{am}}\Delta T_g^{am}(t) + c_g^{fT_{av}}\Delta T_g^{av}(t); \quad (1)$$

– L'équation qui détermine le différentiel d'épaisseur en sortie de la cage

$$\begin{aligned}\Delta h_g(t) = &\left(\frac{w_g}{(l_g^v)^2 K_g^h} + \frac{6w_g}{b_g^2 K_g^f}\right)\left(\Delta P_g(t) + 2P_g\right) Z_g(t) + \\ &\frac{1}{K_g^l}\Delta P_g(t) + \frac{w_g}{l_g^v}\Delta S_g(t) - \frac{w_g P_g}{l_g^v (K_g^h)^2}\Delta K_g(t);\end{aligned} \quad (2)$$

– L'équation qui détermine l'angle α_g entre la bande et l'axe de laminage

$$\begin{aligned}\dot{\alpha}_g(t) = &\frac{s_g}{w_g}\left(\frac{c_g^{gh}}{1+g_g} + \frac{1}{h_g}\right)\Delta h_g(t) + \frac{s_g}{w_g}\left(\frac{c_{g-1}^{gh}}{1+g_g} - \frac{1}{h_{g-1}}\right)\Delta h_{g-1}(t) + \\ &\frac{s_g}{w_g}\frac{c_g^{gT_{av}}}{(1+g_g)}\Delta T_g^{av}(t) + \frac{s_g}{w_g}\frac{c_g^{gT_{am}}}{(1+g_g)}\Delta T_g^{am}(t);\end{aligned} \quad (3)$$

– L'équation qui détermine le décentrement de bande

$$\dot{Z}_g(t) = s_g\,\alpha_g(t); \quad (4)$$

– L'équation qui détermine le différentiel de traction amont à la cage

$$\begin{aligned}\Delta T_g^{am}(t) = &3\left(\frac{w_g E_g}{(l_g^0)^2} + \frac{T_g^{am}}{w_g}\right)\left(Z_g(t) - Z_{g-1}(t)\right) + \\ &\frac{w_g E_g}{l_g^0}\left(2\alpha_g(t) - \alpha_{g-1}(t)\right) + 3\frac{l_g^0 T_g^{am}}{w_g}\alpha_g(t);\end{aligned} \quad (5)$$

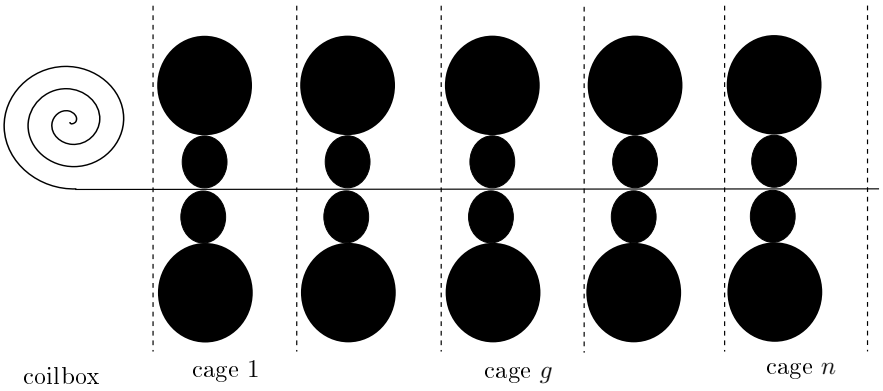

Figure 2: Vue lateral du laminoir

– L'équation qui détermine le couplage entre deux cages successives

$$\Delta T_{g-1}^{av}(t) = -\Delta T_{g}^{am}(t); \tag{6}$$

Nous pouvons associer deux variables d'état à chaque cage: le décentrement de bande Z_g et l'angle α_g. En accord avec les précédentes équations physiques, le processus complet peut être décrit par le système différentiel non-linéaire en temps continu:

$$\dot{x}(t) = f(x, u, d, t) \tag{7}$$

où

$$x(t) = \begin{bmatrix} x_1'(t) & x_2'(t) \end{bmatrix}' = \begin{bmatrix} \alpha_1(t), \ldots, \alpha_n(t), Z_1(t), \ldots, Z_n(t) \end{bmatrix}' \in \mathbb{R}^{2n}$$

est l'état du système, $u(t) \in \mathbb{R}^r$ est la commande (le différentiel de serrage $\Delta S(t)$) et $d(t) = Z_0(t) \in \mathbb{R}$ est la perturbation, pour $t \geq 0$. Il existe n cameras qui mesurent les décentrements de bande $Z_1, \ldots, Z_n$. Dans la suite, nous considérerons seulement une perturbation, c'est-à-dire le décentrement de bande en entrée de la première cage, qui est dû aux vibrations du "coilbox" (le dispositif utilisé pour introduire les bandes dans le train finisseur). Il y a aussi d'autres perturbations dans le système, mais elles sont négligeables par rapport au décentrement initial.

Un simulateur du système a été développé sous *Matlab-Simulink*. Il est adaptable à chaque usine, au prix de caler le modèle et de développer une base de données de produits spécifiques. Le calage pour l'usine d'Eisenhüttenstadt donne de bons résultats avec la majorité des produits. Un exemple est présenté sur la Fig. 3. Le trait plein représente le décentrement de bande mesuré par la camera tandis que le trait discontinu représente le décentrement de bande calculé par le simulateur.

1.2.2 Linéarisation du système

L'objectif principal du système de contrôle d'un laminoir est de maintenir la bande centrée dans l'axe de laminage. Ce but peut être atteint en modifiant le différentiel

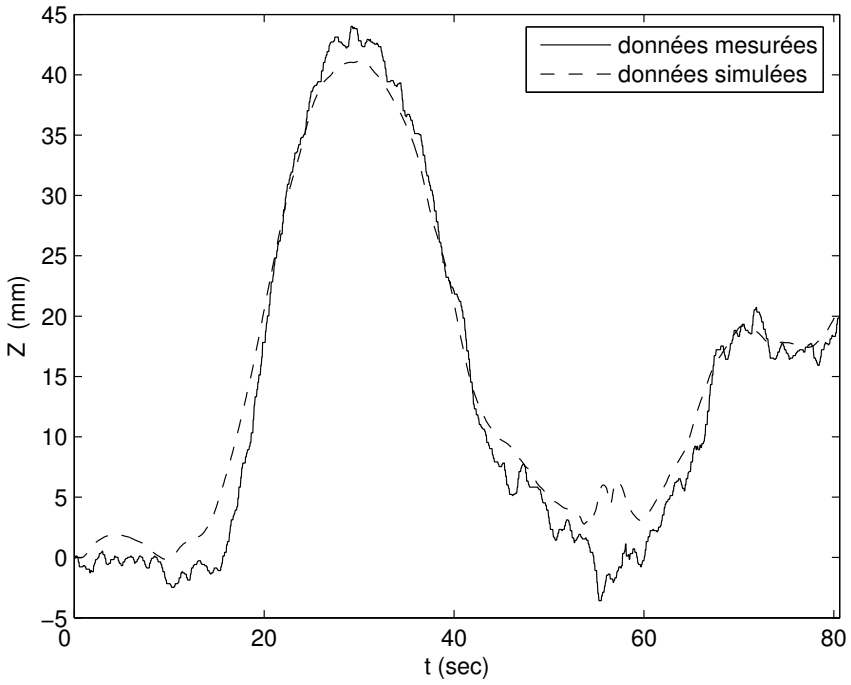

Figure 3: Comparaison entre le décentrement de bande mesuré et simulé

de force de laminage ΔP de manière à guider la bande dans la trajectoire désirée. Néanmoins, si la valeur de ΔP est trop élevée nous engendrons un coin Δh excessif, ce qui équivaut à obtenir une tôle avec un profil trapezoïdal (Figs. 4.a et 5), tandis que le profil idéal d'une tôle devrait être rectangulaire ($\Delta h(t) = 0$). En général, un coin en sortie de la dernière cage qui appartient à l'intervalle $-10\,\mu m < \Delta h_n(t) < 10\,\mu m$ respecte le cahier des charges. La force de laminage dépend du différentiel de serrage ΔS, qui est limité à $\pm 0.6\ mm$ pour les trois premières cages et à $\pm 0.1\ mm$ pour les deux dernières cages, afin de respecter le cahier des charges. Ces contraintes ont été prises en compte dans la synthèse du correcteur. Puisque nous considérons seulement des petites déviations autour du point de fonctionnement idéal ($\alpha_g(t) = Z_g(t) = \Delta h_g(t) = 0$), afin de synthétiser la loi de contrôle nous pouvons utiliser le modèle linéarisé

$$\begin{cases} \dot{x}(t) = M(\varepsilon)x(t) + N_u(\varepsilon)u(t) + N_d(\varepsilon)d(t) \\ y(t) = C_y x(t), \end{cases} \tag{8}$$

où $y(t) \in \mathbb{R}^m$ est la sortie mesurée et $\varepsilon > 0$ est un scalaire, pour tous $t \geq 0$. La dynamique d'un laminoir possède deux échelles de temps différentes car les angles α sont des variables rapides par rapport aux décentrements de bande Z. Les systèmes avec plusieurs échelles de temps sont souvent caractérisés par des problèmes numériques lors de la synthèse du correcteur. Ces problèmes sont dus au fait que les équations du système sont mal conditionnées [KKO86]. De plus, dans un laminoir, la dynamique correspondant aux angles ne peut pas être

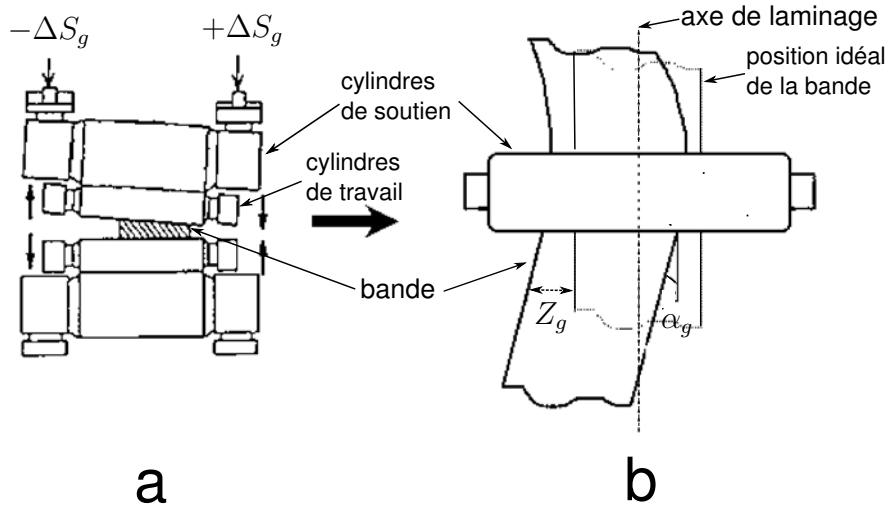

Figure 4: Description de la cage g : vue de face (a) et vue de dessus (b)

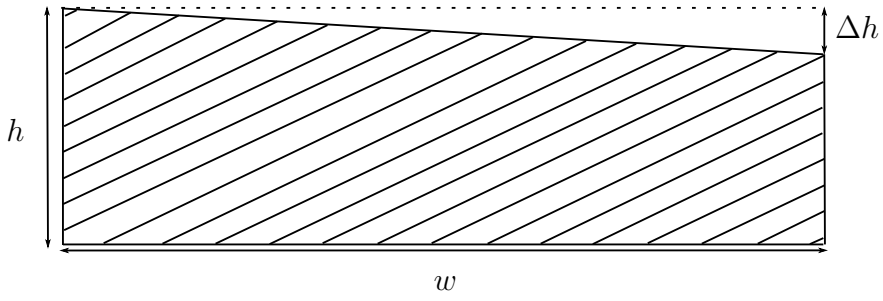

Figure 5: Profil de la tôle

contrôlée directement car les actionneurs du système ont une vitesse limitée. Tous ces problèmes peuvent être résolus en utilisant la méthode d'approximation des perturbations singulières. Il s'agit de décrire le comportement du système par la variété lente. Les équations différentielles qui concernent les variables rapides sont remplacées par des équations algébriques. En décomposant l'état du système en une partie rapide x_1 et une partie lente x_2, nous obtenons:

$$\begin{cases} \varepsilon \dot{x}_1(t) = M_{11}x_1(t) + M_{12}x_2(t) + N_{u,1}u(t) + N_{d,1}d(t) \\ \dot{x}_2(t) = M_{21}x_1(t) + M_{22}x_2(t) + N_{u,2}u(t) + N_{d,2}d(t) \\ y(t) = C_{y,2}x_2(t), \end{cases} \tag{9}$$

où

$$
\begin{aligned}
M(\varepsilon) &= \begin{bmatrix} \varepsilon^{-1} I_n & 0 \\ 0 & I_n \end{bmatrix} \begin{bmatrix} M_{11} & M_{12} \\ M_{21} & M_{22} \end{bmatrix}, \\
N_u &= \begin{bmatrix} \varepsilon^{-1} I_n & 0 \\ 0 & I_n \end{bmatrix} \begin{bmatrix} N_{u,1} \\ N_{u,2} \end{bmatrix}, \\
N_d &= \begin{bmatrix} \varepsilon^{-1} I_n & 0 \\ 0 & I_n \end{bmatrix} \begin{bmatrix} N_{d,1} \\ N_{d,2} \end{bmatrix}, \\
C_y &= \begin{bmatrix} C_{y,1} & C_{y,2} \end{bmatrix} = \begin{bmatrix} 0_{n \times n} & I_n \end{bmatrix},
\end{aligned}
\tag{10}
$$

avec M_{11} matrice Hurwitz. Nous supposons que la paire $(M(\varepsilon), N_u(\varepsilon))$ est contrôlable.

En accord avec l'implémentation pratique, le correcteur doit être synthétisé en temps discret, avec un période d'échantillonnage $T_s = 0.05$. Donc, dans la suite nous considérerons seulement la version discrétisée du système (9) [KI86]:

$$
\begin{cases}
x_1(s+1) = \varepsilon \tilde{A}_{11} x_1(s) + \tilde{A}_{12} x_2(s) + \tilde{B}_{u,1} u(s) + \tilde{B}_{d,1} d(s) \\
x_2(s+1) = \varepsilon \tilde{A}_{21} x_1(s) + \tilde{A}_{22} x_2(s) + \tilde{B}_{u,2} u(s) + \tilde{B}_{d,2} d(s) \\
y(s) = C_{y,2} x_2(s),
\end{cases}
\tag{11}
$$

avec $x_1(s) \in \mathbb{R}^{n_1}$, $x_2(s) \in \mathbb{R}^{n_2}$, $u(s) \in \mathbb{R}^r$, $d(s) \in \mathbb{R}$ and $y(s) \in \mathbb{R}^m$, pour $s \in \mathbb{Z}^+$. De plus,

$$
\tilde{A}(\varepsilon) = \begin{bmatrix} \varepsilon \tilde{A}_{11} & \tilde{A}_{12} \\ \varepsilon \tilde{A}_{21} & \tilde{A}_{22} \end{bmatrix}, \quad \tilde{B}_u = \begin{bmatrix} \tilde{B}_{u,1} \\ \tilde{B}_{u,2} \end{bmatrix}, \quad \tilde{B}_d = \begin{bmatrix} \tilde{B}_{d,1} \\ \tilde{B}_{d,2} \end{bmatrix}.
\tag{12}
$$

En posant $\varepsilon = 0$, nous obtenons le sous système lent:

$$
\begin{cases}
x_s(s+1) = \tilde{A}_s x_s(s) + \tilde{B}_{u,s} u_s(s) + \tilde{B}_{d,s} d(s) \\
y_s(s) = \tilde{C}_{y,s} x_s(s),
\end{cases}
\tag{13}
$$

avec $\tilde{A}_s = \tilde{A}_{22}$, $\tilde{B}_{u,s} = \tilde{B}_{u,2}$, $\tilde{B}_{d,s} = \tilde{B}_{d,2}$ and $\tilde{C}_{y,s} = C_{y,2}$.

Dans Tab. 1, nous comparons le spectre de la matrice $\tilde{A}(\varepsilon)$, qui correspond au système à deux échelles de temps (11), et le spectre de la matrice $\tilde{A}_s$, qui correspond au système au système (13). Nous pouvons noter que la séparation des échelles de temps justifie l'utilisation de la seule dynamique lente, afin de la synthétiser du correcteur.

Pour conclure, dans cette section nous avons présenté un modèle non-linéaire du laminoir qui a été calé en comparant les sorties mesurées et simulées du laminoir d'Eisenhüttenstadt. Ensuite, nous avons linéarisé le modèle et nous sommes parvenus à une forme réduite en utilisant l'approximation des perturbations singulières. Enfin, nous avons obtenu le modèle linéaire (13), qui contient seulement la dynamique contrôlable. Afin de synthétiser le correcteur, nous avons supposé que le système travaille toujours autour du point de fonctionnement et que la dynamique rapide peut être négligée. Toutes ces hypothèses ont été validées dans [DBI+08], où le modèle (1)-(6) a été utilisé pour synthétiser un correcteur LQ pour un produit spécifique.

Table 1: Comparaison des valeurs propres

$\xi\{\tilde{A}(\varepsilon)\}$	$\xi\{\tilde{A}_s\}$
0.9455 + 0.0055i	0.9469 + 0.0075i
0.9455 - 0.0055i	0.9469 - 0.0075i
0.9015 + 0.0302i	0.9066 + 0.0279i
0.9015 - 0.0302i	0.9066 - 0.0279i
0.8101	0.8154
0.2793	
0.0697	
0.0017 + 0.0241i	
0.0017 - 0.0241i	
0.0076	

1.3 Modélisation polytopique

Le fait qu'un laminoir travaille avec un ensemble de produits très hétérogènes peut être modélisé comme une incertitude sur chaque paramètre du produit. Les incertitudes dépendent des paramètres physiques de la tôle (largeur, épaisseur, température, etc.) et des paramètres du laminoir (rayon vitesse de rotation des cylindres, force de laminage, etc.). Les paramètres du laminoir sont liés à la tôle mais fixés par un opérateur, donc chaque produit est caractérisé par ses paramètres de tôle et par ses paramètres du laminoir.

Dans cette subsection, nous présentons la méthode utilisée pour décrire le système comme un problème convexe en utilisant une approche polytopique, qui nous permettra d'appliquer des techniques LMI dans la synthèse du correcteur. Un laminoir avec 5 cages possède 70 paramètres incertains. Pour un problème de cette dimension, la synthèse du correcteur basée sur la résolution de LMI peut échouer, c'est-à-dire que les solveurs n'arrivent pas à trouver une solution. Nous montrons comment la complexité du problème peut être réduite en exploitant les relations physiques entre les différents paramètres du produit. De plus, puisque les produits laminés peuvent être très différents, nous proposons de les diviser en plusieurs familles. Pour chaque famille, nous synthétiserons un correcteur robuste différent de manière à améliorer les performances du système. Considérons le modèle incertain du laminoir dans la forme polytopique:

$$\begin{cases} x(s+1) = \mathfrak{A}(s)x(s) + \mathfrak{B}_u(s)u(s) + \mathfrak{B}_d(s)d(s) \\ q(s) = C_q x(s) + D_{qu}u(s) \\ y(s) = C_y x(s), \end{cases} \tag{14}$$

où $q(s) \in \mathbb{R}^w$ est la sortie contrôlée,

$$\mathfrak{A}(s) = \sum_{l=1}^{N_V} \lambda_l(s)\tilde{A}^l(\varepsilon), \quad \mathfrak{B}_u(s) = \sum_{l=1}^{N_V} \lambda_l(s)\tilde{B}_u^{i,l}, \quad \mathfrak{B}_d(s) = \sum_{l=1}^{N_V} \lambda_l(s)\tilde{B}_d^l,$$

$l \in \mathcal{L} = \{1, ..., N_V\}$ dénote les sommets du polytope. λ_l dénote l'incertitude et appartient au simplexe unitaire

$$\mathfrak{Y}(s) = \{\sum_{l=1}^{N_V} \lambda_l(s) = 1, \ \lambda_l(s) \geq 0\},$$

pour $s \in \mathbb{Z}^+$. Chaque sommet du polytope peut être caractérisé par un modèle linéaire à deux échelles de temps:

$$\begin{cases} x(s+1) = \tilde{A}^l(\varepsilon)x(s) + \tilde{B}_u^l u(s) + \tilde{B}_d^l d(s) \\ q(s) = C_q x(s) + D_{qu} u(s) \\ y(s) = C_y x(s), \end{cases} \tag{15}$$

avec

$$\tilde{A}^l(\varepsilon) = \begin{bmatrix} \varepsilon\tilde{A}_{11}^l & \tilde{A}_{12}^l \\ \varepsilon\tilde{A}_{21}^l & \tilde{A}_{22}^l \end{bmatrix}, \quad \tilde{B}_u^l = \begin{bmatrix} \tilde{B}_{u,1}^l \\ \tilde{B}_{u,2}^l \end{bmatrix}, \quad \tilde{B}_d^l = \begin{bmatrix} \tilde{B}_{d,1}^l \\ \tilde{B}_{d,2}^l \end{bmatrix},$$
$$C_q = \begin{bmatrix} C_{q,1} & C_{q,2} \end{bmatrix}, \quad C_y = \begin{bmatrix} C_{y,1} & C_{y,2} \end{bmatrix}.$$

$N_V = 2^{\mathcal{D}}$ est le nombre de sommets et $\mathcal{D}$ est la dimension du polytope, qui est égale au nombre de paramètres incertains $\mathcal{D} = card\{\mathcal{U}\}$, qui dans notre système vaut $\mathcal{U} = 70$. Les solveurs LMI n'arrivent pas à trouver une solution pour un problème de cette dimension. Néanmoins, puisque la plupart des paramètres sont liés par des relations physiques, nous pouvons déterminer un ensemble de paramètres indépendants $\mathcal{U}^m \subset \mathcal{U}$ tels que la dynamique du système est similaire, pour deux produits qui possèdent le même ensemble $\mathcal{U}^m$. Nous définissons aussi l'ensemble $\mathcal{U}^s = \{\mathcal{U} \setminus \mathcal{U}^m\}$ comme l'ensemble des paramètres restants, qui dépendront de $\mathcal{U}^m$. L'ensemble $\mathcal{U}^s$ peut être divisé en deux sous-ensembles $\mathcal{U}^s = \{\mathcal{U}_{op}^s, \mathcal{U}_{fnc}^s\}$. Le premier sous-ensemble $\mathcal{U}_{op}^s$ contient les paramètres choisis par l'opérateur, comme les caractéristiques des cylindres. L'une des tâches principales des opérateurs est de prévenir les incidents dans le laminoir. Donc, ils doivent assurer une configuration du système garantissant un comportement standard ainsi que la sûreté du système. Cela revient à dire qu'ils utiliseront un sous-ensemble $\mathcal{U}_{op}^s$ similaire pour laminer des produits avec les mêmes caractéristiques de façon à obtenir la même dynamique pour le système. Étant donné que l'ensemble $\mathcal{U}^m$ inclut les caractéristiques physiques les plus importantes du produit, nous pouvons supposer que pour deux produits avec le même ensemble $\mathcal{U}^m$, l'opérateur choisira le même sous-ensemble $\mathcal{U}_{op}^s$. Le dernier sous-ensemble $\mathcal{U}_{fnc}^s$ peut être calculé en utilisant des fonctions analytiques en connaissant les valeurs de $\mathcal{U}^m$ et $\mathcal{U}_{op}^s$. Par exemple, la relation entre la vitesse de rotation et l'épaisseur de sortie de deux cages adjacentes est donnée par la loi de conservation de la matière. Alors, des produits

qui ont le même ensemble $\mathcal{U}^m$ auront aussi le même ensemble $\mathcal{U}^s$, en première approximation.

Nous avons trouvé $\mathcal{U}^m = \{w, h_n, \sigma_1^0, \sigma_n^0\}$, où w est la largeur de la tôle, h_n est l'épaisseur de sortie de la tôle dans la dernière cage et σ_1^0 et σ_n^0 représentent la dureté de la tôle dans la première et dans la dernière cage, respectivement.

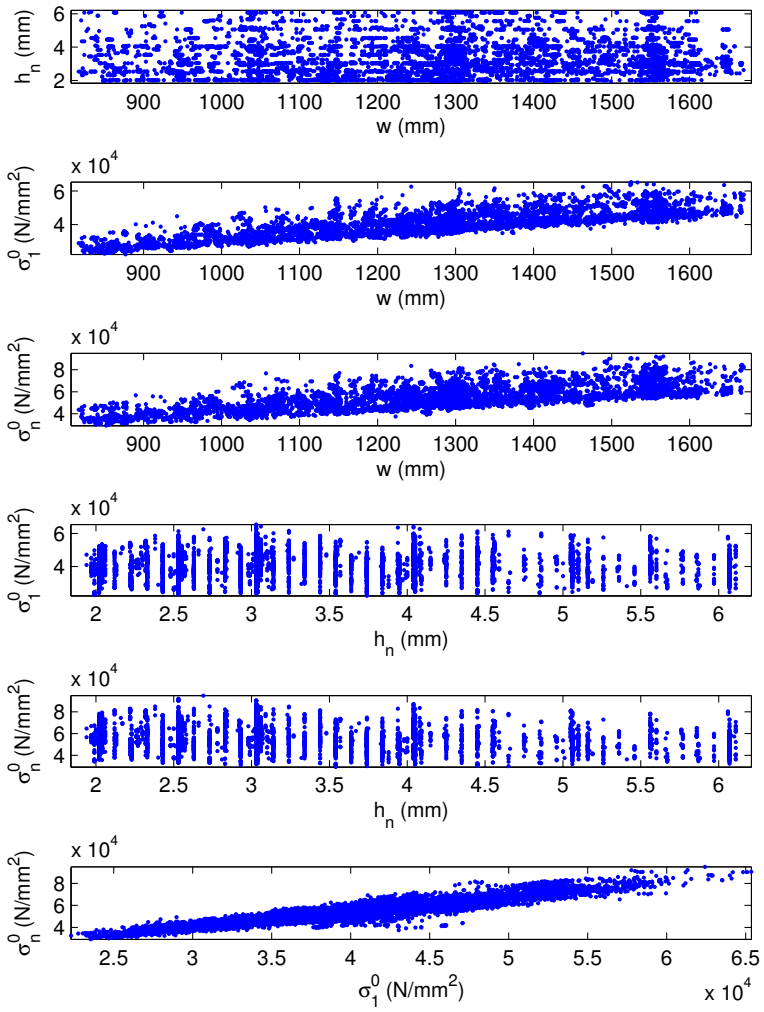

Figure 6: Base de données du HSM ArcelorMittal d'Eisenhüttenstadt

Au but de valider ce choix de $\mathcal{U}^m$, nous considérons la base de données du HSM d'Eisenhüttenstadt (Fig. 6), qui contient environ 10000 produits. L'entière

variation des paramètres principaux dans la base de données est:

$$\begin{array}{c} w = 810 - 1670\, mm \\ h_n = 1.9 - 6.2\, mm \\ \sigma_1^0 = 22 - 65\, KN/mm^2 \\ \sigma_n^0 = 30 - 90\, KN/mm^2 \end{array} \tag{16}$$

Fig. 7 montre l'évolution des valeurs propres en boucle ouverte pour la variation

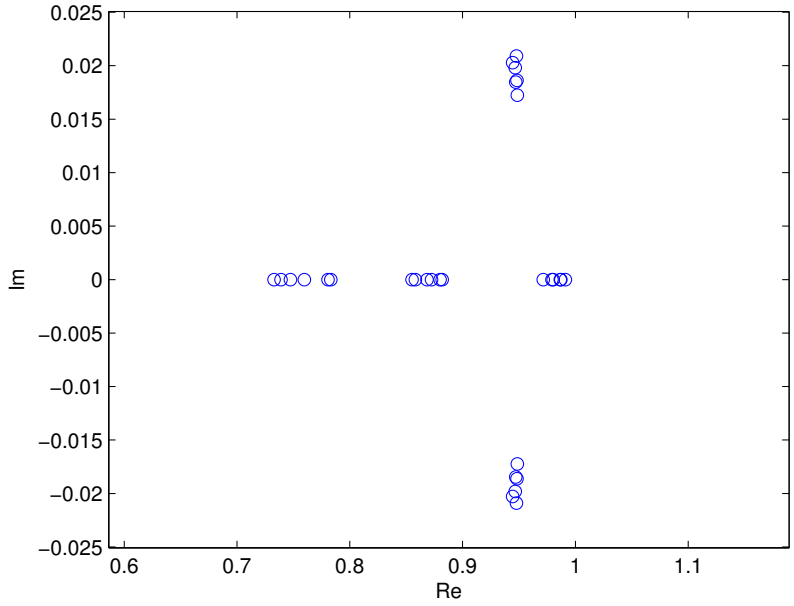

Figure 7: Évolution des valeurs propres en boucle ouverte

des paramètres principaux suivante:

$$\begin{array}{c} w = 1150 - 1180\, mm \\ h_n = 2 - 2.2\, mm \\ \sigma_1^0 = 50 - 52\, KN/mm^2 \\ \sigma_n^0 = 35 - 37\, KN/mm^2 \end{array} \tag{17}$$

Nous pouvons noter comme toutes les valeurs propres ont des variations très limitées. De plus, cette différence de dynamique est due principalement à la variation des paramètres (17). On peut conclure que les paramètres secondaires aussi, qui contribuent à la dynamique du système, bougent dans une zone très limitée lorsque l'ensemble des paramètres principaux ne change pas.

Le polytope qui contient l'ensemble des produits traités peut être divisé dans N_F polytopes plus petits afin de concevoir des correcteurs spécifiques et donc améliorer les performances du système de contrôle.

1.4 Synthèse du correcteur H_2

Dans cette section, nous présentons le correcteur H_2. Considérons le système incertain aux perturbations singulières en temps discret

$$\begin{cases} x(s+1) = \mathfrak{A}(s)x(s) + \mathfrak{B}_u(s)u(s) + \mathfrak{B}_d(s)d(s) \\ q(s) = C_q x(s) + D_{qu}u(s) \\ y(s) = C_y x(s). \end{cases} \tag{18}$$

Puisque les actionneurs du laminoir ont une vitesse limitée, la dynamique rapide, qui est stable en boucle ouverte, ne peut pas être contrôlée. Par conséquent, nous sommes obligés d'utiliser une loi de contrôle réduite. Le modèle linéaire qui correspond à chaque sommet est:

$$\begin{cases} x_1(s+1) = \varepsilon\tilde{A}^l_{11}x_1(s) + \tilde{A}^l_{12}x_2(s) + \tilde{B}^l_{u,1}u(s) + \tilde{B}^l_{d,1}d(s) \\ x_2(s+1) = \varepsilon\tilde{A}^l_{21}x_1(s) + \tilde{A}^l_{22}x_2(s) + \tilde{B}^l_{u,2}u(s) + \tilde{B}^l_{d,2}d(s) \\ q(s) = C_{q,1}x_1(k) + C_{q,2}x_2(k) + D_{qu}u(s) \\ y(s) = C_{y,1}x_1(s) + C_{y,2}x_2(s), \end{cases}$$

avec $\varepsilon = 0.05$, $C_{q,1} = 0$ et $C_{y,1} = 0$. Le sous système lent correspondant est:

$$\begin{cases} x_s(s+1) = \tilde{A}^l_s x_s(s) + \tilde{B}^l_{u,s}u_s(s) + \tilde{B}^l_{d,s}d(s) \\ q(s) = \tilde{C}_s x_s(s) + \tilde{D}_s u_s(s), \end{cases}$$

où $\tilde{A}^l_s = \tilde{A}^l_{22}$, $\tilde{B}^l_{u,s} = \tilde{B}^l_{u,2}$ et $\tilde{B}^l_{d,s} = \tilde{B}^l_{d,2}$. $\tilde{C}_s = C_{q,2} = \begin{bmatrix} I_n \\ 0_{r\times n} \end{bmatrix}$, $\tilde{D}_s = D_{qu} = \begin{bmatrix} 0_{n\times r} \\ D^0_{qu} \end{bmatrix}$ sont deux matrices de poids qui respectent l'hypothèse d'orthogonalité $\tilde{C}_s'\tilde{D}_s = 0$, $\tilde{D}_s'\tilde{D}_s \succ 0$. La paire $(\tilde{A}^l_s, \tilde{B}^l_{u,s})$ est supposé être contrôlable.

Nous avons décidé de synthétiser un correcteur H_2 par retour d'état, qui permet de déterminer une solution robuste par rapport aux incertitudes. De plus, ce type de technique permet de minimiser les effets des perturbations extérieures. Étant donnée la loi de contrôle

$$u_s(s) = K_s x_s(s),$$

nous pouvons définir la matrice de transfert entre q et d

$$H^l_{dq}(\varsigma) = (\tilde{C}_s + \tilde{D}_s K_s)(\varsigma I_n - \tilde{A}^l_s - \tilde{B}^l_{u,s}K_s)^{-1}\tilde{B}^l_{d,s}$$

et sa norme H_2

$$\|H^l_{dq}\|_2^2 = \frac{1}{2\pi}\int_{-\pi}^{\pi} Tr\{H^l_{dq}(\varsigma)^* H^l_{dq}(\varsigma)\}d\omega \tag{19}$$

avec $\varsigma = e^{j\omega}$, pour chaque $l \in \mathcal{L}$. Le théorème suivant permet de calculer un correcteur à retour d'état qui stabilise asymptotiquement le système polytopique (18) et minimise sa dynamique lente, avec $K = [0 \;\; K_s]$.

Théorème 1 *S'il existe des matrices $W_s = W_s' \succ 0$, $P_s = P_s' \succ 0$, Z_s de dimension appropriée, et un scalaire $\mu > 0$ tels que les LMIs*

$$Tr\left(W_s\right) < \mu \tag{20}$$

$$\begin{bmatrix} W_s & \tilde{C}_s P_s + \tilde{D}_s Z_s \\ (\star)' & P_s \end{bmatrix} \succ 0, \tag{21}$$

et

$$\begin{bmatrix} P_s & \tilde{A}_s^l P_s + \tilde{B}_{u,s}^l Z_s & \tilde{B}_{d,s}^l \\ (\star)' & P_s & 0 \\ (\star)' & (\star)' & I_n \end{bmatrix} \succ 0 \tag{22}$$

sont vérifiés pour chaque $l \in \mathcal{L}$, alors il existe un scalaire $\varepsilon_{max} > 0$ tel que le correcteur $K = [0 \;\; K_s]$, avec $K_s = Z_s P_s^{-1}$, stabilise asymptotiquement le système en boucle fermée (18), $\forall \varepsilon \in (0, \varepsilon_{max}]$. De plus, le correcteur K_s solution du problème:

$$\begin{aligned} &\underset{W_s, Z_s, P_s}{min} \; \mu \\ &sujet \;\; à \quad (20)\text{-}(22) \end{aligned} \tag{23}$$

minimise la norme H_2 (19).

Preuve 1 *L'existence d'un ensemble de matrices de Lyapunov*

$$P^l(\varepsilon) = P^l(\varepsilon)' = \begin{bmatrix} \varepsilon^{-1} P_f^l & P_2^l + O(\varepsilon) \\ P_2^{l'} + O(\varepsilon) & P_s + O(\varepsilon) \end{bmatrix} \succ 0, \tag{24}$$

et d'une matrice

$$Z(\varepsilon) = \begin{bmatrix} 0 & Z_s + O(\varepsilon) \end{bmatrix}$$

telles que les LMI

$$\begin{aligned} &\tilde{A}^l(\varepsilon) P^l(\varepsilon) \tilde{A}^l(\varepsilon)' + \tilde{A}^l(\varepsilon) Z(\varepsilon)' \tilde{B}_u^{l'} + \tilde{B}_u^l Z(\varepsilon) \tilde{A}^l(\varepsilon)' + \\ &\tilde{B}_u^l Z(\varepsilon) P^l(\varepsilon)^{-1} Z(\varepsilon)' \tilde{B}_u^{l'} - P^l(\varepsilon) + \tilde{B}_d^l \tilde{B}_d^{l'} \prec 0 \end{aligned} \tag{25}$$

sont vérifiées, $\forall\, l \in \mathcal{L}$, représente une condition suffisante pour la stabilité asymptotique du système en boucle fermée (18). En décomposant la condition (25), nous obtenons:

$$\begin{bmatrix} \varepsilon^{-1}(X_1^l + O(\varepsilon)) & X_2^l + O(\varepsilon) \\ X_2^{l'} & X_3^l + O(\varepsilon) \end{bmatrix} \prec 0, \tag{26}$$

avec

$$X_1^l = -P_f^l \prec 0, \tag{27}$$

$$X_2^l = \tilde{A}_{12}^l P_s \tilde{A}_s^{l'} + \tilde{A}_{12}^l Z_s' \tilde{B}_{d,s}^{l'} + \tilde{B}_{d,1}^l Z_s \tilde{A}_s^{l'} + \tilde{B}_{u,1}^l Z_s P_s^{-1} Z_s' \tilde{B}_{u,s}^{l'} + \tilde{B}_{u,1}^l \tilde{B}_{u,s}^{l'} - P_2^l, \tag{28}$$

$$X_3^l = \tilde{A}_s^l P_s \tilde{A}_s^{l'} + \tilde{A}_s^l Z_s' \tilde{B}_{u,s}^{l'} + \tilde{B}_{u,s}^l Z_s \tilde{A}_s^{l'} + \tilde{B}_{u,s}^l Z_s P_s^{-1} Z_s' \tilde{B}_{u,s}^{l'} + \tilde{B}_{d,s}^l \tilde{B}_{d,s}^{l'} - P_s \prec 0. \tag{29}$$

En appliquant le complément de Schur, la condition (29) est équivalent à la condition (22). Donc, elle est satisfaite par hypothèse, avec $P_s \succ 0$*, ce qui signifie qu'il existe des matrices* $P_f^l \succ 0$ *et an scalaire* $\varepsilon_1 > 0$ *tel quel'inegalité*

$$X_1^l - \varepsilon(X_2^l(X_3^l + O(\varepsilon))^{-1}X_2^{l'} + O(\varepsilon)) + O(\varepsilon) \prec 0$$

est vérifié, $\forall\, l \in \mathcal{L}$ *et* $\forall\, \varepsilon \in (0, \varepsilon_1]$*. En appliquant le complément de Schur, (26) tient* $\forall\, \varepsilon \in (0, \varepsilon_1]$*. De plus, il existe un scalaire* $\varepsilon_2 > 0$ *tel que l'inegalité*

$$P_f^l - \varepsilon P_2^l(P_s + O(\varepsilon))^{-1}P_2^{l'} + O(\varepsilon^2) \succ 0$$

est vérifié, $\forall\, l \in \mathcal{L}$ *et* $\forall\, \varepsilon \in (0, \varepsilon_2]$*. Par conséquent, en utilisant le complément de Schur,* $P^l(\varepsilon) \succ 0$*,* $\forall\, l \in \mathcal{L}$ *et* $\forall\, \varepsilon \in (0, \varepsilon_2]$*. Donc, il existe des matrices* P_s*,* Z_s*,* P_f^l*,* P_2^l *et un scalaire* $\varepsilon_{max} = min\{\varepsilon_1, \varepsilon_2\}$ *qui vérifient la contrainte (24)-(25),* $\forall\, l \in \mathcal{L}$ *et* $\forall\, \varepsilon \in (0, \varepsilon_{max}]$*. En outre, quand* $\varepsilon \to 0$*, nous obtenons* $K = Z(\varepsilon)P^l(\varepsilon)^{-1} = \begin{bmatrix} 0 & Z_s P_s^{-1} \end{bmatrix}$.

Afin de montrer que le correcteur K *minimise la norme* H_2 *(19),* $\forall\, l \in \mathcal{L}$ *et* $\forall\, \varepsilon \in (0, \varepsilon_{max}]$*, considérons l'index de performance*

$$J_s = Tr\left(\begin{bmatrix} \tilde{C}_s'\tilde{C}_s & 0 \\ 0 & \tilde{D}_s'\tilde{D}_s \end{bmatrix}\begin{bmatrix} P_s & Z_s' \\ Z_s & Z_s P_s^{-1} Z_s' \end{bmatrix}\right).$$

En appliquant le complément de Schur à (21), nous obtenons :

$$W_s \succ \tilde{C}_s P_s \tilde{C}_s' + \tilde{D}_s Z_s P_s^{-1} Z_s{}' \tilde{D}_s'.$$

D'où

$$Tr(W_s) \succ Tr(\ \tilde{C}_s P_s \tilde{C}_s' + \tilde{D}_s Z_s P_s^{-1} Z_s' \tilde{D}_s') = J_s.$$

Minimiser J_s *équivaut à minimiser la norme* H_2 *(19) [PG94], si nous choisissons* $\tilde{B}_{d,s}^l = x_s^{0,l}$*. En conséquent,* $\|H_{dq}^l\|_2^2 \leq \mu$*,* $\forall\, l \in \mathcal{L}$*, qui conclut la preuve.*

1.5 Résultats

Dans cette section, nous appliquons la loi de contrôle décrite dans les sections précédentes au laminoir ArcelorMittal situé dans l'usine d'Eisenhüttenstadt. Nous avons divisé l'ensemble des produits traités en N_F familles et, pour chaque famille, nous avons synthétisé un correcteur différent. Cette stratégie permet d'améliorer les performances du système, par rapport aux performances obtenues en utilisant un seul correcteur pour tous les produits. En revanche, le nombre de familles doit être limité afin de ne pas compliquer la gestion des données dans l'usine.

1.5.1 Boite à Outils *RSCT*

Afin d'obtenir une procédure simple et systématique qui permet d'étendre le contrôle de déport de bande dans plusieurs usines, nous avons développé une boite

Table 2: Bornes des Familles

Familles \ Données	w	h_n	σ_1^0	σ_n^0
1	$810-1200$	$1.9-3$	$22-65$	$30-95$
2	$810-1200$	$3-4.5$	$22-65$	$30-95$
3	$810-1200$	$4.5-6.2$	$22-65$	$30-95$
4a	$1200-1400$	$1.9-3$	$22-65$	$30-95$
4b	$1400-1670$	$1.9-3$	$22-65$	$30-95$
5	$1200-1670$	$3-4.5$	$22-65$	$30-95$
6	$1200-1670$	$4.5-6.2$	$22-65$	$30-95$

à outils *Matlab*, appelée *Robust Steering Control Toolbox* (*RSCT*) [MBS+08]. Elle donne la possibilité de construire une base de données de produits et d'implémenter l'algorithme décrit dans la section précédente. Ceci permet de diviser la base de données en N_F familles, de calculer les produits correspondants aux sommets, $\forall f \in \mathcal{F} = \{1, ..., N_F\}$, et le système linéaire correspondant à chaque produit. Ces informations seront utilisées pour calculer les gains des correcteurs K^f, utilisant le Théorème 1. La boite à outils contient aussi le simulateur du laminoir qui permet d'analyser le comportement du système. Le problème LMI (20)-(22) a été résolu utilisant le solveur LMI *SeDuMi* [Stu99] et la boite à outils *Matlab* *YALMIP*, qui fournit une interface simple pour les solveurs LMI les plus utilisés [LÖ4].

1.5.2 Calcul des Régulateurs

Les essais expérimentaux effectués nous ont conduit à diviser la base de données en $N_F = 7$ familles, en fonction de l'ensemble des paramètres principaux $\mathcal{U}^m = \{w, h_n, \sigma_1^0, \sigma_n^0\}$. Les bornes des familles sont résumées dans la table 2.

Le système de contrôle a été synthétisé en temps discret, avec un période d'échantillonnage $T_s = 0.05$ *sec* (une borne inférieure pour T_s est imposée par les limites des actionneurs). Le Théorème 1 permet de déterminer un gain K^f qui garantit la stabilité robuste du système en boucle fermée pour chaque famille $f \in \mathcal{F}$.

1.5.3 Résultats de Simulation

Dans la suite, nous présentons les résultats de simulation pour un produit avec $\mathcal{U}^m = \{967, 2.02, 27.9, 40.1\}$, qui appartient à la famille 1 (table 2). La figure 8 montre l'évolution de la sortie Z.

Le trait plein représente l'évolution de Z avec le gain de régulation K^1. Le trait discontinu montre l'évolution de Z avec un correcteur LQ classique, synthétisé pour un produit moyen par rapport à la famille 1. Le trait pointillé montre l'évolution de Z avec un correcteur LQ classique synthétisé pour un produit moyen par rapport à l'ensemble de la base de données. Ce dernier correcteur est

présenté dans [DBI+08].

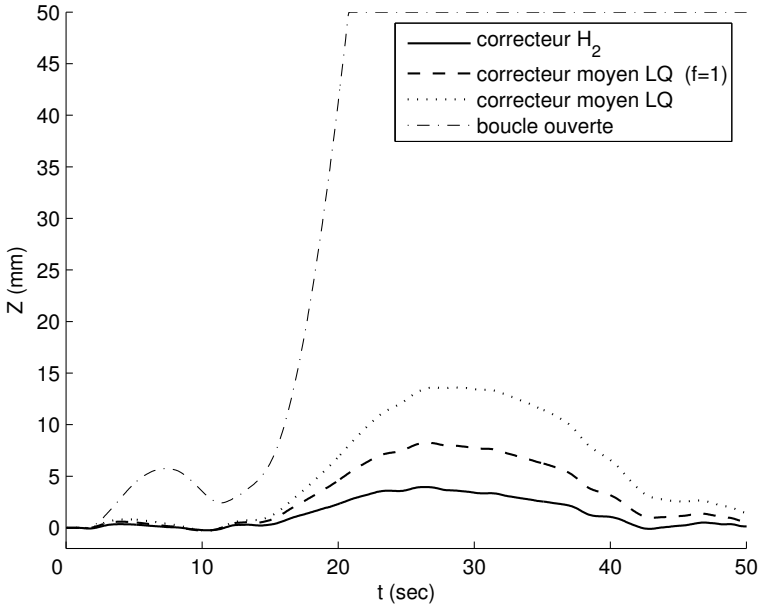

Figure 8: Évolution du décentrement de bande en sortie du système

Comme attendu, la division de la base de données en plusieurs familles améliore les performances du système. De plus, le correcteur H_2 permet de tenir compte des paramètres incertains et de minimiser les effets de la perturbation extérieure, qui est due aux vibrations du "coilbox". La dernière ligne montre l'évolution de Z sans correcteur. Nous pouvons noter que dans ce cas la sortie est sujette à saturation, c'est-à-dire que la tôle frotte contre les guides à cause de la valeur élevée de Z. La tôle risque de se déchirer ou de se replier sur elle-même. Outre le fait que cette tôle devient inutilisable, un incident de laminage de ce type peut engendrer de sérieux défauts sur les cylindres de travail.

1.5.4 Résultats Expérimentaux

Ici, nous présentons quelques résultats expérimentaux. La figure 9 montre l'évolution du décentrement d'un produit avec $\mathcal{U}^m$ ={895, 2.42, 30.4, 37.4} (famille 1). Lorsque le produit rentre dans le laminoir, le contrôle est actif (Fig. 9.b) et la valeur du décentrement de bande est maintenue proche de zéro (Fig. 9.a). En l'instant $N_s = 1050$, le système de contrôle est désactivé et la commande u est fixée à une valeur constante par l'opérateur. Comme attendu, la valeur de Z croît rapidement, de 10 à 30 mm.

Sur la figure 10, nous montrons l'évolution de Z pour deux produits consécutifs et avec le même $\mathcal{U}^m$ ={1510, 2.02, 59.1, 72.5} (famille 4). Le trait plein correspond à l'évolution de Z lorsque le système de contrôle est actif, tandis que le trait pointillé correspond à l'évolution de Z en boucle ouverte. L'amélioration des performances, par rapport à la valeur de Z, est évidente.

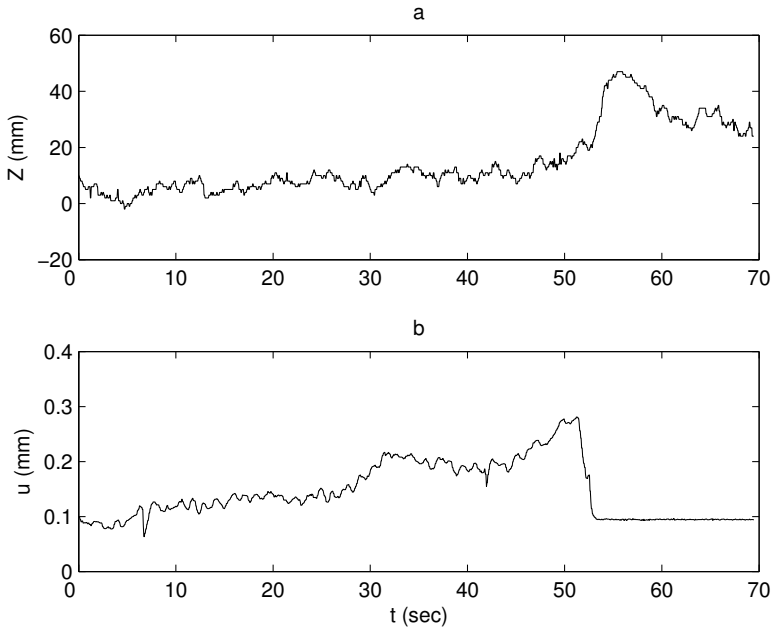

Figure 9: Évolution du décentrement de bande et de la commande

Dans la suite, nous montrons quelques statistiques. Sur la Fig. 11, nous comparons l'écart type du décentrement de bande $\sigma_x(Z)$ obtenu utilisant le système de contrôle basé sur le correcteur H_2, et l'écart type du décentrement de bande $\sigma_x(Z)$ obtenu avec le système en boucle ouverte. Les statistiques concernent 100 tôles contrôlées et 200 tôles en boucle ouverte. Toutes les familles ont été testées. L'amélioration des performances est évidente. Lorsque le système travaille en boucle ouverte, le décentrement de bande augmente d'environ 125%. Les bornes sur ΔS ont été toujours respectées et le coin Δh_n a été toujours maintenu dans les limites du cahier des charges ($\pm 10\,\mu m$).

Sur la Fig. 12, nous comparons l'écart type du décentrement de bande $\sigma_x(Z)$ obtenu utilisant le système de contrôle basée sur le correcteur H_2, et l'écart type du décentrement de bande $\sigma_x(Z)$ utilisant le système de contrôle basé sur le correcteur moyen LQ décrit dans [DBI+08]. Les statistiques concernent 44 tôles appartenant à toutes les familles. Afin de garantir des conditions équivalentes de laminage (paramètres des tôles, caractéristiques des cylindres, température extérieure, asymétries dans le système, etc.) et donc d'obtenir des résultats cohérents, nous avons confronté des tôles identiques. Nous pouvons observer une amélioration des performances lorsque le système de contrôle H_2 est actif (environ le 35%). L'écart type du coin $\sigma_x(\Delta h_n)$ a été aussi amélioré en passant de $7.82\,\mu m$ (LQ) à $5.56\,\mu m$ (H_2).

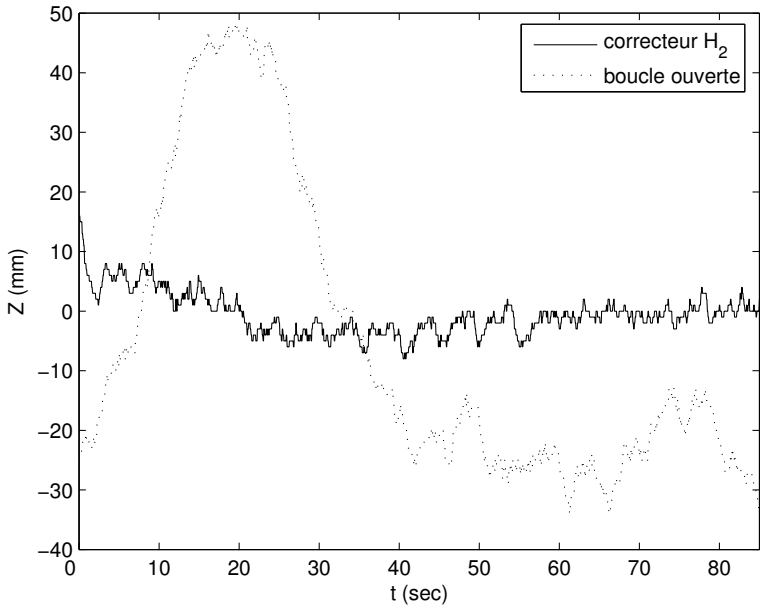

Figure 10: Évolution du décentrement de bande

1.6 Conclusion

Dans cette section, nous avons proposé un correcteur robuste H_2 capable de garantir la stabilité du laminoir et d'améliorer ses performances. Nous avons créé une base de données qui décrit l'ensemble des produits traités par le système, et nous l'avons divisée en sept familles de produits. De plus, nous avons présenté une méthode qui permet de réduire la complexité du problème en exploitant les relations physiques entre les paramètres. Cette méthode permet de formuler le problème de stabilisation comme un problème convexe et, par conséquent, de synthétiser un correcteur H_2 différent pour chaque famille en utilisant des techniques LMI.

Nous avons aussi montré des résultats en simulation et tests expérimentaux qui concernent le laminoir ArcelorMittal d'Eisenhüttenstadt, qui prouvent l'efficacité de la méthode proposée. Le décentrement de bande a été réduit de façon significative, par rapport aux résultats de la boucle ouverte et de la boucle fermée avec le système de contrôle existant qui ne prenait pas en compte les incertitudes.

Le contrôle de décentrement de bande dans un laminoir est un sujet important dans la production d'acier. Afin d'adapter la méthode présentée pour d'autres laminoirs, nous avons développé une procédure systématique. Naturellement, un calage du modèle et la construction d'une base de données de produits sont nécessaires.

Dans la suite, nous nous proposons de résoudre le problème de stabilisation concernant la phase "queue de bande", qui est la dernière phase du processus de laminage à chaud. Dans cette phase, la tôle quitte les cages l'une après l'autre et, chaque fois que la tôle quitte une cage, la dynamique du système change. Donc,

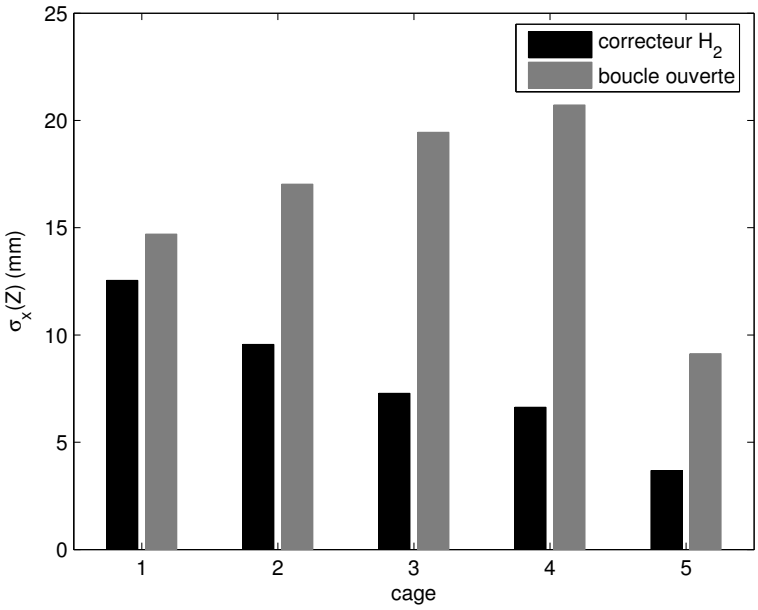

Figure 11: Comparaison de $\sigma_x(Z)$: système contrôlé par le correcteur H_2 et en boucle ouverte

le laminoir peut alors être décrit comme un système à commutations.

2 Stabilisation des systèmes à commutation à deux échelles de temps

2.1 Introduction

Un système à commutation en temps continu est composé d'une famille d'équations différentielles, où chaque équation décrit le comportement d'un sous système, et d'une loi de commutation qui gouverne les commutations parmi les sous systèmes. Dans les dernières années, cette classe de systèmes, qui permet de représenter une large gamme de systèmes physiques, a reçu beaucoup d'attention par la communauté scientifique. Dans le cadre des systèmes de contrôle, une des propriétés les plus étudiées des systèmes à commutation est la stabilité [Lib03], [SWM+07], [LA09]. Afin d'assurer cette propriété, différents types d'approches ont été proposés: méthodes basées sur la recherche d'une fonction quadratique de Lyapunov commune à tous les sous systèmes [SN02], [SN03], ou d'une fonction de Lyapunov multiple [Bra98], [DRI02], [BMS07], méthodes qui cherchent à établir un temps de séjour minimal pour chaque sous système afin de garantir la stabilité du système à commutation [HM99], [Mor96], [ZHYM01].

En pratique, nous pouvons rencontrer beaucoup de systèmes qui présentent une dynamique à deux échelles de temps, par exemple dans les systèmes élec-

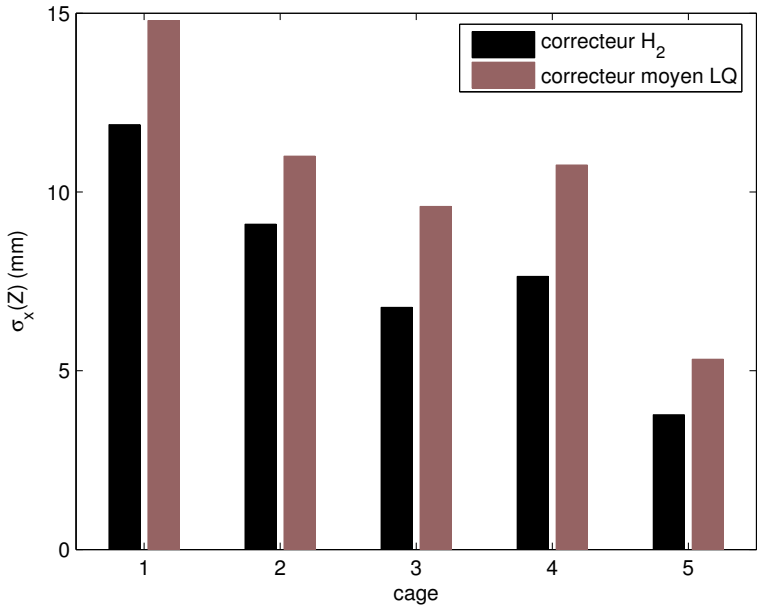

Figure 12: Comparaison de $\sigma_x(Z)$: système contrôlé par le correcteur H_2 et par le correcteur LQ

triques, les systèmes aéronautiques, la robotique, la chimie ou la biologie [Nai02]. Dans ce cas, les techniques de contrôle classiques se trouvent confrontées à des problèmes de mauvais conditionnement. La méthode des perturbations singulières est particulièrement recommandée pour éviter ce type de problèmes : le système original est décomposé en plusieurs sous systèmes, un pour chaque échelle de temps, et un correcteur différent est synthétisé pour chaque sous système [KKO86], [KS68]. On rencontre les systèmes à commutation avec plusieurs échelles de temps dans plusieurs applications réelles. Un exemple est donné par le contrôle de guidage de bande dans un laminoir finisseur [MDI+09e]. Néanmoins, cette classe de systèmes n'a pas reçu beaucoup d'attention jusqu'à maintenant et à notre connaissance la seule contribution dans ce domaine concerne l'extension des conditions pour calculer le temps de séjour minimal [ZHYM01] au cas des systèmes à commutation en temps continu avec retard et à deux échelles de temps [ALI08].

Les méthodes de contrôle classiques concernant les systèmes linéaires à deux échelles de temps s'appuient sur le fait que les dynamiques lente et rapide peuvent être considérées comme découplées, afin de vérifier la stabilité du système en boucle ouverte ou synthétiser une loi de contrôle stabilisante. Donc, la stabilité asymptotique des sous systèmes lent et rapide est une condition suffisante pour la stabilité du système à deux échelles de temps. Dans cette section, nous montrons que ceci n'est plus vrai pour les systèmes à commutation. En effet, la stabilité des sous systèmes à commutation lent et rapide n'est pas une condition suffisante pour la stabilité du système à commutation à deux échelles de temps lorsque la loi de

commutation est arbitraire [MDI09b]. Il est nécessaire de considérer dans ce cas une condition supplémentaire qui tient compte du couplage entre les dynamiques lente et rapide. Ensuite, nous proposons des conditions suffisantes, formulées sous la forme d'inégalités matricielles linéaires (LMI), qui permettent de vérifier la stabilité d'un système à commutation à deux échelles de temps en boucle ouverte et de synthétiser des correcteurs stabilisants, indépendamment de la valeur de ε. Ces conditions impliquent une contrainte additionnelle qui exprime le couplage entre les sous systèmes lent et rapide lorsque la loi de commutation est arbitraire. À notre connaissance, ceci est le premier travail qui met en évidence explicitement le fait que la stabilité asymptotique des sous systèmes lent et rapide n'est pas une condition suffisante pour la stabilité asymptotique du système à commutation à deux échelles de temps lorsque la loi de commutation est arbitraire, et qui établit des conditions de stabilité pour ce type de systèmes.

2.2 Motivations

Considérons le système linéaire singulièrement perturbé

$$\dot{x}(t) = M(\varepsilon)x(t), \tag{30}$$

où $\varepsilon > 0$ est un scalaire, $x(t) = \begin{bmatrix} x_1(t)' & x_2(t)' \end{bmatrix}'$ est le vecteur d'état, avec $x_1(t) \in \mathbb{R}^{n_1}$ et $x_2(t) \in \mathbb{R}^{n_2}$, pour $t \geq 0$, et

$$M(\varepsilon) = \begin{bmatrix} \varepsilon^{-1} I_{n_1} & 0 \\ 0 & I_{n_2} \end{bmatrix} \begin{bmatrix} M_{11} & M_{12} \\ M_{21} & M_{22} \end{bmatrix}, \tag{31}$$

avec M_{11} matrice non-singulière. Les dynamiques lente et rapide peuvent être découplées en utilisant la transformé suivante [Kok75]:

$$\begin{bmatrix} x_f(t) \\ x_s(t) \end{bmatrix} = \begin{bmatrix} I_{n_1} & L(\varepsilon) \\ -\varepsilon H(\varepsilon) & I_{n_2} - \varepsilon H(\varepsilon)L(\varepsilon) \end{bmatrix} \begin{bmatrix} x_1(t) \\ x_2(t) \end{bmatrix}, \tag{32}$$

avec

$$M_{12} - M_{11}L(\varepsilon) + \varepsilon L(\varepsilon)(M_{22} - M_{21}L(\varepsilon)) = 0, \tag{33}$$

$$M_{21} - H(\varepsilon)M_{11} + \varepsilon(M_{22} - M_{21}L(\varepsilon))H(\varepsilon) - \varepsilon H(\varepsilon)L(\varepsilon)M_{21} = 0. \tag{34}$$

Étant donné un scalaire $\varepsilon_{max} > 0$, l'équation algébrique non-symétrique de Riccati (33) et l'équation de Sylvester (34) admettent la solution approximative $L(\varepsilon) = M_{11}^{-1}M_{12} + O(\varepsilon)$, $H(\varepsilon) = M_{21}M_{11}^{-1} + O(\varepsilon)$ quelle que soit la valeur de $\varepsilon \in (0, \varepsilon_{max}]$. La transformé (32) nous donne le système découplé suivante:

$$\begin{cases} \varepsilon \dot{x}_f(t) = (M_{11} + O(\varepsilon))x_f(t) \\ \dot{x}_s(t) = (M_s + O(\varepsilon))x_s(t). \end{cases} \tag{35}$$

Par conséquent, la stabilité asymptotique des sous systèmes lent et rapide (c'est-à-dire les matrices $M_s = M_{22} - M_{21}{M_{11}}^{-1}M_{12}$ et M_{11} sont Hurwitz) implique la

stabilité asymptotique du système à deux échelles de temps (30) quelle que soit la valeur de $\varepsilon \in (0, \varepsilon_{max}]$. Dans le cas des systèmes à commutation à deux échelles de temps, cette propriété est vérifiée au prix d'imposer un temps de séjour minimal [ALI08]. En revanche, le cas des systèmes à commutation avec des lois de commutations arbitraires ne vérifie pas cette propriété. Le système à commutation à deux échelles de temps peut être instable quelle que soit la valeur de $\varepsilon > 0$, même si les sous systèmes lent et rapide sont stables asymptotiquement quelque soit la loi de commutation. L'interprétation de ce phénomène est que pour un $\varepsilon > 0$ fixé, nous pouvons toujours trouver une loi de commutation avec une fréquence de commutation suffisamment élevée qui déstabilise le système à commutation à deux échelles de temps même si les sous systèmes lent et rapide sont stables asymptotiquement. Considérons un système à commutation autonome en temps continu avec perturbations singulières décrit par:

$$\dot{x}(t) = M^{\sigma(t)}(\varepsilon)x(t), \tag{36}$$

où $\{(M^i(\varepsilon)) : i \in \mathcal{I} = \{1,...,N\}\}$ est une famille de matrices et

$$M^i(\varepsilon) = \begin{bmatrix} \varepsilon^{-1} I_{n_1} & 0 \\ 0 & I_{n_2} \end{bmatrix} \begin{bmatrix} M^i_{11} & M^i_{12} \\ M^i_{21} & M^i_{22} \end{bmatrix}, \tag{37}$$

avec M^i_{11} matrice non-singulière pour chaque $i \in \mathcal{I}$. De plus, $\sigma : \mathbb{R}^+ \rightarrow \mathcal{I}$ est le signal de commutation, qui est supposé inconnu a priori. Afin de montrer que la stabilité asymptotique des sous systèmes lent et rapide n'implique pas la stabilité asymptotique du système à commutation à deux échelles de temps, nous choisissons $\mathcal{I} = \{1, 2\}$ et

$$M^1(\varepsilon) = \begin{bmatrix} -\varepsilon^{-1} & 5\varepsilon^{-1} \\ 0 & -1 \end{bmatrix}, \quad M^2(\varepsilon) = \begin{bmatrix} -\varepsilon^{-1} & 0 \\ 5 & -1 \end{bmatrix}. \tag{38}$$

Le système à commutation (36)-(38) possède une dynamique à deux échelles de temps et les matrices $M^i(\varepsilon)$ sont Hurwitz pour chaque $i \in \mathcal{I}$ et chaque valeur de $\varepsilon > 0$. En général, la stabilité de chaque sous système $i \in \mathcal{I}$ ne représente pas une condition suffisante pour la stabilité d'un système à commutation, si la loi de commutation $\sigma(t)$ est arbitraire [Lib03]. Néanmoins, dans notre cas, puisque $M^1_{11} = M^2_{11} = -1$ le sous système à commutation rapide

$$\varepsilon \dot{x_f}(t) = M^{\sigma(t)}_{11} x_f(t) \tag{39}$$

est stable asymptotiquement quelque soit la loi de commutation. Puisque $M^1_s = M^2_s = -1$, aussi le sous système à commutation lent

$$\dot{x_s}(t) = M^{\sigma(t)}_s x_s(t), \tag{40}$$

est stable asymptotiquement quelque soit la loi de commutation, avec

$$M^i_s = M^i_{22} - M^i_{21} {M^i_{11}}^{-1} M^i_{12}. \tag{41}$$

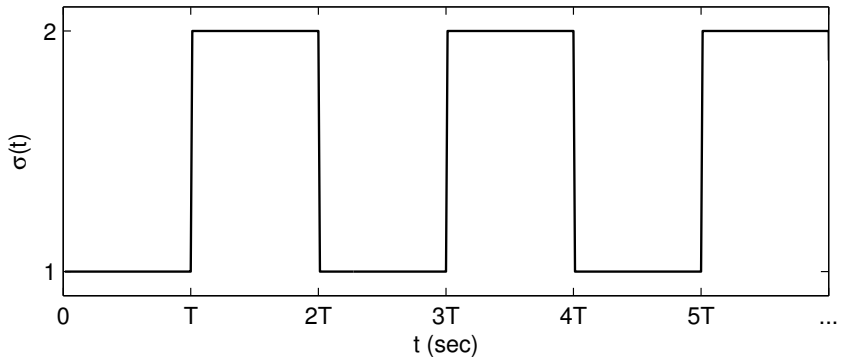

Figure 13: Loi de commutation $\sigma(t)$

Étant donnée la loi de commutation périodique montrée sur la Fig. 13, avec $T = \varepsilon$ *sec*, nous obtenons un système dynamique périodique qui peut être caractérisé par la matrice

$$D(\varepsilon) = e^{M^1(\varepsilon)T} e^{M^2(\varepsilon)T}.$$

Puisque le calcul du rayon spectral de la matrice $D(\varepsilon)$ nous donne

$$\rho(D(\varepsilon)) = 1 + 9.5529\varepsilon - 28.7211\varepsilon^2 + O(\varepsilon^3) > 1$$

pour chaque période $2T$ et chaque $\varepsilon \in (0, \varepsilon_{max}]$, la loi de commutation proposée destabilise le systeme à commutation à deux échelles de temps (36)-(38) quelque soit $\varepsilon \in (0, \varepsilon_{max}]$, même si les sous systèmes à commutation lent et rapide sont stables asymptotiquement.

Dans les prochaines sections, nous proposons des conditions de stabilité pour les systèmes à commutations avec perturbations singulières indépendantes de ε lorsque la loi de commutation est arbitraire. Nous montrons que cela revient à vérifier les conditions de stabilité pour les sous systèmes à commutations lent et rapide et une contrainte additionnelle qui tient compte du couplage entre les sous systèmes lent et rapide lorsqu'une commutation se produit.

2.3 Analyse de stabilité

Considérons le système à commutation linéaire autonome singulièrement perturbé

$$\dot{x}(t) = M^{\sigma(t)}(\varepsilon)x(t), \tag{42}$$

avec $M^i(\varepsilon)$ définie dans l'équation (37) pour chaque $i \in \mathcal{I}$. L'existence d'une fonction de Lyapunov quadratique $V(x(t), \varepsilon) = x(t)'P(\varepsilon)x(t)$ telle que $V(x(t), \varepsilon) > 0$ et $\dot{V}(x(t), \varepsilon) < 0$ est une condition suffisante pour la stabilité asymptotique du système (42).

Lemme 1 *S'il existe des matrices* $P(\varepsilon) = P(\varepsilon)' \succ 0$ *et* $Q^i(\varepsilon) = Q^i(\varepsilon)' \succ 0$ *de dimension appropriée telles que les LMIs*

$$M^i(\varepsilon)P(\varepsilon) + P(\varepsilon)M^i(\varepsilon)' + Q^i(\varepsilon) \prec 0 \tag{43}$$

sont vérifiés $\forall\, i \in \mathcal{I}$, *alors le système à commutation (42) est stable asymptotiquement quelle que soit la loi de commutation.*

Lorsque le scalaire ε est petit, la détermination de la matrice $P(\varepsilon)$ est compliquée à cause des problèmes de mauvais conditionnement de la condition (43). Ce type de problème peut être évité en décomposant le système à commutation à deux échelles de temps en deux sous systèmes bien conditionnés qui correspondent à la dynamique rapide et lente, respectivement [KKO86]. Le théorème suivant donne des conditions de stabilité basées sur des inégalités matricielles linéaires pour tester la stabilité du système à commutation (42), indépendamment de ε et quelle que soit la loi de commutation.

Théorème 2 *S'il existe des matrices* $P_f = P_f{}' \succ 0$, $Q_f^i = Q_f^{i\,\prime} \succ 0$, $P_s = P_s{}' \succ 0$, $Q_s^i = Q_s^{i\,\prime} \succ 0$ *de dimension appropriée telles que les LMIs*

$$M_{11}^i P_f + P_f M_{11}^{i\,\prime} + Q_f^i \prec 0, \tag{44}$$

$$M_s^i P_s + P_s M_s^{i\prime} + Q_s^i \prec 0, \tag{45}$$

$$\begin{bmatrix} Q_f^i & -(M_{11}^i Y^i + P_f M_{21}^{i\,\prime}) \\ (\star)' & Q_s^i - M_{21}^i Y^i - Y^{i\prime} M_{21}^{i\,\prime} \end{bmatrix} \succ 0 \tag{46}$$

sont vérifiées $\forall\, i \in \mathcal{I}$, *avec* $Y^i = -\sum_{h=1, h\neq i}^{N} M_{11}^{h\,-1} M_{12}^h P_s$, *alors il existe un scalaire* $\varepsilon_{max} > 0$ *tel que le système à commutation (42) est stable asymptotiquement* $\forall\, \varepsilon \in (0, \varepsilon_{max}]$ *et quelle que soit la loi de commutation.*

Preuve 2 *Considérons*

$$P(\varepsilon) = \begin{bmatrix} P_1(\varepsilon) & P_2(\varepsilon) \\ P_2(\varepsilon)' & P_3(\varepsilon) \end{bmatrix} \succ 0, \tag{47}$$

$$Q^i(\varepsilon) = \begin{bmatrix} Q_1^i(\varepsilon) & Q_2^i(\varepsilon) \\ Q_2^i(\varepsilon)' & Q_3^i(\varepsilon) \end{bmatrix} \succ 0, \tag{48}$$

avec

$$P_1(\varepsilon) = P_f + \varepsilon P_2 P_s^{-1} P_2', \quad P_2(\varepsilon) = \varepsilon P_2 = -\varepsilon \sum_{h=1}^{N} M_{11}^{h\,-1} M_{12}^h P_s, \quad P_3(\varepsilon) = \varepsilon P_s, \tag{49}$$

$$Q_1^i(\varepsilon) = \varepsilon^{-1} Q_f^i, \quad Q_2^i(\varepsilon) = -M_{11}^i Y^i + P_f {M_{21}^i}', \quad Q_3^i(\varepsilon) = \varepsilon(Q_s^i - M_{21}^i Y^i - Y^{i\prime} {M_{21}^i}') \tag{50}$$

et

$$Y^i = -\sum_{h=1, h\neq i}^{N} {M_{11}^h}^{-1} M_{12}^h P_s. \tag{51}$$

Substituant (37) et (47)-(48) dans (43), nous obtenons:

$$\begin{bmatrix} X_1^i(\varepsilon) & X_2^i(\varepsilon) \\ X_2^i(\varepsilon)' & X_3^i(\varepsilon) \end{bmatrix} \prec 0 \tag{52}$$

avec

$$X_1^i(\varepsilon) = \varepsilon^{-1}(M_{11}^i P_1(\varepsilon) + P_1(\varepsilon){M_{11}^i}' + M_{12}^i P_2(\varepsilon)' + P_2(\varepsilon){M_{12}^i}' + Q_1^i(\varepsilon)),$$

$$X_2^i(\varepsilon) = \varepsilon^{-1} M_{11}^i P_2(\varepsilon) + \varepsilon^{-1} M_{12}^i P_3(\varepsilon) + P_1(\varepsilon){M_{21}^i}' + P_2(\varepsilon)' {M_{22}^i}' + Q_2^i(\varepsilon),$$

$$X_3^i(\varepsilon) = M_{22}^i P_3(\varepsilon) + P_3(\varepsilon){M_{22}^i}' + M_{21}^i P_2(\varepsilon) + P_2(\varepsilon)' {M_{21}^i}' + Q_3(\varepsilon).$$

Remplaçant les valeurs de $P(\varepsilon)$, $Q^i(\varepsilon)$ et les équations (41), (49)-(51), nous obtenons:

$$X_1^i(\varepsilon) = \varepsilon^{-1}(M_{11}^i P_f + P_f {M_{11}^i}' + Q_f^i + O(\varepsilon)) = \varepsilon^{-1}(X_f^i + O(\varepsilon)),$$

$$X_2^i(\varepsilon) = \varepsilon(P_2' {M_{22}^i}' + O(\varepsilon)) = \varepsilon(X_2^i + O(\varepsilon)),$$

$$X_3^i(\varepsilon) = \varepsilon(M_s^i P_s + P_s {M_s^i}' + Q_s^i + O(\varepsilon)) = \varepsilon(X_s^i + O(\varepsilon)).$$

Nous pouvons réécrire (52) comme

$$\begin{bmatrix} \varepsilon^{-1}(X_f^i + O(\varepsilon)) & \varepsilon(X_2^i + O(\varepsilon)) \\ (\star)' & \varepsilon(X_s^i + O(\varepsilon)) \end{bmatrix} \prec 0.$$

Si les conditions (44) et (45) sont satisfaites, alors $X_f^i \prec 0$ et $X_s^i \prec 0$, ce qui revient à dire qu'il existe un scalaire $\varepsilon_{max} > 0$ tel que $X_s^i + O(\varepsilon) \prec 0$ et $X_f^i - \varepsilon^2 X_2^i {X_s^i}^{-1} X_2^{i\prime} + O(\varepsilon) \prec 0$, $\forall\, i \in \mathcal{I}$ et $\forall\, \varepsilon \in (0, \varepsilon_{max}]$. Par conséquent, en utilisant le complément de Schur, la condition LMI (43) est vérifiée [BGFB94]. Puisque $P_f \succ 0$ et $P_s \succ 0$, l'inégalité (47) est vérifiée. De plus, (48) peut être réécrit comme

$$Q^i(\varepsilon) = \begin{bmatrix} \varepsilon^{-1} I_{n_1} & 0 \\ 0 & I_{n_2} \end{bmatrix} \begin{bmatrix} Q_f^i & -(M_{11}^i Y^i + P_f {M_{21}^i}') \\ (\star)' & Q_s^i - M_{21}^i Y^i - Y^{i\prime} {M_{21}^i}' \end{bmatrix} \begin{bmatrix} I_{n_1} & 0 \\ 0 & \varepsilon I_{n_2} \end{bmatrix} \succ 0$$

qui est non négative définie à cause de (46), ce qui conclut la preuve.

Remarque 1 *Le Théorème 2 donne des conditions de stabilité indépendantes pour les sous systèmes rapide et lent (44) et (45), respectivement, et la condition de couplage (46). Cet ensemble de conditions permet de vérifier les conditions de stabilité données dans le Lemme 1, pour chaque $\varepsilon \in (0, \varepsilon_{max}]$. $P(\varepsilon)$ et $Q^i(\varepsilon)$ sont définies dans les inégalités (47) et (48), pour chaque $i \in \mathcal{I}$.*

Remarque 2 *Nous pouvons obtenir une évaluation de la valeur de ε_{max} en résolvant le problème d'optimisation suivant:*

$$\varepsilon_{max} = max\ \varepsilon > 0 \tag{53}$$

$$sous\ \ M^i(\varepsilon)P(\varepsilon) + P(\varepsilon)M^i(\varepsilon)' + Q^i(\varepsilon) \prec 0,\ \ i \in \mathcal{I},$$

où les matrices $M^i(\varepsilon)$, $P(\varepsilon)$, et $Q^i(\varepsilon)$ ont été définies dans les équations (55) et (47)-(48), respectivement. De plus, les valeurs de P_f, Q^i_f, P_s et Q^i_s peuvent être calculées par le Théorème 2, pour chaque $i \in \mathcal{I}$.

2.4 Synthèse du correcteur

Considérons le système à commutation avec perturbations singulières

$$\dot{x}(t) = M^{\sigma(t)}(\varepsilon)x(t) + N^{\sigma(t)}(\varepsilon)u(t), \tag{54}$$

où $u(t) \in \mathbb{R}^r$ est la commande, $\{(M^i(\varepsilon), N^i(\varepsilon)) : i \in \mathcal{I}\}$ est une famille de matrices et

$$\begin{aligned} M^i(\varepsilon) &= \begin{bmatrix} \varepsilon^{-1}I_{n_1} & 0 \\ 0 & I_{n_2} \end{bmatrix} \begin{bmatrix} M^i_{11} & M^i_{12} \\ M^i_{21} & M^i_{22} \end{bmatrix}, \\ N^i(\varepsilon) &= \begin{bmatrix} \varepsilon^{-1}I_{n_1} & 0 \\ 0 & I_{n_2} \end{bmatrix} \begin{bmatrix} N^i_1 \\ N^i_2 \end{bmatrix}, \end{aligned} \tag{55}$$

pour chaque $i \in \mathcal{I}$. Nous définissons les matrices

$$\begin{aligned} M^i_s &= M^i_{22} - M^i_{21}{M^i_{11}}^{-1}M^i_{12} \\ N^i_s &= N^i_2 - M^i_{21}{M^i_{11}}^{-1}N^i_1. \end{aligned} \tag{56}$$

Les paires (M^i_s, N^i_s) er (M^i_{11}, N^i_1) sont supposées être stabilisable pour chaque $i \in \mathcal{I}$, ce qui signifie que chaque valeur propre de M^i_s ou M^i_{11} qui est dans le demi-plan complexe gauche est contrôlable. Le but de cette section est de synthétiser une commande par retour d'état

$$u(t) = K^{\sigma(t)}(\varepsilon)x(t) \tag{57}$$

qui stabilise le système en boucle fermée (54) quelle que soit la loi de commutation.

Lemme 2 *S'il existe des matrices $P(\varepsilon) = P(\varepsilon)' \succ 0$, $Q^i(\varepsilon) = Q^i(\varepsilon)' \succ 0$ et $Z^i(\varepsilon)$ de dimension appropriée telles que les LMIs*

$$\begin{aligned} &M^i(\varepsilon)P(\varepsilon) + P(\varepsilon)M^i(\varepsilon)' + N^i(\varepsilon)Z^i(\varepsilon) + \\ &Z^i(\varepsilon)'N^i(\varepsilon)' + Q^i(\varepsilon) \prec 0 \end{aligned} \tag{58}$$

sont vérifiés $\forall\, i \in \mathcal{I}$, alors la loi de contrôle (57) stabilise asymptotiquement le système à commutation (54) quelle que soit la loi de commutation, avec $K^i(\varepsilon) = Z^i(\varepsilon)P(\varepsilon)^{-1}$.

De la même manière que pour l'analyse de stabilité, les petites valeurs du scalaire ε peuvent engendrer un mauvais conditionnement de la contrainte (58) et rendre difficile le calcul des gains $K^i(\varepsilon)$. Le théorème suivant fournit des conditions basées sur des inégalités matricielles linéaires qui vérifient la stabilité du système (54), indépendamment de ε, quelle que soit la loi de commutation.

Théorème 3 *S'il existe des matrices* $P_f = P_f{}' \succ 0$, $Q_f^i = Q_f^{i\,\prime} \succ 0$, Z_f^i, $P_s = P_s{}' \succ 0$, $Q_s^i = Q_s^{i\,\prime} \succ 0$ *et* Z_s^i *de dimension appropriée telles que les LMIs*

$$M_{11}^i P_f + P_f M_{11}^{i\,\prime} + N_1^i Z_f^i + Z_f^{i\,\prime} N_1^{i\prime} + Q_f^i \prec 0, \tag{59}$$

$$M_s^i P_s + P_s M_s^{i\prime} + N_s^i Z_s^i + Z_s^{i\prime} N_s^{i\prime} + Q_s^i \prec 0, \tag{60}$$

$$\begin{bmatrix} Q_f^i & F^i & N_1^i Z_f^i & 0 \\ (\star)' & G^i & Y^{i\prime} & N_2^i Z_f^i + Y^{i\prime} \\ (\star)' & (\star)' & P_f & 0 \\ (\star)' & (\star)' & (\star)' & P_f \end{bmatrix} \succ 0 \tag{61}$$

sont vérifiées $\forall\, i \in \mathcal{I}$, *avec* $Y^i = -\sum_{h=1, h\neq i}^{N} M_{11}^{h\,-1}(M_{12}^h P_s + N_1^h Z_s^h)$, $F^i = -(M_{11}^i Y^i + P_f M_{21}^{i\,\prime} + Z_f^{i\,\prime} N_2^{i\prime})$ *et* $G^i = Q_s^i - M_{21}^i Y^i - Y^{i\prime} M_{21}^{i\,\prime}$, *alors il existe un scalaire* $\varepsilon_{max} > 0$ *tel que le correcteur à retour d'état*

$$K^i = \begin{bmatrix} K_f^i & K_s^i + K_f^i M_{11}^{i\,-1}(M_{12}^i + N_1^i K_s^i) \end{bmatrix}, \tag{62}$$

avec $K_f^i = Z_f^i P_f^{-1}$ *et* $K_s^i = Z_s^i P_s^{-1}$, *stabilise asymptotiquement le système à commutation en boucle fermée (54),* $\forall\, \varepsilon \in (0, \varepsilon_{max}]$ *et quelle que soit la loi de commutation.*

Preuve 3 *Considérons*

$$P(\varepsilon) = \begin{bmatrix} P_1(\varepsilon) & P_2(\varepsilon) \\ P_2(\varepsilon)' & P_3(\varepsilon) \end{bmatrix} \succ 0, \tag{63}$$

$$Z^i(\varepsilon) = \begin{bmatrix} Z_1^i(\varepsilon) & Z_2^i(\varepsilon) \end{bmatrix}, \tag{64}$$

$$Q^i(\varepsilon) = \begin{bmatrix} Q_1^i(\varepsilon) & Q_2^i(\varepsilon) \\ Q_2^i(\varepsilon)' & Q_3^i(\varepsilon) \end{bmatrix} \succ 0, \tag{65}$$

avec

$$P_1(\varepsilon) = P_f + \varepsilon P_2 P_s^{-1} P_2', \tag{66}$$

$$P_2(\varepsilon) = \varepsilon P_2 = -\varepsilon \sum_{h=1}^{N} {M_{11}^h}^{-1}(M_{12}^h P_s + N_1^h Z_s^h), \tag{67}$$

$$P_3(\varepsilon) = \varepsilon P_s, \tag{68}$$

$$Z_1^i(\varepsilon) = Z_f^i + \varepsilon Z_s^i P_s^{-1} P_2', \tag{69}$$

$$Z_2^i(\varepsilon) = \varepsilon(Z_s^i + Z_f^i P_f^{-1} Y^i), \tag{70}$$

$$Q_1^i(\varepsilon) = \varepsilon^{-1} Q_f^i, \tag{71}$$

$$Q_2^i(\varepsilon) = -((M_{11}^i + N_1^i Z_f^i P_f^{-1})Y^i + P_f {M_{21}^i}' + Z_f^{i'} N_2^{i'}), \tag{72}$$

$$Q_3^i(\varepsilon) = \varepsilon(Q_s^i - (M_{21}^i + N_2^i Z_f^i P_f^{-1})Y^i - Y^{i'}({M_{21}^i}' + P_f^{-1} Z_f^{i'} N_2^{i'})) \tag{73}$$

and

$$Y^i = -\sum_{h=1, h\neq i}^{N} {M_{11}^h}^{-1}(M_{12}^h P_s + N_1^h Z_s^h). \tag{74}$$

Substituant (55) et (63)-(65) dans (58), nous obtenons:

$$\begin{bmatrix} X_1^i(\varepsilon) & X_2^i(\varepsilon) \\ X_2^i(\varepsilon)' & X_3^i(\varepsilon) \end{bmatrix} \prec 0 \tag{75}$$

avec

$$\begin{aligned} X_1^i(\varepsilon) =& \varepsilon^{-1}(M_{11}^i P_1(\varepsilon) + P_1(\varepsilon){M_{11}^i}' + M_{12}^i P_2(\varepsilon)' + P_2(\varepsilon){M_{12}^i}' + \\ & N_1^i Z_1^i(\varepsilon) + Z_1^i(\varepsilon)' N_1^{i'} + Q_1^i(\varepsilon)), \end{aligned} \tag{76}$$

$$\begin{aligned} X_2^i(\varepsilon) =& \varepsilon^{-1} M_{11}^i P_2(\varepsilon) + \varepsilon^{-1} M_{12}^i P_3(\varepsilon) + P_1(\varepsilon){M_{21}^i}' + P_2(\varepsilon)' {M_{22}^i}' + \\ & \varepsilon^{-1} N_1^i Z_2^i(\varepsilon) + Z_1^i(\varepsilon)' N_2^{i'} + Q_2^i(\varepsilon), \end{aligned} \tag{77}$$

$$\begin{aligned} X_3^i(\varepsilon) =& M_{22}^i P_3(\varepsilon) + P_3(\varepsilon){M_{22}^i}' + M_{21}^i P_2(\varepsilon) + P_2(\varepsilon)' {M_{21}^i}' + \\ & N_2^i Z_2^i(\varepsilon) + Z_2^i(\varepsilon)' N_2^{i'} + Q_3(\varepsilon). \end{aligned} \tag{78}$$

Remplaçant les valeurs de $P(\varepsilon), Z^i(\varepsilon), Q^i(\varepsilon)$ et les équations (56), (66)-(74), nous obtenons les équations

$$X_1^i(\varepsilon) = \varepsilon^{-1}(M_{11}^i P_f + P_f {M_{11}^i}' + N_1^i Z_f^i + Z_f^{i'} N_1^{i'} + Q_f^i + O(\varepsilon)) = \varepsilon^{-1}(X_f^i + O(\varepsilon)), \tag{79}$$

$$X_2^i(\varepsilon) = \varepsilon(P_2' {M_{22}^i}' + O(\varepsilon)) = \varepsilon(X_2^i + O(\varepsilon)), \tag{80}$$

$$X_3^i(\varepsilon) = \varepsilon(M_s^i P_s + P_s {M_s^i}' + N_s^i Z_s^i + Z_s^{i'} N_s^{i'} + Q_s^i + O(\varepsilon)) = \varepsilon(X_s^i + O(\varepsilon)). \tag{81}$$

Nous pouvons réécrire (75) comme

$$\begin{bmatrix} \varepsilon^{-1}(X_f^i + O(\varepsilon)) & \varepsilon(X_2^i + O(\varepsilon)) \\ (\star)' & \varepsilon(X_s^i + O(\varepsilon)) \end{bmatrix} \prec 0. \tag{82}$$

Pour hypothèse, nous avons $X_f^i \prec 0$ et $X_s^i \prec 0$, ce qu'équivaut à dire qu'il existe un scalaire $\varepsilon_{max} > 0$ tel que $X_s^i + O(\varepsilon) \prec 0$ et $X_f^i - \varepsilon^2 X_2^i {X_s^i}^{-1} {X_2^i}' + O(\varepsilon) \prec 0$, $\forall\, i \in \mathcal{I}$ et $\forall\, \varepsilon \in (0, \varepsilon_{max}]$. Par conséquent, en utilisant le complément de Schur, l a condition LMI (58) est vérifiée. Puisque $P_f \succ 0$ et $P_s \succ 0$, l'inégalité (63) est vérifiée. De plus, en substituant les équations (71)-(73) dans (65), nous obtenons l'inégalité

$$\begin{aligned} Q^i(\varepsilon) = &\begin{bmatrix} \varepsilon^{-1} I_{n_1} & 0 \\ 0 & I_{n_2} \end{bmatrix} \times \\ &\begin{bmatrix} Q_f^i & -((M_{11}^i + N_1^i Z_f^i P_f^{-1}) Y^i + P_f {M_{21}^i}' + Z_f^{i'} N_2^{i'}) \\ (\star)' & Q_s^i - (M_{21}^i + N_2^i Z_f^i P_f^{-1}) Y^i - Y^{i'} ({M_{21}^i}' + P_f^{-1} Z_f^{i'} N_2^{i'}) \end{bmatrix} \times \\ &\begin{bmatrix} I_{n_1} & 0 \\ 0 & \varepsilon I_{n_2} \end{bmatrix} \succ 0 \end{aligned} \tag{83}$$

qui, en utilisant le complément de Schur, est vérifiée si et seulement si l'inégalité

$$\begin{bmatrix} Q_f^i + N_1^i Z_f^i P_f^{-1} {Z_f^i}' {N_1^i}' & H^i & N_1^i Z_f^i & 0 \\ (\star)' & L^i & Y^{i'} & N_2^i Z_f^i + Y^{i'} \\ (\star)' & (\star)' & P_f & 0 \\ (\star)' & (\star)' & (\star)' & P_f \end{bmatrix} \succ 0 \tag{84}$$

tient, avec $H^i = -(M_{11}^i Y^i + P_f {M_{21}^i}' + Z_f^{i'} N_2^{i'})$ et $L^i = Q_s^i - M_{21}^i Y^i - Y^{i'} {M_{21}^i}' + N_2^i Z_f^i P_f^{-1} {Z_f^i}' {N_2^i}' + Y^{i'} P_f^{-1} Y^i$. (61) est non négative définie, ce qui implique que la contrainte (84) est vérifiée $\forall\, i \in \mathcal{I}$.

Afin de calculer le gain K^i, considérons

$$u_s(t) = K_s^i x_s(t) = Z_s^i P_s^{-1} x_s(t) \tag{85}$$

et

$$u_f(t) = K_f^i x_f(t) = Z_f^i P_f^{-1} x_f(t). \tag{86}$$

Le correcteur composé est

$$u_c(t) = u_s(t) + u_f(t) = K_s^i x_s(t) + K_f^i x_f(t). \tag{87}$$

Par $x_s(t) = x_2(t)$ et $x_f(t) = x_1(t) + {M_{11}^i}^{-1}(M_{12}^i x_s(t) + N_1^i u_s(t)) = x_1(t) + {M_{11}^i}^{-1}(M_{12}^i + N_1^i K_s^i) x_s(t)$, nous obtenons

$$u_c(t) = Z_s^i P_s^{-1} x_2(t) + Z_f^i P_f^{-1} x_1(t) + Z_f^i P_f^{-1} {M_{11}^i}^{-1} (M_{12}^i + N_1^i Z_s^i P_s^{-1}) x_2(t). \tag{88}$$

Lorsque $\varepsilon \to 0$, substituant (63) et (64) dans $K^i(\varepsilon) = Z^i(\varepsilon) P(\varepsilon)^{-1}$ et appliquant la formule d'inversion des matrices par bloc, nous trouvons (88), qui conclut la preuve.

Remarque 3 *Les conditions basées sur des inégalités matricielles linéaires du Théorème 3 avec $Z_f^i = 0$, $i \in \mathcal{I}$, nous donnent la loi de contrôle réduite*

$$u(t) = \begin{bmatrix} 0 & K_s^{\sigma(t)} \end{bmatrix} \begin{bmatrix} x_1(t) \\ x_2(t) \end{bmatrix}, \tag{89}$$

qui stabilise asymptotiquement le système à commutation (54) quelle que soit la valeur de $\varepsilon \in (0, \varepsilon_{max}]$ et chaque loi de commutation. Dans ce cas, l'inégalité (59) implique que le sous système rapide doit être stable asymptotiquement en boucle ouverte.
5

2.5 Exemple numérique

Considérons le système à commutation singulièrement perturbé (54), avec $\mathcal{I} = \{1, 2\}$, $\varepsilon = 0.005$ et

$$\begin{aligned}
M_{11}^1 &= \begin{bmatrix} 0 & 1 \\ -1 & -2 \end{bmatrix}, M_{12}^1 = \begin{bmatrix} 0 & 0 \\ 1.5 & 0 \end{bmatrix}, \\
M_{21}^1 &= \begin{bmatrix} 0 & 0 \\ -0.6 & -0.5 \end{bmatrix}, M_{22}^1 = \begin{bmatrix} 0 & 1 \\ 2.1 & 0 \end{bmatrix}, \\
N_1^1 &= \begin{bmatrix} 0 \\ -1 \end{bmatrix}, N_2^1 = \begin{bmatrix} 0 \\ 0 \end{bmatrix}, \\
M_{11}^2 &= \begin{bmatrix} 0 & 1 \\ -3 & -5 \end{bmatrix}, M_{12}^2 = \begin{bmatrix} 0 & 0 \\ 0 & 0 \end{bmatrix}, \\
M_{21}^2 &= \begin{bmatrix} 0 & 0 \\ -0.3 & -0.2 \end{bmatrix}, M_{22}^2 = \begin{bmatrix} 0 & 0.7 \\ 0 & 0 \end{bmatrix}, \\
N_1^2 &= \begin{bmatrix} 0 \\ -1 \end{bmatrix}, N_2^2 = \begin{bmatrix} 0 \\ 0 \end{bmatrix}.
\end{aligned}$$

Le sous système 1 est instable en boucle ouverte et le sous système 2 est carac-

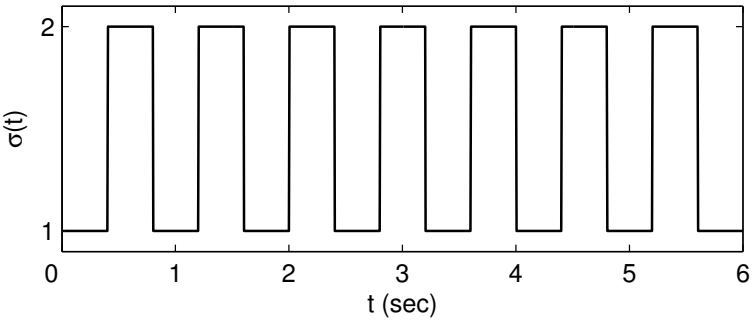

Figure 14: Loi de commutation $\sigma(t)$

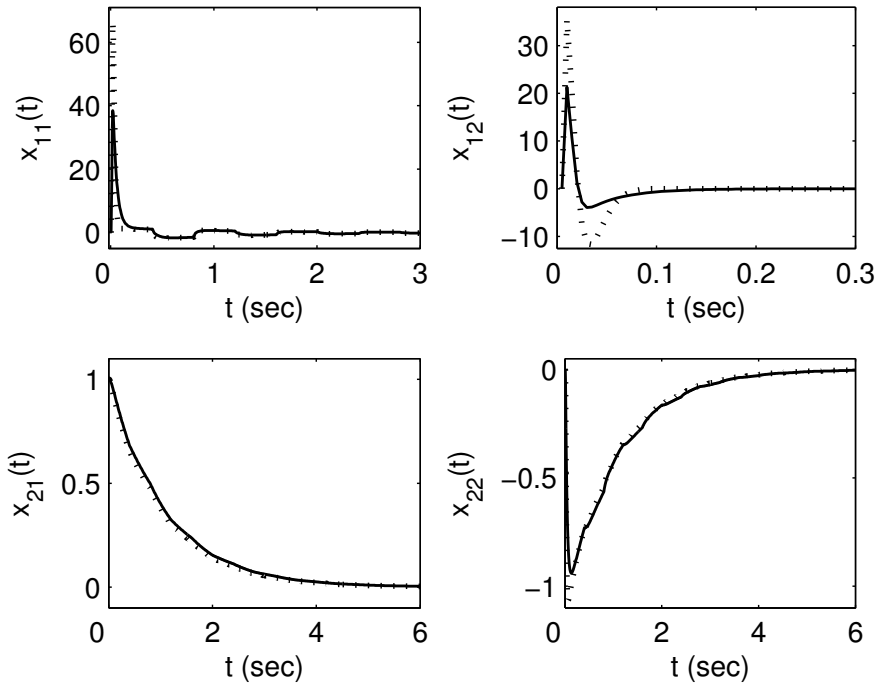

Figure 15: Évolution des variables d'état avec le correcteur complet (trait plein) et le correcteur réduit (trait pointillé)

térisé par une matrice d'état qui a des valeurs propres nulles. En appliquant le Théorème 3, nous obtenons les correcteurs suivants:

$$K^1 = \begin{bmatrix} 0.4040 & 0.1511 & -65.3601 & -60.3074 \end{bmatrix},$$
$$K^2 = \begin{bmatrix} -0.4110 & -0.5931 & -147.6057 & -137.0206 \end{bmatrix}.$$

Puisque M_{11}^1 et M_{11}^2 sont Hurwitz, nous pouvons aussi proposer une loi de contrôle réduite:

$$K_r^1 = \begin{bmatrix} 0 & 0 & -99.0779 & -88.5710 \end{bmatrix},$$
$$K_r^2 = \begin{bmatrix} 0 & 0 & -347.0992 & -310.4213 \end{bmatrix}.$$

Considérons la loi de commutation donnée sur la Fig. 14 et les conditions initiales $x(0) = \begin{bmatrix} 0 & 0 & 1 & 0 \end{bmatrix}'$. L'évolution du système en boucle fermée est donnée sur la Fig. 15, avec $x(t) = \begin{bmatrix} x_{11}(t) & x_{12}(t) & x_{21}(t) & x_{22}(t) \end{bmatrix}'$. Le trait plein représente l'évolution des variables d'état en utilisant les correcteurs complets K^1 et K^2 tandis que le trait pointillé représsente l'évolution des variables d'état en utilisant les correcteurs réduits K_r^1 et K_r^2. Sur la Fig. 16, nous montrons la commande.

2.6 Conclusion

Dans cette section, nous avons considéré le problème de stabilité des systèmes à commutation à deux échelles de temps dans le temps continu. Nous avons

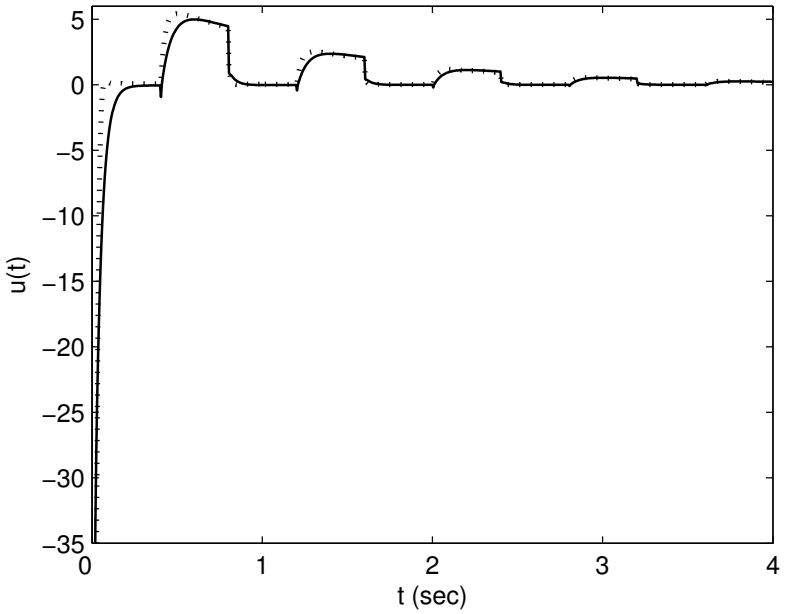

Figure 16: Évolution de la commande avec le correcteur complet (trait plein) et le correcteur réduit (trait pointillé)

montré que la stabilité asymptotique des sous systèmes à commutation lent et rapide ne représente pas une condition suffisante pour la stabilité asymptotique du système à commutation à deux échelles de temps lorsque la loi de commutation est arbitraire. Une condition de couplage entre la dynamique lente et rapide doit être considérée. Ensuite, nous avons proposé des conditions suffisantes, formulées sous la forme d'inégalités matricielles linéaires, qui permettent de vérifier la stabilité asymptotique en boucle ouverte et de synthétiser des correcteurs stabilisants pour cette classe de systèmes.

3 Une approche pour maîtriser les discontinuités de la commande

3.1 Introduction

La majorité des systèmes physiques sont non linéaires. Dans le cadre des systèmes de contrôle il est assez fréquent d'utiliser différents correcteurs linéaires pour commander le même système non linéaire. Cependant, quand on commute les correcteurs, un transitoire s'instaure à cause de la discontinuité sur la commande, ce qui peut dégrader les performances du système. Ceci, ajouté au fait que les systèmes industriels sont souvent caractérisés par des saturations à cause des limitations liées aux actionneurs, peut dégrader les performances voire déstabiliser le système en boucle fermée.

Les méthodes qui traitent ce problème sont communément regroupées sous le vocable "bumpless transfer methods". Les plus populaires sont données dans [Han88], [KCMN94] et [EP98]. Plus récemment, des solutions alternatives ont été proposées par [TW00]et [ZT05]. Ces méthodes ont aussi été testées dans des cas pratiques [ZLW+04], [TAB+06].

La stratégie utilisée dans la plupart de ces méthodes consiste à initialiser tous les correcteurs hors-ligne afin de minimiser la discontinuité dans la commande à l'instant de commutation. Cette méthode est efficace si le temps de séjour entre deux commutations est relativement grand. Dans le cas des systèmes à commutation [Lib03], le temps de séjour peut être trés court, ce qui remet en cause l'application de ces méthodes. Une approche différente consiste à agir sur la commande après la commutation. C'est le cas par exemple du travail présenté dans [DW06], où on utilise une approche LMI [BGFB94] pour minimiser le saut sur la commande dans le cas des systèmes linéaires à temps continu à paramètres variants (LPV). Ici, pour les systèmes linéaires à commutation en temps discret, on propose d'utiliser une méthode d'optimisation linéaire quadratique [MHD+08], [MHD+09].

3.2 Position du problème

Nous considérons un système à commutation en temps discret

$$\begin{cases} x(k+1) = A^{\sigma(k)}x(k) + B^{\sigma(k)}u(k) \\ y(k) = C^{\sigma(k)}x(k) \end{cases} \tag{90}$$

où $x(k) \in \mathbb{R}^n$ est l'état du système, qui est accessible à la mesure, $u(k) \in \mathbb{R}^r$ la commande, $y(k) \in \mathbb{R}^m$ le signal de sortie et $\sigma : \mathbb{Z}^+ \to \mathcal{I} = \{1, ..., N\}$ est la loi de commutation, qui est supposée inconnue a priori mais accessible en temps réel, pour tous $k \in \mathbb{Z}^+$. De plus, $\{(A^i, B^i, C^i) : i \in \mathcal{I}\}$ est une famille de matrices et la paire (A^i, B^i) est supposée contrôlable, pour chaque $i \in \mathcal{I}$. Nous considérons un correcteur par retour d'état

$$u(k) = K^{\sigma(k)}x(k), \tag{91}$$

qui stabilise asymptotiquement le système en boucle fermée (90)-(91) pour une loi de commutation arbitraire. Nous définissons aussi l'intervalle de temps minimal $\Delta^i \in \mathbb{Z}^+$ dans lequel le système reste dans le sous système i, qui est supposé être connu pour chaque $i \in \mathcal{I}$.

Lorsqu'une commutation se produit, la commutation du correcteur engendre une discontinuité sur la commande à appliquer, ceci implique un comportement transitoire et un fort risque de saturation. Une solution consiste à concevoir un correcteur supplémentaire qui soit activée à l'instant de commutation t_i, qui représente l'instant de commutation dans le i^{me} sous système, pour une période

de temps $\tau_i^M < \Delta^i$. Donc, pour chaque mode i, nous avons:

$$u(k) = \begin{cases} K^i x(k) + u^{bt,i}(k) & if \quad t_i \leq k < t_i + \tau_i^M \\ K^i x(k) & sinon, \end{cases} \tag{92}$$

où $u^{bt,i}(k) \in \mathbb{R}^r$ est la sortie du correcteur bumpless transfer, pour $k \in [t_i, t_i + \tau_i^M)$. Le système en boucle fermée (90)-(92) est représenté dans la Fig. 17.

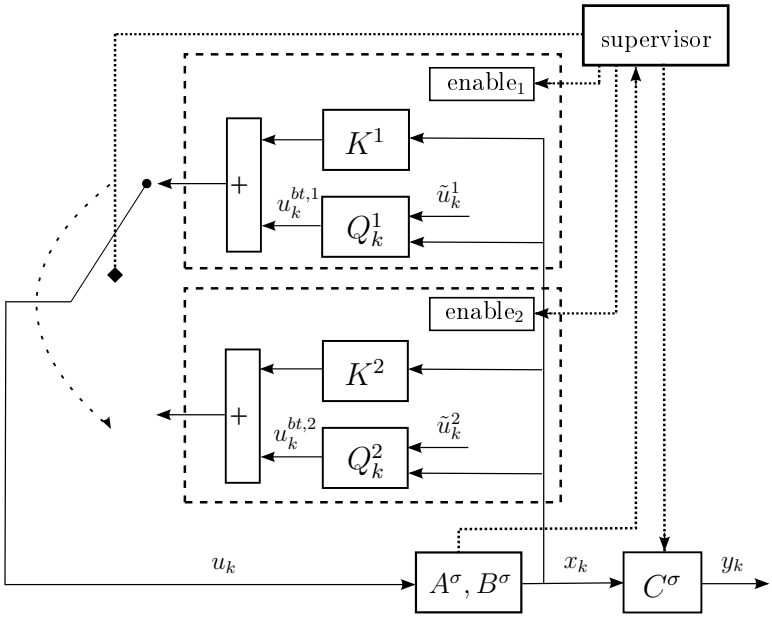

Figure 17: Système en boucle fermée avec $\mathcal{I} = \{1, 2\}$

La synthèse de la loi de contrôle bumpless $u^{bt,i}$, qui dépend du profil désiré pour la commande et des matrices d'état du système, sera présentée dans la section suivante. Pour des raisons de simplicité, on choisit une droite comme profil. Si l'on appelle t_i l'instant de commutation entre le sous système j et le sous système i, pour chaque $(j, i) \in \mathcal{I} \times \mathcal{I}$. on peut définir la commande désirée comme:

$$\tilde{u}^i(k) = \begin{cases} \tilde{u}^{i,0}(k) + (k - t_i + 1)p^i(k) & if \quad t_i \leq k < t_i + \tau_i^M \\ 0 & sinon, \end{cases} \tag{93}$$

où

$$\tilde{u}^{i,0}(k) = K^j x(t_i - 1) \tag{94}$$

est la valeur de la commande à l'instant avant la commutation et p^i détermine la pente du profil désiré:

$$p^i(k) = \frac{1}{\tau_i^M}(K^i x(t_i) - K^j x(t_i - 1)). \tag{95}$$

Nous obtenons une valeur de p^i qui dépend de la discontinuité de la commande (Fig. 18).

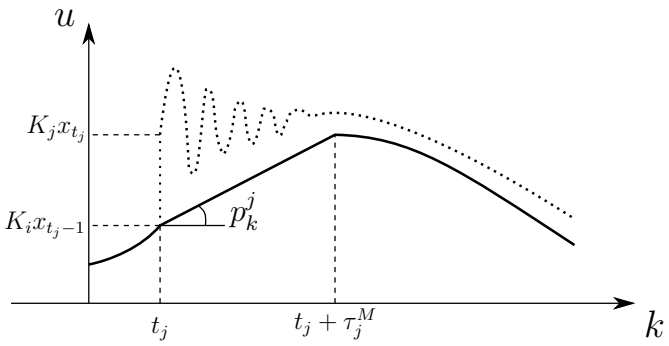

Figure 18: Évolution de la commande avec correcteur bumpless actif (trait continu) et inactif (trait pointillé)

3.3 Synthèse du correcteur bumpless transfer

Dans cette section, une méthode basée sur l'optimisation linéaire quadratique est utilisée pour synthétiser le correcteur bumpless transfer. Ce type d'approche a déjà été utilisée par [TW00], où on minimise la différence entre la sortie du correcteur en-ligne et ceux prévus hors-ligne avant la commutation, de façon à minimiser le transitoire dû au saut sur le signal de contrôle. Ici, on envisage le cas des systèmes à commutation où le temps de séjour n'est pas forcement grand et on propose d'agir directement après l'instant de commutation t_i. Pour chaque sous système $i \in \mathcal{I}$, la loi de contrôle bumpless est basée sur la minimisation de la fonction de coût quadratique suivante:

$$J^i = \phi^i(t_i + \tau_i^M) + \frac{1}{2} \sum_{k=t_i}^{t_i+\tau_i^M-1} [z^{u,i'}(k) W_u^i z^{u,i}(k) + z^{y,i'}(k) W_y^i z^{y,i}(k)], \tag{96}$$

with

$$z^{u,i}(k) = u(k) - \tilde{u}^i(k) \tag{97}$$

$$z^{y,i}(k) = y(k) - \tilde{y}^i(k) \tag{98}$$

$$\phi^i(t_i + \tau_i^M) = \frac{1}{2} z^{u,i'}(t_i + \tau_i^M) X^i z^{u,i}(t_i + \tau_i^M) \tag{99}$$

où $W_u^i \succ 0$, $W_y^i \succ 0$ et $X^i \succeq$ sont de matrices de poids. La commande désirée $\tilde{u}^i$ a été définie dans (93) tandis que le signal de sortie désiré est choisi $\tilde{y}^i = 0$ pour des raisons de simplicité. Le théorème suivant permet de calculer la commande $u^{bt,i}$ qui minimise la fonction de côut J_i, pour chaque $i \in \mathcal{I}$.

Théorème 4 *Étant donné le système à commutation en boucle fermée (90)-(92), l'instant initial t_i et l'instant final $t_i+\tau_i^M$, la loi de contrôle bumpless qui minimise*

la fonction de coût quadratique (96) est donnée par

$$u^{bt,i}(k) = Q^i(k) \begin{bmatrix} x(k) \\ \tilde{u}^i(k) \\ g^i(k+1) \end{bmatrix}, \tag{100}$$

avec

$$Q^i(k) = \begin{bmatrix} (\tilde{N}^i(k+1)\Pi^i(k+1)A^i - K^i)' \\ (I_r + \tilde{N}^i(k+1)\Pi^i(k+1)B^i)' \\ -\tilde{N}^{i'}(k+1) \end{bmatrix}' \tag{101}$$

and

$$\tilde{N}^i(k+1) = -{W_u^i}^{-1} B^{i'}(I - \Pi^i(k+1)\tilde{B}^i)^{-1}, \tag{102}$$

$\forall\, i \in \mathcal{I}$. *On peut calculer les valeurs de* Π^i *et* g^i *par les équations*

$$\Pi^i(k) = A^{i'}(I_n - \Pi^i(k+1)\tilde{B}^i)^{-1}\Pi^i(k+1)A^i + \tilde{C}^i \tag{103}$$

et

$$g^i(k) = A^{i'}(I_n - \Pi^i(k+1)\tilde{B}^i)^{-1}(g^i(k+1) - \Pi^i(k+1)B^i\tilde{u}^i(k)), \tag{104}$$

avec $\tilde{B}^i = -B^i{W_u^i})^{-1}B^{i'}$ *et* $\tilde{C}^i = C^{i'}W_y^iC^i$. *Les conditions aux limites sont données par:*

$$\Pi^i(t_i + \tau_i^M) = 0,\ g^i(t_i + \tau_i^M) = 0. \tag{105}$$

Remarque 4 *Il n'est pas toujours possible d'utiliser directement une approche à horizon fini, car il faut connaître les valeurs futures de* $\tilde{u}^i$ *pour résoudre l'équation (104). Néanmoins, dans notre cas, on est en mesure de calculer toutes les valeurs de* $\tilde{u}^i$ *sur l'horizon fini* $[t_i, t_i + \tau_M^i)$ *directement à partir des équations (93)-(95). Il suffit de connaître la valeur des vecteurs d'état* $x(t_i - 1)$ *and* $x(t_i)$, *qui est accessible à l'instant de commutation* t_i.

3.4 Exemple numérique

Dans cette section, nous synthétisons un correcteur bumpless pour un produit spécifique du laminoir d'Eisenhüttenstadt. Afin de réduire les sauts sur la commande u, nous pouvons appliquer la commande modifiée (92) pour une période de temps τ_i^M, pour $i \in \{2, 3, 4\}$. Puisque le système ne commute jamais vers le premier sous système, nous ne synthétisons pas de correcteur pour $i = 1$. Le signal $u^{bt,i}$ est calculé par le Théorème 4. Les équations (101) et (103) peuvent être résolues hors-line tandis que l'équation (104) peut être résolue à l'instant de commutation t_i, lorsque la valeur de $x(t_i - 1)$ est connue. La sortie mesurée y correspond au décentrement de bande, qui doit être minimisé. Donc, nous choisissons $\tilde{y} = 0$. Sur la Fig. 19, nous proposons un zoom de l'évolution de la

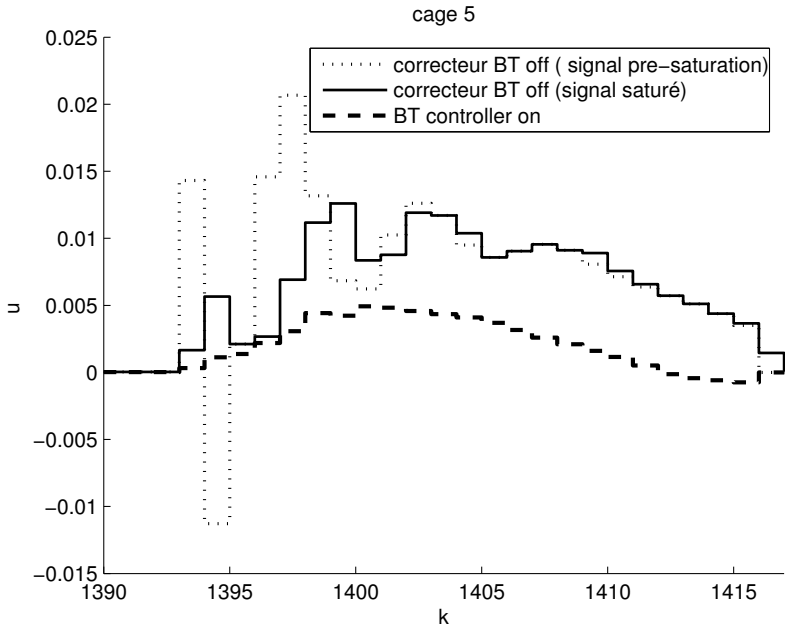

Figure 19: Évolution de la commande u

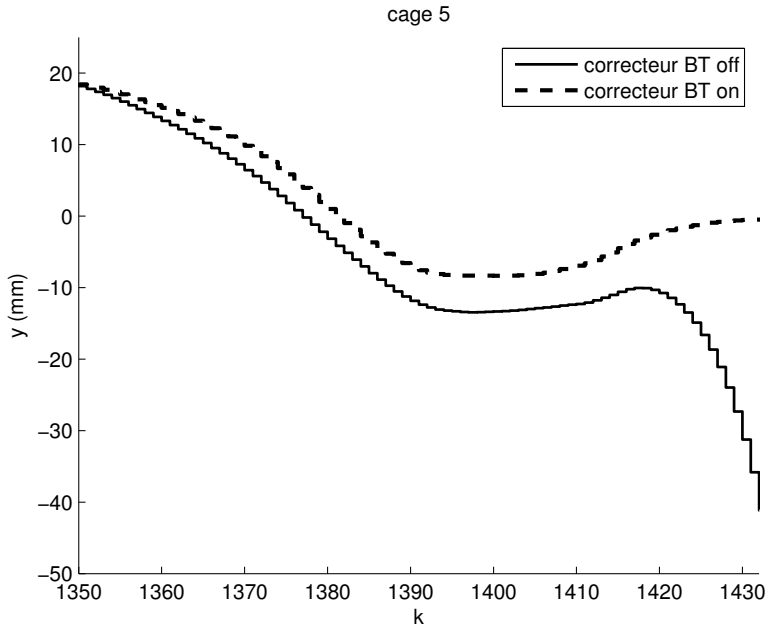

Figure 20: Évolution de la sortie mesurée output y

commande u dans la dernière cage. Le trait pointillé montre la commande calculée par la loi de contrôle (91), lorsque le correcteur bumpless n'est pas actif. Nous pouvons noter un saut assez élevé causé par la commutation à l'instant $k = 1392$, et le transitoire correspondant. Comme les actionneurs du laminoir

sont sujets à des saturations, la commande qui est réellement appliquée au système est le signal saturé donné par le trait continu. Dans ce cas, la stabilité n'est plus garantie. Finalement, le trait discontinu montre la commande calculée par la loi de contrôle (92), c'est-à-dire quand le correcteur bumpless est actif. Dans ce cas, la commande n'est pas sujette à des saturations. Sur la Fig. 20, nous proposons un zoom de l'évolution de la sortie mesurée y dans la dernière cage. Nous pouvons noter que le décentrement de bande a été réduit lorsque le correcteur bumpless est actif.

3.5 Conclusion

Dans cette section, nous avons présenté une méthode pour maîtriser les discontinuités de commande dans le cadre des systèmes à commutation en temps discret. Le correcteur bumpless transfer, qui permet de minimiser les discontinuités sur la commande, a été synthétisé en utilisant une méthode d'optimisation LQ. L'idée est de forcer le signal de contrôle à suivre un profil désiré. Une minimisation de la distance entre la sortie réelle et la sortie désirée est également proposée.

Conclusion générale

Dans ce chapitre, nous avons présenté un résumé du mémoire de thèse. Dans cette thèse, nous avons cherché de résoudre un certain nombre de problèmes qui apparaissent lorsque nous traitons des problèmes concrêts de contrôle: phénomènes à plusieurs échelles de temps, discontinuités de la commande lors du basculement d'un correcteur à un autre, nécessité de concevoir un nombre limité de correcteurs différents malgré une gamme très importante des produits traités. Pour illustrer concrètement les résultats obtenus, nous nous sommes appuyés sur un exemple industriel concret, le contrôle de guidage de bande durant le processus de laminage dans un laminoir à chaud. D'abord, nous avons proposé une solution au problème de commande optimale linéaire quadratique pour les systèmes linéaires à deux échelles de temps en temps discret. Nous avons montré que cette solution peut être étendue directement aux systèmes avec des incertitudes polytopiques. De plus, nous avons établi des conditions suffisantes, formulées sous la forme d'inégalités matricielles linéaires, qui permettent de vérifier la stabilité d'un système à commutation à deux échelles de temps et de synthétiser des correcteurs stabilisants. Nous avons aussi proposé dans ce travail une méthode pour minimiser les discontinuités sur la commande dans le cadre des systèmes à commutation. Dans le contexte du contrôle de guidage de bande pour un laminoir à chaud, nous ne pouvions pas négliger l'influence des paramètres incertains, qui sont dus principalement au fait que ce genre de système traite une gamme de produits très large. Par conséquent, dans la synthèse du correcteur, nous avons pris en compte ces variations en divisant l'ensemble des produits en plusieurs familles et en synthétisant un correcteur différent pour chaque famille de produits. Cette stratégie nous a permis d'atteindre le même niveau de performances pour la ma-

jorité des produits laminés. Les résultats expérimentaux obtenus pour le laminoir d'Eisenhüttenstadt prouvent l'efficacité de notre approche.

Chapter 1

Switched system modeling of hot strip mill

1.1 Introduction

In the steel production framework, the *steering control* denotes the strategies to guide a metal strip during the rolling process, which consists of crushing a metal strip between two rolls in inverse rotation to obtain a strip with constant and desired thickness [Tak01], [VFBO07]. Moreover, some geometrical, metallurgical and mechanical characteristics must be given to the rolled product. A *hot strip finishing mill* is the association of several stands in a line, where each stand is comprised of a set of rolls (Fig. 1.1). The lateral movement of the strip

Figure 1.1: A global view of hot strip mill

with respect to the mill axis, which is called *strip off-center* (Fig. 1.4), is the consequence of rolling asymmetries such as differential stand stretching, work rolls tilting, initial off-center, strip thickness profile or thermal differential profile. Strip off-center may decrease the quality of the product and damage the rolls, if the strip crashes against the side guides of the mill. Hence, this displacement must be reduced to improve process reliability and product quality.

To this aim, several steering control methods have been developed. In general, the strip off-center of each stand is considered as the differential force image of the same stand. Different approaches have been proposed to compute the stand tilt: PID controllers [MN80], [KT83], [KT86], [FFT92], [SP98] (for a hot strip reversing mill), optimal regulators [SS92], state feedback pole assignment [OH97], and sliding mode techniques [OMAH05]. Nevertheless, the law linking the differential force and the strip off-center is nonlinear, and each stand is coupled to the others by the traction of the strip. Thus, SISO approaches are subject to significant performance degradation. In order to overcome this problem, [DBI+08] proposed a multi variable LQ control design while [CRCF08] suggested a model predictive control approach. In metallurgy, MIMO strategies have already been used in the mill loopers regulation, which prevent abrupt tension variations that could compromise the product quality [BKG02], [CRF07], [YHF08], and in the strip shape control during the cold rolling process [GF82], [GP98], [PS08].

All the above solutions refer to a nominal framework. However, a mill treats thousands of different products and the design of a specific controller for each product would be difficult, in a practical application. Despite the robustness properties of the linear quadratic (LQ) control, the average controller presented by [DBI+08] cannot guarantee the same level of performances for the whole set of products. The objective of this chapter is to provide a general model of hot strip mill for robust control purposes. We will start by the nonlinear model established by *ArcelorMittal* researchers and tuned during experimental trials [DBI+08]. This model takes into account the coupling between the stands and the law linking the differential force and the strip off-center. Since the system is subject to small deviations around the operating point, a linear model has been drawn up. Moreover, the system has two time scale dynamics. The fast dynamics is stable and impossible to control from a practical point of view due to the actuators limitations. We will resort to the singular perturbation approach to obtain a reduced order linear model, which will depend on the mill parameters (e.g. roll radius, roll speed, roll force) and on the products characteristics (e.g. strip width, thickness, hardness, temperature), and then formulate the control design problem in the slow manifold [KKO86]. Furthermore, in the last phase of the rolling process, called *tail end phase*, the strip leaves the stands one after the other. Each time the strip leaves a stand, the system dynamics changes. In this phase, the crashes against the side-guides are more frequent and dangerous because the loss of traction due to the switchings makes the system unstable. This kind of behavior may be described recurring to the switched systems theory [Lib03], [SWM+07]. Finally, we obtain a two time scale switched linear model of the system that takes into account the changes on the system dynamics [MDI+09e], [MDIS09], and the

uncertainties related to the fact that a mill treats many different strips [MDI+ar], [MDI+09d], [MDI+09c].

1.2 Description of physical system

A hot strip mill (HSM) is made up of $n \in \{5, 6, 7\}$ stands. Each stand contains one set of rolls (composed of two work rolls and two support rolls, Fig. 1.2) and the strip in the inter-stand on the front. For each stand $g \in \mathcal{G} = \{1, ..., n\}$,

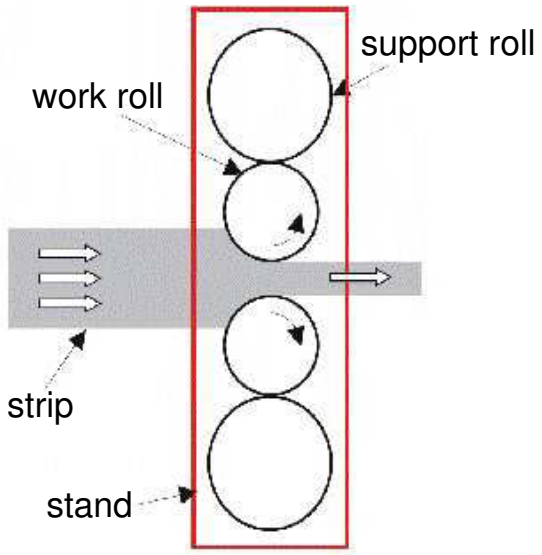

Figure 1.2: Stand lateral view

the main physical parameters are the strip width w_g, the strip thickness h_g, the back strip tension T_g^{am}, the front strip tension T_g^{av}, the screw interaxis length l_g^v, the interstand length l_g^0, the work roll length b_g, the work roll speed s_g and the Young's modulus E_g. Also the following constants are necessary to completely define a strip: c_g^{fh}, $c_g^{fT_{am}}$, $c_g^{fT_{av}}$, c_g^{gh}, $c_g^{gT_{am}}$, $c_g^{gT_{av}}$, K_g^h, K_g^f, K_g^l, P_g and g_g. The main asymmetries are the strip off-center $Z_g(t)$, the strip thickness profile (wedge) $\Delta h_g(t)$, the stand tilt $\Delta S_g(t)$, the differential stand stretch $\Delta K_g(t)$, the differential rolling force $\Delta P_g(t)$, the upstream differential of strip tension $\Delta T_g^{am}(t)$ and the downstream differential of strip tension $\Delta T_g^{av}(t)$, for all $t \geq 0$.

As long as the strip remains connected to the coilbox, which is the device used to coil the strips into the finishing train, the HSM model does not change (Fig. 1.3). Otherwise, in the last phase of the rolling process, the tail end phase, the strip leaves the stands, one after the other. Each time the strip leaves a stand the system dynamics changes. Hence, the HSM can be modeled as a switched system. The first subsystem (the strip has not yet left the first stand) is called n-stands subsystem. The subsystem active after the j^{th} switching, which occurs when the strip leaves the j^{th} stand, is called $(n-j)$-stands subsystem. The following main equations, which are relevant for $g > j$, govern the system dynamics:

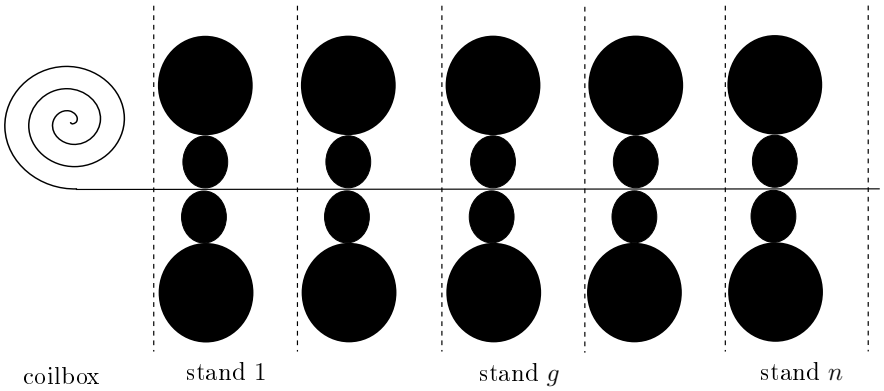

Figure 1.3: HSM lateral view

– The differential rolling force equation:

$$\Delta P_g(t) = c_{g-1}^{fh}\Delta h_{g-1}(t) + c_g^{fh}\Delta h_g(t) + c_g^{fT_{am}}\Delta T_g^{am}(t) + c_g^{fT_{av}}\Delta T_g^{av}(t); \quad (1.1)$$

– The exit stand wedge equation:

$$\begin{aligned}\Delta h_g(t) = &\left(\tfrac{w_g}{(l_g^v)^2 K_g^h} + \tfrac{6w_g}{b_g^2 K_g^f}\right)\left(\Delta P_g(t) + 2P_g\right) Z_g(t) + \\ &\frac{1}{K_g^l}\Delta P_g(t) + \frac{w_g}{l_g^v}\Delta S_g(t) - \frac{w_g P_g}{l_g^v (K_g^h)^2}\Delta K_g(t);\end{aligned} \quad (1.2)$$

– The angle α_g between the strip and the mill axis equation:

$$\begin{aligned}\dot{\alpha}_g(t) = &\frac{s_g}{w_g}\left(\tfrac{c_g^{gh}}{1+g_g} + \tfrac{1}{h_g}\right)\Delta h_g(t) + \frac{s_g}{w_g}\left(\tfrac{c_{g-1}^{gh}}{1+g_g} - \tfrac{1}{h_{g-1}}\right)\Delta h_{g-1}(t) + \\ &\frac{s_g}{w_g}\frac{c_g^{gT_{av}}}{(1+g_g)}\Delta T_g^{av}(t) + \frac{s_g}{w_g}\frac{c_g^{gT_{am}}}{(1+g_g)}\Delta T_g^{am}(t);\end{aligned} \quad (1.3)$$

– The strip off-center equation:

$$\dot{Z}_g(t) = s_g\,\alpha_g(t); \quad (1.4)$$

Moreover, for $g > j+1$ we have:

– The upstream differential of strip tension equation:

$$\begin{aligned}\Delta T_g^{am}(t) = &3\left(\tfrac{w_g E_g}{(l_g^0)^2} + \tfrac{T_g^{am}}{w_g}\right)\left(Z_g(t) - Z_{g-1}(t)\right) + \\ &\frac{w_g E_g}{l_g^0}\left(2\alpha_g(t) - \alpha_{g-1}(t)\right) + 3\frac{l_g^0 T_g^{am}}{w_g}\alpha_g(t);\end{aligned} \quad (1.5)$$

– The coupling between two successive stand equations:

$$\Delta T_{g-1}^{av}(t) = -\Delta T_g^{am}(t); \quad (1.6)$$

For the last two equations, there exists an exception. When the n-stands subsystem is on, the equations (1.5) and (1.6) hold for any stand $g \in \mathcal{G}$. In this case, the upstream differential of strip tension in the first stand ΔT_1^{am} can take two different values. It corresponds to the downstream tension of the coilbox $\Delta T_1^{am}(t) = -\Delta T_0^{av}(t)$ when the strip is connected to the coilbox (most of the time), and to zero after the strip left the coilbox. This last phase with $\Delta T_1^{am}(t) = 0$ and $\Delta T_2^{am}(t) \neq 0$ (the strip left the coilbox but did not leave the first stand yet) has not been considered in the switched system model because is very short and its dynamics is similar to the case $\Delta T_1^{am}(t) = -\Delta T_0^{av}(t)$ and $\Delta T_2^{am}(t) \neq 0$. When the strip leaves the first stand the system switches to the $(n-1)$-stands subsystem and the equations (1.5) and (1.6) are relevant for $g > j+1$.

The equation (1.6) represents the main difference between the model (1.1)-(1.6), introduced by Daafouz et al. [DBI+08], and previous HSM models. The contributions that can be found in literature are based on the steering growth model proposed by Nakajima et al. [NKK+80], where the strip off-center is computed stand by stand. In fact, each stand is linked to the other by the differential of strip tension (see equation (1.6) and Fig. 1.4).

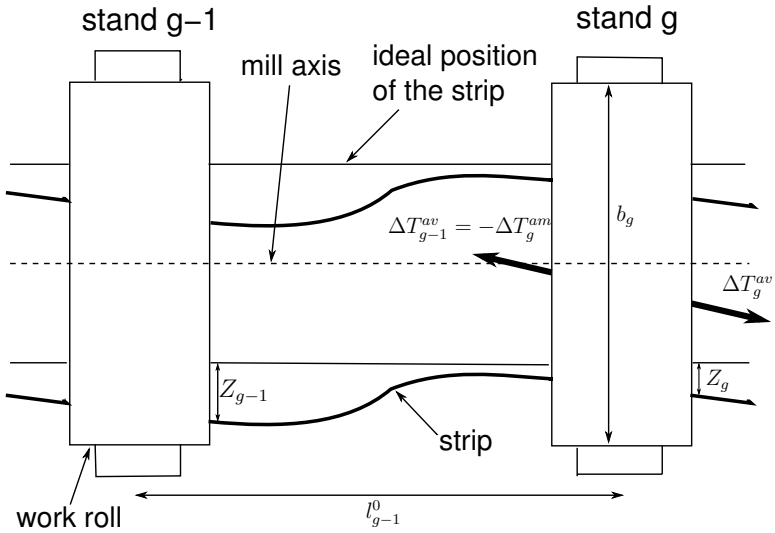

Figure 1.4: Strip behavior between two stands: top view

According to the previous physical equations, the system is described by the continuous time switched nonlinear system

$$\begin{cases} \dot{z}(t) = f^{\sigma(t)}(z, u, d, t) \\ y(t) = \bar{C}_y^{\sigma(t)} z(t) \end{cases} \tag{1.7}$$

where

$$z(t) = \left[\alpha_1(t), \ldots, \alpha_n(t), Z_1(t), \ldots, Z_n(t)\right]' \in \mathbb{R}^{2n} \tag{1.8}$$

is the state vector,

$$u(t) = \Delta S(t) = \left[\Delta S_1(t), \ldots, \Delta S_n(t)\right]' \in \mathbb{R}^r \tag{1.9}$$

is the control signal, $d(t) = Z_0(t) \in \mathbb{R}$ is the external perturbation and $y(t) \in \mathbb{R}^m$ is the measured output signal, for all $t \geq 0$. $\{f^i : i \in \mathcal{I} = \{1, ..., N\}\}$ is a family of sufficient regular functions, N represents the number of subsystems and $\sigma : \mathbb{R}^+ \to \mathcal{I}$ is a piecewise constant function, called switching rule, which orchestrates the switchings between the subsystems. There are n cameras to measure the state variables $Z_1, \ldots, Z_n$. Hence, $\bar{C}_y^i = \begin{bmatrix} 0 & I \end{bmatrix}$, for any $i \in \mathcal{I}$.

Only one perturbation will be considered: the strip off-center at the input of the first stand due to the vibrations of the coilbox. There are other perturbations, but their effects are negligible compared to the strip off-center initial. The model is easily adaptable to any HSM. However, tuning it requires industrial trials and a specific database of products. A strip off-center simulator has been developed under *Matlab-Simulink*. The tuning for the Eisenhüttenstadt HSM corresponds well with most of the products. In Fig. 1.5, an example is presented. The solid line shows the strip off-center measured by a camera while the dashed line shows the simulated strip off-center provided by our model.

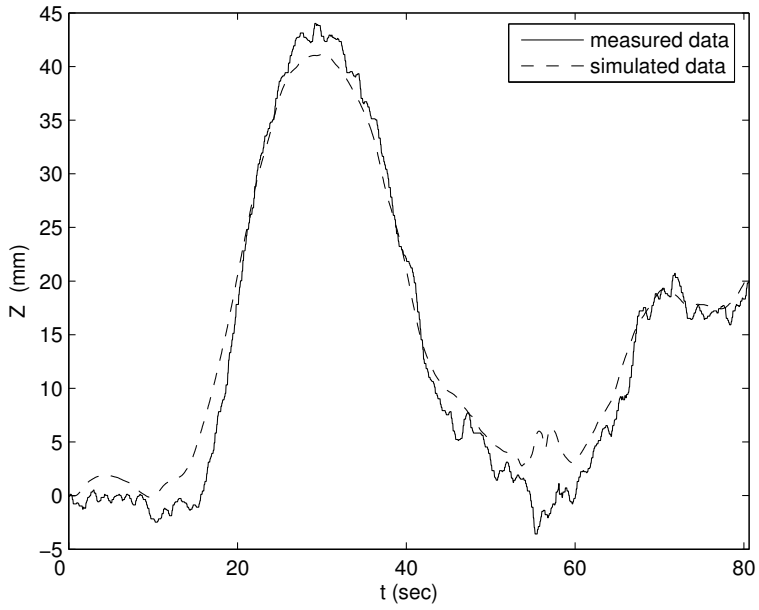

Figure 1.5: Comparison between measured and simulated strip off-center at Eisenhüttenstadt HSM

1.3 System linearization

The main task of the steering control is to maintain the strip close to the mill axis. The target may be reached by modifying the differential rolling force $\Delta P(t) = \begin{bmatrix} \Delta P_1(t), \ldots, \Delta P_n(t) \end{bmatrix}'$ in order to drive the strip into the desired trajectory. In fact, an excessive ΔP yields a high strip wedge $\Delta h(t) = \begin{bmatrix} \Delta h_1(t), \ldots, \Delta h_n(t) \end{bmatrix}'$.

This means that the strip profile becomes trapezoidal (Fig. 1.6.a and Fig. 1.7), whereas the ideal strip profile should be rectangular ($\Delta h(t) = 0$, for all $t \geq 0$). In general, a final wedge belonging to the interval $-10\,\mu m < \Delta h_n(t) < 10\,\mu m$ ensures a good product quality. The rolling force depends on the stand tilt ΔS. In order to respect the limits of the wedge value, ArcelorMittal engineers imposed a constraint on ΔS, which must be bounded between $\pm 0.6\ mm$ for the three first stands and $\pm 0.3\ mm$ for the two last stands (for 5-stands HSM).

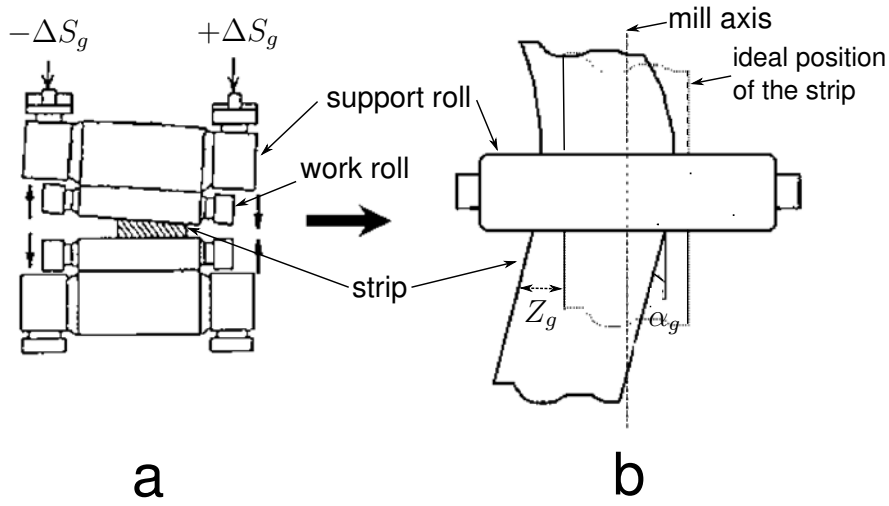

Figure 1.6: Stand g description: front view (a) and top view (b)

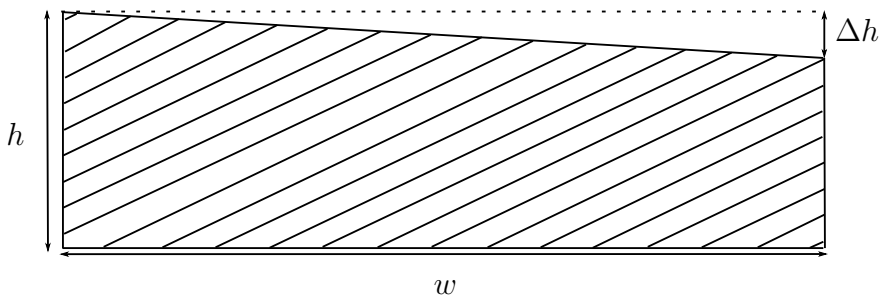

Figure 1.7: Strip profile

Since we assume that only small deviations are possible around the ideal operating point, that is $\alpha_g(t) = Z_g(t) = \Delta h_g(t) = 0$ for any $g \in \mathcal{G}$ and all $t \geq 0$, for control design purposes we can consider the following linearized switched model:

$$\begin{cases} \dot{z}(t) = \bar{M}^{\sigma(t)} z(t) + \bar{N}_u^{\sigma(t)} u(t) + \bar{N}_d^{\sigma(t)} d(t) \\ y(t) = \bar{C}_y^{\sigma(t)} z(t). \end{cases} \tag{1.10}$$

1.4 Model reduction

The HSM system has two time scale dynamics: the angles α are fast variables compared to the strips off-center Z [MDI+ar]. Multi time scale scale systems may lead to numerical problems due to the stiffness of this kind of structure. Moreover, the system actuators have a limited rate. This means that the dynamics corresponding to the angles cannot be controlled directly. In this case, the singular perturbation approximation may be used to control design purposes [KKO86]. It consists in decomposing the system dynamics into fast and slow dynamics and in designing a different controller for each of them. Consider the following subsystem, which corresponds to the mode $i \in \mathcal{I}$ of the switched linear system (1.10):

$$\begin{cases} \dot{z}(t) = \bar{M}^i z(t) + \bar{N}_u^i u(t) + \bar{N}_d^i d(t) \\ y(t) = \bar{C}_y^i z(t). \end{cases} \tag{1.11}$$

In order to express the model (1.11) in the singular perturbation form, the components of the state vector z which belong to the fast and slow dynamics must be associated to two different state vectors, called x_1 and x_2, respectively. In the n-stands subsystem, the state vector corresponding to the slow subsystem x_2 is composed by the n strip off-center variables. In the tail end subsystems, the state vector corresponding to the slow subsystem x_2 is composed by the strips off-center variables of the operating stands and the value of the angle corresponding to the first active stand. Hence, the components and the dimension of x_1 and x_2 change at each switching time. A set of matrices $\{E^i : i \in \mathcal{I}\}$, with pseudo-inverse $E^{i\dagger} = E^{i\prime}(E^i E^{i\prime})^{-1} = E^{i\prime}$, may be chosen such that the change of basis

$$x^i(t) = E^i z(t) \tag{1.12}$$

yields a system state vector in the form :

$$x^i(t) = \begin{bmatrix} x_1^i(t) \\ x_2^i(t) \end{bmatrix},$$

with $x_1^i(t) \in \mathbb{R}^{n_1^i}$ and $x_2^i(t) \in \mathbb{R}^{n_2^i}$, for any $i \in \mathcal{I}$ and for all $t \geq 0$. We obtain:

$$\begin{aligned} M^i(\varepsilon) &= E^i \bar{M}^i E^{i\prime} = \begin{bmatrix} \varepsilon^{-1} I_{n_1} & 0 \\ 0 & I_{n_2} \end{bmatrix} \begin{bmatrix} M_{11}^i & M_{12}^i \\ M_{21}^i & M_{22}^i \end{bmatrix}, \\ N_u^i &= E^i \bar{N}_u^i = \begin{bmatrix} \varepsilon^{-1} I_{n_1} & 0 \\ 0 & I_{n_2} \end{bmatrix} \begin{bmatrix} N_{u,1}^i \\ N_{u,2}^i \end{bmatrix}, \\ N_d^i &= E^i \bar{N}_d^i = \begin{bmatrix} \varepsilon^{-1} I_{n_1} & 0 \\ 0 & I_{n_2} \end{bmatrix} \begin{bmatrix} N_{d,1}^i \\ N_{d,2}^i \end{bmatrix}, \\ C_y^i &= \bar{C}_y^i E^{i\prime} = \begin{bmatrix} 0 & C_{y,2}^i \end{bmatrix}, \end{aligned} \tag{1.13}$$

with the choice $\varepsilon = 0.05$. The subsystem corresponding to the i^{th} mode of the switched system (1.11) can be written in the standard singular perturbation form:

$$\begin{cases} \varepsilon \dot{x}_1^i(t) = M_{11}^i x_1^i(t) + M_{12}^i x_2^i(t) + N_{u,1}^i u(t) + N_{d,1}^i d(t) \\ \dot{x}_2^i(t) = M_{21}^i x_1^i(t) + M_{22}^i x_2^i(t) + N_{u,2}^i u(t) + N_{d,2}^i d(t) \\ y(t) = C_{y,2}^i x_2^i(t), \end{cases} \tag{1.14}$$

where M_{11}^i is assumed to be Hurwitz for any $i \in \mathcal{I}$.

Consider the following state matrices, corresponding to the 4-stands subsystem of an average product of the Eisenhüttenstadt HSM database:

$$\bar{M}^4 = \begin{bmatrix} 0 & 0 & 0 & 0 & 0 & 0 & 0 & 0 & 0 & 0 \\ 0 & -1.60 & -5.87 & 0 & 0 & 0 & 0.0006 & -0.0016 & 0 & 0 \\ 0 & -20.34 & -76.5 & -6.155 & 0 & 0 & 0.0069 & -0.017 & -0.002 & 0 \\ 0 & -7.5 & -51.5 & -71.18 & 15 & 0 & 0.0026 & 0.0145 & -0.022 & 0.004 \\ 0 & -9.548 & -49.2 & -73.93 & -82 & 0 & 0.0033 & 0.0044 & 0.0132 & -0.02 \\ 0 & 0 & 0 & 0 & 0 & 0 & 0 & 0 & 0 & 0 \\ 0 & 4174 & 0 & 0 & 0 & 0 & 0 & 0 & 0 & 0 \\ 0 & 0 & 7466 & 0 & 0 & 0 & 0 & 0 & 0 & 0 \\ 0 & 0 & 0 & 11610 & 0 & 0 & 0 & 0 & 0 & 0 \\ 0 & 0 & 0 & 0 & 15918 & 0 & 0 & 0 & 0 & 0 \end{bmatrix}$$

and

$$\bar{N}_u^4 = \begin{bmatrix} 0 & 0 & 0 & 0 & 0 \\ 0 & 0.076 & 0 & 0 & 0 \\ 0 & 0.15 & 0.767 & 0 & 0 \\ 0 & 0.155 & 0.595 & 1.577 & 0 \\ 0 & 0.197 & 0.757 & 1.8 & 3.38 \\ 0 & 0 & 0 & 0 & 0 \\ 0 & 0 & 0 & 0 & 0 \\ 0 & 0 & 0 & 0 & 0 \\ 0 & 0 & 0 & 0 & 0 \\ 0 & 0 & 0 & 0 & 0 \end{bmatrix}.$$

We have:

$$E^4 = \begin{bmatrix} 0 & 0 & 1 & 0 & 0 & 0 & 0 & 0 & 0 & 0 \\ 0 & 0 & 0 & 1 & 0 & 0 & 0 & 0 & 0 & 0 \\ 0 & 0 & 0 & 0 & 1 & 0 & 0 & 0 & 0 & 0 \\ 0 & 1 & 0 & 0 & 0 & 0 & 0 & 0 & 0 & 0 \\ 0 & 0 & 0 & 0 & 0 & 0 & 1 & 0 & 0 & 0 \\ 0 & 0 & 0 & 0 & 0 & 0 & 0 & 1 & 0 & 0 \\ 0 & 0 & 0 & 0 & 0 & 0 & 0 & 0 & 1 & 0 \\ 0 & 0 & 0 & 0 & 0 & 0 & 0 & 0 & 0 & 1 \end{bmatrix},$$

and then $x^4 = \begin{bmatrix} x_1^4 \\ x_2^4 \end{bmatrix}$, with $x_1^4 = \begin{bmatrix} \alpha_3 & \alpha_4 & \alpha_5 \end{bmatrix}'$, $x_2^4 = \begin{bmatrix} \alpha_2 & Z_2 & Z_3 & Z_4 & Z_5 \end{bmatrix}'$, and

$$
\begin{aligned}
M_{11}^4 &= \begin{bmatrix} -3.825 & -0.3077 & 0 \\ -2.575 & -3.559 & 0.75 \\ -2.46 & -3.696 & -4.1 \end{bmatrix}, \\
M_{12}^4 &= \begin{bmatrix} -1.017 & 0.0003 & -0.0008 & -0.0001 & 0 \\ -0.375 & 0.0001 & 0.0007 & -0.0011 & 0.0002 \\ -0.477 & 0.0001 & 0.0002 & 0.0006 & -0.001 \end{bmatrix}, \\
M_{21}^4 &= 10^4 \begin{bmatrix} -0.0005 & 0 & 0 \\ 0 & 0 & 0 \\ 0.7466 & 0 & 0 \\ 0 & 1.161 & 0 \\ 0 & 0 & 1.5918 \end{bmatrix}, \\
M_{22}^4 &= 10^3 \begin{bmatrix} -0.0016 & 0.0000 & -0.0000 & 0 & 0 \\ 4.174 & 0 & 0 & 0 & 0 \\ 0 & 0 & 0 & 0 & 0 \\ 0 & 0 & 0 & 0 & 0 \\ 0 & 0 & 0 & 0 & 0 \end{bmatrix}, \\
N_{u,1}^4 &= \begin{bmatrix} 0.0075 & 0.0383 & 0 & 0 \\ 0.0077 & 0.0297 & 0.0788 & \\ 0 & & & \\ 0.0098 & 0.0378 & 0.09 & 0.169 \end{bmatrix}, \quad N_{u,2}^4 = \begin{bmatrix} 0.076 & 0 & 0 & 0 \\ 0 & 0 & 0 & 0 \\ 0 & 0 & 0 & 0 \\ 0 & 0 & 0 & 0 \\ 0 & 0 & 0 & 0 \end{bmatrix}.
\end{aligned}
\tag{1.15}
$$

When the 4-stands subsystem is on, the strip has already left the first stand. Therefore, the state variables α_1 and Z_1 do not have any physical meaning and are set to zero.

According to the practical implementation, the controller must be designed in discrete-time, with a sampling time of $T_s = 0.05$ *sec*. We have [Nai02]:

$$
\begin{cases}
x_1^i(s+1) = \varepsilon \tilde{A}_{11}^i x_1^i(s) + \tilde{A}_{12}^i x_2^i(s) + \tilde{B}_{u,1}^i u(s) + \tilde{B}_{d,1}^i d(s) \\
x_2^i(s+1) = \varepsilon \tilde{A}_{21}^i x_1^i(s) + \tilde{A}_{22}^i x_2^i(s) + \tilde{B}_{u,2}^i u(s) + \tilde{B}_{d,2}^i d(s) \\
y(s) = C_{y,2}^i x_2^i(s),
\end{cases}
\tag{1.16}
$$

where $x_1^i(s) \in \mathbb{R}^{n_1^i}$, $x_2^i(s) \in \mathbb{R}^{n_2^i}$, $u(s) \in \mathbb{R}^r$, $d(s) \in \mathbb{R}$ and $y(s) \in \mathbb{R}^m$, for any $i \in \mathcal{I}$ and for all $s \in \mathbb{Z}^+$. Moreover, we have:

$$
\tilde{A}^i(\varepsilon) = \begin{bmatrix} \varepsilon \tilde{A}_{11}^i & \tilde{A}_{12}^i \\ \varepsilon \tilde{A}_{21}^i & \tilde{A}_{22}^i \end{bmatrix}, \quad \tilde{B}_u^i = \begin{bmatrix} \tilde{B}_{u,1}^i \\ \tilde{B}_{u,2}^i \end{bmatrix}, \quad \tilde{B}_d^i = \begin{bmatrix} \tilde{B}_{d,1}^i \\ \tilde{B}_{d,2}^i \end{bmatrix}. \tag{1.17}
$$

Putting $\varepsilon = 0$, we obtain the slow model of the subsystem corresponding to i^{th} mode:

$$
\begin{cases}
x_s^i(s+1) = \tilde{A}_s^i x_s^i(s) + \tilde{B}_{u,s}^i u_s(s) + \tilde{B}_{d,s}^i d(s) \\
y_s(s) = \tilde{C}_{y,s}^i x_s^i(s),
\end{cases}
\tag{1.18}
$$

Table 1.1: Eigenvalues Comparison

$\xi\{\tilde{A}^4(\varepsilon)\}$	$\xi\{\tilde{A}_s^4\}$
1.0169	1.0211
0.9675	0.9821
0.9179	0.9108
0.8347	0.8831
0.8132	0.8132
0.0314	
0.0024 + 0.0186i	
0.0024 - 0.0186i	

with $x_s^i(s) = x_2^i(s)$, $\tilde{A}_s^i = \tilde{A}_{22}^i$, $\tilde{B}_{u,s}^i = \tilde{B}_{u,2}^i$, $\tilde{B}_{d,s}^i = \tilde{B}_{d,2}^i$ and $\tilde{C}_{y,s}^i = C_{y,2}^i$, for any $i \in \mathcal{I}$ and for all $s \in \mathbb{Z}^+$. In Table 1.1, the spectrum $\xi\{\tilde{A}^4(\varepsilon)\}$ of the state matrix corresponding to the two time scale system (1.16) and the spectrum $\xi\{\tilde{A}_s^4\}$ of the state matrix corresponding to the slow subsystem (1.18) are given. Notice that the time scale separation justifies the use of the only slow subsystem for control design purposes.

1.5 Polytopic uncertainties

An HSM treats products with very heterogeneous properties. The scheduling of the rolled products is assumed to be known in real time. Since the controller is computed off-line, from a control design point of view the only available information concerns the minimum and maximum bound of each parameter. Thus, the physical parameters must be considered as bounded uncertainties and a robust controller is needed. The uncertain two time scale switched system can be written in the polytopic form:

$$\begin{cases} x^{\sigma(s)}(s+1) = \mathfrak{A}^{\sigma(s)}(s)x^{\sigma(s)}(s) + \mathfrak{B}_u^{\sigma(s)}(s)u(s) + \mathfrak{B}_d^{\sigma(s)}(s)d(s) \\ y(s) = C_y^{\sigma(s)}x^{\sigma(s)}(s) \end{cases} \tag{1.19}$$

where $\sigma : \mathbb{Z}^+ \to \mathcal{I}$ is the switching rule for all $s \in \mathbb{Z}^+$. Further, for any $i \in \mathcal{I}$, we have:

$$\mathfrak{A}^i(s) = \sum_{l=1}^{N_V} \lambda_l(s)\tilde{A}^{i,l}(\varepsilon), \quad \mathfrak{B}_u^i(s) = \sum_{l=1}^{N_V} \lambda_l(s)\tilde{B}_u^{i,l}, \quad \mathfrak{B}_d^i(s) = \sum_{l=1}^{N_V} \lambda_l(s)\tilde{B}_d^{i,l},$$

where $l \in \mathcal{L} = \{1, ..., N_V\}$ denotes the vertices of the convex hull, N_V is the number of uncertain parameters and λ_l denotes the uncertainty and belongs to the unit simplex

$$\mathfrak{Y}(s) = \{\sum_{l=1}^{N_V} \lambda_l(s) = 1, \ \lambda_l(s) \geq 0\}.$$

1.6 Conclusion

The lateral movement of the strip during the rolling process reduces the product quality and damages the rolls, if the strip crashes against the mill side guides. The goal of the HSM steering control consists in limiting this displacement for improving the reliability and the process quality. In order to implement an effective solution, several phenomena arising on the system should be taken into account on the control design. First, an HSM can treat products with very heterogeneous properties. Thus, the physical products parameters must be considered as bounded uncertainties and a robust controller is needed. Moreover, the system has two time scale dynamics and the fast dynamics cannot be controlled because of the limits on the actuators rate. Further, during the tail end phase, the system is subject to hard traction losses due to the fact that the strip leaves the stands one after the other. Hence, sudden modifications of dynamics arise and the state variables corresponding to the slow and fast manifolds may vary. In particular, each time the strip leaves a stand the state variables corresponding to the left stand do not influence any longer the system and the angle between the strip and the mill axis on the first active stand, which was a state variable belonging to the fast manifold, becomes a state variable of the slow manifold. Because of the changes on the system dynamics, different controllers must be designed, one for each operating point, and a rule orchestrating the controller switchings is needed. At last, switching among different controllers implies undesired transient behaviors due to large discontinuities on the control signal. This phenomenon may affect the system performances and, in the worst case, destabilize the system.

Despite its importance on the steel production framework, there exist few studies dealing with steering control of HSM. Further, most of these works do not consider the uncertainties on the products parameters and the tail end phase switchings. In this chapter, a two time scale switched model of the HSM system has been proposed for steering control purposes. Parametric uncertainties in the polytopic form have also been taken into account. In the next three chapters, we will provide some theoretical results useful for solving different problems concerned with the steering control of HSM. In Chapter 2, we will present a convex solution of the LQ optimization problem of discrete two time scale LTI systems. These results will be extended to uncertain systems in the polytopic form, under the assumption of asymptotically stable fast dynamics. Chapter 3 deals with two time scale switched systems. First, we will show that asymptotic stability of the slow and fast switched subsystems under an arbitrary switching rule is not sufficient for assessing asymptotic stability of the original two time scale switched system. Therefore, we will propose LMI based conditions independent of the singular perturbation parameter which guarantee asymptotic stability of the two time scale switched system, in the continuous and discrete-time frameworks. In Chapter 4, a method for reducing the control signal discontinuities of discrete-time switched linear systems is proposed. Many of these results will be retrieved in the last chapter, where a robust steering control design of HSM is presented.

Chapter 2

A convex solution of the discrete-time LQ control design for two time scale systems

2.1 Introduction

In practice, many systems involve dynamics operating on different time scales, such as electric power systems, aerospace systems, robotics, chemical and biological systems [Nai02]. In this case, standard control techniques lead to ill-conditioning problems and singular perturbation methods may be used to avoid such numerical phenomena [KKO86], [Nai88]. They consist in decomposing the system into several subsystems, one for each time scale. Thus, a different controller is designed for each of them. Singular perturbation techniques also allow to neglect high-frequency dynamics and then reduce the controller order [KS68]. This property can be very useful when the system order is high [And93]. Consider the two time scale model:

$$\varepsilon \dot{x}_1(t) = f(x_1(t), x_2(t), \varepsilon, t) \tag{2.1a}$$

$$\dot{x}_2(t) = g(x_1(t), x_2(t), \varepsilon, t) \tag{2.1b}$$

where f and g are assumed to be continuously differentiable functions of their arguments $x_1(t), x_2(t), \varepsilon, t$, $x_1(t) \in \mathbb{R}^{n_1}$ is the state vector corresponding to the fast dynamics, $x_2(t) \in \mathbb{R}^{n_2}$ is the state vector corresponding to the slow dynamics, for all $t \geq t_0$, $x(t_0) = \begin{bmatrix} x_1(t_0)' & x_2(t_0)' \end{bmatrix}'$ is the initial condition and the scalar $\varepsilon > 0$ represents the singular perturbation parameter. Setting $\varepsilon = 0$, the dimension of the state space of (2.1) is reduced from $n_1 + n_2$ to n_2 because (2.1a) degenerates into the algebraic or transcendental equation:

$$f(\bar{x}_1(t), \bar{x}_2(t), 0, t) = 0, \tag{2.2}$$

where $\bar{x}_1$ and $\bar{x}_2$ denote x_1 and x_2 when $\varepsilon = 0$. The model (2.1) is said to be in the *standard form* if (2.2) has $p \geq 1$ distinct real roots:

$$\bar{x}_1(t) = h_i(\bar{x}_2(t), t) \tag{2.3}$$

for all $t \geq t_0$, with $i = 1, 2, ..., p$. This ensures the existence of a well-defined n_2-dimension *reduced model* to each root of (2.3). Substituting (2.3) into (2.1b), we obtain the i^{th} reduced model (also called *slow model* or *quasi-steady-state model*):

$$\dot{\bar{x}}_2(t) = g(h_i(\bar{x}_2(t), t), \bar{x}_2(t), 0, t), \tag{2.4}$$

with $x_2(t_0) - \bar{x}_2(t_0) = O(\varepsilon)$. We assume that the fast transient, which corresponds to the difference between the response of the original system (2.1) and the slow model (2.4), is:

$$x_2(t) - \bar{x}_2(t) = O(\varepsilon) \tag{2.5}$$

for any $t \in [t_0, t_{fin}]$ on which $\bar{x}_2(t)$ exists. Let us study the behavior of the fast state vector x_1. For $\varepsilon = 0$, its initial condition $\bar{x}_1(t_0) = h(\bar{x}_2(t_0), t_0)$ is constrained and cannot be free to start from $x_1(t_0)$. Hence, the condition

$$x_1(t) - \bar{x}_1(t) = O(\varepsilon) \tag{2.6}$$

can be obtained only for $t \in [t_1, t_{fin}]$, with $t_1 > t_0$. The approximation (2.6) states that during the initial interval $[t_0, t_1]$, called *boundary layer interval*, the original variable x_1 tends to $\bar{x}_1$ and that remains close to $\bar{x}_1$ for $[t_1, t_{fin}]$. To prove that this assumption holds, let apply the stretching transformation:

$$\varepsilon \frac{dx_1}{dt} = \frac{dx_1}{d\tau}.$$

This yields the *fast time variable*

$$\tau = \frac{t - t_0}{\varepsilon},$$

with $\tau = 0$ at $t = t_0$. Notice that when $\varepsilon \to 0$, $\tau \to \infty$, also for a little amount of time $t - t_0$. This means that when $\varepsilon \to 0$, $t - t_0$ is "stretched" to an infinity interval. To describe the behavior of x_1 in the fast time scale, let us define the boundary layer correction $\hat{x}_1 = x_1 - \bar{x}_1$ satisfying the boundary layer system:

$$\frac{d\hat{x}_1}{d\tau} = f(\hat{x}_1(\tau) + \bar{x}_1(t_0), x_2(t_0), 0, t_0), \tag{2.7}$$

with $\hat{x}_1(0) = x_1(t_0) - \bar{x}_1(t_0)$. Fixed t_0 and $x_2(t_0)$, the solution $\hat{x}_1$ of (2.7) may be used as a boundary layer correction of (2.6) for the following uniform approximation of x_1:

$$x_1(t) = \bar{x}_1(t) + \hat{x}_1(\tau) + O(\varepsilon). \tag{2.8}$$

$\bar{x}_1(t)$ and $\hat{x}_1(\tau)$ represent the slow and the fast transient of $x_1(t)$, respectively. The equation (2.8) will quickly converge to (2.6) only if $\hat{x}_1(\tau)$ decays to an $O(\varepsilon)$ quantity for $\tau \to \infty$ (which corresponds to a short interval of time in the slow time scale t). The following theorem gives the stability conditions ensuring the validity of the approximation (2.5), (2.8) [Tik48], [Vas63].

Theorem 1 *([KKO86]) Assume that the equilibrium $\hat{x}_1(\tau) = 0$ of (2.7) is asymptotically stable uniformly in t_0 and $x_2(t_0)$, and that $\hat{x}_1(0) = x_1(t_0) - \bar{x}_1(t_0)$ belongs to its domain of attraction. Further, assume that the eigenvalues of $\frac{\partial f}{\partial x_1}$ evaluated along $\bar{x}_1$ and $\bar{x}_2$ for $\varepsilon = 0$ have negative real parts. Hence, the approximation (2.5), (2.8) holds for any $t \in [t_0, t_{fin}]$, and there exists $t_1 > t_0$ such that (2.6) holds for any $t \in [t_1, t_{fin}]$.*

The first assumption of Theorem 1 implies that $\lim_{\tau \to \infty} \hat{x}_1(\tau) = 0$ uniformly in t_0 and $x_2(t_0)$. Thus, x_1 will be close to $\bar{x}_1$ at some time $t_1 > t_0$. The second assumption ensures that x_1 stays close to $\bar{x}_1$ for any $t \in [t_1, t_{fin}]$.

In the LQ optimal control framework, first contributions to the singular perturbation theory were proposed in the continuous-time case by Kokotovic and Sannuti [KS68], [San68], [SK69]. Garcia et al. proposed an alternative convex solution for the continuous-time LQ optimal control design of two time scale LTI systems [PG94], [GDB98], [GDB02]. However, most of modern control systems work in discrete time. In this case, there exist two main control design approaches, depending on the sampling rate. The reason is that since digital controllers critically depend on the sampling time, different choices of the sampling rate lead to different control laws. The first approach is based on a fast sampling model derived by numerical approximations such as the Euler approximation: a hybrid solution containing a continuous-time slow subsystem and a discrete-time fast subsystem is obtained [Bla81], [LK84]. This model allows to design a control law independently of the stability properties of the fast dynamics. Namely, the sampling rate is assumed to be fast enough for influencing the transient behavior of the system. The second method resorts to a slow sampling model based on a singular perturbed difference equation [RN82], [KI83]. A control law designed through this approach cannot influence the fast transient behavior of the system. Nevertheless, there are many practical applications having asymptotically stable fast dynamics and subject to a constraint on the sampling time, due to the limitation on the actuators rate. An example is given by the hot strip mill system presented in Chapter 1. In this case, the slow sampling model is often more appropriate for control purposes. More complex solutions, which are not investigated in this work, look for a multi-rate control law [KI86].

The aim of this chapter is to extend the results of [GDB02] to discrete-time singularly perturbed LTI systems, for both fast and slow sampling models [MDIB09]. Hence, LMI techniques can be directly applied for control design purposes [BGFB94]. The main advantage of LMI techniques is that there exist efficient algorithms which provide a solution also for high dimension problems [NN94]. Furthermore, we will show that the convexity properties of the solution allows a direct extension of the reduced controller to uncertain systems in the polytopic form.

Consider the two time scale LTI system :

$$\begin{cases} \varepsilon \dot{x}_1(t) = M_{11}x_1(t) + M_{12}x_2(t) + N_1 u(t) \\ \dot{x}_2(t) = M_{21}x_1(t) + M_{22}x_2(t) + N_2 u(t), \end{cases} \tag{2.9}$$

where $u(t) \in \mathbb{R}^r$ is the control signal, for all $t \geq t_0$. We assume that the problem is in the standard form, that is equivalent to assume M_{11} non-singular, in the LTI systems case. Let us apply the mode-decoupling transformation [Kok75]:

$$\begin{aligned} \begin{bmatrix} x_f(t) \\ x_s(t) \end{bmatrix} &= \begin{bmatrix} I_{n_1} & L(\varepsilon) \\ -\varepsilon H(\varepsilon) & I_{n_2} - \varepsilon H(\varepsilon)L(\varepsilon) \end{bmatrix} \begin{bmatrix} x_1(t) \\ x_2(t) \end{bmatrix}, \\ \begin{bmatrix} x_1(t) \\ x_2(t) \end{bmatrix} &= \begin{bmatrix} I_{n_1} - \varepsilon L(\varepsilon)H(\varepsilon) & -L(\varepsilon) \\ \varepsilon H(\varepsilon) & I_{n_2} \end{bmatrix} \begin{bmatrix} x_f(t) \\ x_s(t) \end{bmatrix}, \end{aligned} \tag{2.10}$$

with

$$M_{12} - M_{11}L(\varepsilon) + \varepsilon L(\varepsilon)(M_{22} - M_{21}L(\varepsilon)) = 0, \tag{2.11}$$

$$M_{21} - H(\varepsilon)M_{11} + \varepsilon(M_{22} - M_{21}L(\varepsilon))H(\varepsilon) - \varepsilon H(\varepsilon)L(\varepsilon)M_{21} = 0. \tag{2.12}$$

Given a scalar $\varepsilon_{max} > 0$, the non-symmetric algebraic Riccati equation (2.11) and the Sylvester equation (2.12) admit the approximated solution $L(\varepsilon) = M_{11}^{-1}M_{12} + O(\varepsilon)$, $H(\varepsilon) = M_{21}M_{11}^{-1} + O(\varepsilon)$, for $\varepsilon \in (0, \varepsilon_{max}]$. By discretizing the continuous-time model (2.9), a different sampling model is obtained depending on the sampling rate [KI86]. The choice of the sampling time as $T_f = \alpha_f \varepsilon$, where $\alpha_f > 0$ is a scalar, leads to the *fast sampling model*:

$$\begin{cases} x_1(k+1) = A_{11}x_1(k) + A_{12}x_2(k) + B_1 u(k) \\ x_2(k+1) = \varepsilon A_{21}x_1(k) + (I_{n_2} + \varepsilon A_{22})x_2(k) + \varepsilon B_2 u(k), \end{cases} \tag{2.13}$$

where $x_1(k) \in \mathbb{R}^{n_1}$, $x_2(k) \in \mathbb{R}^{n_2}$ and $u(k) \in \mathbb{R}^r$, for all $k \in \mathbb{Z}^+ \geq t_0$. Neglecting $O(\varepsilon)$ errors, we have :

$$\begin{aligned} A_{11} &= exp\left(\alpha_f M_{11}\right), \\ A_{12} &= \left(exp\left(\alpha_f M_{11}\right) - I_{n_1}\right) M_{11}^{-1}M_{12}, \\ A_{21} &= M_{21}M_{11}^{-1}\left(exp\left(\alpha_f M_{11}\right) - I_{n_1}\right), \\ A_{22} &= \alpha_f M_s + M_{21}M_{11}^{-1}\left(exp\left(\alpha_f M_{11}\right) - I_{n_1}\right) M_{11}^{-1}M_{12}, \\ B_1 &= \left(exp\left(\alpha_f M_{11}\right) - I_{n_1}\right) M_{11}^{-1}N_1, \\ B_2 &= \alpha_f N_s + M_{21}M_{11}^{-1}\left(exp\left(\alpha_f M_{11}\right) - I_{n_1}\right) M_{11}^{-1}N_1, \end{aligned} \tag{2.14}$$

with $M_s = M_{22} - M_{21}M_{11}^{-1}M_{12}$ and $N_s = N_2 - M_{21}M_{11}^{-1}N_1$.

By choosing the sampling time as $T_s = \alpha_s[1/\varepsilon]T_f \approx \alpha_s\alpha_f$, where $\alpha_s > 0$ is a scalar and $[1/\varepsilon]$ is the largest integer $\leq 1/\varepsilon$, we obtain the *slow sampling model*:

$$\begin{cases} x_1(s+1) = \varepsilon\tilde{A}_{11}x_1(s) + \tilde{A}_{12}x_2(s) + \tilde{B}_1 u(s) \\ x_2(s+1) = \varepsilon\tilde{A}_{21}x_1(s) + \tilde{A}_{22}x_2(s) + \tilde{B}_2 u(s), \end{cases} \tag{2.15}$$

where $k = s[1/\varepsilon]$, $x_1(s) \in \mathbb{R}^{n_1}$, $x_2(s) \in \mathbb{R}^{n_2}$ and $u(s) \in \mathbb{R}^r$, for all $s \in \mathbb{Z}^+ \geq t_0$. Neglecting $O(\varepsilon)$ errors, we have:

$$\begin{aligned}
\tilde{A}_{11} &= M_{11}^{-1} M_{12} exp\left(\alpha_s \alpha_f M_s\right) M_{21} M_{11}^{-1} + \varepsilon^{-1} exp\left(\frac{\alpha_s \alpha_f M_{11}}{\varepsilon}\right), \\
\tilde{A}_{12} &= -M_{11}^{-1} M_{12} exp\left(\alpha_s \alpha_f M_s\right), \\
\tilde{A}_{21} &= -exp\left(\alpha_s \alpha_f M_s\right) M_{21} M_{11}^{-1}, \\
\tilde{A}_{22} &= exp\left(\alpha_s \alpha_f M_s\right), \\
\tilde{B}_1 &= -M_{11}^{-1} M_{12} \left(exp\left(\alpha_s \alpha_f M_s\right) - I_{n_2}\right) M_s^{-1} N_s - M_{11}^{-1} N_1, \\
\tilde{B}_2 &= \left(exp\left(\alpha_s \alpha_f M_s\right) - I_{n_2}\right) M_s^{-1} N_s.
\end{aligned} \tag{2.16}$$

Since $exp\left(\frac{\alpha_s \alpha_f M_{11}}{\varepsilon}\right) \approx O(\varepsilon)$ only if the matrix M_{11} is Hurwitz, the slow sampling model is valid only if the fast dynamics is asymptotically stable.

2.2 Discrete-time LQ optimal problem

2.2.1 Fast sampling control law

Consider the fast sampling model (2.13):

$$\begin{cases}
x_1(k+1) = A_{11} x_1(k) + A_{12} x_2(k) + B_1 u(k) \\
x_2(k+1) = \ \varepsilon A_{21} x_1(k) + (I_{n_2} + \varepsilon A_{22}) x_2(k) + \varepsilon B_2 u(k) \\
q(k) = C_1 x_1(k) + C_2 x_2(k),
\end{cases} \tag{2.17}$$

where $x(k) = \begin{bmatrix} x_1(k)' & x_2(k)' \end{bmatrix}'$, $q(k) \in \mathbb{R}^w$ is the controlled output, for all $k \in \mathbb{Z}^+ \geq t_0$, and

$$A(\varepsilon) = \begin{bmatrix} A_{11} & A_{12} \\ \varepsilon A_{21} & (I_{n_2} + \varepsilon A_{22}) \end{bmatrix}, \quad B(\varepsilon) = \begin{bmatrix} B_1 \\ \varepsilon B_2 \end{bmatrix}, \quad C = \begin{bmatrix} C_1 & C_2 \end{bmatrix}. \tag{2.18}$$

Let the fast sampling LQ optimization problem :

$$\min_u J(\varepsilon) = \frac{\varepsilon}{2} \sum_{k=t_0}^{\infty} (q(k)' q(k) + u(k)' R u(k)) \tag{2.19}$$

$$subject\ \ to \quad \begin{cases} x(k+1) = A(\varepsilon) x(k) + B(\varepsilon) u(k) \\ q(k) = C x(k), \end{cases} \qquad x(t_0) = \begin{bmatrix} x_1(t_0) \\ x_2(t_0) \end{bmatrix}$$

where $R = R' \succ 0$ is a weighting matrix. Assume that the pair $(A(\varepsilon), B(\varepsilon))$ is stabilizable and the pair $(C, A(\varepsilon))$ is detectable in the discrete-time sense, which means that each eigenvalue of $A(\varepsilon)$ which has modulus equal or greater than one is controllable and observable. Hence, there exists a stabilizing solution $S(\varepsilon) \succ 0$ for the algebraic Riccati equation:

$$\begin{aligned}
&A(\varepsilon)' S(\varepsilon) A(\varepsilon) - A(\varepsilon)' S(\varepsilon) B(\varepsilon) (R + B(\varepsilon)' S(\varepsilon) B(\varepsilon))^{-1} \\
&B(\varepsilon)' S(\varepsilon) A(\varepsilon) - S(\varepsilon) + C'C = 0.
\end{aligned} \tag{2.20}$$

The optimal solution is :

$$u(k) = K(\varepsilon)x(k), \tag{2.21}$$

with

$$K(\varepsilon) = -(R + B(\varepsilon)'S(\varepsilon)B(\varepsilon))^{-1}B(\varepsilon)'S(\varepsilon)A(\varepsilon)$$

and optimal cost

$$J^*(\varepsilon) = \frac{\varepsilon}{2}x(t_0)'S(\varepsilon)x(t_0).$$

When $\varepsilon \to 0$, standard techniques may lead to ill-conditioning controllers. To avoid such numerical problems, the criterion (2.19) and its associated Riccati equation (2.20) may be decomposed into two different well-behaved subproblems, independently of the singular parameter ε.

Slow subproblem: To derive the slow subsystem of (2.17), we assume that $x_2(k) = x_s(k)$ and $x_1(k) = \bar{x}_1(k) = (I_{n_1} - A_{11})^{-1}(A_{12}x_s(k) + B_1u_s(k))$, during the steady state. These hypotheses are equivalent to the continuous-time assumption (2.5) and (2.6). We obtain [Nai02]:

$$x_s(k+1) = (I_{n_2} + \varepsilon A_s)x_s(k) + \varepsilon B_s u_s(k),$$

which can be written in the time scale $t = \varepsilon k$ as

$$x_s(\varepsilon k + \varepsilon) - x_s(\varepsilon k) = \varepsilon A_s x_s(\varepsilon k) + \varepsilon B_s u_s(\varepsilon k).$$

Dividing both sides by ε, for $\varepsilon \to 0$ we get the approximated continuous-time subproblem:

$$\begin{aligned} &\min_{u_s} J_s = \frac{1}{2}\int_{t_0}^{\infty} \left(q_s(t)'q_s(t) + u_s(t)'R_s u_s(t)\right) dt \\ &\textit{subject to} \begin{cases} \dot{x}_s(t) = A_s x_s(t) + B_s u_s(t) \\ q_s(t) = C_s x_s(t) + D_s u_s(t), \end{cases} \quad x_s^0 = x_2(t_0) \end{aligned} \tag{2.22}$$

where the matrix $(I_{n_1} - A_{11})$ is assumed to be non-singular,

$$\begin{aligned} A_s &= A_{22} + A_{21}(I_{n_1} - A_{11})^{-1}A_{12}, \\ B_s &= B_2 + A_{21}(I_{n_1} - A_{11})^{-1}B_1, \\ C_s &= C_2 + C_1(I_{n_1} - A_{11})^{-1}A_{12}, \\ D_s &= C_1(I_{n_1} - A_{11})^{-1}B_1, \end{aligned} \tag{2.23}$$

and $R_s = R_s' = R + D_s'D_s \succ 0$. Notice that x_s corresponds to the state vector $\bar{x}_2$ introduced in (2.2). Assume that the pair (A_s, B_s) is stabilizable and the pair (C_s, A_s) is detectable in the continuous-time sense, which means that each eigenvalue of A_s that is in the right-half complex plane is controllable and observable. Hence, there exists a stabilizing solution $S_s \succ 0$ for the algebraic Riccati equation:

$$\begin{aligned} &(A_s - B_s R_s^{-1}D_s'C_s)'S_s + S_s(A_s - B_s R_s^{-1}D_s'C_s) - \\ &S_s B_s R_s^{-1}B_s'S_s + C_s'(I_{n_1} - D_s R_s^{-1}D_s')C_s = 0. \end{aligned}$$

The optimal solution is:

$$u_s(t) = K_s x_s(t), \tag{2.24}$$

with $K_s = -R_s^{-1}(B_s'S_s + D_s'C_s)$ and optimal cost $J_s^* = \frac{1}{2}x_s^{0\prime}S_s x_s^0$. The state-feedback law (2.24) guarantees the condition $Re\{\xi(A_s+B_sK_s)\} < 0$. This implies the asymptotic stability of the slow subsystem, for a sufficiently small ε.

Fast subproblem: To derive the fast subsystem of (2.17), we assume that $x_s(k+1) = x_s(k)$ and $x_f(k) = x_1(k) - \bar{x}_1(k)$ during the fast transient. The relation $x_f(k+1) = x_1(k+1) - \bar{x}_1(k+1)$ yields the following fast subproblem [Nai02]:

$$\min_{u_f} J_f = \frac{1}{2}\sum_{k=t_0}^{\infty}(q_f(k)'q_f(k) + u_f(k)'Ru_f(k))$$

$$subject\ \ to\ \ \begin{cases} x_f(k+1) = A_{11}x_f(k) + B_1u_f(k) \\ q_f(k) = C_1x_f(k), \end{cases} \qquad x_f^0 = x_1(t_0) - \bar{x}_1(t_0)$$

with $\bar{x}_1(t_0) = (I_{n_1} - A_{11})^{-1}A_{12}x_2(t_0)$. If the pair (A_{11}, B_1) is stabilizable and the pair (C_1, A_{11}) is detectable in the discrete-time sense, there exists a stabilizing solution $S_f \succ 0$ for the algebraic Riccati equation:

$$A_{11}'S_fA_{11} - A_{11}'S_fB_1(R + B_1'S_fB_1)^{-1}B_1'S_fA_{11} - S_f + C_1'C_1 = 0.$$

The optimal solution is:

$$u_f(k) = K_f x_f(k), \tag{2.25}$$

with $K_f = -(R + B_1'S_fB_1)^{-1}B_1'S_fA_{11}$ and optimal cost $J_f^* = \frac{1}{2}x_f^{0\prime}S_f x_f^0$.

Composite control: The control laws (2.24) and (2.25) are designed using independent gains K_s and K_f. Since (2.24) has been designed in the continuous-time framework while (2.25) has been designed in the discrete-time one, we obtain a hybrid control law. Setting $u_s(t) = u_s(k) = K_sx_s(k)$ constant for $k\varepsilon \leq t < (k+1)\varepsilon$, we have the composite control law :

$$u(k) = u_s(k) + u_f(k) = K\begin{bmatrix} x_1(k) \\ x_2(k) \end{bmatrix}, \tag{2.26}$$

with $K = \begin{bmatrix} K_f & K_s - K_f(I_{n_1} - A_{11})^{-1}(A_{12} + B_1K_s) \end{bmatrix}$. When $\varepsilon \to 0$, (2.26) is close to the optimal solution (2.21).

2.2.2 Slow sampling control law

Consider the slow sampling model (2.15):

$$\begin{cases} x_1(s+1) = \varepsilon\tilde{A}_{11}x_1(s) + \tilde{A}_{12}x_2(s) + \tilde{B}_1u(s) \\ x_2(s+1) = \varepsilon\tilde{A}_{21}x_1(s) + \tilde{A}_{22}x_2(s) + \tilde{B}_2u(s) \\ q(s) = C_1x_1(s) + C_2x_2(s), \end{cases} \tag{2.27}$$

where $x(s) = \begin{bmatrix} x_1(s)' & x_2(s)' \end{bmatrix}'$, $q(s) \in \mathbb{R}^w$ is the controlled output, for all $s \in \mathbb{Z}^+ \geq t_0$, and

$$\tilde{A}(\varepsilon) = \begin{bmatrix} \varepsilon\tilde{A}_{11} & \tilde{A}_{12} \\ \varepsilon\tilde{A}_{21} & \tilde{A}_{22} \end{bmatrix}, \quad \tilde{B} = \begin{bmatrix} \tilde{B}_1 \\ \tilde{B}_2 \end{bmatrix}, \quad C = \begin{bmatrix} C_1 & C_2 \end{bmatrix}. \tag{2.28}$$

A model discretized using a slow sampling time cannot take into account the fast transient. Hence, we consider $C_1 = 0$. Let the slow sampling LQ optimization problem :

$$\min_u J(\varepsilon) = \frac{1}{2}\sum_{s=t_0}^{\infty}(q(s)'q(s) + u(s)'Ru(s)) \tag{2.29}$$

$$\textit{subject to} \quad \begin{cases} x(s+1) = \tilde{A}(\varepsilon)x(s) + \tilde{B}u(s) \\ q(s) = Cx(s) \end{cases} \qquad x(t_0) = \begin{bmatrix} x_1(t_0) \\ x_2(t_0) \end{bmatrix}.$$

If the pair $(\tilde{A}(\varepsilon), \tilde{B})$ is stabilizable and the pair $(C, \tilde{A}(\varepsilon))$ is detectable, there exists a stabilizing solution $S(\varepsilon) \succ 0$ for the algebraic Riccati equation:

$$\tilde{A}(\varepsilon)'S(\varepsilon)\tilde{A}(\varepsilon) - \tilde{A}(\varepsilon)'S(\varepsilon)\tilde{B}(R + \tilde{B}'S(\varepsilon)\tilde{B})^{-1}\tilde{B}'S(\varepsilon)\tilde{A}(\varepsilon) - S(\varepsilon) + C'C = 0. \tag{2.30}$$

The optimal solution is :

$$u(s) = K(\varepsilon)x(s), \tag{2.31}$$

with

$$K(\varepsilon) = -(R + \tilde{B}'S(\varepsilon)\tilde{B})^{-1}\tilde{B}'S(\varepsilon)\tilde{A}(\varepsilon)$$

and optimal cost

$$J^*(\varepsilon) = \frac{1}{2}x(t_0)'S(\varepsilon)x(t_0).$$

As in the fast sampling case, the criterion (2.29) and its associate Riccati equation (2.30) may be decomposed into two different well-behaved subproblems, independently of the singular parameter ε.

Slow subproblem: Setting $\varepsilon = 0$, we obtain the following slow subproblem:

$$\begin{aligned} &\min_{u_s} J_s = \frac{1}{2}\sum_{s=t_0}^{\infty}(q_s(s)'q_s(s) + u_s(s)'Ru_s(s)) \\ &\textit{subject to} \quad \begin{cases} x_s(s+1) = \tilde{A}_s x_s(s) + \tilde{B}_s u_s(s) \\ q_s(s) = \tilde{C}_s x_s(s), \end{cases} \qquad x_s^0 = x_2(t_0) \end{aligned} \tag{2.32}$$

with $x_s(s) = x_2(s)$ and

$$\tilde{A}_s = \tilde{A}_{22}, \quad \tilde{B}_s = \tilde{B}_2, \quad \tilde{C}_s = C_2. \tag{2.33}$$

If the pair $(\tilde{A}_s, \tilde{B}_s)$ is stabilizable and the pair $(\tilde{C}_s, \tilde{A}_s)$ is detectable, there exists a stabilizing solution $S_s \succ 0$ for the algebraic Riccati equation:

$$\tilde{A}_s' S_s \tilde{A}_s - \tilde{A}_s' S_s \tilde{B}_s (R + \tilde{B}_s' S_s \tilde{B}_s)^{-1} \tilde{B}_s' S_s \tilde{A}_s - S_s + \tilde{C}_s' \tilde{C}_s = 0.$$

The optimal solution is:

$$u_s(s) = K_s x_s(s), \tag{2.34}$$

with $K_s = -(R + \tilde{B}_s' S_s \tilde{B}_s)^{-1} \tilde{B}_s' S_s \tilde{A}_s$ and optimal cost $J_s^* = \frac{1}{2} x_s^{0\prime} S_s x_s^0$.

Clearly, a controller designed using a slow sampling time T_s cannot influence the fast transient. Hence, for $\varepsilon \to 0$ we have $K_f = 0$ and

$$u(s) = K \begin{bmatrix} x_1(s) \\ x_2(s) \end{bmatrix}, \tag{2.35}$$

with $K = \begin{bmatrix} 0 & K_s \end{bmatrix}$. Since M_{11} was assumed to be Hurwitz, the closed loop system (2.27) will be asymptotically stable, for an ε small enough.

2.3 LMI based solution

In this section, we present an alternative LMI based solution to the discrete-time LQ optimal problem for two time scale linear systems. In general, LMI tools are considered more effective than Riccati equation solutions in front of the increase of dimensions [BGFB94].

2.3.1 Fast sampling control law

The fast sampling LQ optimization problem (2.19) may be formulated in a convex form [GDB02], [MDIB09]. Let define the sets

$$\mathcal{P}_\varepsilon = \left\{ \bar{P}(\varepsilon) = \begin{bmatrix} P(\varepsilon) & Z(\varepsilon)' \\ Z(\varepsilon) & U(\varepsilon) \end{bmatrix} \succeq 0,\ P(\varepsilon) \succ 0 \right\} \tag{2.36}$$

and

$$\mathcal{Q}_\varepsilon = \left\{ \begin{array}{l} \bar{P}(\varepsilon) \in \mathcal{P}_\varepsilon :\ A(\varepsilon)P(\varepsilon)A(\varepsilon)' + A(\varepsilon)Z(\varepsilon)'B(\varepsilon)' + B(\varepsilon)Z(\varepsilon)A(\varepsilon)' + \\ B(\varepsilon)Z(\varepsilon)P(\varepsilon)^{-1}Z(\varepsilon)'B(\varepsilon)' - P(\varepsilon) + x(t_0)x(t_0)' \prec 0 \end{array} \right\}. \tag{2.37}$$

An alternative LMI based solution to the problem (2.19) is obtained solving the problem [PG94]:

$$\underset{\bar{P}(\varepsilon) \in \mathcal{Q}_\varepsilon}{min}\ J(\varepsilon) = \varepsilon Tr \left(\begin{bmatrix} C'C & 0 \\ 0 & R \end{bmatrix} \bar{P}(\varepsilon) \right). \tag{2.38}$$

Furthermore, if $\bar{P}^*(\varepsilon)$ is optimal, it can be written as:

$$\bar{P}^*(\varepsilon) = \begin{bmatrix} P^*(\varepsilon) & Z^*(\varepsilon)' \\ Z^*(\varepsilon) & U^*(\varepsilon) \end{bmatrix} = \begin{bmatrix} P^*(\varepsilon) & P^*(\varepsilon)K(\varepsilon)' \\ K(\varepsilon)P^*(\varepsilon) & K(\varepsilon)P^*(\varepsilon)K(\varepsilon)' \end{bmatrix},$$

where $K(\varepsilon) = Z^*(\varepsilon)P^*(\varepsilon)^{-1}$ is the optimal gain and

$$\lim_{\varepsilon \to 0} K(\varepsilon) = K = Z^* P^{*-1}. \tag{2.39}$$

Hence, (2.38) may be reformulated as:

$$\begin{aligned} \min_{P(\varepsilon)\succ 0, Z(\varepsilon)} J(\varepsilon) &= \varepsilon Tr\left(\begin{bmatrix} C'C & 0 \\ 0 & R \end{bmatrix} \begin{bmatrix} P(\varepsilon) & Z(\varepsilon)' \\ Z(\varepsilon) & Z(\varepsilon)P(\varepsilon)^{-1}Z(\varepsilon)' \end{bmatrix} \right) \\ subject\ \ to\ & \begin{array}{l} A(\varepsilon)P(\varepsilon)A(\varepsilon)' + A(\varepsilon)Z(\varepsilon)'B(\varepsilon)' + B(\varepsilon)Z(\varepsilon)A(\varepsilon)' + \\ B(\varepsilon)Z(\varepsilon)P(\varepsilon)^{-1}Z(\varepsilon)'B(\varepsilon)' - P(\varepsilon) + x(t_0)x(t_0)' \prec 0. \end{array} \end{aligned} \tag{2.40}$$

When ε is small, numerical difficulties to minimize the criterion $J(\varepsilon)$ arise. This problem is due to the ill-conditioning of the constraint (2.37). As in the LQ classical solution, we can decompose the original problem (2.40) into two well-behaved subproblems :

$$J(\varepsilon) = \varepsilon Tr \left(\begin{array}{c} \begin{bmatrix} C_1' \\ C_2' \end{bmatrix} \begin{bmatrix} C_1 & C_2 \end{bmatrix} \begin{bmatrix} P_1(\varepsilon) & P_2(\varepsilon) \\ P_2(\varepsilon)' & P_3(\varepsilon) \end{bmatrix} + \\ R \begin{bmatrix} Z_1(\varepsilon) & Z_2(\varepsilon) \end{bmatrix} \begin{bmatrix} P_1(\varepsilon) & P_2(\varepsilon) \\ P_2(\varepsilon)' & P_3(\varepsilon) \end{bmatrix}^{-1} \begin{bmatrix} Z_1(\varepsilon)' \\ Z_2(\varepsilon)' \end{bmatrix} \end{array} \right),$$

where

$$P(\varepsilon) = P(\varepsilon)' = \begin{bmatrix} P_1(\varepsilon) & P_2(\varepsilon) \\ P_2(\varepsilon)' & P_3(\varepsilon) \end{bmatrix} = \varepsilon^{-1} \begin{bmatrix} P_1 + O(\varepsilon) & P_2 + O(\varepsilon) \\ P_2' + O(\varepsilon) & P_3 + O(\varepsilon) \end{bmatrix} \succ 0 \tag{2.41}$$

and

$$Z(\varepsilon) = \begin{bmatrix} Z_1(\varepsilon) & Z_2(\varepsilon) \end{bmatrix} = \varepsilon^{-1} \begin{bmatrix} Z_1 + O(\varepsilon) & Z_2 + O(\varepsilon) \end{bmatrix}. \tag{2.42}$$

Given $F(\varepsilon) = P_1(\varepsilon) - P_2(\varepsilon)P_3(\varepsilon)^{-1}P_2(\varepsilon)'$, we obtain:

$$\begin{aligned} J(\varepsilon) =& J_s(\varepsilon) + J_f(\varepsilon) = \\ & \varepsilon Tr\left(\begin{bmatrix} C_1 & C_2 + C_1P_2(\varepsilon)P_3(\varepsilon)^{-1} \end{bmatrix} \begin{bmatrix} F(\varepsilon) & 0 \\ 0 & P_3(\varepsilon) \end{bmatrix} [\star]' \right) + \\ & \varepsilon Tr\left(R \begin{bmatrix} Z_1(\varepsilon) - Z_2(\varepsilon)P_3(\varepsilon)^{-1}P_2(\varepsilon)' & Z_2(\varepsilon) \end{bmatrix} \begin{bmatrix} F(\varepsilon)^{-1} & 0 \\ 0 & P_3(\varepsilon)^{-1} \end{bmatrix} [\star]' \right) \end{aligned}$$

with

$$\begin{aligned} J_s(\varepsilon) =\ & \varepsilon Tr((C_2 + C_1P_2(\varepsilon)'P_3(\varepsilon)^{-1})P_3(\varepsilon) \times \\ & (C_2 + C_1P_2(\varepsilon)'P_3(\varepsilon)^{-1})' + RZ_2(\varepsilon)P_3(\varepsilon)^{-1}Z_2(\varepsilon)'), \\ J_f(\varepsilon) =\ & \varepsilon Tr((C_1(P_1(\varepsilon) - P_2(\varepsilon)P_3(\varepsilon)^{-1}P_2(\varepsilon)')C_1' + R(Z_1(\varepsilon) - Z_2(\varepsilon)P_3(\varepsilon)^{-1} \times \\ & P_2(\varepsilon)')(P_1(\varepsilon) - P_2(\varepsilon)P_3(\varepsilon)^{-1}P_2(\varepsilon)')^{-1}(Z_1(\varepsilon) - Z_2(\varepsilon)P_3(\varepsilon)^{-1}P_2(\varepsilon)')'). \end{aligned}$$

Let us define

$$P_2 = (I_{n_1} - A_{11})^{-1}(A_{12}P_3 + B_1Z_2), \tag{2.43}$$

$$P_s = P_3,\ Z_s = Z_2, \tag{2.44}$$

$$P_f = P_1 - P_2 P_3^{-1} P_2', \; Z_f = Z_1 - Z_2 P_3^{-1} P_2'. \tag{2.45}$$

Hence:

$$\lim_{\varepsilon \to 0} (C_2 + C_1 P_2(\varepsilon) P_3(\varepsilon)^{-1}) =$$
$$C_2 + C_1 (I_{n_1} - A_{11})^{-1} A_{12} + C_1 (I_{n_1} - A_{11})^{-1} B_1 Z_s P_s^{-1} = C_s + D_s Z_s P_s^{-1},$$

$$\lim_{\varepsilon \to 0} J_s(\varepsilon) = J_s = Tr(C_s P_s C_s' + C_s Z_s' D_s' + D_s Z_s C_s' + D_s Z_s P_s^{-1} Z_s' D_s' + R Z_s P_s^{-1} Z_s'),$$

$$\lim_{\varepsilon \to 0} J_f(\varepsilon) = J_f = Tr(C_1 P_f C_1' + R Z_f P_f^{-1} Z_f').$$

The last two equations can be written in the form:

$$J_s = Tr\left(\begin{bmatrix} C_s' C_s & C_s' D_s \\ D_s' C_s & D_s' D_s + R \end{bmatrix} \begin{bmatrix} P_s & Z_s' \\ Z_s & Z_s P_s^{-1} Z_s' \end{bmatrix} \right), \tag{2.46}$$

$$J_f = Tr\left(\begin{bmatrix} C_1' C_1 & 0 \\ 0 & R \end{bmatrix} \begin{bmatrix} P_f & Z_f' \\ Z_f & Z_f P_f^{-1} Z_f' \end{bmatrix} \right), \tag{2.47}$$

with

$$J = J_s + J_f. \tag{2.48}$$

In terms of variables, J_s depends on P_s and Z_s while J_f depends on P_f and Z_f. Thus, two independent optimization subproblems can be defined:

Slow subproblem:

$$\min_{\bar{P}_s \in \mathcal{Q}_s} Tr\left(\begin{bmatrix} C_s' C_s & C_s' D_s \\ D_s' C_s & D_s' D_s + R \end{bmatrix} \bar{P}_s \right), \tag{2.49}$$

with

$$\mathcal{P}_s = \left\{ \bar{P}_s = \begin{bmatrix} P_s & Z_s' \\ Z_s & V_s \end{bmatrix} \succ 0 \right\}$$

and

$$\mathcal{Q}_s = \left\{ \bar{P}_s \in \mathcal{P}_s : A_s P_s + P_s A_s' + B_s Z_s + Z_s' B_s' + x_s^0 x_s^{0\prime} \prec 0 \right\}.$$

Fast subproblem:

$$\min_{\bar{P}_f \in \mathcal{Q}_f} Tr\left(\begin{bmatrix} C_1' C_1 & 0 \\ 0 & R \end{bmatrix} \bar{P}_f \right), \tag{2.50}$$

with

$$\mathcal{P}_f = \left\{ \bar{P}_f = \begin{bmatrix} P_f & Z_f' \\ Z_f & V_f \end{bmatrix} \succ 0 \right\}$$

and

$$\mathcal{Q}_f = \left\{ \bar{P}_f \in \mathcal{P}_f : A_{11} P_f A_{11}' + A_{11} Z_f' B_1' + B_1 Z_f A_{11}' + B_1 Z_f P_f^{-1} Z_f' B_1' - P_f \prec 0 \right\}$$

which, using the Schur complement [BGFB94], becomes

$$\mathcal{Q}_f = \left\{ \bar{P}_f \in \mathcal{P}_f : \begin{bmatrix} P_f & A_{11}P_f + B_1 Z_f \\ (\star)' & P_f \end{bmatrix} \succ 0 \right\}.$$

The following theorem gives a suboptimal solution of the problem (2.38).

Theorem 2 *Assume that the problems (2.49) and (2.50) admit, respectively, the solutions*

$$\bar{P}_s = \begin{bmatrix} P_s & Z_s' \\ Z_s & V_s \end{bmatrix}, \; \bar{P}_f = \begin{bmatrix} P_f & Z_f' \\ Z_f & V_f \end{bmatrix}.$$

Hence, there exists a positive scalar ε_{max} such that the solution $\bar{P}(\varepsilon)$ of the problem (2.38) exists $\forall\, \varepsilon \in (0, \varepsilon_{max}]$ and

$$\lim_{\varepsilon \to 0} J(\varepsilon) = J = J_s + J_f = Tr\left(\begin{bmatrix} C'C & 0 \\ 0 & R \end{bmatrix} \begin{bmatrix} P & Z' \\ Z & ZP^{-1}Z' \end{bmatrix} \right),$$

with

$$P = \begin{bmatrix} P_f + P_2 P_s^{-1} P_2' & P_2 \\ P_2' & P_s \end{bmatrix} \tag{2.51}$$

and

$$Z = \begin{bmatrix} Z_f + Z_s P_s^{-1} P_2' & Z_s \end{bmatrix}. \tag{2.52}$$

Moreover, the composite controller gain (2.39), which guarantees the asymptotic stability of the system (2.17) $\forall\, \varepsilon \in (0, \varepsilon_{max}]$, is:

$$K = \begin{bmatrix} Z_f P_f^{-1} & Z_s P_s^{-1} - Z_f P_f^{-1} (I_{n_1} - A_{11})^{-1} (A_{12} + B_1 Z_s P_s^{-1}) \end{bmatrix}.$$

Proof. See Appendix B.1. ■

Remark 1 *An evaluation of the upper bound ε_{max} is obtained solving the following optimization problem:*

$$\varepsilon_{max} = max\ \varepsilon > 0 \tag{2.53}$$

$$subject\ \ to\ \ P(\varepsilon) \succ 0, \quad \begin{array}{l} A(\varepsilon)P(\varepsilon)A(\varepsilon)' + A(\varepsilon)Z(\varepsilon)'B(\varepsilon)' + B(\varepsilon)Z(\varepsilon)A(\varepsilon)' + \\ B(\varepsilon)Z(\varepsilon)P(\varepsilon)^{-1}Z(\varepsilon)'B(\varepsilon)' - P(\varepsilon) + x(t_0)x(t_0)' \prec 0, \end{array}$$

where $A(\varepsilon)$, $B(\varepsilon)$, $P(\varepsilon)$ and $Z(\varepsilon)$ are defined in (2.18) and (2.41)-(2.45), respectively. The values of P_f, Z_f, P_s and Z_s can be computed by Theorem 2.

Remark 2 *The conditions of Theorem 2 with $Z_f = 0$ lead to the reduced control law:*

$$u(k) = \begin{bmatrix} 0 & K_s \end{bmatrix} \begin{bmatrix} x_1(k) \\ x_2(k) \end{bmatrix}, \tag{2.54}$$

where $K_s = Z_s P_s^{-1}$ is the optimal controller gain of the slow subsystem. Notice that, in this case, the fast subproblem (2.50) has a solution only if A_{11} is Schur.

2.3.2 Slow sampling control law

The slow sampling LQ optimization problem (2.29) may be formulated in a convex form using a similar procedure to the fast sampling control design illustrated in the previous section. Let define the sets

$$\mathcal{P}_\varepsilon = \left\{ \bar{P}(\varepsilon) = \begin{bmatrix} P(\varepsilon) & Z(\varepsilon)' \\ Z(\varepsilon) & U(\varepsilon) \end{bmatrix} \succeq 0,\ P(\varepsilon) \succ 0 \right\} \tag{2.55}$$

and

$$\mathcal{Q}_\varepsilon = \left\{ \begin{array}{l} \bar{P}(\varepsilon) \in \mathcal{P}_\varepsilon :\ \tilde{A}(\varepsilon)P(\varepsilon)\tilde{A}(\varepsilon)' + \tilde{A}(\varepsilon)Z(\varepsilon)'\tilde{B}' + \tilde{B}Z(\varepsilon)\tilde{A}(\varepsilon)' + \\ \tilde{B}Z(\varepsilon)P(\varepsilon)^{-1}Z(\varepsilon)'\tilde{B}' - P(\varepsilon) + x(t_0)x(t_0)' \prec 0 \end{array} \right\}. \tag{2.56}$$

From

$$\min_{\bar{P}(\varepsilon)\in\mathcal{Q}_\varepsilon} J(\varepsilon) = Tr\left(\begin{bmatrix} C'C & 0 \\ 0 & R \end{bmatrix} \bar{P}(\varepsilon) \right), \tag{2.57}$$

$$\bar{P}^*(\varepsilon) = \begin{bmatrix} P^*(\varepsilon) & Z^*(\varepsilon)' \\ Z^*(\varepsilon) & U^*(\varepsilon) \end{bmatrix} = \begin{bmatrix} P^*(\varepsilon) & P^*(\varepsilon)K(\varepsilon)' \\ K(\varepsilon)P^*(\varepsilon) & K(\varepsilon)P^*(\varepsilon)K(\varepsilon)' \end{bmatrix},$$

where $K(\varepsilon) = Z^*(\varepsilon)P^*(\varepsilon)^{-1}$ is the optimal gain and

$$\lim_{\varepsilon\to 0} K(\varepsilon) = K = Z^* P^{*-1}. \tag{2.58}$$

We obtain:

$$\min_{P(\varepsilon)\succ 0, Z(\varepsilon)} J(\varepsilon) = Tr\left(\begin{bmatrix} C'C & 0 \\ 0 & R \end{bmatrix} \begin{bmatrix} P(\varepsilon) & Z(\varepsilon)' \\ Z(\varepsilon) & Z(\varepsilon)P(\varepsilon)^{-1}Z(\varepsilon)' \end{bmatrix} \right) \tag{2.59}$$

$$subject\ \ to \quad \begin{array}{l} \tilde{A}(\varepsilon)P(\varepsilon)\tilde{A}(\varepsilon)' + \tilde{A}(\varepsilon)Z(\varepsilon)'\tilde{B}' + \tilde{B}Z(\varepsilon)\tilde{A}(\varepsilon)' + \\ \tilde{B}Z(\varepsilon)P(\varepsilon)^{-1}Z(\varepsilon)'\tilde{B}' - P(\varepsilon) + x(t_0)x(t_0)' \prec 0. \end{array}$$

Decomposing the criterion

$$J(\varepsilon) = Tr\left(\begin{array}{c} \begin{bmatrix} 0 \\ C_2' \end{bmatrix} \begin{bmatrix} 0 & C_2 \end{bmatrix} \begin{bmatrix} P_1(\varepsilon) & P_2(\varepsilon) \\ P_2(\varepsilon)' & P_3(\varepsilon) \end{bmatrix} + \\ R \begin{bmatrix} Z_1(\varepsilon) & Z_2(\varepsilon) \end{bmatrix} \begin{bmatrix} P_1(\varepsilon) & P_2(\varepsilon) \\ P_2(\varepsilon)' & P_3(\varepsilon) \end{bmatrix}^{-1} \begin{bmatrix} Z_1(\varepsilon)' \\ Z_2(\varepsilon)' \end{bmatrix} \end{array} \right),$$

with

$$P(\varepsilon) = P(\varepsilon)' = \begin{bmatrix} P_1(\varepsilon) & P_2(\varepsilon) \\ P_2(\varepsilon)' & P_3(\varepsilon) \end{bmatrix} = \begin{bmatrix} \varepsilon^{-1}P_1 & P_2 + O(\varepsilon) \\ P_2' + O(\varepsilon) & P_3 + O(\varepsilon) \end{bmatrix} \succ 0 \tag{2.60}$$

and

$$Z(\varepsilon) = \begin{bmatrix} Z_1(\varepsilon) & Z_2(\varepsilon) \end{bmatrix} = \begin{bmatrix} O(\varepsilon) & Z_2 + O(\varepsilon) \end{bmatrix}, \tag{2.61}$$

and defining

$$P_f = P_1,\ P_s = P_3,\ Z_s = Z_2, \tag{2.62}$$

we have:

$$\lim_{\varepsilon\to 0} J(\varepsilon) = J_s = Tr(\tilde{C}_s P_s \tilde{C}_s' + R Z_s P_s^{-1} Z_s') = Tr\left(\begin{bmatrix} \tilde{C}_s'\tilde{C}_s & 0 \\ 0 & R \end{bmatrix} \begin{bmatrix} P_s & Z_s' \\ Z_s & Z_s P_s^{-1} Z_s' \end{bmatrix}\right). \tag{2.63}$$

The *slow subproblem* is:

$$\min_{\bar{P}_s \in \mathcal{Q}_s} Tr\left(\begin{bmatrix} \tilde{C}_s'\tilde{C}_s & 0 \\ 0 & R \end{bmatrix} \bar{P}_s\right), \tag{2.64}$$

with

$$\mathcal{P}_s = \left\{ \bar{P}_s = \begin{bmatrix} P_s & Z_s' \\ Z_s & V_s \end{bmatrix} \succ 0 \right\}$$

and

$$\mathcal{Q}_s = \left\{ \bar{P}_s \in \mathcal{P}_s : \begin{bmatrix} P_s & \tilde{A}_s P_s + \tilde{B}_s Z_s & x_s^0 \\ (\star)' & P_s & 0 \\ (\star)' & (\star)' & I_{n_2} \end{bmatrix} \succ 0 \right\}.$$

The following theorem gives a suboptimal solution of the problem (2.57).

Theorem 3 *Assume that the problem (2.64) admits the solution*

$$\bar{P}_s = \begin{bmatrix} P_s & Z_s' \\ Z_s & V_s \end{bmatrix}.$$

Hence, there exists a positive scalar ε_{max} such that the solution $\bar{P}(\varepsilon)$ of the problem (2.57) exists $\forall\, \varepsilon \in (0, \varepsilon_{max}]$ and

$$\lim_{\varepsilon\to 0} J(\varepsilon) = J_s = Tr\left(\begin{bmatrix} \tilde{C}_s'\tilde{C}_s & 0 \\ 0 & R \end{bmatrix} \begin{bmatrix} P_s & Z_s' \\ Z_s & Z_s P_s^{-1} Z_s' \end{bmatrix}\right).$$

Moreover, the composite controller gain (2.58), which guarantees the asymptotic stability of the closed loop system (2.27) $\forall\, \varepsilon \in (0, \varepsilon_{max}]$, is $K = \begin{bmatrix} 0 & Z_s P_s^{-1} \end{bmatrix}$.

Proof. From (2.60), we have:

$$P(\varepsilon)^{-1} = \begin{bmatrix} \varepsilon(P_1 + O(\varepsilon))^{-1} & -\varepsilon(P_1 + O(\varepsilon))^{-1} P_2(\varepsilon) P_3(\varepsilon)^{-1} \\ (\star)' & P_3(\varepsilon)^{-1} + O(\varepsilon) \end{bmatrix} \succ 0. \tag{2.65}$$

Substituting (2.28), (2.33), (2.60), (2.61), (2.62) and (2.65) in (2.56), we obtain:

$$\begin{bmatrix} \varepsilon^{-1} X_1(\varepsilon) & X_2(\varepsilon) \\ X_2(\varepsilon)' & X_3(\varepsilon) \end{bmatrix} \prec 0, \tag{2.66}$$

with

$$X_1(\varepsilon) = \varepsilon(\tilde{A}_{12} + \tilde{B}_1 Z_s P_s^{-1}) P_s (\tilde{A}_{12} + \tilde{B}_1 Z_s P_s^{-1})' + \varepsilon x_1^0 x_1^{0\prime} - P_f + O(\varepsilon^2),$$

$$X_2(\varepsilon) = \tilde{A}_{12}P_s\tilde{A}_s' + \tilde{A}_{12}Z_s'\tilde{B}_s' + \tilde{B}_1Z_s\tilde{A}_s' + \tilde{B}_1Z_sP_s^{-1}Z_s'\tilde{B}_s' + x_1^0x_s^{0\prime} - P_2 + O(\varepsilon),$$
$$X_3(\varepsilon) = \tilde{A}_sP_s\tilde{A}_s' + \tilde{A}_sZ_s'\tilde{B}_s' + \tilde{B}_sZ_s\tilde{A}_s' + \tilde{B}_sZ_sP_s^{-1}Z_s'\tilde{B}_s' + x_s^0x_s^{0\prime} - P_s + O(\varepsilon).$$

When $\varepsilon \to 0$, we get:

$$X_1 = -P_f \prec 0, \tag{2.67}$$

$$X_2 = \tilde{A}_{12}P_s\tilde{A}_s' + \tilde{A}_{12}Z_s'\tilde{B}_s' + \tilde{B}_1Z_s\tilde{A}_s' + \tilde{B}_1Z_sP_s^{-1}Z_s'\tilde{B}_s' + x_1^0x_s^{0\prime} - P_2, \tag{2.68}$$

$$X_3 = \tilde{A}_sP_s\tilde{A}_s' + \tilde{A}_sZ_s'\tilde{B}_s' + \tilde{B}_sZ_s\tilde{A}_s' + \tilde{B}_sZ_sP_s^{-1}Z_s'\tilde{B}_s' + x_s^0x_s^{0\prime} - P_s \prec 0. \tag{2.69}$$

Using the Schur complement, the condition (2.69) represents the constraint of slow the subproblem (2.64). Hence, it is satisfied by assumption, with $P_s \succ 0$. Replacing (2.67)-(2.69) in (2.66), we obtain:

$$\begin{bmatrix} \varepsilon^{-1}(X_1 + O(\varepsilon)) & X_2 + O(\varepsilon) \\ X_2' & X_3 + O(\varepsilon) \end{bmatrix} \prec 0. \tag{2.70}$$

The condition $X_1 \prec 0$ implies that there exist matrices $P_f \succ 0$, P_2 and a scalar $\varepsilon_1 > 0$ such that the inequality

$$X_1 - \varepsilon(X_2(X_3 + O(\varepsilon))^{-1}X_2' + O(\varepsilon)) + O(\varepsilon) \prec 0$$

holds $\forall\, \varepsilon \in (0, \varepsilon_1]$. Hence, using the Schur complement, also (2.70) holds $\forall\, \varepsilon \in (0, \varepsilon_1]$. Moreover, there exists a scalar $\varepsilon_2 > 0$ such that the inequality

$$P_f - \varepsilon P_2(P_s + O(\varepsilon))^{-1}P_2' + O(\varepsilon^2) \succ 0$$

holds, $\forall\, \varepsilon \in (0, \varepsilon_2]$. Hence, using the Schur complement, $P(\varepsilon) \succ 0\ \forall\, \varepsilon \in (0, \varepsilon_2]$. Thus, there exist matrices P_s, Z_s and P_f and a scalar $\varepsilon_{max} = min\{\varepsilon_1, \varepsilon_2\}$ that verify the constraints (2.55)-(2.56) of the problem (2.57), $\forall\, \varepsilon \in (0, \varepsilon_{max}]$.

When $\varepsilon \to 0$, from (2.61) and (2.65) we have

$$K = Z(\varepsilon)P(\varepsilon)^{-1} = \begin{bmatrix} 0 & Z_sP_s^{-1} \end{bmatrix},$$

which concludes the proof. ■

Remark 3 *An evaluation of the upper bound ε_{max} is obtained solving the following optimization problem:*

$$\varepsilon_{max} = \max_{P_f}\ \varepsilon > 0 \tag{2.71}$$
$$\text{subject to } P(\varepsilon) \succ 0, \quad \begin{array}{l} \tilde{A}(\varepsilon)P(\varepsilon)\tilde{A}(\varepsilon)' + \tilde{A}(\varepsilon)Z(\varepsilon)'\tilde{B}' + \tilde{B}Z(\varepsilon)\tilde{A}(\varepsilon)' + \\ \tilde{B}Z(\varepsilon)P(\varepsilon)^{-1}Z(\varepsilon)'\tilde{B}' - P(\varepsilon) + x(t_0)x(t_0)' \prec 0, \end{array}$$

where $\tilde{A}(\varepsilon)$, $\tilde{B}$, $P(\varepsilon)$ and $Z(\varepsilon)$ are defined in (2.28) and (2.60)-(2.62), respectively. The values of P_s and Z_s are given by Theorem 3. Since a control law based on the slow sampling model cannot influence the fast transient, Theorem 3 does not provide a solution for the fast subproblem. Hence, the value of P_f can be chosen in order to maximize the value of ε_{max}, under the constraints of the problem 2.71.

2.3.3 Numerical example

Consider the state matrices (1.15), introduced in Chapter 1. They correspond to the 4-stands subsystem of an average product of the Eisenhüttenstadt HSM database, with $\varepsilon = 0.05$. Let us assume, in a first moment, that there exist no bounds on the rate actuators. In this case, we could resort to the fast sampling model (2.13) in order to control both slow and fast dynamics. Choosing $\alpha_f = 0.1$, we have $T_f = 0.005\,sec$. Using formulae (2.14), we get the following discrete-time state matrices:

$$A_{11} = \begin{bmatrix} 0.6849 & -0.0212 & -0.0008 \\ -0.1837 & 0.6938 & 0.0509 \\ -0.1325 & -0.2486 & 0.6543 \end{bmatrix},$$

$$A_{12} = \begin{bmatrix} -0.0841 & 0.0000 & -0.0000 & -0.0000 & -0.0000 \\ -0.0223 & 0.0000 & 0.0000 & -0.0000 & 0.0000 \\ -0.0252 & 0.0000 & 0.0000 & 0.0000 & -0.0000 \end{bmatrix},$$

$$A_{21} = 10^3 \begin{bmatrix} -0.0004 & 0.0000 & 0.0000 \\ 0 & 0 & 0 \\ 0.6211 & -0.009 & -0.0002 \\ -0.1198 & 0.974 & 0.0338 \\ -0.1318 & -0.227 & 1.3 \end{bmatrix},$$

$$A_{22} = 10^2 \begin{bmatrix} -0.0013 & 0.0000 & -0.0000 & 0.0000 & 0.0000 \\ 4.1744 & 0 & 0 & 0 & 0 \\ -0.3345 & 0.0001 & -0.0002 & -0.0000 & -0.0000 \\ -0.1565 & 0.0000 & 0.0004 & -0.0005 & 0.0000 \\ -0.2525 & 0.0000 & 0.0001 & 0.0005 & -0.0007 \end{bmatrix},$$

$$B_1 = \begin{bmatrix} 0.0006 & 0.0031 & -0.0000 & -0.0000 \\ 0.0006 & 0.0022 & 0.0069 & 0.0004 \\ 0.0006 & 0.0023 & 0.0062 & 0.0138 \end{bmatrix},$$

$$B_2 = \begin{bmatrix} 0.0093 & 0.0095 & -0.0045 & -0.002 \\ 0 & 0 & 0 & 0 \\ -2.224 & -12.113 & 5.74 & 2.59 \\ 2.108 & 16.784 & -46.07 & -31.82 \\ 2.526 & 4.011 & 73.13 & -35.17 \end{bmatrix},$$

$$C_1 = \begin{bmatrix} 1 & 0 & 0 \\ 0 & 1 & 0 \\ 0 & 0 & 1 \\ 0 & 0 & 0 \\ 0 & 0 & 0 \end{bmatrix}, \; C_2 = \begin{bmatrix} 1 & 0 & 0 & 0 & 0 \\ 0 & 1 & 0 & 0 & 0 \\ 0 & 0 & 1 & 0 & 0 \\ 0 & 0 & 0 & 1 & 0 \\ 0 & 0 & 0 & 0 & 1 \end{bmatrix}.$$

Let the weighting matrix $R = 100I_5$. Theorem 2 leads to the following controller gain:

$$K = \begin{bmatrix} -0.1 & 0 & 0 & -97.883 & -0.1052 & -0.0034 & 0.0034 & -0.0038 \\ 0 & -0.1 & 0 & -22.1287 & -0.0076 & 0.0551 & -0.0434 & -0.0158 \\ 0 & 0 & -0.1 & 9.5851 & 0.01 & -0.014 & 0.0115 & -0.0366 \\ 0 & 0 & 0 & -15.3011 & -0.004 & 0.0392 & 0.0741 & 0.0112 \end{bmatrix}.$$

Now, let consider the real scenario of Eisenhüttenstadt HSM, where the lower bound on the sampling time is fixed to $T_{low} = 0.04\,sec$, due to the limitations on the actuators rate. Hence the fast dynamics, which is open loop stable, cannot be controlled. In this case, it is quite natural to design a reduced control law using the slow sampling model (2.15). Let choose $\alpha_s = 0.5$. We obtain $T_s = 0.05\,sec$. Using formulae (2.16), we obtain the following discrete-time state matrices:

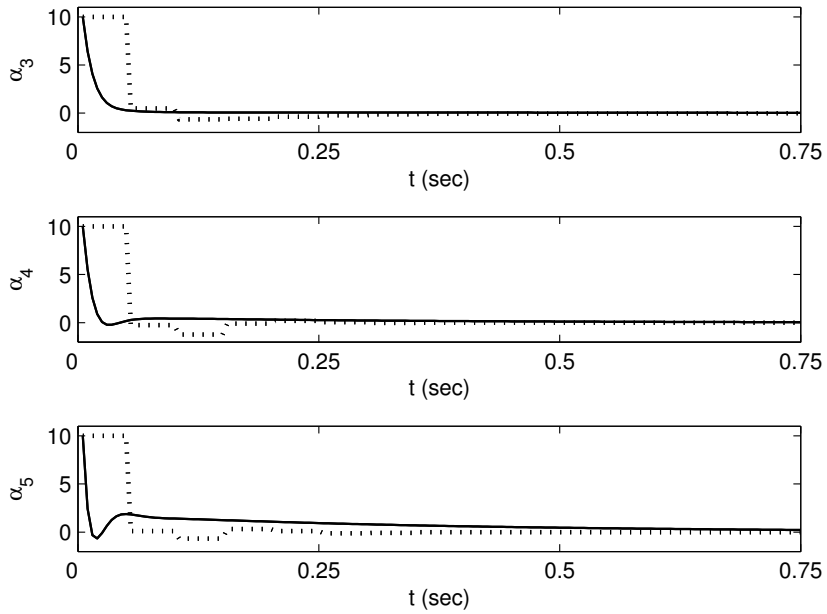

Figure 2.1: Closed loop response of x_1^4 using the fast sampling controller (solid line, $T_f = 0.005$) and the slow sampling controller (dotted-line, $T_s = 0.05$)

$$\tilde{A}_{11} = \begin{bmatrix} 0.5549 & -0.127 & -0.0467 \\ -0.3236 & -0.407 & 0.1387 \\ 0.4222 & 0.41 & -0.6266 \end{bmatrix},$$

$$\tilde{A}_{12} = \begin{bmatrix} -0.23 & 0.0000 & -0.0002 & -0.0000 & -0.0000 \\ 0.038 & -0.0000 & 0.0002 & -0.0001 & 0.0000 \\ -0.0008 & 0.0000 & -0.0000 & 0.0002 & -0.0002 \end{bmatrix},$$

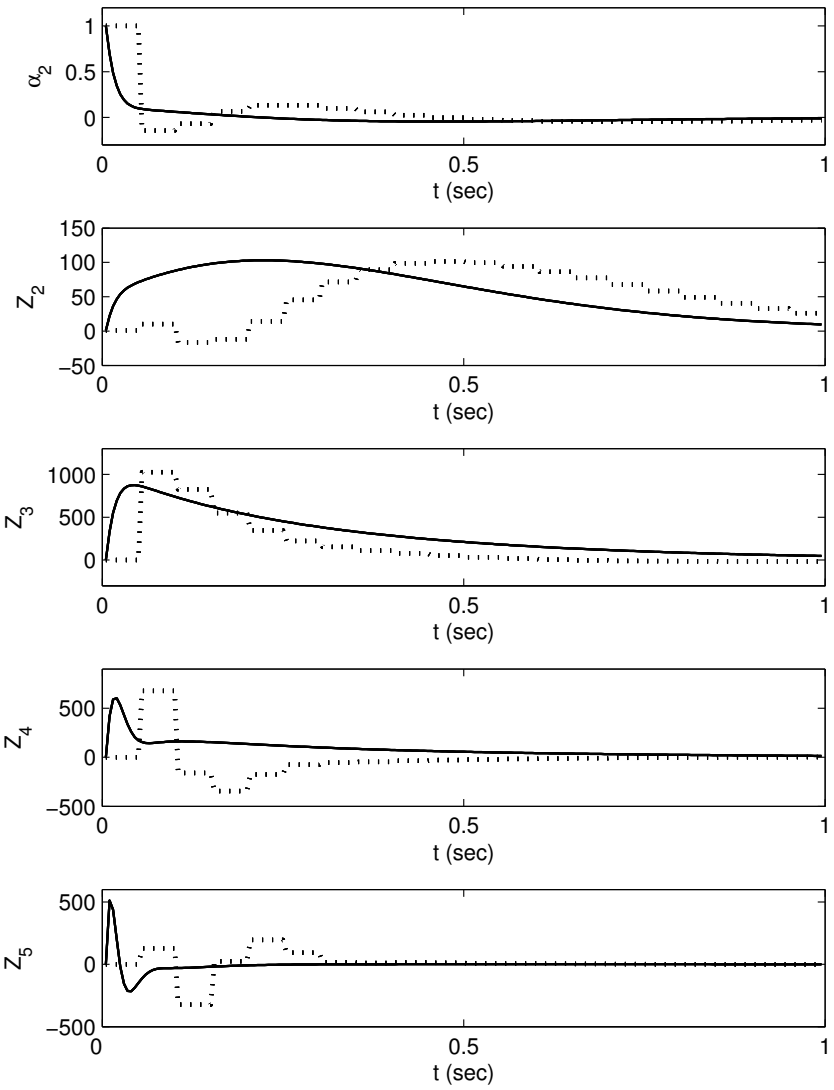

Figure 2.2: Closed loop response of x_2^4 using the fast sampling controller (solid line, $T_f = 0.005$) and the slow sampling controller (dotted-line, $T_s = 0.05$)

$$\tilde{A}_{21} = 10^3 \begin{bmatrix} -0.0016 & 0.0001 & 0.0000 \\ -0.3417 & 0.0254 & 0.0046 \\ 2.0446 & -0.1558 & -0.0289 \\ -1.6887 & 2.52 & 0.469 \\ -0.5125 & -2.0625 & 2.812 \end{bmatrix},$$

$$\tilde{A}_{22} = 10^2 \begin{bmatrix} 0.01 & 0.0000 & -0.0000 & 0.0000 & 0.0000 \\ 2.087 & 0.01 & -0.0000 & 0.0000 & 0.0000 \\ -0.937 & 0.0003 & 0.0091 & -0.0000 & -0.0000 \\ 0.353 & -0.0001 & 0.0018 & 0.0087 & 0.0000 \\ -0.111 & 0.0000 & -0.0005 & 0.0024 & 0.0082 \end{bmatrix},$$

$$\tilde{B}_1 = \begin{bmatrix} 0.0009 & 0.0097 & -0.002 & -0.0006 \\ 0.0012 & 0.0024 & 0.02 & 0.0068 \\ 0.0004 & 0.0016 & 0.0057 & 0.03 \end{bmatrix},$$

$$\tilde{B}_2 = \begin{bmatrix} 0.0032 & -0.0029 & 0.0006 & 0.0002 \\ 0.3386 & -0.304 & 0.06 & 0.019 \\ 0.5154 & 3.666 & -0.73 & -0.24 \\ 0.627 & 1.166 & 12.93 & 4.226 \\ 0.3476 & 1.36 & 2.98 & 25.6 \end{bmatrix},$$

$$C_1 = \begin{bmatrix} 0 & 0 & 0 \\ 0 & 0 & 0 \\ 0 & 0 & 0 \\ 0 & 0 & 0 \\ 0 & 0 & 0 \end{bmatrix}, \; C_2 = \begin{bmatrix} 1 & 0 & 0 & 0 & 0 \\ 0 & 1 & 0 & 0 & 0 \\ 0 & 0 & 1 & 0 & 0 \\ 0 & 0 & 0 & 1 & 0 \\ 0 & 0 & 0 & 0 & 1 \end{bmatrix}.$$

Theorem 3 yields the following controller gain:

$$K = \begin{bmatrix} 0 & 0 & 0 & -73.898 & -0.0857 & -0.0151 & 0.0016 & -0.0004 \\ 0 & 0 & 0 & 61.091 & 0.0013 & -0.0481 & -0.0007 & -0.0012 \\ 0 & 0 & 0 & -2.1477 & 0.0007 & -0.0297 & -0.0408 & 0.0054 \\ 0 & 0 & 0 & -1.1542 & -0.0005 & 0.006 & -0.0226 & -0.0271 \end{bmatrix}.$$

Consider the initial conditions

$$x^4(0) = \begin{bmatrix} x_1^4(0)' & x_2^4(0)' \end{bmatrix}' = \begin{bmatrix} 10 & 10 & 10 & 1 & 1 & 1 & 1 & 1 \end{bmatrix}',$$

where $x_1^4 = \begin{bmatrix} \alpha_3 & \alpha_4 & \alpha_5 \end{bmatrix}'$ is the state vector corresponding to the fast dynamics and $x_2^4 = \begin{bmatrix} \alpha_2 & Z_2 & Z_3 & Z_4 & Z_5 \end{bmatrix}'$ is the state vector corresponding to the slow dynamics. Fig. 2.1 shows the closed loop response corresponding to x_1^4 using the fast sampling controller (solid line) and the slow sampling controller (dotted-line). Fig. 2.2 shows the closed loop response corresponding to x_2^4 using the fast sampling controller (solid line) and the slow sampling controller (dotted-line).

2.4 An extension to uncertain systems in the polytopic form

2.4.1 Slow sampling control law

This section aims at extending the results of Theorem 3 to uncertain two time scale systems in the polytopic form and designing a H_2 robust controller for this class of systems. Consider the slow sampling two time scale system:

$$\begin{cases} x(s+1) = \mathfrak{A}(s)x(s) + \mathfrak{B}_u(s)u(s) + \mathfrak{B}_d(s)d(s) \\ q(s) = Cx(s) + Du(s), \end{cases} \tag{2.72}$$

where $d(s) \in \mathbb{R}^h$ is the external perturbation, for all $s \in \mathbb{Z}^+ \geq t_0$, and

$$\mathfrak{A}(s) = \sum_{l=1}^{N_V} \lambda_l(s)\tilde{A}^l(\varepsilon), \quad \mathfrak{B}_u(s) = \sum_{l=1}^{N_V} \lambda_l(s)\tilde{B}_u^l, \quad \mathfrak{B}_d(s) = \sum_{l=1}^{N_V} \lambda_l(s)\tilde{B}_d^l,$$

with $l \in \mathcal{L}$. λ_l denotes the uncertainty and belongs to the unit simplex

$$\mathfrak{Y}(s) = \{\sum_{l=1}^{N_V} \lambda_l(s) = 1, \ \lambda_l(s) \geq 0\}.$$

The matrices $\tilde{A}^l(\varepsilon)$, $\tilde{B}_u^l$, $\tilde{B}_d^l$ and C are defined as:

$$\tilde{A}^l(\varepsilon) = \begin{bmatrix} \varepsilon\tilde{A}_{11}^l & \tilde{A}_{12}^l \\ \varepsilon\tilde{A}_{21}^l & \tilde{A}_{22}^l \end{bmatrix}, \quad \tilde{B}_u^l = \begin{bmatrix} \tilde{B}_{u,1}^l \\ \tilde{B}_{u,2}^l \end{bmatrix}, \quad \tilde{B}_d^l = \begin{bmatrix} \tilde{B}_{d,1}^l \\ \tilde{B}_{d,2}^l \end{bmatrix}, \quad C = \begin{bmatrix} 0 & C_2 \end{bmatrix}, \tag{2.73}$$

for any $l \in \mathcal{L}$. The two time scale linear system corresponding to each vertex l of (2.72) may be written in the form:

$$\begin{cases} x_1(s+1) = \varepsilon\tilde{A}_{11}^l x_1(s) + \tilde{A}_{12}^l x_2(s) + \tilde{B}_{u,1}^l u(s) + \tilde{B}_{d,1}^l d(s) \\ x_2(s+1) = \varepsilon\tilde{A}_{21}^l x_1(s) + \tilde{A}_{22}^l x_2(s) + \tilde{B}_{u,2}^l u(s) + \tilde{B}_{d,2}^l d(s), \\ q(s) = C_2 x_2(s) + Du(s). \end{cases}$$

Its slow subsystem is:

$$\begin{cases} x_s(s+1) = \tilde{A}_s^l x_s(s) + \tilde{B}_{u,s}^l u_s(s) + \tilde{B}_{d,s}^l d(s) \\ q(s) = \tilde{C}_s x_s(s) + \tilde{D}_s u_s(s), \end{cases}$$

where $\tilde{A}_s^l = \tilde{A}_{22}^l$, $\tilde{B}_{u,s}^l = \tilde{B}_{u,2}^l$, $\tilde{B}_{d,s}^l = \tilde{B}_{d,2}^l$, $\tilde{C}_s = C_2$ and $\tilde{D}_s = D$. The pair $(\tilde{A}_s^l, \tilde{B}_{u,s}^l)$ is assumed to be controlable, for any $l \in \mathcal{L}$. For simplicity reasons, we assume that the weighting matrices $\tilde{C}_s$ and $\tilde{D}_s$ respect the orthogonality hypothesis $\tilde{C}_s'\tilde{D}_s = 0$, $\tilde{D}_s'\tilde{D}_s \succ 0$. Consider the state-feedback control law

$$u_s(s) = K_s x_s(s),$$

the transfer matrix between q and d is

$$H_{dq}^l(\varsigma) = (\tilde{C}_s + \tilde{D}_s K_s)(\varsigma I_{n_2} - \tilde{A}_s^l - \tilde{B}_{u,s}^l K_s)^{-1}\tilde{B}_{d,s}^l$$

and its H_2 norm is

$$\|H_{dq}^l\|_2^2 = \frac{1}{2\pi}\int_{-\pi}^{\pi} Tr\{H_{dq}^l(\varsigma)^* H_{dq}^l(\varsigma)\}d\omega \tag{2.74}$$

with $\varsigma = e^{j\omega}$, for any $l \in \mathcal{L}$. The following theorem designs a suboptimal state-feedback control law

$$u(s) = Kx(s) \tag{2.75}$$

which asymptotically stabilizes the polytopic two time scale system (2.72) and minimizes the H_2 norm of its slow dynamics, with $K = [0 \ K_s]$.

Theorem 4 *Assume that there exist matrices $W_s = W_s' \succ 0$, $P_s = P_s' \succ 0$, Z_s of appropriate dimensions, and a scalar $\mu > 0$ such that LMIs*

$$Tr\left(W_s\right) < \mu \tag{2.76}$$

$$\begin{bmatrix} W_s & \tilde{C}_s P_s + \tilde{D}_s Z_s \\ (\star)' & P_s \end{bmatrix} \succ 0, \tag{2.77}$$

and

$$\begin{bmatrix} P_s & \tilde{A}_s^l P_s + \tilde{B}_{u,s}^l Z_s & \tilde{B}_{d,s}^l \\ (\star)' & P_s & 0 \\ (\star)' & (\star)' & I_{n_2} \end{bmatrix} \succ 0 \tag{2.78}$$

are verified $\forall\, l \in \mathcal{L}$. Hence, there exists a positive scalar ε_{max} such that the state-feedback controller gain $K = [0 \;\; K_s]$, with $K_s = Z_s P_s^{-1}$, stabilizes asymptotically the closed loop system (2.72), $\forall\, \varepsilon \in (0, \varepsilon_{max}]$. Moreover, the controller gain K_s solution of the problem:

$$\min_{W_s, Z_s, P_s} \mu \tag{2.79}$$

$$\textit{subject to} \quad (2.76)\text{-}(2.78)$$

minimizes the H_2 norm (2.74).

Proof. A well-known sufficient condition for asymptotic stability of the closed loop system (2.72) is to find a set of Lyapunov matrices

$$P^l(\varepsilon) = P^l(\varepsilon)' = \begin{bmatrix} \varepsilon^{-1} P_f^l & P_2^l + O(\varepsilon) \\ P_2^{l'} + O(\varepsilon) & P_s + O(\varepsilon) \end{bmatrix} \succ 0, \tag{2.80}$$

and a matrix

$$Z(\varepsilon) = \begin{bmatrix} 0 & Z_s + O(\varepsilon) \end{bmatrix} \tag{2.81}$$

such that the inequality

$$\begin{aligned} &\tilde{A}^l(\varepsilon) P^l(\varepsilon) \tilde{A}^l(\varepsilon)' + \tilde{A}^l(\varepsilon) Z(\varepsilon)' \tilde{B}_u^{l'} + \tilde{B}_u^l Z(\varepsilon) \tilde{A}^l(\varepsilon)' + \\ &\tilde{B}_u^l Z(\varepsilon) P^l(\varepsilon)^{-1} Z(\varepsilon)' \tilde{B}_u^{l'} - P^l(\varepsilon) + \tilde{B}_d^l \tilde{B}_d^{l'} \prec 0 \end{aligned} \tag{2.82}$$

holds, $\forall\, l \in \mathcal{L}$. Decomposing the inequality (2.82) as in the LTI case, we find:

$$\begin{bmatrix} \varepsilon^{-1}(X_1^l + O(\varepsilon)) & X_2^l + O(\varepsilon) \\ X_2^{l'} & X_3^l + O(\varepsilon) \end{bmatrix} \prec 0, \tag{2.83}$$

with

$$X_1^l = -P_f^l \prec 0, \tag{2.84}$$

$$X_2^l = \tilde{A}_{12}^l P_s \tilde{A}_s^{l'} + \tilde{A}_{12}^l Z_s' \tilde{B}_{d,s}^{l'} + \tilde{B}_{d,1}^l Z_s \tilde{A}_s^{l'} + \tilde{B}_{u,1}^l Z_s P_s^{-1} Z_s' \tilde{B}_{u,s}^{l'} + \tilde{B}_{u,1}^l \tilde{B}_{u,s}^{l'} - P_2^l, \tag{2.85}$$

$$X_3^l = \tilde{A}_s^l P_s \tilde{A}_s^{l'} + \tilde{A}_s^l Z_s' \tilde{B}_{u,s}^{l'} + \tilde{B}_{u,s}^l Z_s \tilde{A}_s^{l'} + \tilde{B}_{u,s}^l Z_s P_s^{-1} Z_s' \tilde{B}_{u,s}^{l'} + \tilde{B}_{d,s}^l \tilde{B}_{d,s}^{l'} - P_s \prec 0. \tag{2.86}$$

Using the Schur complement, the condition (2.86) corresponds to (2.78). Hence, it is satisfied by assumption, with $P_s \succ 0$. This means that there exist matrices $P_f^l \succ 0$ and a scalar $\varepsilon_1 > 0$ such that the inequality

$$X_1^l - \varepsilon(X_2^l(X_3^l + O(\varepsilon))^{-1} X_2^{l'} + O(\varepsilon)) + O(\varepsilon) \prec 0$$

holds, $\forall\, l \in \mathcal{L}$ and $\forall\, \varepsilon \in (0, \varepsilon_1]$. Thus, using the Schur complement, (2.83) holds $\forall\, \varepsilon \in (0, \varepsilon_1]$. Moreover, there exists a scalar $\varepsilon_2 > 0$ such that the inequality

$$P_f^l - \varepsilon P_2^l (P_s + O(\varepsilon))^{-1} P_2^{l'} + O(\varepsilon^2) \succ 0$$

holds, $\forall\, l \in \mathcal{L}$ and $\forall\, \varepsilon \in (0, \varepsilon_2]$. Hence, using the Schur complement, $P^l(\varepsilon) \succ 0$, $\forall\, l \in \mathcal{L}$ and $\forall\, \varepsilon \in (0, \varepsilon_2]$. Thus, there exist matrices P_s, Z_s, P_f^l, P_2^l and a scalar $\varepsilon_{max} = min\{\varepsilon_1, \varepsilon_2\}$ which verify the constraint (2.80)-(2.82), $\forall\, l \in \mathcal{L}$ and $\forall\, \varepsilon \in (0, \varepsilon_{max}]$. Further, when $\varepsilon \to 0$, we have $K = Z(\varepsilon) P^l(\varepsilon)^{-1} = \begin{bmatrix} 0 & Z_s P_s^{-1} \end{bmatrix}$.

To prove that the controller K minimizes the H_2 norm (2.74), $\forall\, l \in \mathcal{L}$ and $\forall\, \varepsilon \in (0, \varepsilon_{max}]$, consider the performance index

$$J_s = Tr\left(\begin{bmatrix} \tilde{C}_s' \tilde{C}_s & 0 \\ 0 & \tilde{D}_s' \tilde{D}_s \end{bmatrix} \begin{bmatrix} P_s & Z_s' \\ Z_s & Z_s P_s^{-1} Z_s' \end{bmatrix} \right).$$

Applying the Schur complement to (2.77), we obtain :

$$W_s \succ \tilde{C}_s P_s \tilde{C}_s' + \tilde{D}_s Z_s P_s^{-1} Z_s{}' \tilde{D}_s'.$$

Thus:

$$Tr(W_s) \succ Tr(\, \tilde{C}_s P_s \tilde{C}_s' + \tilde{D}_s Z_s P_s^{-1} Z_s' \tilde{D}_s') = J_s.$$

Under the choice $\tilde{B}_{d,s}^l = x_s^{0,l}$, minimizing J_s corresponds to minimize the H_2 norm (2.74) [PG94]. Hence, $\|H_{dq}^l\|_2^2 \leq \mu$, $\forall\, l \in \mathcal{L}$, which concludes the proof. ■

Remark 4 *An evaluation of the upper bound ε_{max} is obtained solving the following optimization problem:*

$$\varepsilon_{max} = \max_{P_f^l} \{\varepsilon > 0, \;\; l \in \mathcal{L}\} \tag{2.87}$$

$$\textit{subject to } P^l(\varepsilon) \succ 0, \quad \begin{array}{l} \tilde{A}^l(\varepsilon) P^l(\varepsilon) \tilde{A}^l(\varepsilon)' + \tilde{A}^l(\varepsilon) Z(\varepsilon)' \tilde{B}_u^{l'} + \tilde{B}_u^l Z(\varepsilon) \tilde{A}^l(\varepsilon)' + \\ \tilde{B}_u^l Z(\varepsilon) P^l(\varepsilon)^{-1} Z(\varepsilon)' \tilde{B}_u^{l'} - P^l(\varepsilon) + \tilde{B}_d^l \tilde{B}_d^{l'} \prec 0 \end{array}$$

where $\tilde{A}^l(\varepsilon)$, $\tilde{B}_u^l$, $\tilde{B}_d^l$, $P^l(\varepsilon)$ and $Z(\varepsilon)$ are defined in (2.73) and (2.80)-(2.81), respectively. The values of P_s and Z_s can be computed by Theorem 4, for any $l \in \mathcal{L}$.

Remark 5 *The extension of the full-order controller designed in Theorem 2 to uncertain systems in the polytopic form cannot be directly done because P_2^l depends on the state matrices A_{11}^l, A_{12}^l and B_1^l, for any $l \in \mathcal{L}$.*

2.4.2 Numerical example

Consider the slow sampling time scale system in the polytopic form (2.72), which can represent a subsystem $i \in \mathcal{I}$ of the switched system (1.19) corresponding to the model of the uncertain HSM system. Assume that the HSM system is subject to four parametric uncertainties: the width of the strip w, the output thickness of the strip in the last stand h_n, the hardness of the strip in the first and in the last stand σ_1^0 and σ_n^0, respectively. Consider the following variation of the uncertain parameters:

$$\begin{array}{c} w \in [800 - 1200]\, mm \\ h_n \in [1.9 - 3]\, mm \\ \sigma_1^0 \in [22 - 56]\, KN/mm^2 \\ \sigma_n^0 \in [30 - 72]\, KN/mm^2. \end{array} \tag{2.88}$$

Here, the aim is to design a robust control law in the form (2.75) that asymptotically stabilizes the 4-stands subsystem of the HSM system for all products belonging to the uncertain set (2.88), which is represented by a convex hull with $N_V = 16$ vertices. Using Theorem 4 with $\tilde{C}_s = \begin{bmatrix} I_5 \\ 0_{4\times 5} \end{bmatrix}$ and $\tilde{D}_s = \begin{bmatrix} 0_{5\times 4} \\ 10 I_4 \end{bmatrix}$, we find:

$$K = \begin{bmatrix} 0 & 0 & 0 & -79.5 & -0.072 & 0.0064 & -0.0072 & 0.01 \\ 0 & 0 & 0 & 31.8 & 0.0175 & -0.0634 & -0.0006 & -0.0013 \\ 0 & 0 & 0 & -0.0075 & 0.0038 & -0.0011 & -0.0273 & 0.0074 \\ 0 & 0 & 0 & 0.51 & 0.0005 & 0.0049 & -0.0055 & -0.0247 \end{bmatrix}.$$

In Fig. 2.3, we show the closed loop evolution of the state variables α_2 and Z_2 for the products corresponding to the convex hull vertices for the initial conditions $x(0) = \begin{bmatrix} 0 & 0 & 0 & 0.01 & 1 & 1 & 1 & 1 \end{bmatrix}'$. The external perturbation is shown in Fig. 2.4.

2.5 Conclusion

In this chapter, a LMI based solution for the LQ control design of singularly perturbed systems in the discrete-time case has been proposed. In general, LMI tools are considered more effective than Riccati equation solutions, when the dimension of the problem is high. In order to design the control law, a model representing the sampling of singularly perturbed continuous-time systems was used. Thus, results can be applied to continuous-time systems controlled by digital devices. Fast sampling and slow sampling state-feedback control designs were investigated.

An extension of the slow sampling controller to uncertain systems in the polytopic form has also been presented. We will resort to this result on the robust steering control design of HSM presented in Chapter 5.

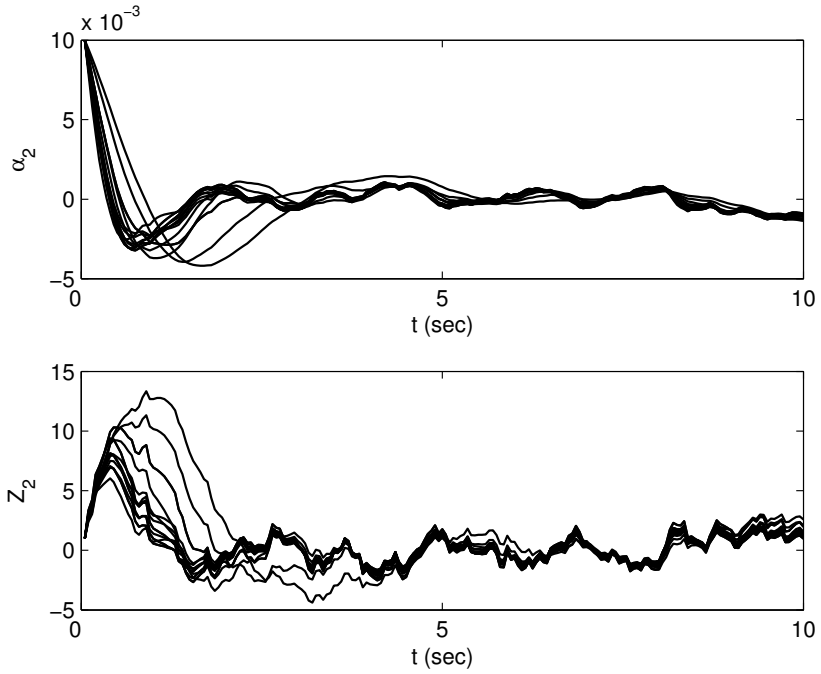

Figure 2.3: Closed loop response

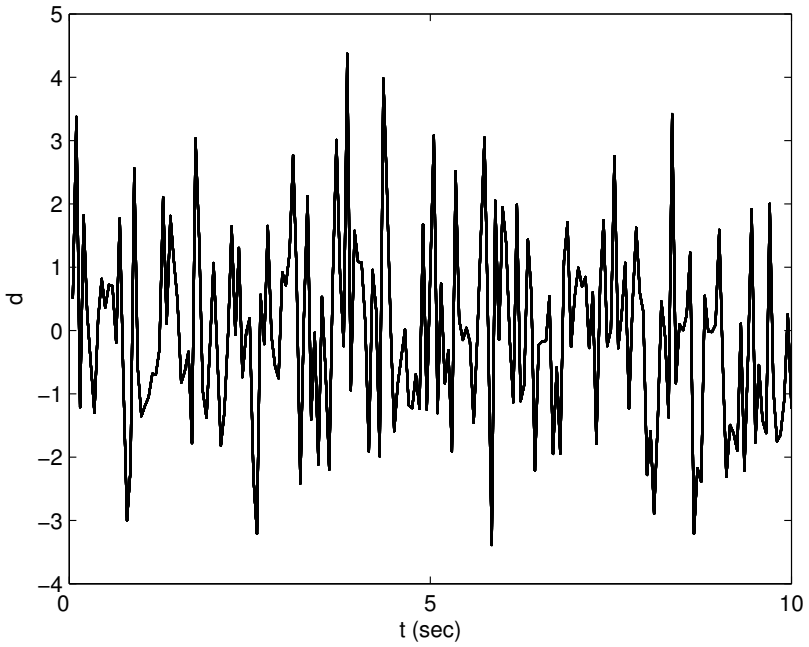

Figure 2.4: External perturbation

Chapter 3

Stability of two time scale switched systems

3.1 Introduction

During last years, *switched systems* have been the subject of a big interest by the scientific community. The main reason is that many physical systems can be modeled using such a framework. Examples of switched systems can be found in event driven systems, robots guidance, network control systems, adaptive control or biologic networks [SWM+07]. An autonomous continuous-time switched system consists of a set of differential equations

$$\dot{x}(t) = f^{\sigma(t)}(x(t), t), \tag{3.1}$$

where $\{f^i : i \in \mathcal{I} = \{1, ..., N\}\}$ is a family of sufficiently regular functions, $\sigma : \mathbb{R}^+ \to \mathcal{I}$ is a piecewise constant function, called switching rule, and $x(t) \in \mathbb{R}^n$ is the state vector, which is assumed to be continuous, for all $t \geq 0$. The switching rule determines which mode i is active at each instant and may depend on the time t, on the system state x or on the evolution of some system parameters. An autonomous discrete-time switched system consists of a set of difference equations

$$x(k+1) = f^{\sigma(k)}(x(k), k), \tag{3.2}$$

where $\sigma : \mathbb{Z}^+ \to \mathcal{I}$ and $x(k) \in \mathbb{R}^n$, for all $k \in \mathbb{Z}^+$. Three basic problems concerning stability of switched systems may be formulated [Lib03]:

- *Problem A:* Find conditions that guarantee the asymptotic stability of the switched system (3.1) (or (3.2)) under arbitrary switchings [LHM99], [DRI02], [SN02].
- *Problem B:* Identify classes of switching rules for which the switched system (3.1) (or (3.2)) is asymptotically stable [Mor96], [LM99], [ZHYM01].

– *Problem C:* Construct a switching rule that makes the switched system (3.1) (or (3.2)) asymptotically stable [SESP99], [SCGB06], [LA07].

In particular, we are interested in studying the stability of *switched linear systems* [LA09]. In this case, all the subsystems are linear and we have:

$$\dot{x}(t) = M^{\sigma(t)}x(t), \tag{3.3}$$

for the continuous-time case, and:

$$x(k+1) = A^{\sigma(k)}x(k), \tag{3.4}$$

for the discrete-time case. $\{M^i : i \in \mathcal{I}\}$ and $\{A^i : i \in \mathcal{I}\}$ are two families of matrices. We first recall three results (Theorems 5, 6 and 7) giving sufficient conditions for stability of switched systems.

In order to verify stability of a continuous-time switched system under arbitrary switchings (*Problem A*), sufficient LMI based conditions for the existence of a *common quadratic Lyapunov function* $V(x(t)) = x(t)'Px(t)$ may be used [BGFB94].

Theorem 5 *Consider the system (3.3). If there exists a matrix* $P = P' \succ 0$ *of appropriate dimension such that the LMI*

$$M^{i'}P + PM^i \prec 0 \tag{3.5}$$

holds $\forall\, i \in \mathcal{I}$*, the quadratic function* $V(x(t)) = x(t)'Px(t)$ *is a Lyapunov function for the system (3.3), i.e. the origin* $x = 0$ *is globally exponentially stable.*

When $V(x(t)) = x(t)'Px(t)$ exists, the system is said to be quadratically stable. This implies that there exists a scalar $\delta > 0$ such that $\dot{V}(x(t)) < -\delta\|x\|$.

Different sufficient conditions for the existence of a common Lyapunov function related to Lie algebra and simultaneous triangulation have been proposed by [MK97], [LHM99] and [Lib03]. The restriction of all these methods is the conservatism, that may be too high [DM99]. In order to reduce this problem, several necessary and sufficient conditions for the existence of a common Lyapunov function have been investigated. For instance, Shorten and Narendra provided a solution for stable second order linear systems and for a pair of stable linear systems whose system matrices are in companion form [SN02], [SN03]. However, all the necessary and sufficient conditions for the existence of a common Lyapunov function present in the literature address particular cases. To overcome the conservatism problem in a general framework, *multiple Lyapunov functions* $V(x(t)) = x(t)'P(\sigma(t), x(t))x(t)$ have been introduced. In this case, the Lyapunov matrix may depend on the switching law or on the state vector [MP89], [OIGH93], [PD91], [Bra98], [DRI02], [BMS07].

A different approach for assessing stability of a switched system consists of assuming a minimal interval of time between two successive switchings (*Problem B*). Consider the continuous-time switched system (3.3) and the switching instants $t_1, t_2, \ldots, t_k$, with $t_i - t_{i-1} \geq \Delta$. Obviously, if the matrix M^i is Hurwitz for any $i \in \mathcal{I}$ and the *dwell time* Δ is large enough to allow each subsystem i to reach the steady-state, the system (3.3) is exponentially stable. The following theorem yields an evaluation of the minimum dwell time Δ between two consecutive switching instants ensuring exponential stability of the switched system (3.3).

Theorem 6 *([Mor96], [LM99]) Consider the switched system (3.3) and assume that the matrix M^i is Hurwitz for any $i \in \mathcal{I}$. If the inequality*

$$ln(\mu) - \nu(t_k - t_{k-1}) \leq 0, \quad k = 1, 2, ... \tag{3.6}$$

holds, then the origin of (3.3) is exponentially stable, where $\mu = \dfrac{\lambda^P_{max}}{\lambda^P_{min}}$, $\lambda^P_{max} = max\{\lambda_{max}(P^i),\ i \in \mathcal{I}\}$, $\lambda^P_{min} = min\{\lambda_{min}(P^i),\ i \in \mathcal{I}\}$, and $P^i = P^{i'} \succ 0$ is a matrix satisfying the Lyapunov equation

$$M^{i'}P^i + P^iM^i = -Q^i, \tag{3.7}$$

with $Q^i = Q^{i'} \succ 0$. Further, ν and c^i are two constants such that $0 < \nu < \lambda^i$, where $\lambda^i = \dfrac{c^i}{\lambda^P_{max}}$, and $\dfrac{\partial V^i(x(t))}{\partial x(t)} M^i x(t) \leq -c^i \|x(t)\|^2 < 0$, for any $i \in \mathcal{I}$.

Condition (3.6) may be written as

$$\Delta = t_k - t_{k-1} = \frac{ln(\mu)}{\nu}, \quad k = 1, 2, \ldots$$

and has been generalized by Hespanha and Morse through the concept of *average dwell time* Δ_{avg} [HM99]. The idea is that the switched system (3.3) is exponentially stable if the switching intervals are in average greater than Δ_{avg}. Zhai et al. extended the results of Theorem 6 to switched systems with stable and unstable subsystems [ZHYM01]. In [GC06a] and [GC06b], Geromel and Colaneri exploit the dwell time knowledge for finding LMI base stability conditions for continuous and discrete-time switched systems, respectively. The following theorem recalls the discrete-time case.

Theorem 7 *([GC06b]) Consider the switched system (3.4). If there exist matrices $P^i = P^{i'} \succ 0$ of appropriate dimensions such that LMIs*

$$A^{i'}P^iA^i - P^i \prec 0, \ \forall\, i \in \mathcal{I},$$

$$(A^{i'})^{\Delta}P^j(A^i)^{\Delta} - P^i \prec 0, \ \forall\, (i, j \neq i) \in \mathcal{I} \times \mathcal{I}$$

hold, then the origin of (3.4) is globally asymptotically stable for a dwell time equal or greater than $\Delta \geq 1 \in \mathbb{Z}^+$.

Notice that the choice $\Delta = 1$ leads to the conditions proposed by [DRI02].

Multi time scale switched systems are of practical interest in many applications. An example is given by the last phase of the rolling process in a hot strip mill, which has been introduced in Chapter 1. However, these dynamical systems have been the subject of few investigations. To our knowledge, the only work addressing two time scale switched systems is [ALI08], where dwell time approach is extended to singularly perturbed continuous-time switched systems with time delay [LSZ03].

In this chapter, we will first recall some results to show that, under dwell time constraints, stability of the slow and fast switched subsystems is sufficient for stability of the original two time scale switched system and then may be evaluated separately, as in the linear systems case. Therefore, we will show that, if no assumption on the minimal dwell is made, this important property is not verified anymore [MDI09a], [MDI09b]. This means that stability of the slow and fast switched subsystems does not guarantee stability of the original two time scale switched system, when the switching rule is arbitrary. In this case, an additional constraint taking into account the coupling between slow and fast subsystems has to be considered. Therefore, we will propose LMI based conditions, independently of the singular parameter ε, for stability analysis and feedback control design of continuous and discrete-time singularly perturbed switched linear systems. These conditions express the fact that a coupling constraint has to be satisfied, in addition to stability of the slow and fast switched subsystems, as far as arbitrary switchings may arise. An interpretation of this constraint in terms of the degree of time scale separation will be given. To our knowledge, this is the first work which points out explicitly the fact that asymptotic stability of slow and fast switched subsystems is not sufficient for asymptotic stability of a two time scale switched system, under an arbitrary switching rule, and which provides a stabilizing control law for this kind of systems.

3.2 Motivation for a new stability condition

Recall that for an autonomous continuous-time LTI system in the singular perturbation form

$$\dot{x}(t) = M(\varepsilon)x(t), \tag{3.8}$$

where $\varepsilon > 0$ is a scalar parameter and

$$M(\varepsilon) = \begin{bmatrix} \varepsilon^{-1} I_{n_1} & 0 \\ 0 & I_{n_2} \end{bmatrix} \begin{bmatrix} M_{11} & M_{12} \\ M_{21} & M_{22} \end{bmatrix},$$

with M_{11} non-singular matrix, the fast and slow dynamics may be separated using the transformation (2.10), which leads to the following decoupled system:

$$\begin{cases} \varepsilon \dot{x}_f(t) = (M_{11} + O(\varepsilon))x_f(t) \\ \dot{x}_s(t) = (M_s + O(\varepsilon))x_s(t). \end{cases}$$

Hence, there exists a scalar $\varepsilon_{max} > 0$ such that asymptotic stability of the slow and fast subsystems (i.e. matrices $M_s = M_{22} - M_{21}M_{11}^{-1}M_{12}$ and M_{11} are Hurwitz) implies asymptotic stability of the two time scale system (3.8), for any $\varepsilon \in (0, \varepsilon_{max}]$ [KKO86].

3.2.1 A dwell-time condition for two time scale switched systems

Consider the autonomous continuous two time scale switched linear system

$$\dot{x}(t) = M^{\sigma(t)}(\varepsilon)x(t), \tag{3.9}$$

with

$$M^i(\varepsilon) = \begin{bmatrix} \varepsilon^{-1}I_{n_1} & 0 \\ 0 & I_{n_2} \end{bmatrix} \begin{bmatrix} M_{11}^i & M_{12}^i \\ M_{21}^i & M_{22}^i \end{bmatrix}, \tag{3.10}$$

and the matrix M_{11}^i is assumed to be non-singular, for any $i \in \mathcal{I}$. The subsystem corresponding to each mode $i \in \mathcal{I}$ can be written in the form:

$$\begin{cases} \varepsilon \dot{x}_1(t) = M_{11}^i x_1(t) + M_{12}^i x_2(t) \\ \dot{x}_2(t) = M_{21}^i x_1(t) + M_{22}^i x_2(t), \end{cases} \tag{3.11}$$

where $x_1(t) \in \mathbb{R}^{n_1}$ and $x_2(t) \in \mathbb{R}^{n_2}$ are the state vectors corresponding to the fast and slow dynamics, respectively, for all $t \geq 0$. The following theorem yields an extension of the dwell time approach [Mor96] for singularly perturbed switched systems. The two time scale switched system (3.9) is considered as an interconnected system where the terms $M_{12}^i x_2$ and $M_{21}^i x_1$ are perturbations that are assumed to be bounded.

Theorem 8 *([ALI08]) Consider the switched system (3.9). Assume that the matrices M_{11}^i and M_{22}^i are Hurwitz, the principal minors of*

$$\hat{M}^i = \begin{bmatrix} -\dfrac{(\lambda_{min}^{Q_f} - \varepsilon_{max}\|P_f^i {M_{11}^i}^{-1} M_{12}^i M_{21}^i\|)}{\varepsilon_{max}\lambda_{max}^{P_f}} & \dfrac{\|P_f^i {M_{11}^i}^{-1} M_{12}^i (M_{22}^i - M_{21}^i {M_{11}^i}^{-1} M_{12}^i)\|}{\lambda_{min}^{P_s}} \\ \dfrac{\|P_s^i M_{21}^i\|}{\lambda_{min}^{P_f}} & -\dfrac{(\lambda_{min}^{Q_s} - \|P_s^i M_{21}^i {M_{11}^i}^{-1} M_{12}^i\|)}{\lambda_{max}^{P_s}} \end{bmatrix}$$

are negative and $\lambda_{max}(\hat{M}^i + \hat{M}^{i'}) \leq \lambda^i$, with $\lambda_{max}^{P_s} = max\{\lambda_{max}(P_s^i),\ i \in \mathcal{I}\}$, $\lambda_{min}^{P_s} = min\{\lambda_{min}(P_s^i),\ i \in \mathcal{I}\}$, $\lambda_{max}^{P_f} = max\{\lambda_{max}(P_f^i),\ i \in \mathcal{I}\}$, $\lambda_{min}^{P_f} = min\{\lambda_{min}(P_f^i),$

$i \in \mathcal{I}\}$, $\lambda_{min}^{Q_s} = min\{\lambda_{min}(Q_s^i),\ i \in \mathcal{I}\}$, $\lambda_{min}^{Q_f} = min\{\lambda_{min}(Q_f^i),\ \ i \in \mathcal{I}\}$, $\lambda^i = min\{\frac{c_s^i}{\lambda_{max}^{P_s}}, \frac{c_f^i}{\lambda_{max}^{P_f}}\}$, $c_s^i = \lambda_{min}(Q_s^i)$ *and* $c_f^i = \lambda_{min}(\varepsilon_{max}^{-1} Q_f^i)$, $\forall\, i \in \mathcal{I}$. *Further,* $P_s^i = P_s^{i'} \succ 0$ *and* $P_f^i = P_f^{i'} \succ 0$ *are matrices satisfying the Lyapunov equations*

$$M_{11}^i P_f^i + P_f^i M_{11}^{i'} = -Q_f^i,$$

$$M_{22}^i P_s^i + P_s^i M_{22}^{i'} = -Q_s^i,$$

with $Q_s^i = Q_s^{i'} \succ 0$, $Q_f^i = Q_f^{i'} \succ 0$, $\forall\, i \in \mathcal{I}$. *If the inequality*

$$ln(2\mu) - \nu(t_k - t_{k-1}) \leq 0, \quad k = 1, 2, ...$$

holds, then there exists ε_{max} *such that the origin of (3.9) is exponentially stable* $\forall\, \varepsilon \in (0, \varepsilon_{max}]$, *where* $\mu = max\{\frac{\lambda_{max}^{P_s}}{\lambda_{min}^{P_s}}, \frac{\lambda_{max}^{P_f}}{\lambda_{min}^{P_f}}\}$ *and* ν *is a constant such that* $0 < \nu < \lambda^i$.

Consider the switched system (3.9), with $\mathcal{I} = \{1, 2\}$ and

$$M^1(\varepsilon) = \begin{bmatrix} -\varepsilon^{-1} & 5\varepsilon^{-1} \\ 0 & -1 \end{bmatrix}, \quad M^2(\varepsilon) = \begin{bmatrix} -\varepsilon^{-1} & 0 \\ 5 & -1 \end{bmatrix}. \tag{3.12}$$

Applying Theorem 8, we find

$$P_s^1 = P_f^1 = Q_s^1 = Q_f^1 = 1,$$

and

$$P_s^2 = P_f^2 = Q_s^2 = Q_f^2 = 1,$$

with $\varepsilon_{max} = 0.076$. Hence, $\mu = 1$, $\lambda^1 = 1$ and $\lambda^2 = 1$. Finally, choosing $\nu = 0.99$, we get the minimal dwell time $\Delta = \dfrac{ln(\mu)}{\nu} = 0.7001$. An example of stabilizing

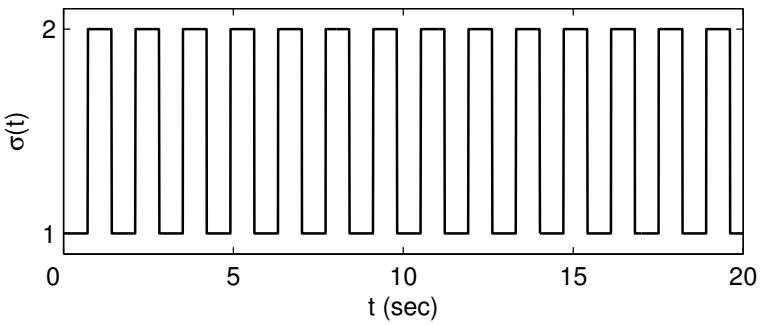

Figure 3.1: Stabilizing switching rule $\sigma(t)$

switching rule for the switched system (3.9)-(3.12) with $\varepsilon = \varepsilon_{max}$ is given in Fig. 3.1, where the system switches between the subsystems 1 and 2 each $\Delta^* = \Delta\, sec.$ Fig. 3.2 shows the convergence of the state trajectories to zero for the initial condition $x(0) = \begin{bmatrix} 1 & 1 \end{bmatrix}'$.

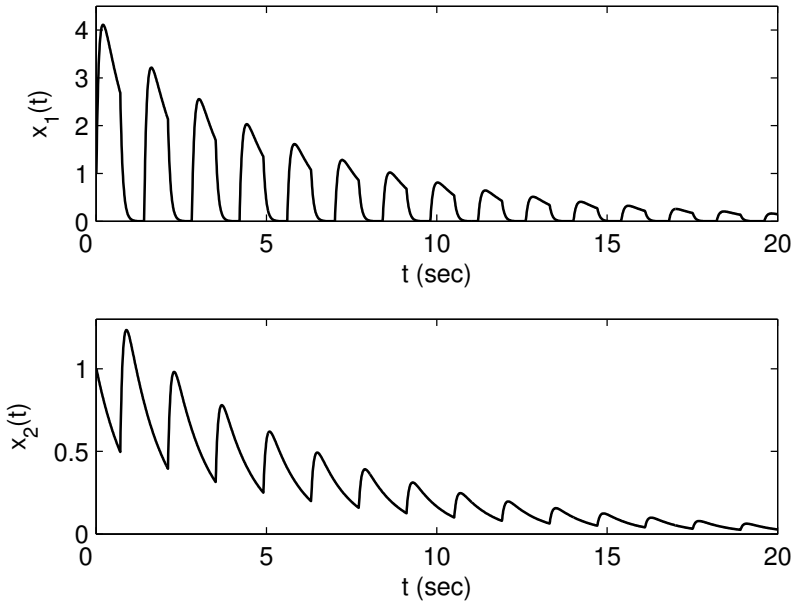

Figure 3.2: State trajectories: Stable behavior

3.2.2 Two time scale switched systems under arbitrary switching rules

Consider the two time scale switched system (3.9)-(3.12). Matrices $M^1(\varepsilon)$ and $M^2(\varepsilon)$ are Hurwitz for any value of $\varepsilon > 0$. Moreover, since $M^1_{11} = M^2_{11} = -1$, the fast switched subsystem

$$\varepsilon \dot{x_f}(t) = M^{\sigma(t)}_{11} x_f(t) \tag{3.13}$$

is asymptotically stable for any switching rule. Also, since $M^1_s = M^2_s = -1$, the slow switched subsystem

$$\dot{x_s}(t) = M^{\sigma(t)}_s x_s(t) \tag{3.14}$$

is asymptotically stable for any switching rule, with

$$M^i_s = M^i_{22} - M^i_{21} {M^i_{11}}^{-1} M^i_{12} \tag{3.15}$$

for any $i \in \mathcal{I}$. However, when the switching rule is arbitrary, the two time scale switched system (3.9)-(3.12) can be unstable for any small value of $\varepsilon > 0$, even if the slow and fast switched subsystems are asymptotically stable. The interpretation of this phenomenon is that for any fixed $\varepsilon \in (0, \varepsilon_{max}]$, a switching rule with a sufficiently high switching frequency which destabilizes the two time scale switched system may be exhibited. For instance, let switching between the subsystems 1 and 2 each $\Delta^* = \varepsilon$ *sec*. We obtain a periodic dynamical system characterized by the matrix

$$D(\varepsilon) = e^{M^1(\varepsilon)\Delta^*} e^{M^2(\varepsilon)\Delta^*}.$$

Since the computation of the spectral radius of $D(\varepsilon)$ yields

$$\rho(D(\varepsilon)) = 1 + 9.5529\varepsilon - 28.7211\varepsilon^2 + O(\varepsilon^3) > 1$$

for every period $2\Delta^*$ and any $\varepsilon \in (0, \varepsilon_{max}]$, the proposed switching rule destabilizes the two time scale switched systems (3.9)-(3.12) for any $\varepsilon \in (0, \varepsilon_{max}]$, even if the slow and fast switched subsystems are asymptotically stable. A simple example of destabilizing switching rule is given in Fig. 3.3, where the system switches between the subsystems 1 and 2 each $\Delta^* = \dfrac{\Delta}{2} = 0.35\,sec$ and $\varepsilon = \varepsilon_{max} = 0.076$. In this case, the state trajectories diverge, as shown in Fig. 3.4 for the initial condition $x(0) = \begin{bmatrix} 1 & 1 \end{bmatrix}'$.

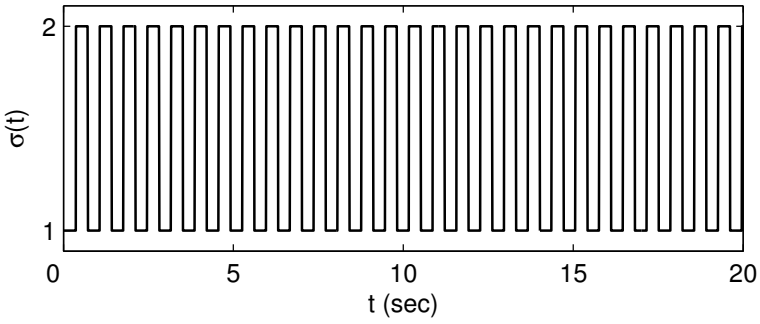

Figure 3.3: Destabilizing switching rule $\sigma(t)$

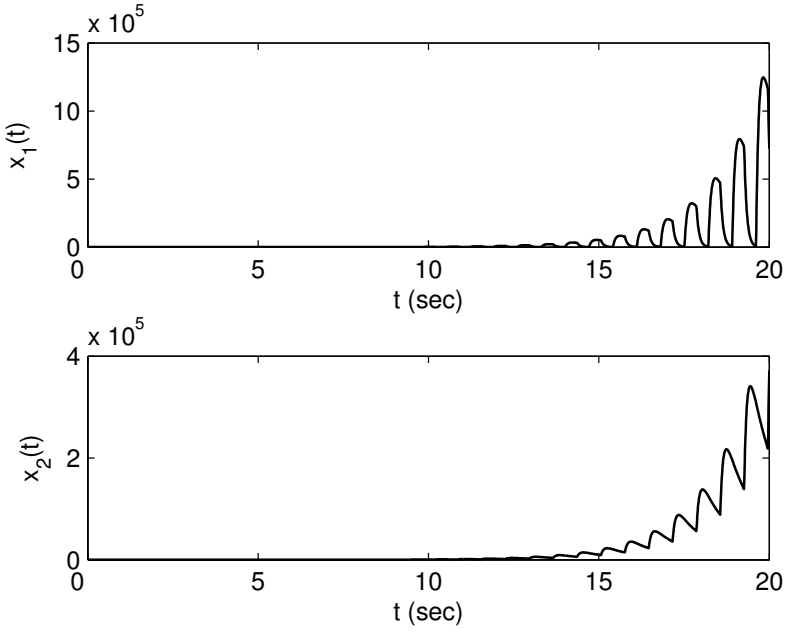

Figure 3.4: State trajectories: Unstable behavior

In the next sections, we will provide LMI based conditions guaranteeing the asymptotic stability of a switched systems in the singular perturbation form under an arbitrary switching rule and independently of the value of ε. We will show that this corresponds to assess the asymptotic stability of the slow and fast switched subsystems and verifying an additional constraint which takes into account the coupling between the fast and slow dynamics when a switching occurs.

3.3 Stability conditions: Continuous-time case

3.3.1 Stability analysis

Consider the autonomous two time scale switched system

$$\dot{x}(t) = M^{\sigma(t)}(\varepsilon)x(t), \tag{3.16}$$

defined in (3.9). The existence of a common quadratic Lyapunov function $V(x(t),\varepsilon) = x(t)'P(\varepsilon)x(t)$ such that $V(x(t),\varepsilon) > 0$ and $\dot{V}(x(t),\varepsilon) < 0$ for all $t \geq 0$ is a well-known sufficient condition for asymptotic stability of the system (3.16). This is equivalent to the existence of matrices $P(\varepsilon) = P(\varepsilon)' \succ 0$ and $Q^i(\varepsilon) = Q^i(\varepsilon)' \succ 0$ of appropriate dimensions such that the LMI

$$M^i(\varepsilon)P(\varepsilon) + P(\varepsilon)M^i(\varepsilon)' + Q^i(\varepsilon) \prec 0 \tag{3.17}$$

holds for any $i \in \mathcal{I}$. The following theorem gives LMI based conditions guaranteeing the stability of the switched system (3.16) independently of ε and for any switching rule.

Theorem 9 *Assume that there exist matrices $P_f = P_f' \succ 0$, $Q_f^i = Q_f^{i\,\prime} \succ 0$, $P_s = P_s' \succ 0$, $Q_s^i = Q_s^{i\,\prime} \succ 0$ of appropriate dimensions such that the LMIs*

$$M_{11}^i P_f + P_f M_{11}^{i\,\prime} + Q_f^i \prec 0, \tag{3.18}$$

$$M_s^i P_s + P_s M_s^{i\prime} + Q_s^i \prec 0, \tag{3.19}$$

$$\begin{bmatrix} Q_f^i & -(M_{11}^i Y^i + P_f M_{21}^{i\,\prime}) \\ (\star)' & Q_s^i - M_{21}^i Y^i - Y^{i\prime} M_{21}^{i\,\prime} \end{bmatrix} \succ 0 \tag{3.20}$$

are verified $\forall\, i \in \mathcal{I}$, with $Y^i = -\sum_{h=1,h\neq i}^{N} M_{11}^{h\,-1} M_{12}^h P_s$. Hence, there exists a positive scalar ε_{max} such that the switched system (3.16) is asymptotically stable $\forall\, \varepsilon \in (0, \varepsilon_{max}]$ and for any switching rule.

Proof. Let us assume

$$P(\varepsilon) = \begin{bmatrix} P_1(\varepsilon) & P_2(\varepsilon) \\ P_2(\varepsilon)' & P_3(\varepsilon) \end{bmatrix} \succ 0, \tag{3.21}$$

$$Q^i(\varepsilon) = \begin{bmatrix} Q_1^i(\varepsilon) & Q_2^i(\varepsilon) \\ Q_2^i(\varepsilon)' & Q_3^i(\varepsilon) \end{bmatrix} \succ 0, \tag{3.22}$$

with

$$P_1(\varepsilon) = P_f + \varepsilon P_2 P_s^{-1} P_2', \quad P_2(\varepsilon) = \varepsilon P_2 = -\varepsilon \sum_{h=1}^{N} {M_{11}^h}^{-1} M_{12}^h P_s, \quad P_3(\varepsilon) = \varepsilon P_s \tag{3.23}$$

$$Q_1^i(\varepsilon) = \varepsilon^{-1} Q_f^i, \quad Q_2^i(\varepsilon) = -M_{11}^i Y^i + P_f {M_{21}^i}', \quad Q_3^i(\varepsilon) = \varepsilon(Q_s^i - M_{21}^i Y^i - Y^{i\prime} {M_{21}^i}') \tag{3.24}$$

and

$$Y^i = -\sum_{h=1, h\neq i}^{N} {M_{11}^h}^{-1} M_{12}^h P_s. \tag{3.25}$$

Substituting (3.10) and (3.21)-(3.22) in (3.17), we have:

$$\begin{bmatrix} X_1^i(\varepsilon) & X_2^i(\varepsilon) \\ X_2^i(\varepsilon)' & X_3^i(\varepsilon) \end{bmatrix} \prec 0 \tag{3.26}$$

with

$$X_1^i(\varepsilon) = \varepsilon^{-1}(M_{11}^i P_1(\varepsilon) + P_1(\varepsilon){M_{11}^i}' + M_{12}^i P_2(\varepsilon)' + P_2(\varepsilon){M_{12}^i}' + Q_1^i(\varepsilon)),$$

$$X_2^i(\varepsilon) = \varepsilon^{-1} M_{11}^i P_2(\varepsilon) + \varepsilon^{-1} M_{12}^i P_3(\varepsilon) + P_1(\varepsilon){M_{21}^i}' + P_2(\varepsilon)' {M_{22}^i}' + Q_2^i(\varepsilon),$$

$$X_3^i(\varepsilon) = M_{22}^i P_3(\varepsilon) + P_3(\varepsilon){M_{22}^i}' + M_{21}^i P_2(\varepsilon) + P_2(\varepsilon)' {M_{21}^i}' + Q_3(\varepsilon).$$

Replacing the values of $P(\varepsilon)$, $Q^i(\varepsilon)$ and the equations (3.15), (3.23)-(3.25), we obtain:

$$X_1^i(\varepsilon) = \varepsilon^{-1}(M_{11}^i P_f + P_f {M_{11}^i}' + Q_f^i + O(\varepsilon)) = \varepsilon^{-1}(X_f^i + O(\varepsilon)),$$

$$X_2^i(\varepsilon) = \varepsilon(P_2' {M_{22}^i}' + O(\varepsilon)) = \varepsilon(X_2^i + O(\varepsilon)),$$

$$X_3^i(\varepsilon) = \varepsilon(M_s^i P_s + P_s M_s^{i\prime} + Q_s^i + O(\varepsilon)) = \varepsilon(X_s^i + O(\varepsilon)).$$

The inequality (3.26) can be written as

$$\begin{bmatrix} \varepsilon^{-1}(X_f^i + O(\varepsilon)) & \varepsilon(X_2^i + O(\varepsilon)) \\ (\star)' & \varepsilon(X_s^i + O(\varepsilon)) \end{bmatrix} \prec 0.$$

Satisfying the conditions (3.18) and (3.19) implies that $X_f^i \prec 0$ and $X_s^i \prec 0$. This means that there exists a scalar $\varepsilon_{max} > 0$ such that $X_s^i + O(\varepsilon) \prec 0$ and

$X_f^i - \varepsilon^2 X_2^i X_s^{i^{-1}} X_2^{i\prime} + O(\varepsilon) \prec 0$, $\forall i \in \mathcal{I}$ and $\forall \varepsilon \in (0, \varepsilon_{max}]$. Hence, using the Schur complement, the LMI (3.17) holds [BGFB94]. Since $P_f \succ 0$ and $P_s \succ 0$, (3.21) holds. Furthermore, (3.22) can be written as

$$Q^i(\varepsilon) = \begin{bmatrix} \varepsilon^{-1} I_{n_1} & 0 \\ 0 & I_{n_2} \end{bmatrix} \begin{bmatrix} Q_f^i & -(M_{11}^i Y^i + P_f M_{21}^{i\prime}) \\ (\star)' & Q_s^i - M_{21}^i Y^i - Y^{i\prime} M_{21}^{i\prime}) \end{bmatrix} \begin{bmatrix} I_{n_1} & 0 \\ 0 & \varepsilon I_{n_2} \end{bmatrix} \succ 0$$

which is non negative definite because of (3.20). This concludes the proof. ■

Remark 6 *Theorem 9 provides two separate LMI based conditions for assessing the asymptotic stability of the fast and slow subsystems (3.18) and (3.19), respectively. Moreover, the coupling condition (3.20) is given. This allows to conclude that there exists ε_{max} such that the classical stability condition (3.17) holds for any $\varepsilon \in (0, \varepsilon_{max}]$. $P(\varepsilon)$ and $Q^i(\varepsilon)$ are defined in (3.21)-(3.25), for any $i \in \mathcal{I}$.*

Remark 7 *An evaluation of the upper bound ε_{max} is obtained solving the following optimization problem:*

$$\varepsilon_{max} = max\ \varepsilon > 0 \tag{3.27}$$

$$subject\ \ to\ \ M^i(\varepsilon)P(\varepsilon) + P(\varepsilon)M^i(\varepsilon)' + Q^i(\varepsilon) \prec 0,\ \ i \in \mathcal{I},$$

where matrices $M^i(\varepsilon)$, $P(\varepsilon)$, and $Q^i(\varepsilon)$ are defined in (3.10) and (3.21)-(3.25), respectively. Moreover, the values of P_f, Q_f^i, P_s and Q_s^i can be computed by Theorem 9, for any $i \in \mathcal{I}$.

3.3.2 Estimation of the degree of time scale separation

In addition to the stability conditions of the fast and slow switched subsystems, Theorem 9 gives the coupling condition that must be satisfied in order to assess the asymptotic stability of the two time scale switched linear system (3.16). The meaning of this condition can be illustrated through the extension of the notion of time scale separation degree given in [Yur04] for LTI systems. In this classical case, the degree of time scale separation of the LTI two time scale systems (3.8) may be expressed as a ratio between the dynamical matrices eigenvalues [Yur04]:

$$\eta^* = \frac{\lambda_{min}(\varepsilon^{-1} M_{11})}{\lambda_{max}(M_s)}.$$

For two time scale switched systems, such a quantity cannot be obtained using the eigenvalues evaluation. The following proposition provides the notion of time scale separation degree for switched linear systems in the singular perturbation form (3.16).

Proposition 1 *Assume that there exist matrices $P_f = P_f' \succ 0$, $Q_f^i = Q_f^{i\prime} \succ 0$, $P_s = P_s' \succ 0$, $Q_s^i = Q_s^{i\prime} \succ 0$, $i \in \mathcal{I}$, such that the stability conditions of Theorem*

9 hold. Hence, an estimation of the degree of time scale separation between the slow and fast dynamics is given by the ratio:

$$\eta = \frac{\lambda_{min}(P_s) min\{\lambda_{min}(Q_f^i),\ i \in \mathcal{I}\}}{\varepsilon \lambda_{max}(P_f) max\{\lambda_{max}(Q_s^i),\ i \in \mathcal{I}\}}.$$

Proof. See Appendix B.2. ■

In order to understand the role played by the condition (3.20), consider the switched system (3.16), with

$$M^1(\varepsilon) = \begin{bmatrix} -\varepsilon^{-1} & \alpha\varepsilon^{-1} \\ 0 & -1 \end{bmatrix}, \quad M^2(\varepsilon) = \begin{bmatrix} -\varepsilon^{-1} & 0 \\ \alpha & -1 \end{bmatrix}. \tag{3.28}$$

We have $M_{11}^1 = M_{11}^2 = -1$ and $M_s^1 = M_s^2 = -1$. Although the fast and slow switched subsystems are asymptotically stable for any value of the parameter α and for any switching rule $\sigma(t)$, the switched system (3.16) may be unstable under an arbitrary switching rule, as shown in section 3.2 for the case $\alpha = 5$. Using Theorem 9, the system has been found asymptotically stable for $-1 < \alpha < 1$, under arbitrary switchings. As the conditions (3.18) and (3.19) are independent of α, the coupling between the fast and slow dynamics is taken into account by the condition (3.20). This means that the Lyapunov matrices assessing stability of the fast and slow switched subsystems must satisfy the coupling condition, which involves the terms $M_{12}^1 = \alpha\varepsilon^{-1}$ and $M_{21}^2 = \alpha$. Hence, the degree of time scale separation between the slow and fast dynamics η depends on the value of α. For several values of $-1 < \alpha < 1$, we solved the conditions of Theorem 9 and computed the corresponding value of the degree of time scale separation η. The result is shown in Fig. 3.5.

On the proposed example, the relation between η and α is direct: a bigger value of $|\alpha|$ yields a smaller value of η and viceversa. In particular, for $\alpha = 0$ we have a linear system ($M^1(\varepsilon) = M^2(\varepsilon)$) and the degree of time scale separation is maximum. However, in a general framework, the evolution of η with respect to M_{12}^i and M_{21}^i, $i \in \mathcal{I}$, is difficult to analyze.

3.3.3 Control design

Consider the two time scale switched system

$$\dot{x}(t) = M^{\sigma(t)}(\varepsilon)x(t) + N^{\sigma(t)}(\varepsilon)u(t), \tag{3.29}$$

where $u(t) \in \mathbb{R}^r$ is the control signal, for all $t \geq 0$,

$$M^i(\varepsilon) = \begin{bmatrix} \varepsilon^{-1} I_{n_1} & 0 \\ 0 & I_{n_2} \end{bmatrix} \begin{bmatrix} M_{11}^i & M_{12}^i \\ M_{21}^i & M_{22}^i \end{bmatrix}, N^i(\varepsilon) = \begin{bmatrix} \varepsilon^{-1} I_{n_1} & 0 \\ 0 & I_{n_2} \end{bmatrix} \begin{bmatrix} N_1^i \\ N_2^i \end{bmatrix}, \tag{3.30}$$

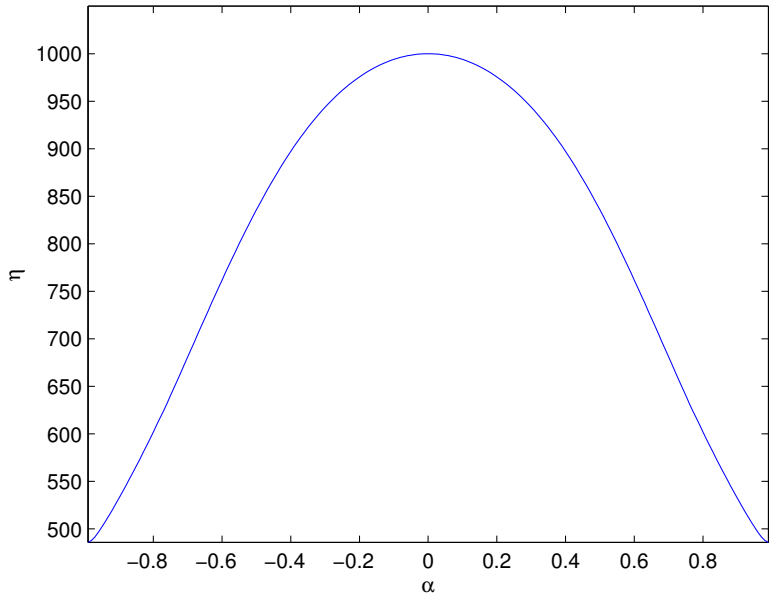

Figure 3.5: Estimation of the time scale separation degree for $\varepsilon = 10^{-3}$

and the matrix M_{11}^i is assumed to be non-singular, for any $i \in \mathcal{I}$. The subsystem corresponding to each mode $i \in \mathcal{I}$ can be written in the form:

$$\begin{cases} \varepsilon \dot{x}_1(t) = M_{11}^i x_1(t) + M_{12}^i x_2(t) + N_1^i u(t) \\ \dot{x}_2(t) = M_{21}^i x_1(t) + M_{22}^i x_2(t) + N_2^i u(t), \end{cases} \tag{3.31}$$

Its slow subsystem is :

$$\dot{x}_s(t) = M_s^i x_s(t) + N_s^i u_s(t) \tag{3.32}$$

with

$$M_s^i = M_{22}^i - M_{21}^i {M_{11}^i}^{-1} M_{12}^i, \quad N_s^i = N_2^i - M_{21}^i {M_{11}^i}^{-1} N_1^i, \tag{3.33}$$

while its fast subsystem is:

$$\varepsilon \dot{x}_f(t) = M_{11}^i x_f(t) + N_1^i u_f(t). \tag{3.34}$$

The pairs (M_s^i, N_s^i) and (M_{11}^i, N_1^i) are assumed to be stabilizable in the continuous-time setting, for any $i \in \mathcal{I}$.

The aim of this section is to design a state-feedback control law

$$u(t) = K^{\sigma(t)}(\varepsilon) x(t) \tag{3.35}$$

asymptotically stabilizing the closed loop system (3.29) for any switching rule. A classical LMI based condition for state-feedback control design of switched

systems consists of checking the existence of matrices $P(\varepsilon) = P(\varepsilon)' \succ 0$, $Q^i(\varepsilon) = Q^i(\varepsilon)' \succ 0$ and $Z^i(\varepsilon)$ of appropriate dimensions such that LMI

$$M^i(\varepsilon)P(\varepsilon) + P(\varepsilon)M^i(\varepsilon)' + N^i(\varepsilon)Z^i(\varepsilon) + Z^i(\varepsilon)'N^i(\varepsilon)' + Q^i(\varepsilon) \prec 0 \tag{3.36}$$

holds for any $i \in \mathcal{I}$. The state-feedback control law (3.35), which asymptotically stabilizes the continuous-time switched system (3.29), is characterized by the gain matrices $K^i(\varepsilon) = Z^i(\varepsilon)P(\varepsilon)^{-1}$, $i \in \mathcal{I}$.

Likewise to the stability analysis case, when ε is small numerical difficulties to find the gains $K^i(\varepsilon)$ arise. This problem is due to the ill-conditioning of the constraint (3.36) and can be avoided decomposing the two time scale system into two well-behaved subsystems, the slow and fast subsystems. The following theorem gives LMI based conditions guaranteeing the asymptotic stability of the system (3.29) independently of ε, for any switching rule.

Theorem 10 *Assume that there exist matrices $P_f = P_f' \succ 0$, $Q_f^i = Q_f^{i\,\prime} \succ 0$, Z_f^i, $P_s = P_s' \succ 0$, $Q_s^i = Q_s^{i\prime} \succ 0$ and Z_s^i of appropriate dimensions such that the LMIs*

$$M_{11}^i P_f + P_f M_{11}^{i\,\prime} + N_1^i Z_f^i + Z_f^{i\,\prime} N_1^{i\prime} + Q_f^i \prec 0, \tag{3.37}$$

$$M_s^i P_s + P_s M_s^{i\prime} + N_s^i Z_s^i + Z_s^{i\prime} N_s^{i\prime} + Q_s^i \prec 0, \tag{3.38}$$

$$\begin{bmatrix} Q_f^i & -(M_{11}^i Y^i + P_f M_{21}^{i\,\prime} + Z_f^{i\,\prime} N_2^{i\prime}) & N_1^i Z_f^i & 0 \\ (\star)' & Q_s^i - M_{21}^i Y^i - Y^{i\prime} M_{21}^{i\,\prime} & Y^{i\prime} & N_2^i Z_f^i + Y^{i\prime} \\ (\star)' & (\star)' & P_f & 0 \\ (\star)' & (\star)' & (\star)' & P_f \end{bmatrix} \succ 0 \tag{3.39}$$

are verified $\forall\, i \in \mathcal{I}$, with $Y^i = -\sum_{h=1, h\neq i}^{N} M_{11}^{h\,-1}(M_{12}^h P_s + N_1^h Z_s^h)$. Hence, there exists a positive scalar ε_{max} such that the state-feedback controller gains

$$K^i = \begin{bmatrix} K_f^i & K_s^i + K_f^i M_{11}^{i\,-1}(M_{12}^i + N_1^i K_s^i) \end{bmatrix}, \tag{3.40}$$

with $K_f^i = Z_f^i P_f^{-1}$ and $K_s^i = Z_s^i P_s^{-1}$, stabilize asymptotically the closed loop switched system (3.29), $\forall\, \varepsilon \in (0, \varepsilon_{max}]$ and for any switching rule.

Proof. See Appendix B.3. ■

Remark 8 *The conditions of Theorem 10 with $Z_f^i = 0$, $i \in \mathcal{I}$, lead to the reduced control law:*

$$u(t) = \begin{bmatrix} 0 & K_s^{\sigma(t)} \end{bmatrix} \begin{bmatrix} x_1(t) \\ x_2(t) \end{bmatrix},$$

which asymptotically stabilizes the switched system (3.29) for any $\varepsilon \in (0, \varepsilon_{max}]$ and any switching rule σ. Notice that in this case (3.37) assumes that the fast subsystem is asymptotically stable in open loop.

3.4 Stability conditions: Discrete-time case

3.4.1 Stability analysis

Consider the autonomous two time scale switched system in the fast sampling model (2.13):

$$x(k+1) = A^{\sigma(k)}(\varepsilon)x(k), \tag{3.41}$$

where

$$A^i(\varepsilon) = \begin{bmatrix} A^i_{11} & A^i_{12} \\ \varepsilon A^i_{21} & (I_{n_2} + \varepsilon A^i_{22}) \end{bmatrix} \tag{3.42}$$

and the matrix $(I_{n_1} - A^i_{11})$ is assumed to be non-singular, for any $i \in \mathcal{I}$. The subsystem corresponding to each mode i may be written in the form:

$$\begin{cases} x_1(k+1) = A^i_{11}x_1(k) + A^i_{12}x_2(k) \\ x_2(k+1) = \varepsilon A^i_{21}x_1(k) + (I_{n_2} + \varepsilon A^i_{22})x_2(k). \end{cases} \tag{3.43}$$

Its slow subsystem is:

$$x_s(k+1) = (I_{n_2} + \varepsilon A^i_s)x_s(k) \tag{3.44}$$

with

$$A^i_s = A^i_{22} + A^i_{21}(I_{n_1} - A^i_{11})^{-1}A^i_{12}, \tag{3.45}$$

while its fast subsystem is:

$$x_f(k+1) = A^i_{11}x_f(k). \tag{3.46}$$

The fast sampling singular perturbation model presents two main advantages, with respect to the other discrete time models of two time scale systems (see [Nai02] for an overview). First, it allows to describe both discretized continuous two time scale systems and pure difference equations. Second, due to the choice of the sampling time as $T_f = \varepsilon$, this model assumes that the sampling rate is fast enough to influence the transient behavior of the system for control purposes, when it represents discretized continuous two time scale systems.

A standard stability condition ensuring the existence of a switched quadratic Lyapunov function $V^{\sigma(k)}(x(k), \varepsilon) = x(k)'S^{\sigma(k)}(\varepsilon)x(k)$ such that $V^{\sigma(k)}(x(k), \varepsilon) > 0$ and $V^{\sigma(k)}(x(k+1), \varepsilon) - V^{\sigma(k)}(x(k), \varepsilon) < 0$ for $k \in \mathbb{Z}^+$, which is a sufficient condition for the asymptotic stability of the switched system (3.41), consists in checking the existence of matrices $P^i(\varepsilon) = P^i(\varepsilon)' = S^i(\varepsilon)^{-1} \succ 0$ and $Q^{ij}(\varepsilon) = Q^{ij}(\varepsilon)' \succ 0$ such that the LMI

$$A^i(\varepsilon)P^i(\varepsilon)A^i(\varepsilon)' - P^j(\varepsilon) + Q^{ij}(\varepsilon) \prec 0 \tag{3.47}$$

holds for any $(i, j) \in \mathcal{I} \times \mathcal{I}$ [DRI02].

When ε is small the computation of $P^i(\varepsilon)$ is complicated due to the ill-conditioning of the constraint (3.47). As in the continuous-time case, the decoupling of the two time scale system into two well-behaved subsystems can solve this problem. Also in this case, it may exist a switching rule destabilizing the two time scale switched system, even if the slow and fast switched subsystems are asymptotically stable. Hence, a coupling condition must be considered. The following theorem gives LMI based conditions guaranteeing the asymptotic stability of the switched system (3.41) independently of ε, for any switching rule.

Theorem 11 *Assume that there exist matrices* $P_f^i = P_f^{i\prime} \succ 0$, $Q_f^i = Q_f^{i\prime} \succ 0$, $P_s = P_s{}' \succ 0$, $Q_s^i = Q_s^{i\prime} \succ 0$ *of appropriate dimensions such that the LMIs*

$$\begin{bmatrix} P_f^j - Q_f^i & A_{11}^i P_f^i \\ (\star)' & P_f^i \end{bmatrix} \succ 0, \tag{3.48}$$

$$A_s^i P_s + P_s A_s^{i\prime} + Q_s^i \prec 0, \tag{3.49}$$

$$\begin{bmatrix} Q_f^i & P_2^j - P_2^i - A_{11}^i P_f^i A_{21}^i{}' \\ (\star)' & Q_s^i - A_{21}^i P_f^i A_{21}^i{}' \end{bmatrix} \succ 0 \tag{3.50}$$

are verified $\forall\,(i,j) \in \mathcal{I} \times \mathcal{I}$, *with* $P_2^i = (I_{n_1} - A_{11}^i)^{-1} A_{12}^i P_s$. *Hence, there exists a positive scalar* ε_{max} *such that the switched system (3.41) is asymptotically stable* $\forall\,\varepsilon \in (0, \varepsilon_{max}]$ *and for any switching rule.*

Proof. Let us assume

$$P^i(\varepsilon) = \begin{bmatrix} P_1^i(\varepsilon) & P_2^i(\varepsilon) \\ P_2^i(\varepsilon)' & P_3(\varepsilon) \end{bmatrix} \succ 0, \tag{3.51}$$

$$Q^{ij}(\varepsilon) = \begin{bmatrix} Q_1^i & Q_2^{ij}(\varepsilon) \\ Q_2^{ij}(\varepsilon)' & Q_3^i(\varepsilon) \end{bmatrix} \succ 0, \tag{3.52}$$

with

$$P_1^i(\varepsilon) = P_f^i + \varepsilon P_2^i P_s^{-1} P_2^{i\prime}, \quad P_2^i(\varepsilon) = \varepsilon P_2^i = \varepsilon (I_{n_1} - A_{11}^i)^{-1} A_{12}^i P_s, \quad P_3(\varepsilon) = \varepsilon P_s, \tag{3.53}$$

$$Q_1^i = Q_f^i, \quad Q_2^{ij}(\varepsilon) = \varepsilon (P_2^j - P_2^i - A_{11}^i P_f^i A_{21}^i{}'), \quad Q_3^i(\varepsilon) = \varepsilon^2 (Q_s^i - A_{21}^i P_f^i A_{21}^i{}'). \tag{3.54}$$

Substituting (3.42), (3.51)-(3.52) in (3.47), we have:

$$\begin{bmatrix} X_1^{ij}(\varepsilon) & X_2^{ij}(\varepsilon) \\ X_2^{ij}(\varepsilon)' & X_3^i(\varepsilon) \end{bmatrix} \prec 0 \tag{3.55}$$

with:

$$X_1^{ij}(\varepsilon) = A_{11}^i P_1^i(\varepsilon) A_{11}^{i\,\prime} + A_{12}^i P_2^i(\varepsilon)' A_{11}^{i\,\prime} + A_{11}^i P_2^i(\varepsilon) A_{12}^{i\,\prime} + A_{12}^i P_3(\varepsilon) A_{12}^{i\,\prime} - P_1^j(\varepsilon) + Q_1^i,$$

$$X_2^{ij}(\varepsilon) = A_{11}^i P_1^i(\varepsilon) A_{21}^{i\,\prime}\varepsilon + A_{12}^i P_2^i(\varepsilon)' A_{21}^{i\,\prime}\varepsilon + A_{11}^i P_2^i(\varepsilon)(I_{n_2} + \varepsilon A_{22}^i)' + A_{12}^i P_3^i(\varepsilon)(I_{n_2} + \varepsilon A_{22}^i)' - P_2^j(\varepsilon) + Q_2^{ij}(\varepsilon),$$

$$X_3^i(\varepsilon) = \varepsilon A_{21}^i P_1^i(\varepsilon) A_{21}^{i\,\prime}\varepsilon + \varepsilon A_{21}^i P_2^i(\varepsilon)(I_{n_2} + \varepsilon A_{22}^i)' + (I_{n_2} + \varepsilon A_{22}^i) P_2^{i\prime}(\varepsilon) A_{21}^{i\,\prime}\varepsilon + (I_{n_2} + \varepsilon A_{22}^i) P_3(\varepsilon)(I_{n_2} + \varepsilon A_{22}^i)' - P_3(\varepsilon) + Q_3(\varepsilon).$$

Replacing the values of $P^i(\varepsilon)$, $Q^{ij}(\varepsilon)$, and the equations (3.45), (3.53)-(3.54), we obtain:

$$X_1^{ij}(\varepsilon) = A_{11}^i P_f^i A_{11}^{i\,\prime} - P_f^j + Q_f^i + O(\varepsilon) = X_1^{ij} + O(\varepsilon),$$

$$X_2^{ij}(\varepsilon) = \varepsilon^2 (A_{12}^i P_2^{i\prime} A_{21}^{i\,\prime} + A_{11}^i P_2^i A_{22}^{i\,\prime} + O(\varepsilon)) = \varepsilon^2 (X_2^i + O(\varepsilon)),$$

$$X_3^i(\varepsilon) = \varepsilon^2 (A_s^i P_s + P_s A_s^{i\prime} + Q_s^i + O(\varepsilon)) = \varepsilon^2 (X_3^i + O(\varepsilon)).$$

The inequality (3.55) can be written as

$$\begin{bmatrix} X_1^{ij} + O(\varepsilon) & \varepsilon^2 (X_2^i + O(\varepsilon)) \\ (\star)' & \varepsilon^2 (X_3^i + O(\varepsilon)) \end{bmatrix} \prec 0.$$

Satisfying the conditions (3.48) and (3.49) implies that $X_1^{ij} \prec 0$ and $X_3^i \prec 0$. This means that there exists a scalar $\varepsilon_{max} > 0$ such that $X_3^i + O(\varepsilon) \prec 0$ and $X_1^{ij} - \varepsilon^2 X_2^i X_3^{i^{-1}} X_2^{i\prime} + O(\varepsilon) \prec 0$, $\forall (i,j) \in \mathcal{I} \times \mathcal{I}$ and $\forall\, \varepsilon \in (0, \varepsilon_{max}]$. Hence, using the Schur complement, the LMI (3.47) holds. Since $P_f \succ 0$ and $P_s \succ 0$, (3.51) holds. Furthermore, (3.52) can be written as

$$Q^{ij}(\varepsilon) = \begin{bmatrix} I_{n_1} & 0 \\ 0 & \varepsilon I_{n_2} \end{bmatrix} \begin{bmatrix} Q_f^i & P_2^j - P_2^i - A_{11}^i P_f^i A_{21}^{i\,\prime} \\ (\star)' & Q_s^i - A_{21}^i P_f^i A_{21}^{i\,\prime} \end{bmatrix} \begin{bmatrix} I_{n_1} & 0 \\ 0 & \varepsilon I_{n_2} \end{bmatrix} \succ 0,$$

which is non negative definite because of (3.50). This concludes the proof. ■

Remark 9 *An evaluation of the upper bound ε_{max} is obtained solving the following optimization problem:*

$$\varepsilon_{max} = max\ \varepsilon > 0 \tag{3.56}$$

$$subject\ \ to\ \ A^i(\varepsilon) P^i(\varepsilon) A^i(\varepsilon)' - P^j(\varepsilon) + Q^{ij}(\varepsilon) \prec 0, \quad (i,j) \in \mathcal{I} \times \mathcal{I},$$

where matrices $A^i(\varepsilon)$, $P^i(\varepsilon)$, and $Q^{ij}(\varepsilon)$ are defined in (3.42) and (3.51)-(3.54), respectively. Moreover, the values of P_f^i, Q_f^i, P_s and Q_s^i can be computed by Theorem 9, for any $(i,j) \in \mathcal{I} \times \mathcal{I}$.

3.4.2 Control design

Consider the two time scale switched system in the fast sampling model (2.13):

$$x(k+1) = A^{\sigma(k)}(\varepsilon)x(k) + B^{\sigma(k)}(\varepsilon)u(k), \tag{3.57}$$

where $u(k) \in \mathbb{R}^r$ is the control signal, for all $k \in \mathbb{Z}^+$,

$$A^i(\varepsilon) = \begin{bmatrix} A^i_{11} & A^i_{12} \\ \varepsilon A^i_{21} & (I_{n_2} + \varepsilon A^i_{22}) \end{bmatrix}, \; B^i(\varepsilon) = \begin{bmatrix} B^i_1 \\ \varepsilon B^i_2 \end{bmatrix}, \tag{3.58}$$

and $(I_{n_1} - A^i_{11})$ is assumed to be a non-singular matrix, for any $i \in \mathcal{I}$. The subsystem corresponding to each mode i may be written in the form:

$$\begin{cases} x_1(k+1) = A^i_{11}x_1(k) + A^i_{12}x_2(k) + B^i_1 u(k) \\ x_2(k+1) = \varepsilon A^i_{21}x_1(k) + (I_{n_2} + \varepsilon A^i_{22})x_2(k) + \varepsilon B^i_2 u(k). \end{cases} \tag{3.59}$$

Its slow subsystem is:

$$x_s(k+1) = (I_{n_2} + \varepsilon A^i_s)x_s(k) + \varepsilon B^i_s u_s(k) \tag{3.60}$$

with

$$A^i_s = A^i_{22} + A^i_{21}(I_{n_1} - A^i_{11})^{-1}A^i_{12}, \quad B^i_s = B^i_2 + A^i_{21}(I_{n_1} - A^i_{11})^{-1}B^i_1, \tag{3.61}$$

while its fast subsystem is:

$$x_f(k+1) = A^i_{11}x_f(k) + B^i_1 u_f(k). \tag{3.62}$$

The pair (A^i_s, B^i_s) is assumed to be stabilizable in the continuous-time setting, and the pair (A^i_{11}, B^i_1) is assumed to be stabilizable in the discrete-time setting, for any $i \in \mathcal{I}$.

The aim of this section is to design a state-feedback control law

$$u(k) = K^{\sigma(k)}(\varepsilon)x(k) \tag{3.63}$$

asymptotically stabilizing the closed loop system (3.57) for any switching rule. The extension of condition (3.47) to state feedback-design leads to check the existence of matrices $P^i(\varepsilon) = P^i(\varepsilon)' \succ 0$, $Q^{ij}(\varepsilon) = Q^{ij}(\varepsilon)' \succ 0$ and $Z^i(\varepsilon)$ of appropriate dimensions such that the inequality

$$\begin{aligned} &A^i(\varepsilon)P^i(\varepsilon)A^i(\varepsilon)' + A^i(\varepsilon)Z^i(\varepsilon)'B^i(\varepsilon)' + B^i(\varepsilon)Z^i(\varepsilon)A^i(\varepsilon)' + \\ &B^i(\varepsilon)Z^i(\varepsilon)P^i(\varepsilon)^{-1}Z^i(\varepsilon)'B^i(\varepsilon)' - P^j(\varepsilon) + Q^{ij}(\varepsilon) \prec 0 \end{aligned} \tag{3.64}$$

holds for any $(i,j) \in \mathcal{I} \times \mathcal{I}$. The state-feedback control law (3.63), with $K^i(\varepsilon) = Z^i(\varepsilon)P^i(\varepsilon)^{-1}$, stabilizes asymptotically the discrete-time switched system (3.57). The following theorem gives LMI based design conditions independent of ε in order to avoid the numerical problems due to the ill-conditioning of (3.64).

Theorem 12 *Assume that there exist matrices* $P_f^i = P_f^{i\prime} \succ 0$, $Q_f^i = Q_f^{i\prime} \succ 0$, Z_f^i, $P_s = P_s{}' \succ 0$, $Q_s^i = Q_s^{i\prime} \succ 0$ *and* Z_s^i *of appropriate dimensions such that the LMIs*

$$\begin{bmatrix} P_f^j - Q_f^i & A_{11}^i P_f^i + B_1^i Z_f^i \\ (\star)' & P_f^i \end{bmatrix} \succ 0, \tag{3.65}$$

$$A_s^i P_s + P_s A_s^{i\prime} + B_s^i Z_s^i + Z_s^{i\prime} B_s^{i\prime} + Q_s^i \prec 0, \tag{3.66}$$

$$\begin{bmatrix} Q_f^i & P_2^j - P_2^i & A_{11}^i P_f^i + B_1^i Z_f^i \\ (\star)' & Q_s^i & A_{21}^i P_f^i + B_2^i Z_f^i \\ (\star)' & (\star)' & P_f^i \end{bmatrix} \succ 0 \tag{3.67}$$

are verified $\forall (i,j) \in \mathcal{I} \times \mathcal{I}$, *with* $P_2^i = (I_{n_1} - A_{11}^i)^{-1}(A_{12}^i P_s + B_1^i Z_s^i)$. *Hence, there exists a positive scalar* ε_{max} *such that the state-feedback controller gains*

$$K^i = \begin{bmatrix} K_f^i & K_s^i - K_f^i (I_{n_1} - A_{11}^i)^{-1}(A_{12}^i + B_1^i K_s^i) \end{bmatrix}, \tag{3.68}$$

with $K_f^i = Z_f^i P_f^{i-1}$ *and* $K_s^i = Z_s^i P_s^{-1}$, *stabilize asymptotically the closed loop switched system (3.57),* $\forall\, \varepsilon \in (0, \varepsilon_{max}]$ *and for any switching rule.*

Proof. See Appendix B.4. ■

Remark 10 *The conditions of Theorem 12 with* $Z_f^i = 0$, $i \in \mathcal{I}$, *lead to the reduced control law:*

$$u(k) = \begin{bmatrix} 0 & K_s^{\sigma(k)} \end{bmatrix} \begin{bmatrix} x_1(k) \\ x_2(k) \end{bmatrix}, \tag{3.69}$$

which asymptotically stabilizes the switched system (3.57) for any $\varepsilon \in (0, \varepsilon_{max}]$ *and any switching rule* σ. *Notice that in this case (3.65) assumes that the fast switched subsystem is asymptotically stable in open loop.*

3.5 Numerical example

Consider the continuous-time switched system (3.29), with $\mathcal{I} = \{1, 2\}$, $\varepsilon = 0.005$ and

$$M_{11}^1 = \begin{bmatrix} 0 & 1 \\ -1 & -2 \end{bmatrix}, M_{12}^1 = \begin{bmatrix} 0 & 0 \\ 1.5 & 0 \end{bmatrix}, M_{21}^1 = \begin{bmatrix} 0 & 0 \\ -0.6 & -0.5 \end{bmatrix}, M_{22}^1 = \begin{bmatrix} 0 & 1 \\ 2.1 & 0 \end{bmatrix},$$
$$N_1^1 = \begin{bmatrix} 0 \\ -1 \end{bmatrix}, N_2^1 = \begin{bmatrix} 0 \\ 0 \end{bmatrix},$$

$$M_{11}^2 = \begin{bmatrix} 0 & 1 \\ -3 & -5 \end{bmatrix}, M_{12}^2 = \begin{bmatrix} 0 & 0 \\ 0 & 0 \end{bmatrix}, M_{21}^2 = \begin{bmatrix} 0 & 0 \\ -0.3 & -0.2 \end{bmatrix}, M_{22}^2 = \begin{bmatrix} 0 & 0.7 \\ 0 & 0 \end{bmatrix},$$
$$N_1^2 = \begin{bmatrix} 0 \\ -1 \end{bmatrix}, N_2^2 = \begin{bmatrix} 0 \\ 0 \end{bmatrix}.$$

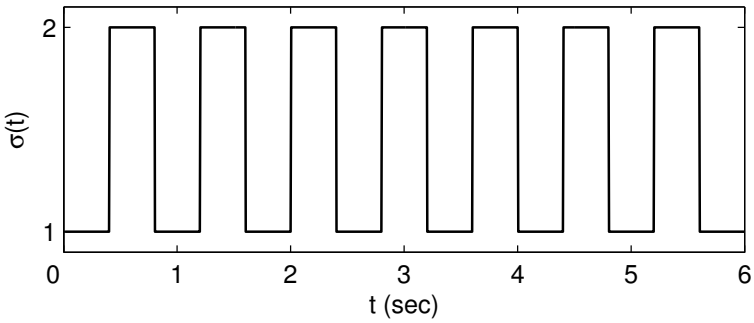

Figure 3.6: Switching rule $\sigma(t)$

The subsystem 1 is open loop unstable while the subsystem 2 is characterized by a state-space matrix with zero eigenvalues. Obviously, this system is unstable under arbitrary switching rules and existing results in the literature do not help in designing a stabilizing switching rule. Theorem 10 leads to the following stabilizing controller gains:

$$K^1 = \begin{bmatrix} 0.4040 & 0.1511 & -65.3601 & -60.3074 \end{bmatrix},$$
$$K^2 = \begin{bmatrix} -0.4110 & -0.5931 & -147.6057 & -137.0206 \end{bmatrix}.$$

For this example, the fast switched system was found asymptotically stable in open loop. Hence, using Remark 8, a reduced control law may also be proposed:

$$K_r^1 = \begin{bmatrix} 0 & 0 & -99.0779 & -88.5710 \end{bmatrix},$$
$$K_r^2 = \begin{bmatrix} 0 & 0 & -347.0992 & -310.4213 \end{bmatrix}.$$

Consider the switching rule given in Fig. 3.6 and the initial condition $x(0) = \begin{bmatrix} 0 & 0 & 1 & 0 \end{bmatrix}'$, Fig. 3.7 shows the state trajectories, with

$$x(t) = \begin{bmatrix} x'_{11}(t) & x'_{12}(t) & x'_{21}(t) & x'_{22}(t) \end{bmatrix}'.$$

The solid line shows the state trajectories using the full state-feedback controller gains K^1 and K^2 while the dotted line shows the state trajectories using the reduced state-feedback controller gains K_r^1 and K_r^2. Fig. 3.8 shows the control signal evolution. Let the corresponding discretized switched system in the singular perturbation form (3.57), with sampling time $T_f = 0.005$ and

$$A_{11}^1 = \begin{bmatrix} 0.7358 & 0.3679 \\ -0.3679 & 0.0000 \end{bmatrix}, \; A_{12}^1 = \begin{bmatrix} 0.3964 & 0 \\ 0.5518 & 0 \end{bmatrix},$$
$$A_{21}^1 = \begin{bmatrix} 0 & 0 \\ -0.4057 & -0.3425 \end{bmatrix}, \; A_{22}^1 = \begin{bmatrix} 0 & 1 \\ 1.8085 & 0 \end{bmatrix},$$
$$B_1^1 = \begin{bmatrix} -0.2642 \\ -0.3679 \end{bmatrix}, \; B_2^1 = \begin{bmatrix} 0 \\ 0.1943 \end{bmatrix},$$

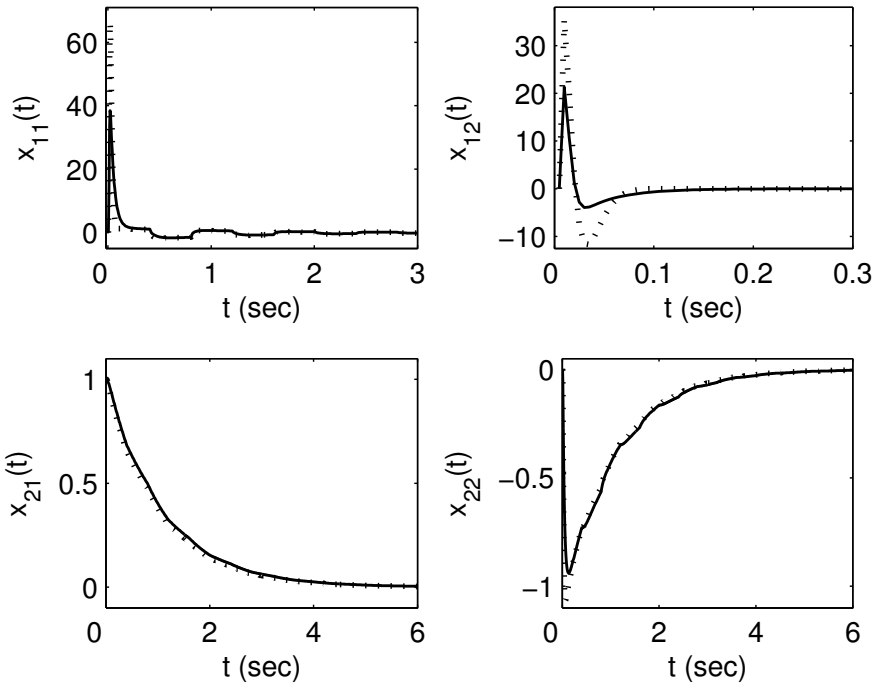

Figure 3.7: Closed loop response in the continuous-time with full state-feedback controller (solid line) and reduced state-feedback controller (dotted line)

$$A_{11}^2 = \begin{bmatrix} 0.5916 & 0.1344 \\ -0.4031 & -0.0801 \end{bmatrix}, A_{12}^2 = \begin{bmatrix} 0 & 0 \\ 0 & 0 \end{bmatrix},$$
$$A_{21}^2 = \begin{bmatrix} 0 & 0 \\ -0.1628 & -0.0677 \end{bmatrix}, A_{22}^2 = \begin{bmatrix} 0 & 0.7 \\ 0 & 0 \end{bmatrix}$$
$$B_1^2 = \begin{bmatrix} -0.1361 \\ -0.1344 \end{bmatrix}, B_2^2 = \begin{bmatrix} 0 \\ 0.0457 \end{bmatrix}.$$

From Theorem 12, we find the controller gains:

$$K^1 = \begin{bmatrix} 0.8565 & 0.6941 & -19.7259 & -9.8473 \end{bmatrix},$$
$$K^2 = \begin{bmatrix} 1.5333 & 0.3934 & -52.0573 & -24.3528 \end{bmatrix}.$$

Using Remark 10, we obtain the reduced controller gains:

$$K_r^1 = \begin{bmatrix} 0 & 0 & -10.0899 & -5.4331 \end{bmatrix}, \quad K_r^2 = \begin{bmatrix} 0 & 0 & -34.9751 & -16.4975 \end{bmatrix}.$$

In Fig. 3.9, the state trajectories are shown for the full state-feedback controller case (solid line) and the reduced state-feedback controller case (dotted line). In Fig. 3.10, the control signal evolution is shown.

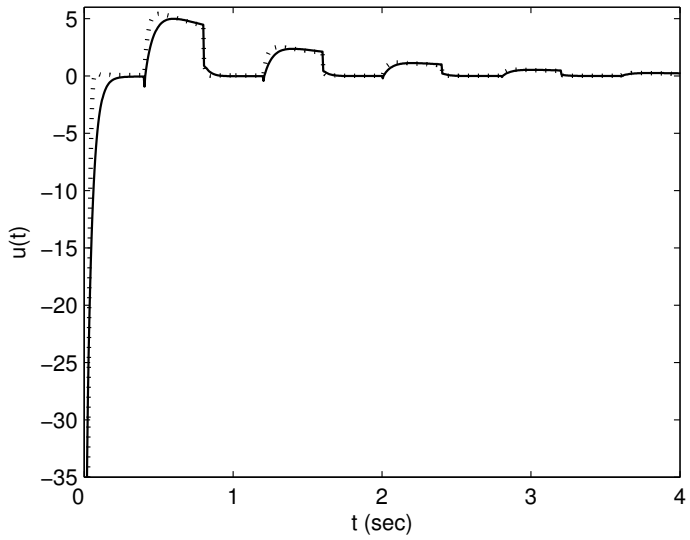

Figure 3.8: Control signal evolution in the continuous-time with full state-feedback controller (solid line) and reduced state-feedback controller (dotted line)

3.6 Conclusion

It is well known that some fundamental properties of linear systems can be lost by switchings. This is the case of stability, observability, controllability, flatness, and so on. In this chapter, we showed that stability of the slow and fast switched subsystems under arbitrary switching rules does not imply the stability of the corresponding two time scale switched system in the singular perturbation form. A coupling constraint, which may be interpreted as a certain level of the degree of time scale separation, has also to be satisfied. This constraint was expressed in terms of LMI based conditions for stability analysis of singularly perturbed switched systems independently of the value of the singular parameter ε and under an arbitrary switching rule, for both continuous and fast sampling discrete time cases. Composite and reduced state-feedback control design problems were investigated in the same framework. As pointed out in Chapter 2, the discrete time model that we utilized, called fast sampling model, presents two main advantages, with respect to the other discrete time models of two time scale systems given in literature. First, it allows to describe both discretized continuous two time scale systems and pure difference equations. Second, due to the choice of the sampling time as $T_f = \varepsilon$, this model assumes that the sampling rate is fast enough to influence the transient behavior of the system for control purposes, when it represents discretized continuous two time scale systems. Thus, from a theoretical point of view, has a larger interest.

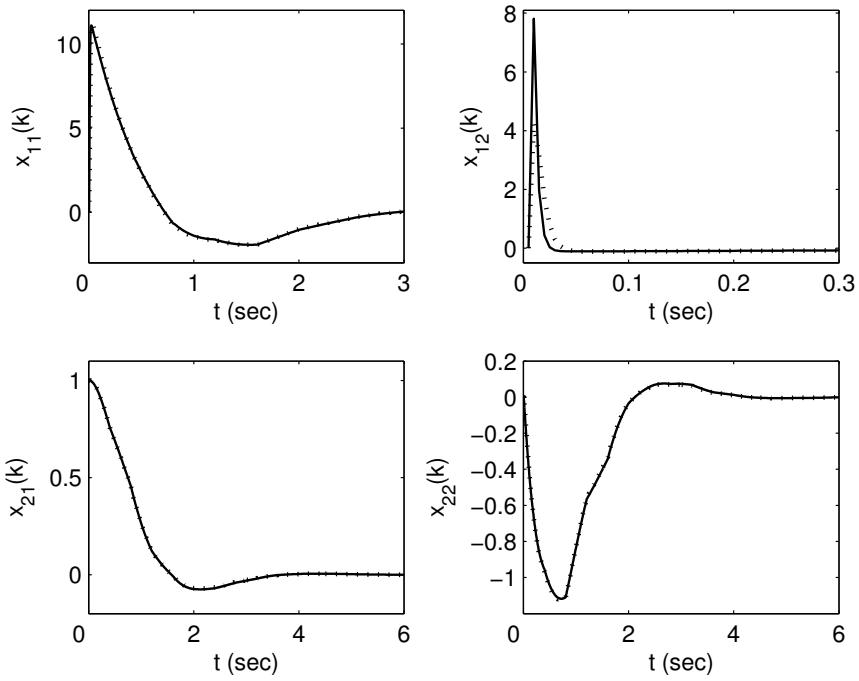

Figure 3.9: Closed loop response in the discrete-time ($T_f = 0.005$) with full state-feedback controller (solid line) and reduced state-feedback controller (dotted line)

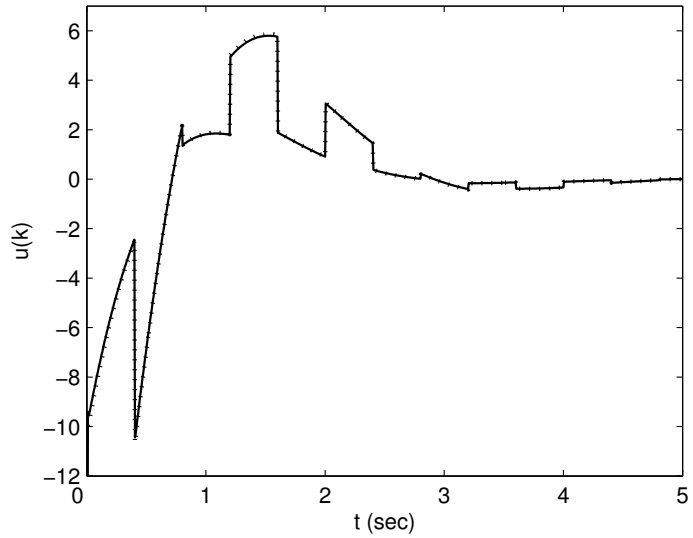

Figure 3.10: Control signal evolution in the discrete-time ($T_f = 0.005$) with full state-feedback controller (solid line) and reduced state-feedback controller (dotted line)

Chapter 4

Bumpless transfer for switched systems

4.1 Introduction

In practical control of nonlinear plants, often a set of discrete-time LTI controllers

$$\begin{cases} x_c(k+1) = A_c^{\sigma(k)} x_c(k) + B_c^{\sigma(k)} y(k) \\ u(k) = C_c^{\sigma(k)} x_c(k) + D_c^{\sigma(k)} y(k) \end{cases} \tag{4.1}$$

is used, where $x_c(k) \in \mathbb{R}^p$ is the controller state, $u(k) \in \mathbb{R}^r$ is the control signal, $y(k) \in \mathbb{R}^m$ is the plant measured output, $\{(A_c^i, B_c^i, C_c^i, D_c^i) : i \in \mathcal{I} = \{1, ..., N\}\}$ is a family of matrices and $\sigma : \mathbb{Z}^+ \to \mathcal{I}$ is the switching rule, which handles the scheduling among the controllers and is assumed to be available in real-time, for any $i \in \mathcal{I}$ and for all $k \in \mathbb{Z}^+$. Each time the operating point of the system changes, the adequate controller is activated by a supervisor. However, switching among different controllers implies undesired transient behaviors due to possible large variations of the control signal. This phenomenon may affect the system performances and, in the worst case, destabilize the closed loop system. The solution of this problem, which has been largely studied in the last few decades, is called bumpless transfer.

A description of most popular strategies for bumpless transfer can been found in [Han88], [KCMN94], [GA96] and [EP98]. One of the first schemes is proposed by Hanus for nonlinear plants [HKH87]. The idea consists in pre-setting the off-line controller state for reducing the transient behavior at the switching time. Turner and Walker generalize the results of Hanus for controllers which are not bi-proper [TW99], [TW00]. Let define the signal

$$\bar{z}_e^i(k) = \alpha^i(k) - e(k),$$

which represents the difference between the i^{th} off-line controller input $\alpha^i(k) \in \mathbb{R}^m$ and the on-line controller input $e(k) = r(k) - y(k)$, where $r(k) \in \mathbb{R}^m$ is the reference; and the signal

$$\bar{z}_u^i(k) = u^i(k) - u(k),$$

which represents the difference between the i^{th} off-line controller output $u^i(k)$ and the on-line controller output $u(k)$, for any $i \in \mathcal{I}$ and for all $k \in \mathbb{Z}^+$. The idea in [TW00] is to minimize the following LQ criterion :

$$\bar{J}^i = \bar{\phi}^i(\bar{T}_f^i) + \frac{1}{2}\sum_{k=t_i}^{\bar{T}_f^i - 1} [\bar{z}_u^{i'}(k)\bar{W}_u^i \bar{z}_u^i(k) + \bar{z}_e^{i'}(k)\bar{W}_e^i \bar{z}_e^i(k)],$$

where

$$\bar{\phi}^i(\bar{T}_f^i) = \frac{1}{2}\bar{z}_u^{i'}(\bar{T}_f^i)\bar{X}^i \bar{z}_u^i(\bar{T}_f^i),$$

$\bar{W}_e^i = \bar{W}_e^{i'} \succ 0$ and $\bar{W}_u^i = \bar{W}_u^{i'} \succ 0$ are weighting matrices, t_i is the switching time to the subsystem corresponding to the mode $i \in \mathcal{I}$, $\bar{T}_f^i$ is the terminal time and $\bar{X}^i = \bar{X}^{i'} \succeq 0$ is a terminal weighting matrix, for any $i \in \mathcal{I}$. Since reference signals are not known a priori, practical implementation requires an extension to an infinite horizon. This approximation yields a constant feedback matrix $\bar{Q}^i$ that preconditions the i^{th} off-line controller (4.1) for obtaining the desired transient behavior at the switching time (Fig. 4.1).

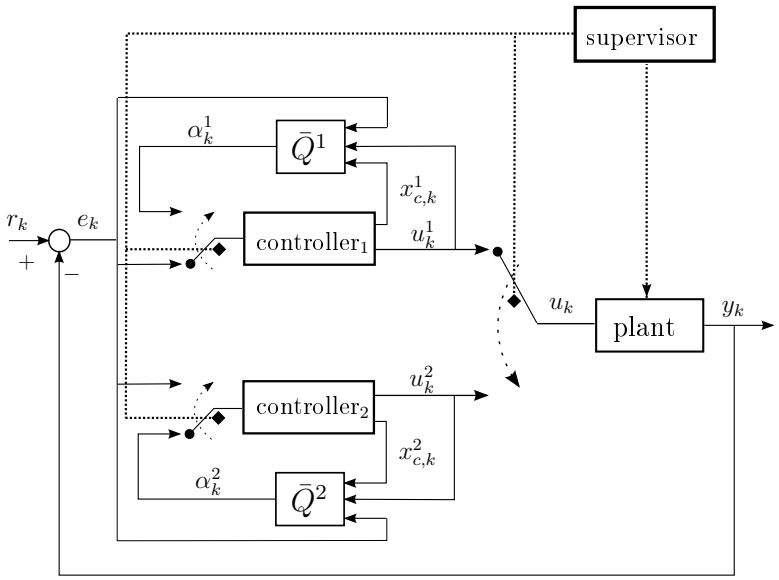

Figure 4.1: Closed loop system with $\mathcal{I} = \{1, 2\}$

In particular, we have:

$$\alpha^i(k) = \bar{Q}^i \begin{bmatrix} x_c(k) \\ u(k) \\ e(k) \end{bmatrix},$$

with

$$\bar{Q}^i = (I_m - \Gamma^i B_c^{i'} \Pi^i B_c^i)^{-1} \Gamma^i \begin{bmatrix} (D_c^{i'} \bar{W}_u^i C_c^i + B_c^{i'} \Pi^i A_c^i)' \\ -(D_c^{i'} \bar{W}_u^i + B_c^{i'}(I_p - M^i)^{-1} U^i)' \\ -(\bar{W}_e^i + B_c^{i'}(I_p - M^i)^{-1} E^i)' \end{bmatrix}',$$

where

$$\begin{aligned}
\Gamma^i &= -(D_c^{i'}\bar{W}_u^i D_c^i + \bar{W}_e^i)^{-1},\\
\bar{A}^i &= A_c^i + B_c^i\Gamma^i D_c^{i'}\bar{W}_u^i C_c^i,\\
\bar{B}^i &= B_c^i\Gamma^i B_c^{i'},\\
M^i &= \bar{A}^{i'}(I_p - \Pi^i\bar{B}^i)^{-1},\\
U^i &= M^i\Pi^i B_c^i\Gamma^i D_c^{i'}\bar{W}_u^i + C_c^{i'}\bar{W}_u^i(I_r + D_c^i\Gamma^i D_c^{i'}\bar{W}_u^i),\\
E^i &= M^i\Pi^i B_c^i\Gamma^i\bar{W}_e^i + C_c^{i'}\bar{W}_u^i D_c^i\Gamma^i\bar{W}_e^i,
\end{aligned}$$

and Π^i is the stabilizing solution to the discrete-time Riccati equation

$$\bar{A}^{i'}(I_n - \Pi^i\bar{B}^i)^{-1}\Pi^i\bar{A}^i - \Pi^i + C_c^{i'}\bar{W}_u^i(I_r + D_c^i\Gamma^i D_c^{i'}\bar{W}_u^i)C_c^i = 0,$$

for any $i \in \mathcal{I}$. LQ bumpless transfer has been one of most celebrated bumpless transfer methods on industrial MIMO applications [TAB+06], [ZLBT06], [ZB09]. This success is due to different factors: the existence of several reliable numerical solvers for Riccati equations, the excellent convergence properties of LQ based feedback controllers, and the fact that no plant knowledge is needed. Nevertheless, the extension to an infinite horizon assumes that the tracking error e and the control signal u are constant. This approximation is effective only if these signals vary slowly enough, with reference to the system dynamics. Another drawback is concerned with the fact that this strategy guarantees the closed loop stability only around a specific operating point. In general, it is assumed that the closed loop stability of the whole process is maintained, if both on-line and off-line control loops are stable. This assumption is justified only if the operating point is subject to "slow" variations.

In [CS08], the discontinuity of the controller output is reduced by resetting the fast dynamics of the controller at the switching time. In [ZT05], the desired transient behavior, called target response, is defined as the ideal closed loop behavior after the controller switching. Hence, the anti bumpless purpose is reached by recovering the target response in a $\mathcal{L}_2$ sense [TK97]. Unlike the previous solutions, this method guarantees the asymptotic stability of the closed loop system for arbitrary switchings of the controller. Nevertheless, these results are limited to the linear plant case.

Although the bumpless transfer problem has been widely studied in literature, only few articles address the switched systems framework. In [AW96], a bumpless transfer solution for continuous-time switched systems is given when the order of the controller is smaller than the order of the plant. The idea is to force the output of the activated controller to be equal to the plant input at the switching time. An analogous strategy is proposed in [DW06] for continuous-time linear parameter varying systems. However, as pointed out by Zaccarian and Teel, a constraint on the only controller output does not imply better performances on the plant output [ZT02], [ZT05].

In this chapter, a bumpless transfer control design for discrete-time switched systems is presented [MHD+08], [MHD+09]. The solution is based on the LQ

optimization theory, which has been introduced on the bumpless transfer framework by Turner and Walker. This method does not guarantee stability of the closed loop switched system as it is well-known that switchings can destabilize the closed loop system, even if all the subsystems are stable [Lib03]. To solve this problem, we propose a LQ bumpless transfer controller which is activated at each switching time. The controller and the plant output are forced to follow a desired profile for a given period of time. A finite horizon approach can be directly applied, which means that no approximation on the tracking error and on the control signal are needed. Asymptotic stability of the closed loop system is verified through dwell time conditions [GC06b].

4.2 Preliminaries

Consider the discrete-time switched system

$$\begin{cases} x(k+1) = A^{\sigma(k)}x(k) + B^{\sigma(k)}u(k) \\ y(k) = C^{\sigma(k)}x(k) \end{cases} \tag{4.2}$$

where $x(k) \in \mathbb{R}^n$ is the state vector, which is assumed to be available for feedback, for all $k \in \mathbb{Z}^+$. Moreover, $\{(A^i, B^i, C^i) : i \in \mathcal{I}\}$ is a family of matrices and the pair (A^i, B^i) is assumed to be controllable for any $i \in \mathcal{I}$. Let the state-feedback control law

$$u(k) = K^{\sigma(k)}x(k), \tag{4.3}$$

which stabilizes the closed loop system (4.2)-(4.3) for any switching law. Further, let us define the minimal interval of time $\Delta^i \in \mathbb{Z}^+$ the system remains in the subsystem corresponding to the mode i until it switches to another subsystem. Δ^i is assumed to be known for any $i \in \mathcal{I}$.

Switching among controllers usually introduces large jumps in the control signal. In order to reduce the amplitude of these jumps, different strategies are possible. In this work, we propose a bumpless transfer controller that is activated at the instant t_i, which represents a switching instant to the i^{th} mode, for a period of time $\tau_i^M < \Delta^i$. Therefore, for each mode $i \in \mathcal{I}$, we have:

$$u(k) = \begin{cases} K^i x(k) + u^{bt,i}(k) & if \quad t_i \leq k < t_i + \tau_i^M \\ K^i x(k) & otherwise, \end{cases} \tag{4.4}$$

where $u^{bt,i}(k) \in \mathbb{R}^r$ is the bumpless transfer controller output, for all $k \in [t_i, t_i + \tau_i^M)$. The closed loop system (4.2)-(4.4) is shown in Fig. 4.2.

The bumpless transfer controller will be designed in the next section. It will depend on the profile of the desired transient behavior and on the state matrices. For simplicity reasons, a straight line is chosen as desired profile. Let t_i be a switching instant from the mode j to the mode i, for all $(j, i) \in \mathcal{I} \times \mathcal{I}$. We can

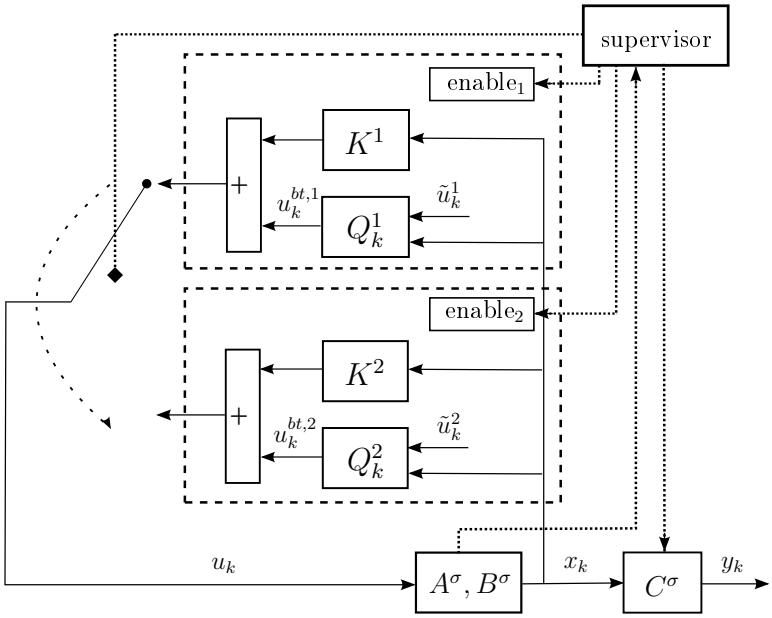

Figure 4.2: Closed loop system with $\mathcal{I} = \{1, 2\}$

define the desired control signal of the subsystem corresponding to the i^{th} mode as:

$$\tilde{u}^i(k) = \begin{cases} \tilde{u}^{i,0}(k) + (k - t_i + 1)p^i(k) & if \quad t_i \leq k < t_i + \tau_i^M \\ 0 & otherwise, \end{cases} \tag{4.5}$$

where

$$\tilde{u}^{i,0}(k) = K^j x(t_i - 1) \tag{4.6}$$

is the control signal value at the instant before the switching and p^i determines the slope of the desired profile, i. e.

$$p^i(k) = \frac{1}{\tau_i^M}(K^i x(t_i) - K^j x(t_i - 1)). \tag{4.7}$$

We obtain a value of p^i that depends on the control signal discontinuity. An illustrative example is given in Fig. 4.3.

4.3 Bumpless transfer control design

In this section, we present the bumpless transfer control design, which is based on the minimization of a LQ criterion. In the bumpless transfer framework, this solution was proposed by [TW00], where the difference between the on-line and the off-line controller input and output are minimized before each switching. This is equivalent to initialize the controller state for reducing the transient behavior on the plant output. Since this method consists in pre-setting the state of the off-line controller before the switching, it does not address control systems without memory, such as state-feedback control laws. Furthermore, the controller

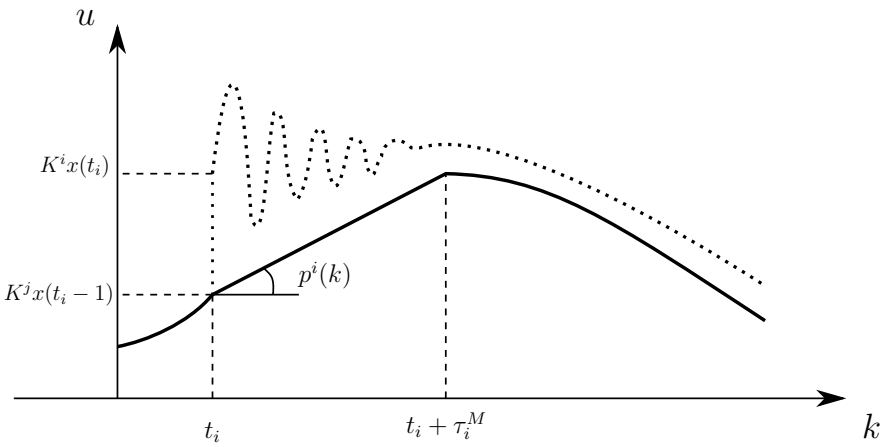

Figure 4.3: Control signal evolution with bumpless transfer controller switched on (solid line) and switched off (dotted line)

input and output cannot be known a priori. Hence, the practical implementation requires an extension to the infinite horizon case. At last, asymptotic stability of the closed loop system is not guaranteed. In general, it is assumed that the closed loop stability of the whole process is maintained, if both on-line and off-line control loops are asymptotically stable. This assumption is justified if we consider that the operating point is subject to slow variations, which is not necessarily the case for switched systems. In this case, switchings can destabilize the closed loop system, even if all the subsystems are asymptotically stable [Lib03].

In order to solve these problems, we propose a bumpless transfer controller which is activated at each switching time t_i. Asymptotic stability conditions for the closed loop system (4.2)-(4.4) are presented in the next section. For each mode $i \in \mathcal{I}$, the bumpless transfer control law is based on the minimization of the following quadratic cost function:

$$J^i = \phi^i(t_i + \tau_i^M) + \frac{1}{2} \sum_{k=t_i}^{t_i+\tau_i^M-1} [z^{u,i'}(k) W_u^i z^{u,i}(k) + z^{y,i'}(k) W_y^i z^{y,i}(k)], \tag{4.8}$$

with

$$z^{u,i}(k) = u(k) - \tilde{u}^i(k), \tag{4.9}$$

$$z^{y,i}(k) = y(k) - \tilde{y}^i(k), \tag{4.10}$$

and

$$\phi^i(t_i + \tau_i^M) = \frac{1}{2} z^{u,i'}(t_i + \tau_i^M) X^i z^{u,i}(t_i + \tau_i^M). \tag{4.11}$$

$W_u^i \succ 0$, $W_y^i \succ 0$ and $X^i \succeq$ are weighting matrices. The desired control signal $\tilde{u}^i$ was defined in (4.5) while the desired output signal is set to $\tilde{y}^i = 0$ for simplicity reasons. The following theorem yields the signal $u^{bt,i}$ that minimizes the cost function J^i, for any $i \in \mathcal{I}$.

Theorem 13 *Given the switched system (4.2)-(4.4), the initial time t_i and the terminal time $t_i + \tau_i^M$, the bumpless transfer control law that minimizes the quadratic cost function (4.8) is*

$$u^{bt,i}(k) = Q^i(k) \begin{bmatrix} x(k) \\ \tilde{u}^i(k) \\ g^i(k+1) \end{bmatrix}, \tag{4.12}$$

with

$$Q^i(k) = \begin{bmatrix} (\tilde{N}^i(k+1)\Pi^i(k+1)A^i - K^i)' \\ (I_r + \tilde{N}^i(k+1)\Pi^i(k+1)B^i)' \\ -\tilde{N}^{i'}(k+1) \end{bmatrix}' \tag{4.13}$$

and

$$\tilde{N}^i(k+1) = -{W_u^i}^{-1} B^{i'} (I_n - \Pi^i(k+1)\tilde{B}^i)^{-1}, \tag{4.14}$$

$\forall\, i \in \mathcal{I}$. *The values of* Π^i *and* g^i *are provided by the equations*

$$\Pi^i(k) = A^{i'}(I_n - \Pi^i(k+1)\tilde{B}^i)^{-1}\Pi^i(k+1)A^i + \tilde{C}^i \tag{4.15}$$

and

$$g^i(k) = A^{i'}(I_n - \Pi^i(k+1)\tilde{B}^i)^{-1}(g^i(k+1) - \Pi^i(k+1)B^i\tilde{u}^i(k)), \tag{4.16}$$

with

$$\tilde{B}^i = -B^i {W_u^i}^{-1} B^{i'},\ \tilde{C}^i = C^{i'} W_y^i C^i. \tag{4.17}$$

The bound conditions are:

$$\Pi^i(t_i + \tau_i^M) = 0,\quad g^i(t_i + \tau_i^M) = 0. \tag{4.18}$$

Proof. Consider

$$\begin{aligned} J^i =& \phi^i(t_i + \tau_i^M) + \frac{1}{2}\sum_{k=t_i}^{t_i+\tau_i^M-1} [(K^i x(k) + u^{bt,i}(k) - \tilde{u}^i(k))' W_u^i \times \\ & (K^i x(k) + u^{bt,i}(k) - \tilde{u}^i(k)) + C^{i'} x(k) W_y^i C^i x(k)]. \end{aligned} \tag{4.19}$$

Introducing a Lagrange multiplier $\lambda^i(k) \in \mathbb{R}^n$, we have:

$$J^i = \phi^i(t_i + \tau_i^M) + \frac{1}{2}\sum_{k=t_i}^{t_i+\tau_i^M-1} [H^i(k) - \lambda^{i'}(k+1)x(k+1)], \tag{4.20}$$

where H^i is the Hamiltonian, defined by

$$\begin{aligned} H^i(k) =& \frac{1}{2}[(K^i x(k) + u^{bt,i}(k) - \tilde{u}^i(k))' W_u^i (K^i x(k) + u^{bt,i}(k) - \tilde{u}^i(k)) + \\ & C^{i'} x(k) W_y^i C^i x(k)] + \lambda^{i'}(k+1)[(A^i + B^i K^i)x(k) + B^i u^{bt,i}(k)]. \end{aligned} \tag{4.21}$$

First order necessary conditions are:

$$x(k+1) = \frac{\partial H^i(k)}{\partial \lambda^i(k+1)} \tag{4.22}$$

$$\lambda^i(k) = \frac{\partial H^i(k)}{\partial x(k)} \tag{4.23}$$

$$\frac{\partial H^i(k)}{\partial u^{bt,i}(k)} = 0 \tag{4.24}$$

$$\lambda^i(t_i + \tau_i^M) = \frac{\partial \phi^i(t_i + \tau_i^M)}{\partial x(t_i + \tau_i^M)}. \tag{4.25}$$

Since the cost function J^i is convex for any $i \in \mathcal{I}$, the conditions (4.22)-(4.25) are also sufficient for optimality. Substituting (4.22)-(4.24), we obtain:

$$\frac{\partial H^i(k)}{\partial \lambda^i(k+1)} = (A^i + B^i K^i)x(k) + B^i u^{bt,i}(k) \tag{4.26}$$

$$\begin{aligned}\frac{\partial H^i(k)}{\partial x(k)} =& (A^i + B^i K^i)'\lambda^i(k+1) + K^{i'} W_u^i K^i x(k) - \\ & K^{i'} W_u^i \tilde{u}^i(k) + K^{i'} W_u^i u^{bt,i}(k) + C^{i'} W_y^i C^i x(k)\end{aligned} \tag{4.27}$$

$$\frac{\partial H^i(k)}{\partial u^{bt,i}(k)} = W_u^i u^{bt,i}(k) + W_u^i K^i x(k) + B^{i'}\lambda^i(k+1) - W_u^i \tilde{u}^i(k). \tag{4.28}$$

Setting the last equation equal to zero, we have:

$$u^{bt,i}(k) = -K^i x(k) - {W_u^i}^{-1} B^{i'} \lambda^i(k+1) + \tilde{u}^i(k). \tag{4.29}$$

Hence, substituting $u^{bt,i}(k)$ in (4.26) and (4.27), we obtain the following non homogeneous difference equation:

$$\begin{cases} x(k+1) = A^i x(k) + \tilde{B}^i \lambda^i(k+1) + B^i \tilde{u}^i(k) \\ \lambda^i(k) = \tilde{C}^i x(k) + A^{i'} \lambda^i(k+1). \end{cases} \tag{4.30}$$

In order to find the solution, we resort to the method of sweep [BH75], where λ^i is given by the equation:

$$\lambda^i(k+1) = \Pi^i(k+1)x(k+1) - g^i(k+1), \tag{4.31}$$

with Π^i and g^i defined in equations (4.15) and (4.16), respectively. Combining the equations (4.30) and (4.31), we have:

$$\begin{cases} \lambda^i(k+1) =& (I_n - \Pi^i(k+1)\tilde{B}^i)^{-1} \times \\ & [\Pi^i(k+1)A^i x(k) + \Pi^i(k+1)B^i \tilde{u}^i(k) - g^i(k+1)] \\ \Pi^i(k)x(k) - g^i(k) = \tilde{C}^i x(k) + A^{i'} \lambda^i(k+1). \end{cases} \tag{4.32}$$

Solving (4.15) and (4.16) implies that (4.32) has a solution on the finite horizon $[t_i, t_i + \tau_M^i)$. The bound condition (4.18) is given by (4.25) and (4.29). Finally, (4.12) is obtained from (4.29) and (4.32). ■

Remark 11 *In the finite horizon case, the knowledge of all the future values of* $\tilde{u}^i$ *is required in order to solve (4.16) backward in time. Hence, in general this method cannot be applied to solve practical problems [TW00]. On the other hand, notice that in our case, from equations (4.5)-(4.7), only the knowledge of* $x(t_i-1)$ *and* $x(t_i)$ *is needed to compute the values of* $\tilde{u}^i$ *on the finite horizon* $[t_i, t_i+\tau_M^i)$*. Since this information is available at each switching time* t_i*, the method can be applied in real problems. Notice that the structure of the desired profile (4.5), composed by the initial offset (4.6) and the slope of the desired profile (4.7), may be easily modified in order to obtain a different desired profile. For instance, the choice*

$$\tilde{u}_k^i = \begin{cases} \tilde{u}_k^{i,0} + (k-t_j+1)^2\gamma^i p_k^i & if \quad t_i \le k < t_i+\tau_i^M \\ 0 & otherwise \end{cases}$$

yields a parabolic profile, with $\gamma^i \in (0,1]$*.*

4.4 Stability analysis

In the previous sections, we assumed that the bumpless transfer controller is switched on for τ_i^M instants. As the original controller (4.3) has been designed without taking into account this fact, , asymptotic stability of the switched system (4.2) is not guaranteed anymore. This section aims at establishing asymptotic stability conditions for the closed loop system (4.2)-(4.4). To this purpose, let us define the additional time variable $\tau_k^i = k - t_i + 1$ that is reset to zero at the instant t_i, which represents a generic switching time from the mode j to the mode i, for any $(i,j) \in \mathcal{I} \times \mathcal{I}$. Therefore, for each mode $i \in \mathcal{I}$, the closed loop system (4.2)-(4.4) can be written as:

$$v(k+1) = Y^i(j, \tau_k^i)v(k), \tag{4.33}$$

where the construction of the time variant state matrix Y^i is detailed in Appendix B.5,

$$v(k) = \begin{bmatrix} x(k) \\ x(k-1) \\ \tilde{u}^{i,0}(k) \\ p^i(k) \end{bmatrix}$$

is the augmented state vector and signals $\tilde{u}^{i,0}$ and p^i are defined in section 4.2. We distinguish two phases on the interval between two switchings:

– *The bumpless transfer phase:* the bumpless transfer controller is on. We have:

$$Y^i(j, \tau_k^i)|_{\tau_k^i=1} = \begin{bmatrix} \bar{H}^i(\tau_k^i+1) & \bar{L}^{ji}(\tau_k^i+1) & 0_{n\times r} & 0_{n\times r} \\ I_n & 0_{n\times n} & 0_{n\times r} & 0_{n\times r} \\ 0_{r\times n} & K^j & 0_{r\times r} & 0_{r\times r} \\ \frac{1}{\tau_i^M}K^i & -\frac{1}{\tau_i^M}K^j & 0_{r\times r} & 0_{r\times r} \end{bmatrix} \tag{4.34}$$

and

$$Y^i(j,\tau_k^i)|_{2\leq\tau_k^i\leq\tau_i^M} = \begin{bmatrix} \bar{A}^i(\tau_k^i+1) & 0_{n\times n} & \bar{U}^i(\tau_k^i+1) & \bar{P}^i(\tau_k^i+1) \\ I_n & 0_{n\times n} & 0_{n\times r} & 0_{n\times r} \\ 0_{r\times n} & 0_{r\times n} & I_r & 0_{r\times r} \\ 0_{r\times n} & 0_{r\times n} & 0_{r\times r} & I_r \end{bmatrix}. \quad (4.35)$$

In this phase, the state matrices of the system (4.33) may have eigenvalues outside the unit circle.

– *The recuperation phase:* the bumpless transfer controller is off. We have:

$$Y^i(j,\tau_k^i)|_{\tau_k^i>\tau_i^M} = Y_s^i = \begin{bmatrix} A^i + B^iK^i & 0_{n\times(n+2r)} \\ I & 0_{n\times(n+2r)} \\ 0_{2r\times n} & 0_{2r\times(n+2r)}. \end{bmatrix}, \quad (4.36)$$

where the matrix Y_s^i is Schur and constant for any $i \in \mathcal{I}$. Equations (4.34)-(4.36) are detailed in Appendix B.5.

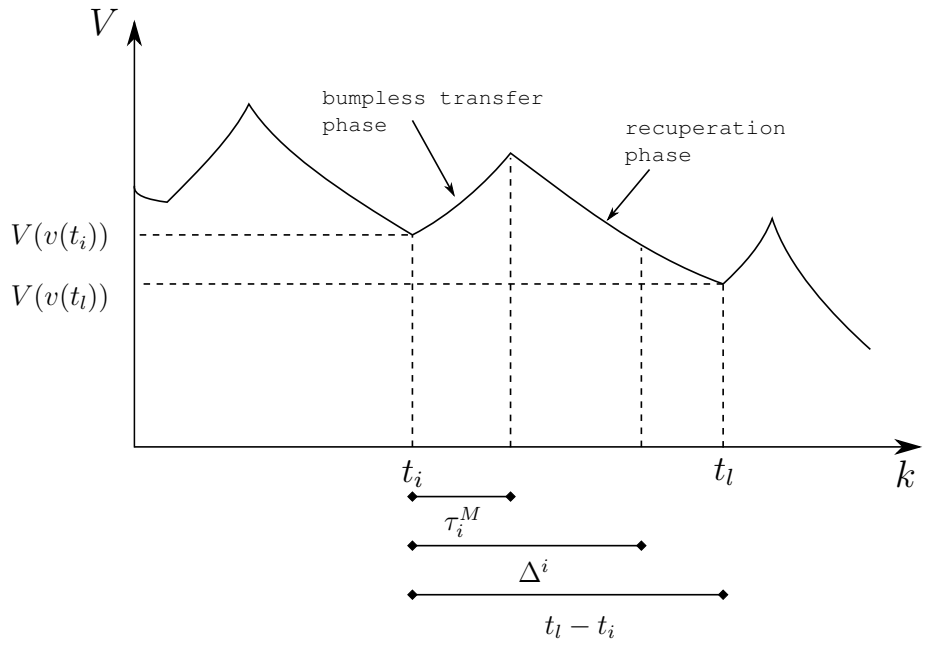

Figure 4.4: Lyapunov function evolution

Assume that for $k \in [t_i, t_l)$ the i^{th} mode is active and, when a switching occurs ($k = t_l$), the system jumps to the l^{th} mode. Moreover, assume that the condition $t_l - t_i \geq \Delta^i \geq 1$, with Δ^i defined in section 4.2, holds for any $(i,l) \in \mathcal{I} \times \mathcal{I}$. The following theorem gives LMI based conditions to check asymptotic stability of the closed loop switched system (4.33).

Theorem 14 *Assume that there exist matrices* $P^i = P^{i'} \succ 0$ *of appropriate dimensions and scalars* $0 \leq \tau_i^M < \Delta^i$ *such that the LMIs*

$$Y_s^{i'} P^i Y_s^i - P^i \prec 0, \tag{4.37}$$

$$\left(\prod_{d=1}^{\tau_i^M} Y^i(j,d) Y_s^{i(\Delta^i - \tau_i^M)}\right)' P^l \left(\prod_{d=1}^{\tau_i^M} Y^i(j,d) Y_s^{i(\Delta^i - \tau_i^M)}\right) - P^i \prec 0 \tag{4.38}$$

hold $\forall\ (j \neq i, l, i) \in \mathcal{I} \times \mathcal{I} \times \mathcal{I}$. *Hence, the switched system (4.33) is asymptotically stable for* $t_l - t_i \geq \Delta^i \geq 1$.

Proof. This proof is based on Theorem 1 of [GC06b]. First, notice that the matrix $\prod_{d=1}^{\tau_i^M} Y^i(j,d)$ represents the evolution of the switched system (4.33) for $k \in [t_i, t_i + \tau_i^M)$ and the matrix $Y_s^{i(t_l - t_i - \tau_i^M)}$ represents the evolution of the switched system (4.33) for $k \in [t_i + \tau_i^M, t_l)$. From (4.38), with $l = i$, the Lyapunov function $V(v(k)) = v(k)' P^i v(k)$ satisfies the inequality

$$V(v(t_i + \Delta^i)) < V(v(t_i)). \tag{4.39}$$

From (4.37), we have:

$$V(v(k+1)) < V(v(k)), \tag{4.40}$$

$\forall\, k \in [t_i + \Delta^i, t_l)$ and $\forall\, i \in \mathcal{I}$. Hence, there exist scalars $\alpha \in (0,1)$ and $\beta > 0$ such that

$$\|v(k)\|^2 \leq \beta \alpha^{k - t_i} V(v(t_i)), \tag{4.41}$$

$k \in [t_i, t_l)$. Moreover, still from (4.38), we obtain:

$$\begin{aligned} V(v(t_l)) &= v(t_l)' P^l v(t_l) \\ &= v(t_i)' \left(\prod_{d=1}^{\tau_i^M} Y^i(j,d) Y_s^{i(t_l - t_i - \tau_i^M)}\right)' P^l \times \\ &\qquad \left(\prod_{d=1}^{\tau_i^M} Y^i(j,d) Y_s^{i(t_l - t_i - \tau_i^M)}\right) v(t_i) \\ &< v(t_i)' Y_s^{i(t_l - t_i - \Delta^i)'} P^i Y_s^{i(t_l - t_i - \Delta^i)} v(t_i) \\ &\leq v(t_i)' P^i v(t_i) = V(v(t_i)). \end{aligned} \tag{4.42}$$

The non strict inequality holds because $t_l - t_i - \Delta^i \geq 0$ and Y_s^i is Schur by assumption, $\forall\, i \in \mathcal{I}$. Hence, given the initial condition of (4.33) $v(0) = v_0$, there exists $\delta \in (0,1)$ such that, after the q^{th} switching, we have:

$$V(v(t_i)) \leq \delta^q V(v_0), \forall\, q \in \mathbb{N}. \tag{4.43}$$

Finally, (4.41) and (4.43) imply that the switched system (4.33) is asymptotically stable. ■

Remark 12 *An evaluation of the maximum value of τ^M that guarantees the asymptotic stability of the closed loop system (4.33) is given by following algorithm:*

$\tau_1^M, ..., \tau_N^M = 0;$
for $h = 1 : max\{\Delta^i, \ i \in \mathcal{I}\}$
  for $i = 1 : N$
    if ($\tau_i^M < \Delta^i$) *and* (LMIs (4.37)-(4.38) hold)
      $\tau_i^M = \tau_i^M + 1;$
    end
  end
end

4.4.1 Numerical example

In this section, we present a bumpless transfer control design to a specific product of the Eisenhüttenstadt HSM. In order to reduce the bumps on the control signal u, the modified control signal (4.4) may be applied to the plant for a period of time τ_i^M, for $i \in \{2, 3, 4\}$. Since the system never switches back to the first subsystem, no bumpless transfer controller is designed for $i = 1$. The signal $u^{bt,i}$ is computed by Theorem 13. Equations (4.13) and (4.15) can be solved off-line whereas equation (4.16) must be solved at the switching time t_i, when the value of $x(t_i - 1)$ is known. The output signal y corresponds to the strip off-center, that must be minimized. Hence, we choose $\tilde{y} = 0$. Given the weighting matrices W_u and W_y, the τ_i^M values allowing to verify the conditions of Theorem 14 can be found by applying the algorithm proposed in Remark 12. Results are summarized in Table 4.1. In Fig. 4.5, we propose a zoom of the control signal u for the last

Table 4.1: BT controller data

i	2	3	4
Δ^i	64	38	30
τ_i^M	30	15	6
W_u^i	I_n	$100I_n$	$10I_n$
W_y^i	I_n	I_n	I_n

stand. The dotted line shows the control signal computed by the control law (4.3), when the bumpless transfer controller is off. One can notice the big bump due to the switching at the instant $k = 1392$ and the corresponding transient behavior. Since the actuators of the hot strip mill system are subject to amplitude and slope saturation, the applied control signal corresponds to the saturated signal (solid

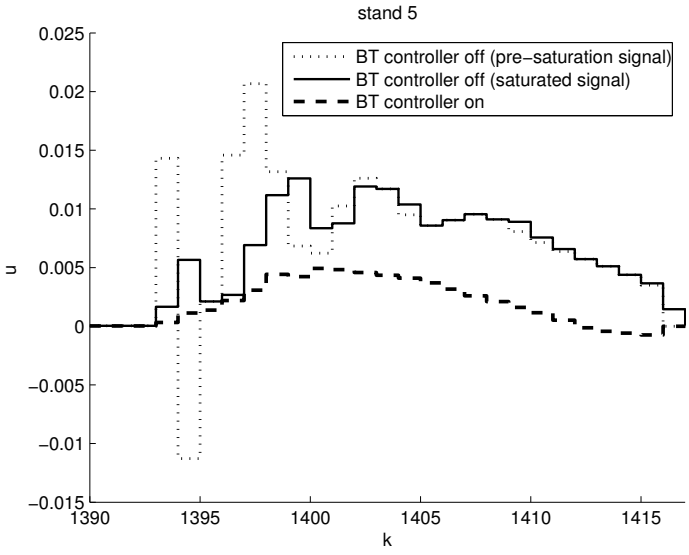

Figure 4.5: Control signal u

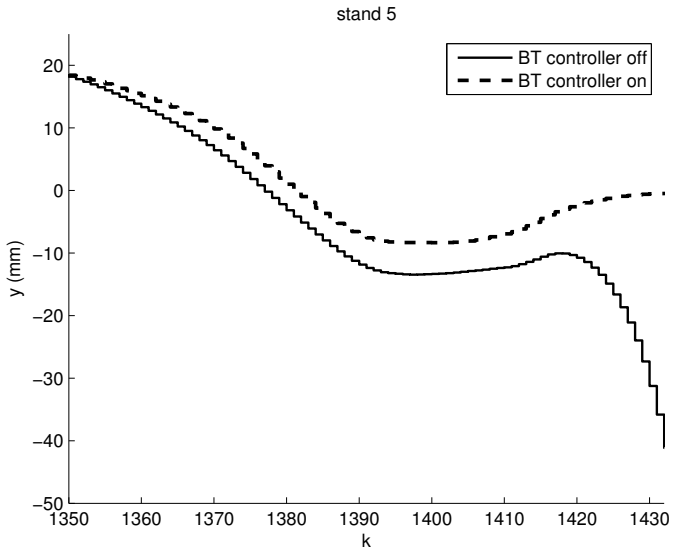

Figure 4.6: Measured output y

line), for which stability is not guaranteed anymore. Finally, the dashed line shows the control signal computed by the control law (4.4), that is the bumpless transfer controller is on. In this case, no saturation occurs. Further, the closed loop asymptotic stability is guaranteed by the conditions of Theorem 14. In Fig. 4.6, we propose a zoom of the measured output y in the last stand, which corresponds to the displacement of the strip with respect to the axis of the mill in the exit of the system. The solid line shows the control signal without bumpless transfer control while the dashed line shows the control signal when the bumpless transfer controller is on. As expected, the displacement of the strip was reduced.

4.5 Conclusion

In this chapter, a bumpless transfer method for switched systems has been presented. The bumpless transfer controller was designed using a finite horizon approach based on the LQ optimization framework. The idea is to force the controller output and the plant output to follow a desired profile. Dwell time conditions for assessing the asymptotic stability of the closed loop switched system were also established. Simulation results concerning the Eisenhüttenstadt HSM system were shown.

Chapter 5

Robust steering control of hot strip mill

5.1 Introduction

In this chapter, a robust steering control design of HSM based on the uncertain switched linear model given in chapter 1 is proposed. The aim is to guarantee the stability of an HSM system and minimize the strip off-center for the whole set of treated products [MDI+ar], [MDI+09d], [MDI+09c], [MDI+09e], [MDIS09].

In an HSM with 5 stands, there are 70 uncertain parameters, which become 110 for HSMs with 7 stands. For a problem of this dimension, LMI techniques suffer from a well-known drawback concerning numerical problems. Therefore, in the first part of this chapter, a method for reducing the number of uncertainties by exploiting the physical relations among the different product parameters will be introduced. Once the simplified polytopic model is obtained, the convex hull corresponding to the whole database may be partitioned into several small convex hulls. The division of the database with respect to the physical parameters of the products, allowing to design a different controller for each family, yields better performances.

The system involves a two time scale dynamics. Since fast dynamics is stable and impossible to control from a practical point of view due to actuators limitations, a robust reduced controller will be designed resorting to the results of Chapter 2.

When the n-stands subsystem is active, the strip is connected to all the stands, and it is subject to a strong perturbation due to the coilbox vibrations. Hence, the main control task is to guarantee a good quality of the rolled product, minimizing the external perturbation. This phase takes the $90\% - 95\%$ of the whole rolling process duration and the system reaches the steady state before the switchings occur. In the tail end phase, traction is lost every time the strip leaves a stand. This increases the difficulties to guide the strip, which becomes free to move in all directions. The result is that the crashes of the strip against the mill side-guides are more frequent. Thus, during the tail end phase the priority of the

control design is the system safety. Moreover, in this phase switchings are very fast and the stability of all subsystems does not guarantee the stability of the whole system. It is also necessary to verify that switchings do not destabilize the system [Mor96], [GC06b].

To our knowledge, the only condition to design a control law which asymptotically stabilizes a two time scale switched systems was proposed in Chapter 3. This condition needs a state vector with constant components and dimension. Nevertheless, in an HSM system, the components and dimension of the state vector change at each switching time. A possible solution consists in designing a robust control law stabilizing each subsystem i separately through the method proposed in Chapter 2. The stability of the tail end switched system will be verified a posteriori. In fact, the switching time depends on the rolled strip and must be estimated on-line. Hence, the switched system stability condition has also to take into account an uncertainty in the switching time.

Finally, simulation and experimental results of the robust steering control design at Eisenhüttenstadt HSM will be presented.

5.2 Polytopic modeling

An HSM can treat products with very heterogeneous properties. Each product is characterized by its physical parameters and by a specific system setup. The scheduling of the rolled products is assumed to be known in real time. Since the controller is computed off-line, from a control design point of view the only available information concerns the minimum and maximum bound of each parameter. Thus, the physical parameters must be considered as bounded uncertainties and a robust controller is needed.

The main objective of this section is to describe the uncertainties of the HSM system as a convex set. LMI techniques can then be applied to design the control law. Two fundamental points are discussed:

- The reduction of the number of convex hull vertices.
- The determination of the convex hull vertices such that the associated physical parameters would reflect a given product.

Once the polytopic model is obtained for the whole database, partitioning it into several small convex hulls can be done quite easily. We only have to choose the number of partitions and compute the vertices of each partition as was done for the original convex set.

Consider the HSM system in the polytopic form (1.19):

$$\begin{cases} x^{\sigma(s)}(s+1) = \mathfrak{A}^{\sigma(s)}(s)x^{\sigma(s)}(s) + \mathfrak{B}_u^{\sigma(s)}(s)u(s) + \mathfrak{B}_d^{\sigma(s)}(s)d(s) \\ q(s) = C_q^{\sigma(s)}x^{\sigma(s)}(s) + D_{qu}^{\sigma(s)}u(s) \\ y(s) = C_y^{\sigma(s)}x^{\sigma(s)}(s), \end{cases} \tag{5.1}$$

where $\sigma : \mathbb{Z}^+ \to \mathcal{I} = \{1, ..., N\}$ is the switching rule, $x^i(s) = \begin{bmatrix} x_1^i(s)' & x_2^i(s)' \end{bmatrix}' \in \mathbb{R}^{2n}$ is the state vector, $u(s) \in \mathbb{R}^r$ is the control signal, $d(s) \in \mathbb{R}$ is the external perturbation, $q(s) \in \mathbb{R}^w$ is the controlled output and $y(s) \in \mathbb{R}^m$ is the measured output, for any $i \in \mathcal{I}$ and for all $s \in \mathbb{Z}^+$. Moreover, we have:

$$\mathfrak{A}^i(s) = \sum_{l=1}^{N_V} \lambda_l(s) \tilde{A}^{i,l}(\varepsilon), \quad \mathfrak{B}_u^i(s) = \sum_{l=1}^{N_V} \lambda_l(s) \tilde{B}_u^{i,l}, \quad \mathfrak{B}_d^i(s) = \sum_{l=1}^{N_V} \lambda_l(s) \tilde{B}_d^{i,l},$$

where $l \in \mathcal{L} = \{1, ..., N_V\}$ denotes the vertices of the convex hull, and λ_l denotes the uncertainty and belongs to the unit simplex

$$\mathfrak{Y}(s) = \{\sum_{l=1}^{N_V} \lambda_l(s) = 1, \ \lambda_l(s) \geq 0\}.$$

Hence, for each subsystem $i \in \mathcal{I}$, we have a different convex hull described by N_V vertices. Each vertex $(i, l) \in \mathcal{I} \times \mathcal{L}$ may be characterized by its corresponding two time scale linear state-space model

$$\begin{cases} x^i(s+1) = \tilde{A}^{i,l}(\varepsilon) x^i(s) + \tilde{B}_u^{i,l} u(s) + \tilde{B}_d^{i,l} d(s) \\ q(s) = C_q^i x^i(s) + D_{qu}^i u(s) \\ y(s) = C_y^i x^i(s), \end{cases} \tag{5.2}$$

with

$$\tilde{A}^{i,l}(\varepsilon) = \begin{bmatrix} \varepsilon \tilde{A}_{11}^{i,l} & \tilde{A}_{12}^{i,l} \\ \varepsilon \tilde{A}_{21}^{i,l} & \tilde{A}_{22}^{i,l} \end{bmatrix}, \quad \tilde{B}_u^{i,l} = \begin{bmatrix} \tilde{B}_{u,1}^{i,l} \\ \tilde{B}_{u,2}^{i,l} \end{bmatrix}, \quad \tilde{B}_d^{i,l} = \begin{bmatrix} \tilde{B}_{d,1}^{i,l} \\ \tilde{B}_{d,2}^{i,l} \end{bmatrix},$$
$$C_q^i = \begin{bmatrix} C_{q,1}^i & C_{q,2}^i \end{bmatrix}, \quad C_y^i = \begin{bmatrix} C_{y,1}^i & C_{y,2}^i \end{bmatrix}.$$

5.2.1 Reduction of the convex hull space dimension

Let $\mathcal{U}$ be the set of uncertain parameters. The space dimension of the convex hull coincides with the number of uncertainties $\mathcal{D} = card(\mathcal{U})$. Hence, $N_V = 2^{\mathcal{D}}$.

In an HSM with 5 stands $\mathcal{D} = 70$ (110 for an HSM with 7 stands). For a problem of this dimension, LMI techniques suffer from a well-known drawback concerning numerical problems. Nevertheless, such numerical problems can be avoided by exploiting the physical relations among the different product parameters for reducing the dimension of the space dimension. Based on the knowledge of the engineers, we chose to use only four main parameters in order to classify the products: the set of independent parameters $\mathcal{U}^m = \{w, h_n, \sigma_1^0, \sigma_n^0\} \subset \mathcal{U}$, where w is the strip width, h_n is the output thickness of the strip in the last stand and σ_1^0 and σ_n^0 are the hardness of the strip in the first and in the last stand, respectively.

The remaining set of parameters $\mathcal{U}^s = \{\mathcal{U} \setminus \mathcal{U}^m\}$ depends on $\mathcal{U}^m$. This means that two products with the same $\mathcal{U}^m$ set have nearly the same $\mathcal{U}^s$ set and thus the same dynamics. To explain this fact, notice that $\mathcal{U}^s$ can be broken down into two subsets $\mathcal{U}^s = \{\mathcal{U}_{op}^s, \mathcal{U}_{fnc}^s\}$:

– The first subset $\mathcal{U}^s_{op}$ concerns the parameters set by the operator, such as roll characteristics. Operators must prevent incidents on the mill and restore eventual damages. Therefore, they look for an HSM setup that guarantees safe and standard system behavior. Their choices are mainly based on past experience, hence, they usually provide a similar $\mathcal{U}^s_{op}$ set for products with similar characteristics (and then with a similar $\mathcal{U}^m$ set).

– The last subset $\mathcal{U}^s_{fnc}$ depends, analytically, on $\mathcal{U}^m$ and $\mathcal{U}^s_{op}$.

Fig. 5.1 shows the evolution of the open loop eigenvalues for 10 products with the following $\mathcal{U}^m$ set:

$$w \in [1150 - 1180]\, mm$$
$$h_n \in [2 - 2.2]\, mm$$
$$\sigma_1^0 \in [50 - 52]\, KN/mm^2$$
$$\sigma_n^0 \in [35 - 37]\, KN/mm^2.$$

Each eigenvalue moves inside a very limited zone. This fact confirms that two products with the same $\mathcal{U}^m$ set have nearly the same $\mathcal{U}^s$ set and so, nearly the same dynamics. Hence, the space dimension of the convex hull can be reduced

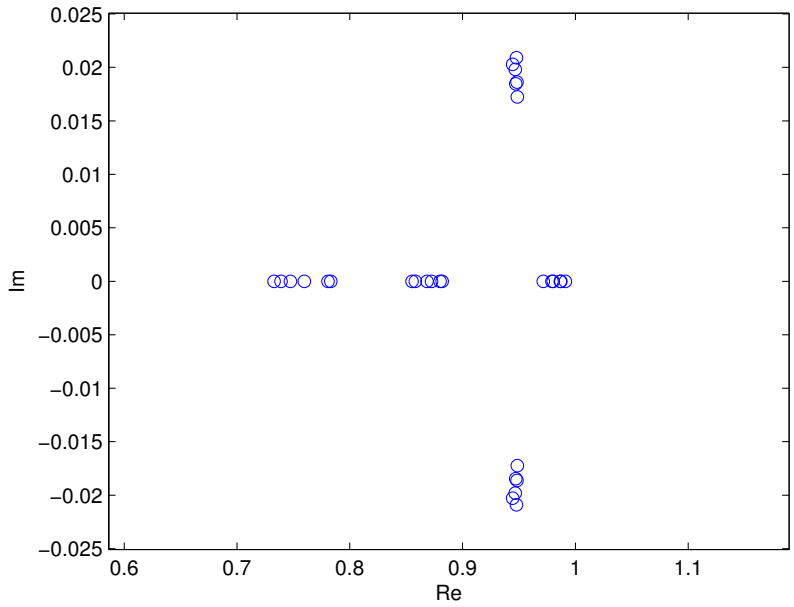

Figure 5.1: Open loop eigenvalues variation

to $\mathcal{D} = card(\mathcal{U}^m) = 4$.

5.2.2 Construction of the convex hull

Each product $p \in \mathcal{P} = \{1, ..., N_P\}$ is characterized by its $\mathcal{U}^m(p)$ set and can then be represented as a point in a 4-dimensional space. Consider the Eisenhüttenstadt HSM database, which contains $N_P = 10000$ products. Fig. 5.2 shows the

projections of the database on the six possible planes. Each point represents a different product. The variation of the independent parameters in the database is:

$$\begin{array}{c} w \in [810 - 1670]\, mm \\ h_n \in [1.9 - 6.2]\, mm \\ \sigma_1^0 \in [22 - 65]\, KN/mm^2 \\ \sigma_n^0 \in [30 - 90]\, KN/mm^2. \end{array} \tag{5.3}$$

Since the combinations among the parameters that belong to $\mathcal{U}^m$ are infinite, the

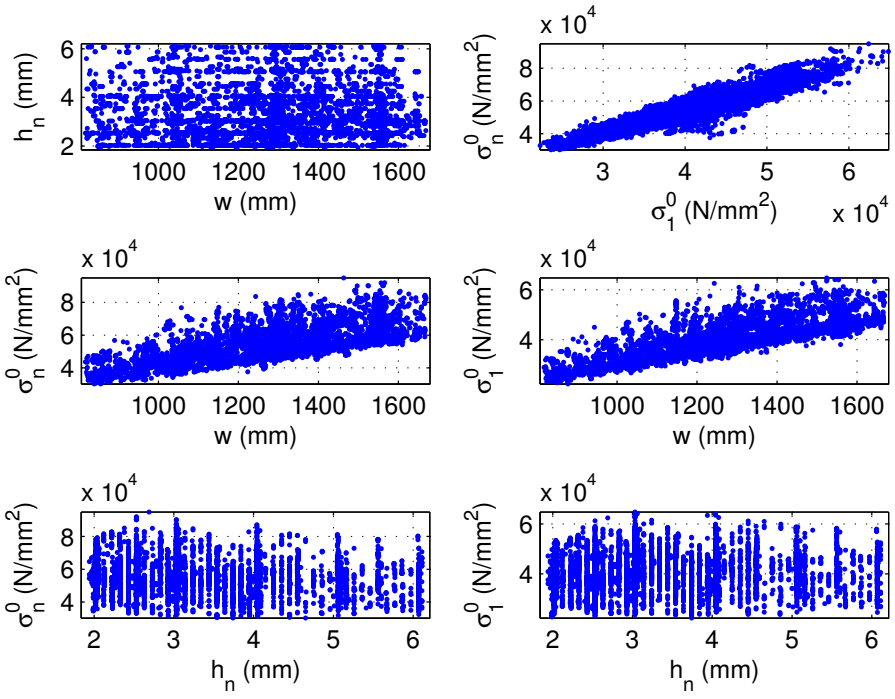

Figure 5.2: ArcelorMittal Eisenhüttenstadt HSM database (2D projection)

products corresponding to the convex hull vertices are not necessarily included in the database. In this case, given the set $\mathcal{U}^m(l)$, the subset $\mathcal{U}^s_{op}(l)$ must be estimated for all the products $l \in \mathcal{L}$. To this aim, the subset $\mathcal{U}^s_{op}(l)$ can be arbitrarily set to be equal to the subset $\mathcal{U}^s_{op}(p^l)$ of the product $p^l \in \mathcal{P}$ "closest" to the vertex l. Therefore, for each vertex $l \in \mathcal{L}$, p^l may be found solving the following minimization problem:

$$D_{min}(l, p^l) = min\{D(l, p), \quad p \in \mathcal{P}\}, \tag{5.4}$$

with

$$\begin{aligned} D(l,p) = \; & [(w(l) - w(p))^2 + (h_n(l) - h_n(p))^2 + \\ & (\sigma_1^0(l) - \sigma_1^0(p))^2 + (\sigma_n^0(l) - \sigma_n^0(p))^2]^{\frac{1}{2}}. \end{aligned}$$

$D(l,p)$ represents the distance, with reference to the set $\mathcal{U}^m$, between the vertex l and the product p, for any $(l,p) \in \mathcal{L} \times \mathcal{P}$. The computation of (5.4) assumes that all the parameters are normalized beforehand into the interval $[-1,1]$. An

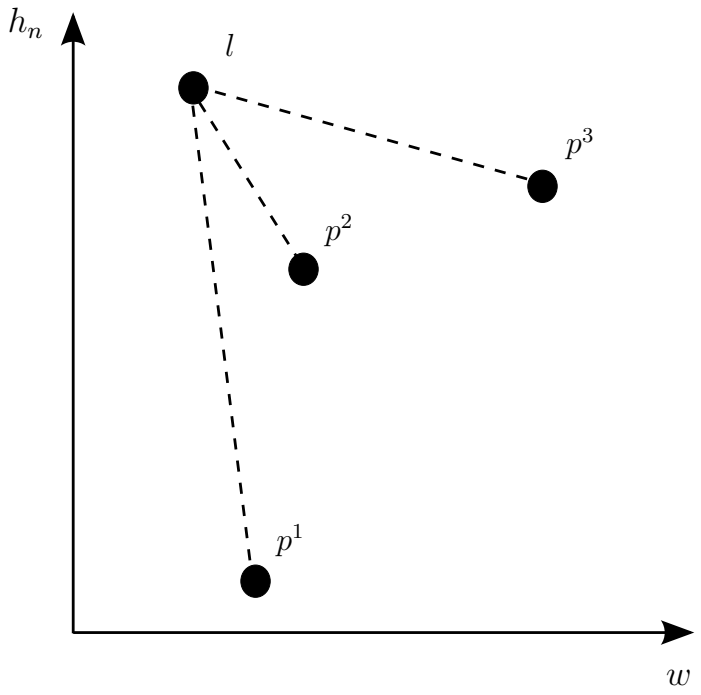

Figure 5.3: D_{min} computation: A two dimensional example

illustrative two dimensional example is proposed in Fig. 5.3. Consider a vertex l and three different products p^1, p^2 and p^3. It is easy to see that

$$D_{min}(l,p^l) = D(l,p^2) = [(w(l) - w(p^2))^2 + (h_n(l) - h_n(p^2))^2]^{\frac{1}{2}}.$$

The convex hull including the whole set of rolled products bounded by (5.3) may be divided into smaller N_F convex hulls for improving the system performances. For each family of products $f \in \mathcal{F} = \{1, ..., N_F\}$, a minimization problem in the form of (5.4) is solved to get the convex hull vertices of this family.

5.3 Robust steering control design

To our knowledge, all the conditions to design a control law stabilizing a two time scale switched system need a state vector with constant components and dimension. Nevertheless, in the HSM system, the components and dimension of the state vector change at each switching time, as explained in section 1.4. A possible solution consists in designing a robust control law stabilizing each subsystem $i \in \mathcal{I}$ of the HSM system (5.1) separately. In this first phase, the effect of the switchings is not taken into account and the i index is omitted.

The stability of the tail end switched system is verified a posteriori. Therefore, consider the subsystem corresponding to the mode $i \in \mathcal{I}$ of (5.1):

$$\begin{cases} x(s+1) = \mathfrak{A}(s)x(s) + \mathfrak{B}_u(s)u(s) + \mathfrak{B}_d(s)d(s) \\ q(s) = C_q x(s) + D_{qu}u(s) \\ y(s) = C_y x(s). \end{cases} \tag{5.5}$$

Due to actuators rate limits, the fast manifold, which is asymptotically stable in open loop, cannot be controlled. Hence, a slow sampling robust control law is able to stabilize asymptotically the uncertain two time scale system (5.5). The slow sampling model corresponding to each vertex $l \in \mathcal{L}$ of (5.5) is:

$$\begin{cases} x_1(s+1) = \varepsilon\tilde{A}_{11}^l x_1(s) + \tilde{A}_{12}^l x_2(s) + \tilde{B}_{u,1}^l u(s) + \tilde{B}_{d,1}^l d(s) \\ x_2(s+1) = \varepsilon\tilde{A}_{21}^l x_1(s) + \tilde{A}_{22}^l x_2(s) + \tilde{B}_{u,2}^l u(s) + \tilde{B}_{d,2}^l d(s) \\ q(s) = C_{q,1}x_1(k) + C_{q,2}x_2(k) + D_{qu}u(s) \\ y(s) = C_{y,1}x_1(s) + C_{y,2}x_2(s), \end{cases}$$

where $x_1(s) \in \mathbb{R}^{n_1}$, $x_2(s) \in \mathbb{R}^{n_2}$, $\varepsilon = 0.05$, $T_s = \alpha_s\alpha_f = 0.05$, $C_{q,1} = 0$ and $C_{y,1} = 0$, for all $s \in \mathbb{Z}^+$. Its corresponding slow subsystem is:

$$\begin{cases} x_s(s+1) = \tilde{A}_s^l x_s(s) + \tilde{B}_{u,s}^l u_s(s) + \tilde{B}_{d,s}^l d(s) \\ q(s) = \tilde{C}_s x_s(s) + \tilde{D}_s u_s(s), \end{cases}$$

where $\tilde{A}_s^l = \tilde{A}_{22}^l$, $\tilde{B}_{u,s}^l = \tilde{B}_{u,2}^l$ and $\tilde{B}_{d,s}^l = \tilde{B}_{d,2}^l$. $\tilde{C}_s = C_{q,2} = \begin{bmatrix} I_{n_2} \\ 0_{r\times n_2} \end{bmatrix}$, $\tilde{D}_s = D_{qu} = \begin{bmatrix} 0_{n_2\times r} \\ D_{qu}^0 \end{bmatrix}$ are two weighting matrices which respect the orthogonality hypothesis $\tilde{C}_s'\tilde{D}_s = 0$, $\tilde{D}_s'\tilde{D}_s \succ 0$. The pair $(\tilde{A}_s^l, \tilde{B}_{u,s}^l)$ is assumed to be controlable. Since the HSM system is subject to a strong external perturbation d, we decided to design the robust steering control law in a H_2 framework. Therefore, Theorem 4 may be applied to design a reduced state-feedback control law

$$u(s) = Kx(s) \tag{5.6}$$

such that the controller gain $K = [0 \;\; K_s]$ stabilizes asymptotically the uncertain two time scale system (5.5) and minimizes the H_2 norm of its slow dynamics.

5.4 Stability analysis of the tail end switched system

The goal of this section is to verify the asymptotic stability of the tail end switched system, for any $(i, l) \in \mathcal{I} \times \mathcal{L}$. The switching time depends on the rolled strip and must be estimated on-line. Hence, the stability condition has also to take

into account an uncertainty in the switching time.

Consider the set of matrices $\{E^i : i \in \mathcal{I}\}$ introduced in Chapter 1. The change of basis

$$z(s) = E^{i'} x^i(s)$$

yields the same state vector $z(s) \in \mathbb{R}^{2n}$ for each subsystem $i \in \mathcal{I}$ and for all $s \in \mathbb{Z}^+$. Hence, we can write the closed loop switched system in the polytopic form:

$$z(s+1) = \mathfrak{T}^{\sigma(s)}(s) z(s) \tag{5.7}$$

with

$$\mathfrak{T}^i(s) = \sum_{l=1}^{N_V} \lambda_{i,l}(s) \bar{T}_{i,l},$$

and $\lambda_{i,l}(s) \in \mathfrak{Y}$. The closed loop matrix $\bar{T}_{i,l} = E^{i'}(\tilde{A}^{i,l} + \tilde{B}_u^{i,l} K^i) E^i$ is Schur, where K^i corresponds to the controller gain of the state-feedback control law (5.6), for any $(i,l) \in \mathcal{I} \times \mathcal{L}$.

In order to prove the asymptotic stability of the closed loop system (5.7), we provide a dwell time condition [GC06b] taking into account the uncertain parameters $l \in \mathcal{L}$ and an uncertainty $\tau^i \in \mathcal{W}^i = \{-N_{\tau^i}, ..., N_{\tau^i}\}$ in the switching time. To this aim, consider three successive switching times t_{q-1}, t_q and t_{q+1}. For $s \in [t_{q-1}, t_q)$ the system is in the subsystem corresponding to $(i_-, l_-, \tau^{i_-}) \in \mathcal{I} \times \mathcal{L} \times \mathcal{W}^{i_-}$, for $s \in [t_q, t_{q+1})$ the system is in the subsystem corresponding to $(i, l, \tau^i) \in \mathcal{I} \times \mathcal{L} \times \mathcal{W}^i$ and, for $s = t_{q+1}$, the system jumps to the subsystem corresponding to $(i_+, l_+, \tau^{i_+}) \in \mathcal{I} \times \mathcal{L} \times \mathcal{W}^{i_+}$. t_{q-1}, t_q and t_{q+1} satisfy $t_q - t_{q-1} = \Delta_{q-1}^{i_-} \geq \Delta^{i_-} \geq 1$, $t_{q+1} - t_q = \Delta_q^i \geq \Delta^i \geq 1$, for any $q \in \mathbb{N}$, where Δ^i is the dwell time of the subsystem i. We assume $N_{\tau^i} + N_{\tau^{i_+}} < \Delta^i$. Hence, the subsystem i is controlled by the wrong gain K^{i_-} for a time $t \in (sT_s, (s+\tau^i)T_s)$ if $\tau^i > 0$, with $\bar{T}_{i_-,l} = E^{i'}(\tilde{A}^{i,l} + \tilde{B}_u^{i,l} K^{i_-}) E^i$. Furthermore, the subsystem i is controlled by the wrong gain K^{i_+} for a time $t \in (sT_s, (s-\tau^{i_+})T_s)$ if $\tau^{i_+} < 0$, with $\bar{T}_{i_+,l} = E^{i'}(\tilde{A}^{i,l} + \tilde{B}_u^{i,l} K^{i_+}) E^i$ (see Fig. 5.4).

Let the transition matrix Q_{π,Δ_q^i}, which represents the system evolution for $s \in [t_q, t_{q+1})$. Its value depends on the sign of τ^i and τ^{i_+}:

$$\begin{cases} if \;\; \tau^i \leq 0, \tau^{i_+} \geq 0: & Q_{\pi,\Delta_q^i} = (\bar{T}_{i,l})^{\Delta_q^i}, \\ if \;\; \tau^i > 0, \tau^{i_+} \geq 0: & Q_{\pi,\Delta_q^i} = (\bar{T}_{i,l})^{\Delta_q^i - \tau^i} (\bar{T}_{i_-,l})^{\tau^i}, \\ if \;\; \tau^i \leq 0, \tau^{i_+} < 0: & Q_{\pi,\Delta_q^i} = (\bar{T}_{i_+,l})^{-\tau^{i_+}} (\bar{T}_{i,l})^{\Delta_q^i + \tau^{i_+}}, \\ if \;\; \tau^i > 0, \tau^{i_+} < 0: & Q_{\pi,\Delta_q^i} = (\bar{T}_{i_+,l})^{-\tau^{i_+}} (\bar{T}_{i,l})^{\Delta_q^i - \tau^i + \tau^{i_+}} (\bar{T}_{i_-,l})^{\tau^i}, \end{cases} \tag{5.8}$$

with $\pi = i, i_- \neq i, i_+ \neq i, l, l_+, \tau^i, \tau^{i_+} \in \Pi = \mathcal{I} \times \mathcal{I} \times \mathcal{I} \times \mathcal{L} \times \mathcal{L} \times \mathcal{W}^i \times \mathcal{W}^{i_+}$. The following theorem gives a generalization of Theorem 7 for uncertain switched systems with an uncertainty in the switching time.

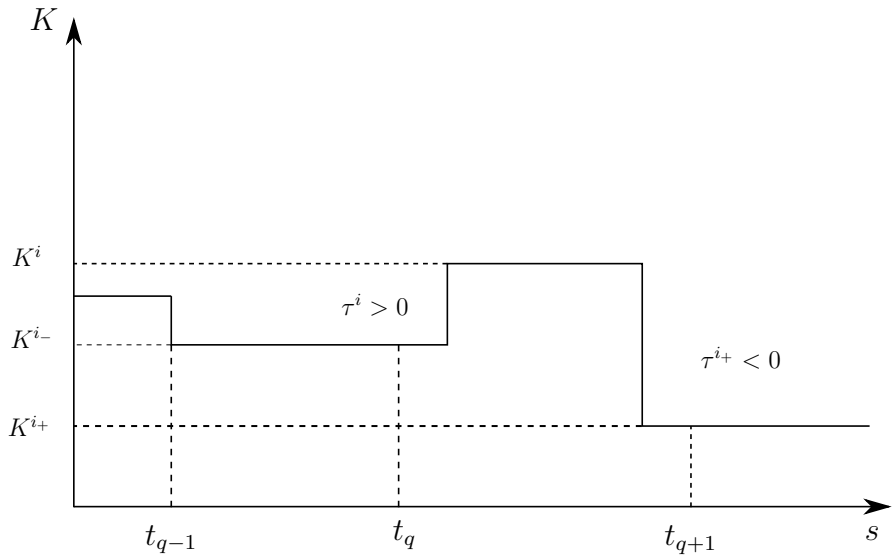

Figure 5.4: Controller switchings

Theorem 15 *Consider the uncertain switched system (5.7) and an uncertainty in the switching time $\tau^i \in \mathcal{W}^i$. If there exist matrices $P_{i,l} = P_{i,l}' \succ 0$ of appropriate dimensions such that the LMIs*

$$\bar{T}_{i,l}' P_{i,l} \bar{T}_{i,l} - P_{i,l} \prec 0, \ \forall\, (i,l) \in \mathcal{I} \times \mathcal{L}, \tag{5.9}$$

$$Q_{\pi,\Delta^i}' P_{i_+,l_+} Q_{\pi,\Delta^i} - P_{i,l} \prec 0, \ \forall\, \pi \in \Pi \tag{5.10}$$

hold, then the switched system (5.7) is asymptotically stable for $\Delta_q^i \geq \Delta^i \geq 1$, $\forall\, (i,l,\tau^i) \in \mathcal{I} \times \mathcal{L} \times \mathcal{W}^i$.

Proof. Let the parameter dependent quadratic Lyapunov function

$$V(s) = z(s)' \sum_{i=1}^{N} \sum_{l=1}^{N_V} \varphi_i(s) \lambda_{i,l}(s) P_{i,l} z(s)$$

where $P_{i,l} = P_{i,l}' \succ 0$, $\varphi_i(s) : \mathbb{N} \to \{0,1\}$, $\sum_{i=1}^{N} \varphi_i(s) = 1$ and $\lambda_{i,l}(s) \geq 0$, $\sum_{l=1}^{N_V} \lambda_{i,l}(s) = 1$, for any $(i,l) \in \mathcal{I} \times \mathcal{L}$ and for all $s \in \mathbb{Z}^+$. The system (5.7) is asymptotically stable if the difference $L(s) = V(s+1) - V(s)$ satisfies the inequality

$$L(s) = z(s)' (\hat{\mathfrak{T}}^{\sigma(s)}(s)' \mathfrak{P}_+(s) \hat{\mathfrak{T}}^{\sigma(s)}(s) - \mathfrak{P}(s)) z(s) \prec 0$$

where

$$\hat{\mathfrak{T}}^{\sigma(s)}(s) = \sum_{i=1}^{N} \mathfrak{T}^i(s) = \sum_{i=1}^{N} \sum_{l=1}^{N_V} \varphi_i(s) \lambda_{i,l}(s) \bar{T}_{i,l},$$

$$\mathfrak{P}(s) = \sum_{i=1}^{N}\sum_{l=1}^{N_V}\varphi_i(s)\lambda_{i,l}(s)P_{i,l},$$

$$\mathfrak{P}_+(s) = \sum_{i=1}^{N}\sum_{l=1}^{N_V}\varphi_i(s+1)\lambda_{i,l}(s+1)P_{i,l} = \sum_{i_+=1}^{N}\sum_{l_+=1}^{N_V}\varphi_{i_+}(s)\lambda_{i_+,l_+}(s)P_{i_+,l_+}$$

for any $(i,l) \in \mathcal{I} \times \mathcal{L}$ and for any $(i_+,l_+) \in \mathcal{I} \times \mathcal{L}$ [HDI06]. From (5.9), for any $s \in [t_q, t_{q+1})$ the Lyapunov function $v(z(s)) = z(s)'P_{i,l}z(s)$ satisfies

$$v(z(s+1)) < v(z(s)).$$

Hence, there exist scalars $\alpha \in (0,1)$ and $\beta > 0$ such that

$$\|z(s)\|^2 \leq \beta\alpha^{s-t_q}v(z(t_q)), \tag{5.11}$$

$s \in [t_q, t_{q+1})$. Moreover, from (5.8), when $\tau^i > 0$ and $\tau^{i_+} < 0$, we have $Q_{\pi,\Delta_q^i} = (\bar{T}_{i_+,l})^{-\tau^{i_+}}(\bar{T}_{i,l})^{\Delta_q^i-\tau^i+\tau^{i_+}}(\bar{T}_{i_-,l})^{\tau^i}$. Hence, using (5.10) we obtain:

$$\begin{aligned}
v(z(t_{q+1})) &= z(t_{q+1})'P_{i_+,l_+}z(t_{q+1}) \\
&= z(t_q)'(\bar{T}_{i_+,l}^{-\tau^{i_+}}\bar{T}_{i,l}^{\Delta_q^i-\tau^i+\tau^{i_+}}\bar{T}_{i_-,l}^{\tau^i})'P_{i_+,l_+}\bar{T}_{i_+,l}^{-\tau^{i_+}}\bar{T}_{i,l}^{\Delta_q^i-\tau^i+\tau^{i_+}}\bar{T}_{i_-,l}^{\tau^i}z(t_q) \\
&< z(t_q)'(\bar{T}_{i_-,l}^{-\tau^i}\bar{T}_{i,l}^{\Delta_q^i-\Delta^i}\bar{T}_{i_-,l}^{\tau^i})'P_{i,l}\bar{T}_{i_-,l}^{-\tau^i}\bar{T}_{i,l}^{\Delta_q^i-\Delta^i}\bar{T}_{i_-,l}^{\tau^i}z(t_q) \\
&\leq z(t_q)'(\bar{T}_{i_-,l}^{\tau^i-\tau^i})'P_{i,l}\bar{T}_{i_-,l}^{\tau^i-\tau^i}z(t_q) \\
&= z(t_q)'P_{i,l}z(t_q) = v(z(t_q)).
\end{aligned} \tag{5.12}$$

The non-strict inequality holds because $\Delta_q^i - \Delta^i \geq 0$ and $\bar{T}_{i,l}$ is Schur. Hence

$$(\bar{T}_{i,l}^{\Delta_q^i-\Delta^i})'\bar{T}_{i_-,l}^{-\tau^{i'}}P_{i,l}\bar{T}_{i_-,l}^{-\tau^i}\bar{T}_{i,l}^{\Delta_q^i-\Delta^i} \preceq \bar{T}_{i_-,l}^{-\tau^{i'}}P_{i,l}\bar{T}_{i_-,l}^{-\tau^i},$$

for any $(i,l) \in \mathcal{I} \times \mathcal{L}$. The relation $v(z(t_{q+1})) < v(z(t_q))$ is verified also for the other cases of (5.8). In order to see it, it is sufficient to substitute the right value of Q_{π,Δ_q^i} in (5.12). Hence, given the initial condition of (5.7) $z(0) = z_0$, there exists $\delta \in (0,1)$ such that

$$v(z(t_q)) \leq \delta^q v(z_0), \forall\, q \in \mathbb{N}. \tag{5.13}$$

Finally, (5.11) and (5.13) imply that the system (5.7) is asymptotically stable. ■

Remark 13 *In order to verify the LMIs (5.9)-(5.10) of Theorem 15, $NN_V + N(N-1)^2N_V^2(N_{\tau^i}+1)^2$ possible combinations have to be considered, in the general case. Nevertheless, in the HSM system case, only $n-1$ switchings occur. Moreover, since the uncertain parameters are constant for each product, switchings are possible only between subsystems with the same l. Hence, only $NN_V + (n-1)N_V(N_{\tau^i}+1)^2$ LMIs have to be verified.*

Table 5.1: Families bounds

Data / Family	$w\,(mm)$	$h_n\,(mm)$	$\sigma_1^0\ \left(\frac{KN}{mm^2}\right)$	$\sigma_n^0\ \left(\frac{KN}{mm^2}\right)$
1	$810-1200$	$1.9-3$	$22-65$	$30-95$
2	$810-1200$	$3-4.5$	$22-65$	$30-95$
3	$810-1200$	$4.5-6.2$	$22-65$	$30-95$
4a	$1200-1400$	$1.9-3$	$22-65$	$30-95$
4b	$1400-1670$	$1.9-3$	$22-65$	$30-95$
5	$1200-1670$	$3-4.5$	$22-65$	$30-95$
6	$1200-1670$	$4.5-6.2$	$22-65$	$30-95$

5.5 Robust steering control implementation

In order to obtain a simple and systematic procedure so as to extend the steering control to different factories, a user-friendly interface, called *Robust Steering Control Toolbox* (*RSCT*) [MBS+08], has been developed under *Matlab*. The software implements the following functions:

- Given the desired family bounds, it computes the $\mathcal{U}^m(l,f)$ set, which contains the information concerning the convex hulls vertices, for any $(l,f) \in \mathcal{L}\times\mathcal{F}$. Hence, the minimization problem (5.4) is solved in order to estimate the $\mathcal{U}^s(l,f)$ set, for any $(l,f) \in \mathcal{L}\times\mathcal{F}$.
- The knowledge of the $\mathcal{U}(l,f)$=$\{\mathcal{U}^m(l,f),\mathcal{U}^s(l,f)\}$ set allows to compute the linear model of the HSM system, for any $(i,l,f) \in \mathcal{I}\times\mathcal{L}\times\mathcal{F}$.
- Therefore, the robust controller gains $K^{i,f}$ are computed solving the LMI based conditions of Theorem 4 for any $(i,f) \in \mathcal{I}\times\mathcal{F}$. To this aim, *RSCT* exploits the LMI solver *SeDuMi* [Stu99] and the *MATLAB* toolbox *YALMIP* [Löf04].
- Finally, the asymptotic stability of the closed loop switched system (5.7) may be verified using Theorem 15.

The main features of *RSCT* features are presented in Appendix C. In the next sections, we present simulation and experimental results at Eisenhüttenstadt HSM. After experimental trials, the whole database was divided into $N_F = 7$ families, with reference to the $\mathcal{U}^m$ set. The families bounds are summarized in Table 5.1. This choice improves system performances, compared to the performances obtained using a single controller for all the products. The number of families has been limited in order to handle the data in the factory more easily. The weighting matrices $\tilde{D}_s^{i,f}$ have been tuned to fulfill the constraints on the stand tilting ΔS described in section 1.3, for any $i \in \mathcal{I}$.

5.6 Simulation results

5.6.1 n-stands subsystem

In this section, simulation results are shown for a product p with $\mathcal{U}^m = \{967,\ 2.02,\ 27.9,\ 40.1\}$. From Table 5.1, p belongs to the first family. Fig. 5.5 shows the evolution of the strip off-center Z in the last stand. The solid line represents the Z evolution using with the H_2 controller gain $K^{n,1}$. The dash-dotted line shows the Z evolution using a classic LQ controller gain, designed for an average product of family 1. The dashed line shows the Z evolution using the classic LQ controller gain, given in [DBI+08], designed for an average product of the whole database. As expected, the division of the whole database into several

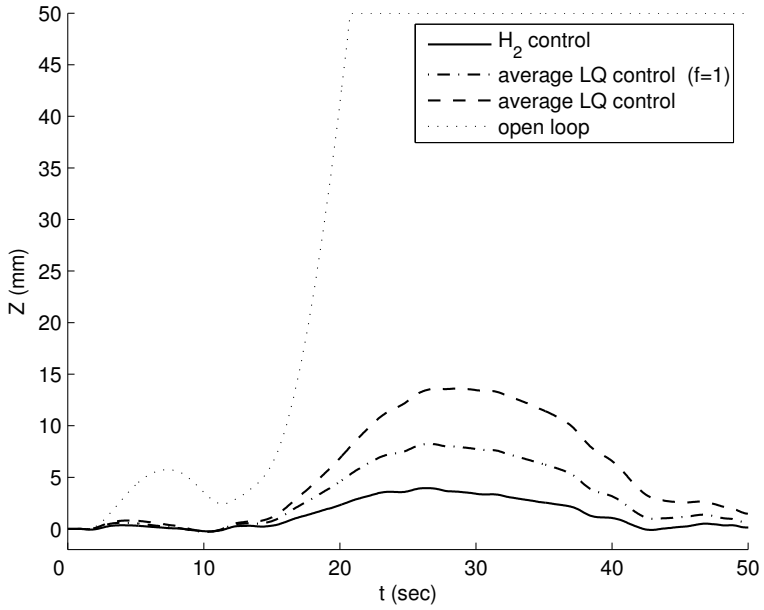

Figure 5.5: Exit strip off-center evolution

families improves system performances. Moreover, the H_2 robust controller takes into account the uncertain parameters and minimizes the effects of the external perturbation, which is due to the coilbox vibrations. The last line, the dotted one, shows the Z evolution without any control. Notice that in this case a saturation occurs: this means that the strip is crashing against the HSM side guides.

5.6.2 Tail end switched system

In this section, we present the simulation results concerned with the tail end phase. Given the controller gains and the dwell time Δ^i, Theorem 15 provides a sufficient condition for the stability of the switched system (5.7) for any $\tau^i \in \mathcal{W}^i$. We found a solution for $N_{\tau^i} \leq 4$, for any $i \in \mathcal{I}$. Since $T_s = 0.05\,sec$, the stability of

the system is guaranteed for a maximum uncertainty of $\pm 0.2\,sec$ in the switching time. From practical experience, this constraint can be respected.

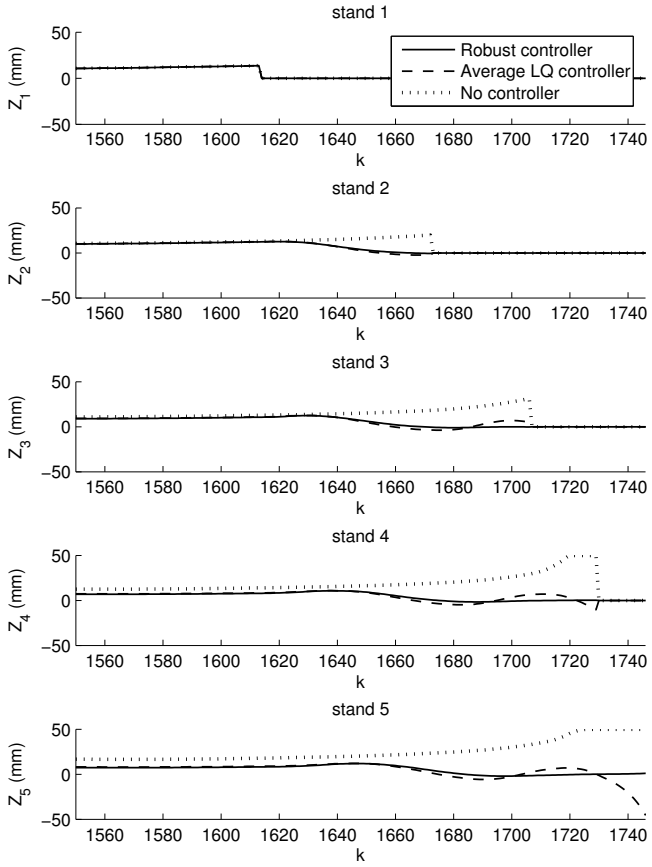

Figure 5.6: Strip off-center evolution: comparison

In Fig. 5.6, the evolution of the strip off-center Z at the exit of each stand is shown. Notice that, when the strip leaves the g^{th} stand, the value of Z_g has not a physical meaning anymore and is set to zero. In this first simulation, no delay in the control signal has been considered. The solid line represents the Z evolution when the system is controlled by the robust controller gain computed using Theorem 4 for each subsystem. The dashed line shows the Z evolution when the system is controlled by the LQ controller gain designed using average state matrices. The dotted line corresponds to the Z evolution when the system works in open loop. We can see that the robust controller is able to keep the Z value close to zero during all the rolling process. Otherwise, the average LQ controller limits the Z value for the first four stands but induces an oscillatory behavior on the strip. Hence, when the strip leaves stand 4, the Z value increases very quickly. This situation can be very dangerous for the system safety. In the

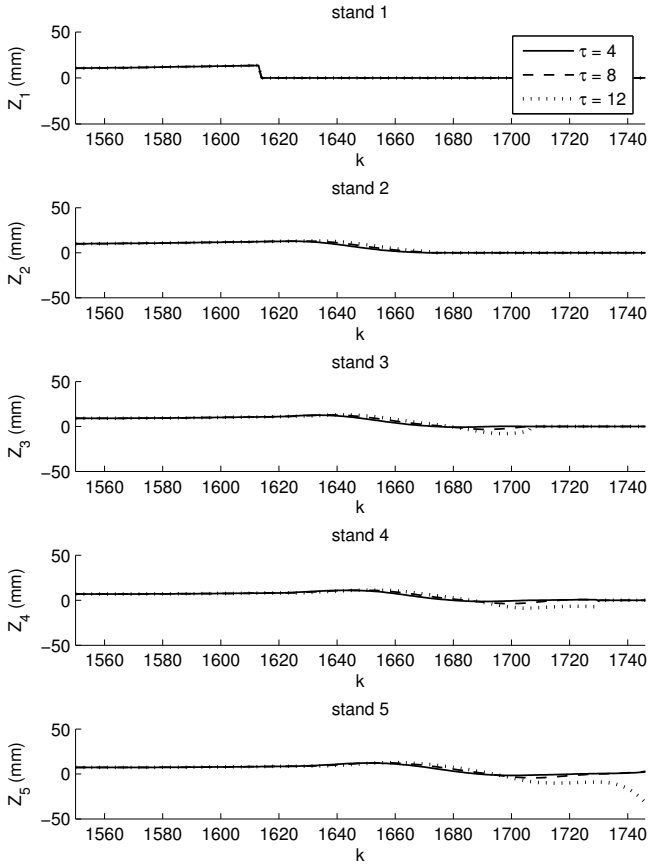

Figure 5.7: Strip off-center evolution with delay in the H_2 robust controller switchings

open loop case, the Z value begins to increase when the strip leaves the first stand ($s = 1613$). Notice that a saturation occurs in stands 4 and 5. This means that the strip is crashing against the side guides. The result is a decrease of the product quality and, in the worst case, the damage of the rolls.

In Fig. 5.7, we introduce an uncertainty in the switching signal when the system is controlled by the H_2 robust control law. In the Eisenhüttenstadt case, the switching time can be estimated online, with an error that has the same sign for any $i \in \mathcal{I}$. Here, the case $\tau^i \geq 0$ is presented. This means that the controller switches to the i-stands subsystem τ^i instants after the strip left the stand. Three different cases are shown: ($\tau = \tau^4 = \tau^3 = \tau^2 = 4$) (solid line), ($\tau = \tau^4 = \tau^3 = \tau^2 = 8$) (dashed line), ($\tau = \tau^4 = \tau^3 = \tau^2 = 12$) (dotted line). Although theoretically the system is stable only for $\tau \leq 4$, notice that until $\tau = 8$ the Z value is kept near to zero. Nevertheless, when $\tau = 12$ the controller performances decrease and the strip almost crashes against the side guides. In

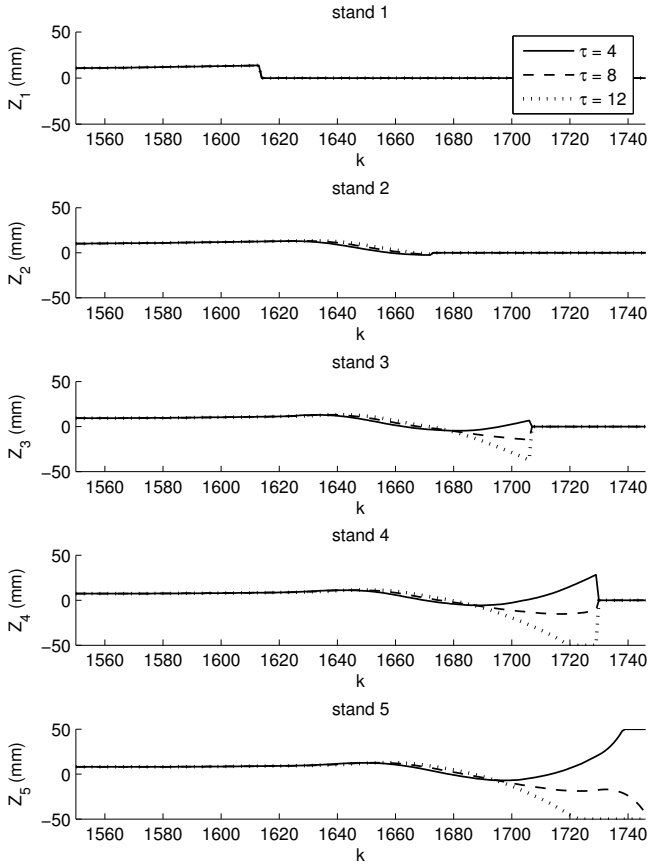

Figure 5.8: Strip off-center evolution with delay in the average LQ controller switchings

this case, the Z value increases in the opposite side of the open loop case.

In Fig. 5.8, we consider the same delay using the average LQ controller. We can see that this kind of controller does not accept uncertainties on the switching time. The system is unstable and the strip crashes against the side guides in each case.

5.7 Industrial system description

The steering control system includes five cameras measuring the strip off-center, the main computer SC and the data connection devices (see Fig. 5.9). The cameras, which are *DAC004* delivered by *Fife*, are protected by a water-cooled housing (the strip can reach $1000°C$) and mounted on dedicated vibration absorbers to avoid high accelerations. A *Profibus* connects each camera to the main

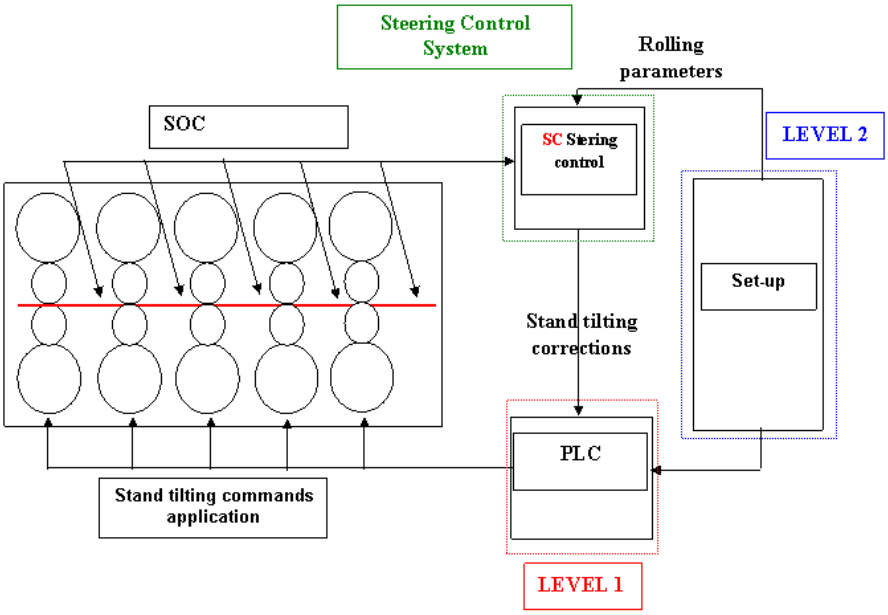

Figure 5.9: Global process information at Eisenhüttenstadt HSM

computer, which is linked to the *PLC* stand by *Profibus* as well. The main computer consists of a *3 GHz Intel-P4* standard personal computer with an integrated *Profibus* interface. The control system is developed in the *C++* language and works under the operating system *Windows XP*. A *TCP/IP* using an *Ethernet* connection communicates the rolling parameters to the *Level 2* system. Filtering, active pixel selection and edge detection are carried out by *FPGA* devices, which are directly located on the cameras. This architecture reduces the amount of data that must be transmitted to the main computer. An edge detection algorithm based on gradient analysis is used to obtain clear information concerning the strip off-center values Z. During the operating phase of the control system, the applied stand tilt is $u(s) = K^{i,f} z(s)$, with $K^{i,f}$ the gain computed off-line by the *RSCT* software, for any $(i, f) \in \mathcal{I} \times \mathcal{F}$. In order to avoid large values of the control signal u, due to measurement errors, a saturation function is applied before sending the stand tilt signal to the *PLC*.

5.8 Experimental results

In Fig. 5.10, we show the exit strip off-center evolution of a product with $\mathcal{U}^m = \{895, 2.42, 30.4, 37.4\}$ (family 1). When the product enters the HSM the steering control is on (Fig. 5.10.b) and the strip off-center value is kept close to zero (Fig. 5.10.a). At the instant $s = 1050$, the steering control system is switched off and the signal u is set to a constant value by the operator. As expected, the Z value increases quickly (from 10 to 30 mm). In Fig. 5.11, we show the exit Z evolution of two consecutive products with the same set $\mathcal{U}^m = \{1510, 2.02, 59.1, 72.5\}$

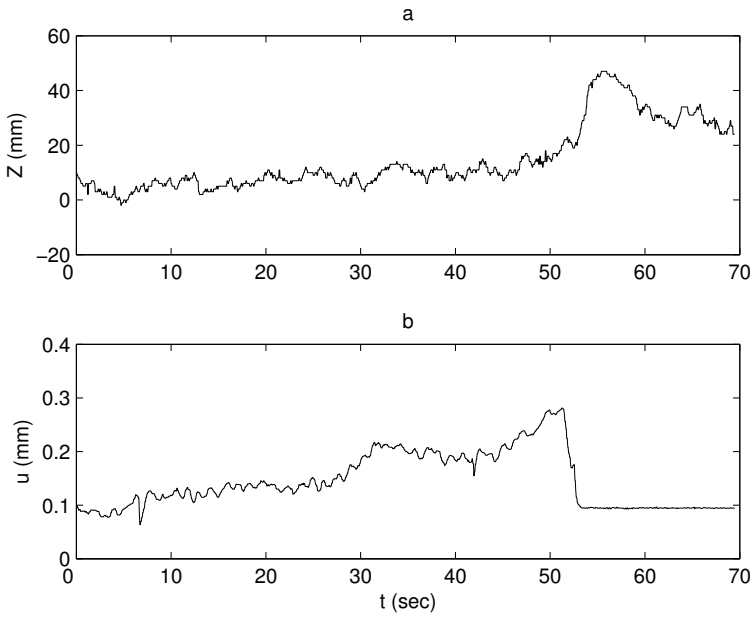

Figure 5.10: Exit strip off-center and control signal evolution

(family 4). The solid line corresponds to the Z evolution with robust steering control whereas the dotted line corresponds to the open loop Z evolution. The performance improvement is demonstrated.

In Fig. 5.12, the standard deviation of the strip off-center values $\sigma_x(Z)$ obtained by applying the H_2 control system are compared with the standard deviation of the strip off-center values obtained in open loop. The statistics concern 100 controlled strips and 200 strips in open loop of all the families. Performance improvement is substantial. When the H_2 steering control is switched off, the strip off-center standard deviation increases more than 125%. The bounds on the stand tilt ΔS maximum values have always been respected and the wedge Δh has always been kept between $\pm 10\,\mu m$. In Fig. 5.13, the standard deviation of the strip off-center values $\sigma_x(Z)$ obtained using the H_2 control system are compared with the standard deviation of the strip off-center values obtained using the average LQ control system proposed by [DBI+08]. The statistics concern 44 strips from all the families. In order to guarantee the same rolling conditions (e.g. strip parameters, roll characteristics, external temperature, system asymmetries) and then obtain coherent results, only identical and consecutive strips have been compared. We observe performance improvement using the H_2 control system (about 35%). Also the standard deviation of the wedge value $\sigma_x(\Delta h_n)$, which gives a measure of the quality of the rolled product, has been improved from $7.82\,\mu m$ (LQ control system) to $5.56\,\mu m$ (H_2 control system).

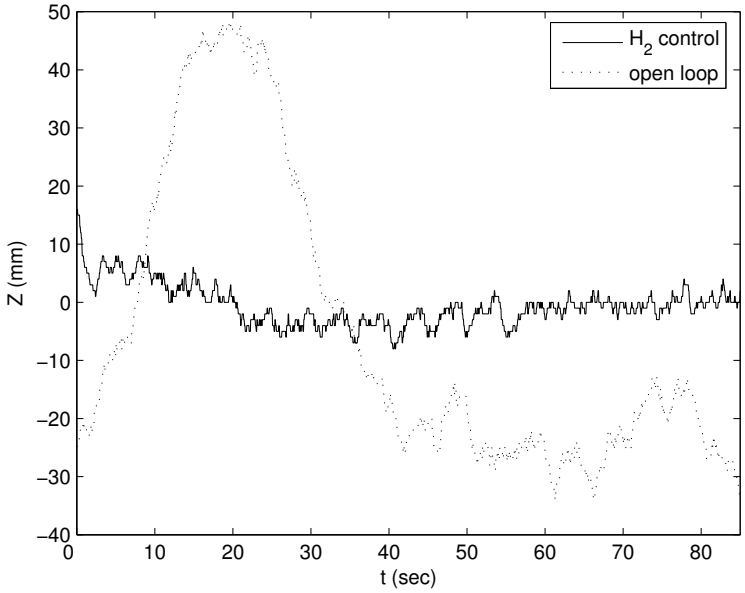

Figure 5.11: Exit strip off-center evolution

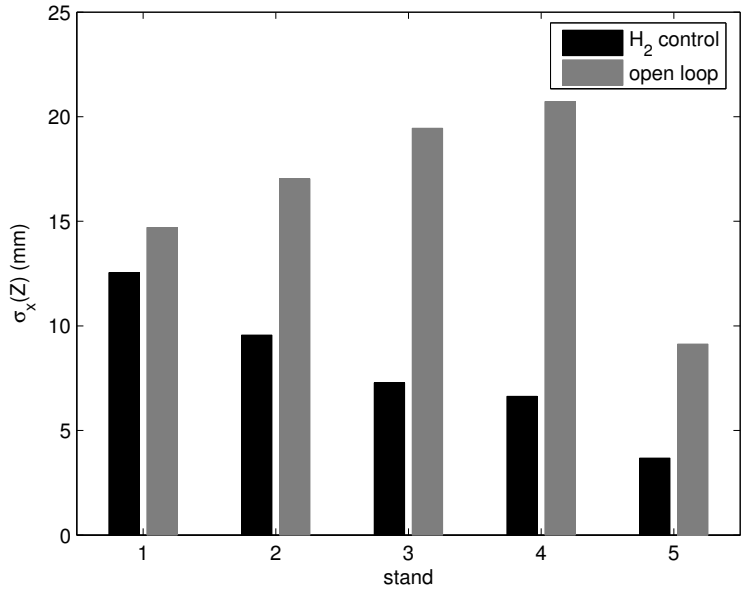

Figure 5.12: $\sigma_x(Z)$ comparison : H_2 steering control and open loop systems

5.9 Conclusion

In this chapter, a robust steering control design has been proposed in order to guarantee the asymptotical stability of the HSM uncertain switched system presented in Chapter 1 and improve its performance. The aim has been achieved

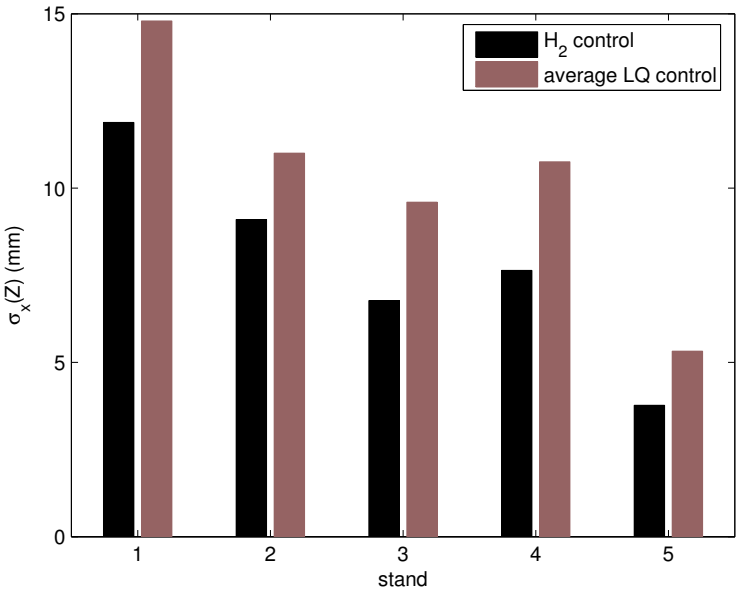

Figure 5.13: $\sigma_x(Z)$ comparison: H_2 and average LQ steering control systems

minimizing the strip movement during the rolling process. Since an HSM treats a set of very heterogeneous products, an extensive database was created and divided into seven families of products. A method for reducing the complexity of the problem exploiting the relations among the different products parameters has also been presented. This method yields a convex formulation of the stabilization problem. Hence, for each family, a different LMI based robust controller was designed. A dwell-time condition verifying the asymptotical stability of the tail end switched system has also been provided. This condition takes into account the uncertainties on the physical parameters and on the controllers switching instants.

Simulations (for both the n-stands subsystem and the tail end subsystem) and experimental results (for the n-stands subsystem) concerning the ArcelorMittal HSM of Eisenhüttenstadt proved the effectiveness of the presented method. The strip off-center was significantly reduced, with respect to the results obtained in open loop and using the old control system.

Steering control is an important framework in steel production. In order to adapt the described method to other mills, a dedicated *Matlab* toolbox, *RSCT*, was developed. Only the model tuning and a specific database of products, which each plant can provide, are required.

General conclusion

This Ph.D. thesis deals with a certain number of problems arising in practical implementation of control systems: multi time scale phenomena, sudden modifications on the system dynamics, discontinuities on the control signal due to controller switchings, the need of design a limited number of controllers in spite of a wide variation on the physical parameters. In order to illustrate the validity of the obtained results, we resorted to a real problem concerning the steel production framework, the robust steering control of hot strip finishing mill.

First, a convex solution of the linear quadratic control design for discrete two time scale linear systems has been proposed. Fast and slow sampling state feedback control designs were investigated. An extension of the slow sampling controller to uncertain systems in the polytopic form has also been presented. Hence, we addressed the stability problem of two time scale switched systems. We showed that asymptotical stability of the slow and fast switched subsystems under arbitrary switching rules does not imply asymptotical stability of the corresponding two time scale switched system in the singular perturbation form. A coupling constraint, expressed in terms of LMIs independent of the value of the singular perturbation parameter, must also be satisfied. A stabilizing state feedback control law was also designed, for the continuous and fast sampling discrete time frameworks. We also introduced a bumpless transfer method for discrete time switched systems, based on a linear quadratic optimization approach, for reducing the control signal discontinuities due to the switchings. Dwell time conditions assessing asymptotical stability of the closed loop switched system were established.

The practical contribution of this thesis, the robust steering control of a hot strip mill, exploits some of the previous theoretical results. The aim is to guarantee asymptotic stability of a hot strip mill system and improve the quality of the rolled products. This purpose was achieved minimizing the strip movement during the rolling process. Since a hot strip mill treats a set of very heterogeneous products, an extensive database was created and divided into seven families of products. A method for reducing the complexity of the problem by exploiting the relations among the different products parameters has also been presented. This method yields a convex formulation of the stabilization problem. Therefore, a different robust controller was designed for each family. A dwell time condition, which verifies asymptotic stability of the tail end switched system, has also been

presented. This condition takes into account the uncertainties on the physical parameters and on the switching instants. In order to adapt this method to other mills, a dedicated *Matlab* toolbox, called *RSCT*, was developed. Simulations and experimental results at Eisenhüttenstadt mill proved the effectiveness of the proposed solution. The lateral movement of the strip was significantly reduced, with respect to the results obtained in open loop and using the old control system.

Multi time scale switched systems offer several future research topics. In this work, we pointed out the fact that classical stability properties of linear systems in the singular perturbation form do not hold, when arbitrary switchings arise. Therefore, we presented sufficient conditions to analyze asymptotic stability and design a stabilizing state feedback control law of two time scale switched linear systems. The extension of these conditions to more general classes of switched systems should be investigated. Further, practical implementation usually requires more complex control techniques, as output feedback, and performance constraints. In physical systems, the time scale of the state variables corresponding to the state space model of the system may change after a switching. An example of this phenomenon is observed during the tail end phase of the rolling process in a hot strip mill. Even if the angles between the strip and the mill axis of each stand are usually "fast" state variables, each time the strip leaves a stand the angle between the strip and the mill axis on the first stand active becomes a "slow" state variable. This behavior was modeled through a two time scale switched system for which the state vectors corresponding to the slow and fast subsystems vary at each switching time. To our knowledge, the stabilization problem of two time scale switched systems with variable state vectors has never been addressed before this work. We avoided the problem by designing an independent control law for each subsystem and verifying the stability of the tail end switched system a posteriori, through a dwell time condition. This approach yields a set of well-behaved controllers and, in the hot strip mill case, guarantees the closed loop asymptotic stability. However, in a general context it presents a drawback. Since the controllers do not take into account the switchings effects, the closed loop stability of the whole switched system is evaluated through a condition that depends on the singular perturbation parameter. Therefore, numerical problems may arise due to ill-conditioning constraints.

In the robust steering control framework, the next step concerns the industrial implementation of the tail end phase regulation at Eisenhüttenstadt plant. The installation of the proposed control system to other mills is also planned.

Appendix A

Formulae

A.1 Schur complement

The LMI $\begin{bmatrix} A & B \\ (\star)' & D \end{bmatrix} \succ 0$, where $A = A'$ and $D = D'$, is equivalent to LMIs $D \succ 0,\ A - BD^{-1}B' \succ 0$, and to LMIs $A \succ 0,\ D - B'A^{-1}B \succ 0$.

A.2 Inverse of a block matrix

Consider an invertible block matrix $\begin{bmatrix} A & B \\ C & D \end{bmatrix}$. Its inverse is

$$\begin{bmatrix} A & B \\ C & D \end{bmatrix}^{-1} = \begin{bmatrix} A^{-1} + A^{-1}B(D - CA^{-1}B)^{-1}CA^{-1} & -A^{-1}B(D - CA^{-1}B)^{-1} \\ -(D - CA^{-1}B)^{-1}CA^{-1} & (D - CA^{-1}B)^{-1} \end{bmatrix}.$$

A.3 Searle's identity

$$(I + AB)^{-1} = I - A(I + AB)^{-1}B.$$

Appendix B

Proofs

B.1 Proof of Theorem 2

From (2.41), let us denote

$$P(\varepsilon)^{-1} = \begin{bmatrix} W(\varepsilon) & Y(\varepsilon) \\ Y(\varepsilon)' & Q(\varepsilon) \end{bmatrix} \succ 0, \tag{B.1}$$

with

$$\begin{aligned} W(\varepsilon) &= (P_1(\varepsilon) - P_2(\varepsilon)P_3(\varepsilon)^{-1}P_2(\varepsilon)')^{-1}, \\ Y(\varepsilon) &= -W(\varepsilon)P_2(\varepsilon)P_3(\varepsilon)^{-1}, \\ Q(\varepsilon) &= P_3(\varepsilon)^{-1} + P_3(\varepsilon)^{-1}P_2(\varepsilon)'W(\varepsilon)P_2(\varepsilon)P_3(\varepsilon)^{-1}. \end{aligned} \tag{B.2}$$

Hence, substituting (2.18), (2.41), (2.42) and (B.1) in (2.37), we obtain:

$$\begin{bmatrix} \varepsilon^{-1}X_1(\varepsilon) & \varepsilon^{-1}X_2(\varepsilon) \\ \varepsilon^{-1}X_2(\varepsilon)' & X_3(\varepsilon) \end{bmatrix} \prec 0, \tag{B.3}$$

with

$$\begin{aligned} X_1(\varepsilon) = \varepsilon(&A_{11}P_1(\varepsilon)A_{11}' + A_{12}P_2(\varepsilon)'A_{11}' + A_{11}P_2(\varepsilon)A_{12}' + A_{12}P_3(\varepsilon)A_{12}' + \\ &A_{11}Z_1(\varepsilon)'B_1' + A_{12}Z_2(\varepsilon)'B_1' + B_1Z_1(\varepsilon)A_{11}' + B_1Z_2(\varepsilon)A_{12}' + \\ &B_1(Z_1(\varepsilon)W(\varepsilon)Z_1(\varepsilon)' + Z_2(\varepsilon)Y(\varepsilon)'Z_1(\varepsilon)' + \ Z_1(\varepsilon)Y(\varepsilon)Z_2(\varepsilon)' + \\ &Z_2(\varepsilon)Q(\varepsilon)Z_2(\varepsilon)')B_1' - P_1(\varepsilon) + x_1^0x_1^{0\prime}), \end{aligned}$$

$$\begin{aligned} X_2(\varepsilon) = \varepsilon(&A_{11}P_1(\varepsilon)A_{21}'\varepsilon + A_{12}P_2(\varepsilon)'A_{21}'\varepsilon + A_{11}P_2(\varepsilon)(I_{n_2} + \varepsilon A_{22})' + \\ &A_{12}P_3(\varepsilon)(I_{n_2} + \varepsilon A_{22})' + A_{11}Z_1(\varepsilon)'B_2'\varepsilon + A_{12}Z_2(\varepsilon)'B_2'\varepsilon + \\ &B_1Z_1(\varepsilon)\varepsilon A_{21}' + B_1Z_2(\varepsilon)(I_{n_2} + \varepsilon A_{22})' + B_1(Z_1(\varepsilon)W(\varepsilon)Z_1(\varepsilon)' + \\ &Z_2(\varepsilon)Y(\varepsilon)'Z_1(\varepsilon)' + Z_1(\varepsilon)Y(\varepsilon)Z_2(\varepsilon)' + Z_2(\varepsilon)Q(\varepsilon)Z_2(\varepsilon)')B_2'\varepsilon - \\ &P_2(\varepsilon) + x_1^0x_2^{0\prime}), \end{aligned}$$

$$\begin{aligned}X_3(\varepsilon) = {} & \varepsilon A_{21}P_1(\varepsilon)A_{21}'\varepsilon + \varepsilon A_{21}P_2(\varepsilon)(I_{n_2}+\varepsilon A_{22})' + (I_{n_2}+\varepsilon A_{22})\times \\ & P_2'(\varepsilon)A_{21}'\varepsilon + (I_{n_2}+\varepsilon A_{22})P_3(\varepsilon)(I_{n_2}+\varepsilon A_{22})' + \varepsilon A_{21}Z_1(\varepsilon)'B_2'\varepsilon + \\ & (I_{n_2}+\varepsilon A_{22})Z_2(\varepsilon)'B_2'\varepsilon + \varepsilon B_2 Z_1(\varepsilon)A_{21}'\varepsilon + \varepsilon B_2 Z_2(\varepsilon)(I_{n_2}+\varepsilon A_{22})' \\ & + \varepsilon B_2(Z_1(\varepsilon)W(\varepsilon)Z_1(\varepsilon)' + Z_2(\varepsilon)Y(\varepsilon)'Z_1(\varepsilon)' + Z_1(\varepsilon)Y(\varepsilon)Z_2(\varepsilon)' + \\ & Z_2(\varepsilon)Q(\varepsilon)Z_2(\varepsilon)')B_2'\varepsilon - P_3(\varepsilon) + x_2^0 x_2^{0\prime}.\end{aligned}$$

When $\varepsilon \to 0$, using (B.2) we have :

$$\begin{aligned}X_1 = {} & A_{11}P_1A_{11}' + A_{12}P_2'A_{11}' + A_{11}P_2A_{12}' + A_{12}P_3A_{12}' + A_{11}Z_1'B_1' + \\ & A_{12}Z_2'B_1' + B_1Z_1A_{11}' + B_1Z_2A_{12}' + B_1Z_1(P_1 - P_2P_3{}^{-1}P_2')^{-1}Z_1'B_1' - \\ & B_1Z_2P_3{}^{-1}P_2'(P_1 - P_2P_3{}^{-1}P_2')^{-1}Z_1'B_1' - B_1Z_1(P_1 - P_2P_3{}^{-1}P_2')^{-1}\times \\ & P_2P_3{}^{-1}Z_2'B_1' + B_1Z_2P_3{}^{-1}Z_2'B_1' + B_1Z_2P_3{}^{-1}P_2'(P_1 - P_2P_3{}^{-1}P_2')^{-1}\times \\ & P_2P_3{}^{-1}Z_2'B_1' - P_1 \prec 0.\end{aligned} \tag{B.4}$$

$$X_2 = A_{11}P_2 + A_{12}P_3 + B_1Z_2 - P_2 = 0, \tag{B.5}$$

$$X_3 = P_2'A_{21}' + A_{21}P_2 + A_{22}P_3 + P_3A_{22}' + Z_2'B_2' + B_2Z_2 + x_2^0x_2^{0\prime} \prec 0. \tag{B.6}$$

Equation (2.43) verifies (B.5). Furthermore, substituting (2.43) and (2.45) in (B.4), we obtain:

$$\begin{aligned}X_1 = {} & A_{11}P_fA_{11}' + A_{11}Z_f'B_1' + B_1Z_fA_{11}' + B_1Z_fP_f^{-1}Z_f'B_1' - P_f + \\ & A_{11}P_2P_3^{-1}(P_2A_{11}' + P_3A_{12}' + Z_2'B_1') + B_1Z_2P_3^{-1}(P_2A_{11}' + \\ & P_3A_{12}' + Z_2'B_1') + A_{12}(P_2A_{11}' + P_3A_{12}' + Z_2'B_1') - P_2P_3^{-1}P_2' = \\ & A_{11}P_fA_{11}' + A_{11}Z_f'B_1' + B_1Z_fA_{11}' + B_1Z_fP_f^{-1}Z_f'B_1' - P_f \prec 0,\end{aligned} \tag{B.7}$$

and, substituting (2.23), (2.43) and (2.44) in (B.6), we get:

$$X_3 = A_sP_s + P_sA_s' + B_sZ_s + Z_s'B_s' + x_s^0x_s^{0\prime} \prec 0. \tag{B.8}$$

(B.7) and (B.8) represent the constraints of the problems (2.50) and (2.49), respectively. Hence, they are satisfied by assumption. Replacing in (B.3) the unknown values of $P_1(\varepsilon)$, $P_2(\varepsilon)$, $P_3(\varepsilon)$, $Z_1(\varepsilon)$, $Z_2(\varepsilon)$ with P_1, P_2, P_3, Z_1, Z_2, we obtain:

$$\begin{bmatrix}\varepsilon^{-1}X_1 & X_4 \\ X_4' & X_3 + O(\varepsilon)\end{bmatrix} \prec 0, \tag{B.9}$$

with

$$\begin{aligned}X_4 = {} & A_{11}P_1A_{21}' + A_{12}P_2'A_{21}' + A_{11}P_2A_{22}' + A_{12}P_3A_{22}' + A_{11}Z_1'B_2' + A_{12}Z_2'B_2' + \\ & B_1Z_1A_{21}' + B_1Z_2A_{22}' + B_1(Z_1WZ_1' + Z_2Y'Z_1' + Z_1YZ_2' + Z_2QZ_2')B_2' + \\ & x_1^0x_2^{0\prime}.\end{aligned}$$

W, Y and Q are obtained replacing $P_1(\varepsilon)$, $P_2(\varepsilon)$, $P_3(\varepsilon)$, $Z_1(\varepsilon)$, $Z_2(\varepsilon)$ in (B.2). The conditions $X_1 \prec 0$ and $X_3 \prec 0$ imply that there exists a scalar $\varepsilon_1 > 0$ such that the inequality

$$X_1 - \varepsilon X_4(X_3 + O(\varepsilon))^{-1}X_4' \prec 0$$

holds $\forall \varepsilon \in (0, \varepsilon_1]$. Hence, using the Schur complement, also (B.9) holds $\forall \varepsilon \in (0, \varepsilon_1]$. Moreover, there exists a scalar $\varepsilon_2 > 0$ such that the inequality

$$\varepsilon P(\varepsilon) = \begin{bmatrix} P_f + P_2 P_s^{-1} P_2' & P_2 \\ P_2' & P_s \end{bmatrix} + O(\varepsilon) \succ 0$$

holds, $\forall \varepsilon \in (0, \varepsilon_2]$. Thus, there exist matrices P_s, Z_s, P_f, Z_f and a scalar $\varepsilon_{max} = min\{\varepsilon_1, \varepsilon_2\}$ which verify the constraints (2.36)-(2.37) of the problem (2.38), $\forall \varepsilon \in (0, \varepsilon_{max}]$.

Consider

$$u_s(k) = K_s x_s(k) = Z_s P_s^{-1} x_s(k)$$

and

$$u_f(k) = K_f x_f(k) = Z_f P_f^{-1} x_f(k).$$

The composite controller is

$$u(k) = u_s(k) + u_f(k) = K_s x_s(k) + K_f x_f(k).$$

Assume $x_s(k) = x_2(k)$ and $x_f(k) = x_1(k) - (I_{n_1} - A_{11})^{-1}(A_{12} x_s(k) + B_1 u_s(k)) = x_1(k) - (I_{n_1} - A_{11})^{-1}(A_{12} + B_1 K_s) x_s(k)$. Hence, we have:

$$\begin{aligned} u(k) = & Z_f P_f^{-1} x_1(k) + Z_s P_s^{-1} x_2(k) - Z_f P_f^{-1} \times \\ & (I_{n_1} - A_{11})^{-1}(A_{12} + B_1 Z_s P_s^{-1}) x_2(k) = K \begin{bmatrix} x_1(k) \\ x_2(k) \end{bmatrix}, \end{aligned}$$

which corresponds to (2.26). Applying the formula of the inverse of block matrix to (2.51), we find:

$$P^{-1} = \begin{bmatrix} P_f^{-1} & -P_f^{-1} P_2 P_s^{-1} \\ -P_s^{-1} P_2' P_f^{-1} & P_s^{-1} + P_s^{-1} P_2' P_f^{-1} P_2 P_s^{-1} \end{bmatrix}.$$

Thus, we get:

$$K = Z P^{-1} = \begin{bmatrix} Z_f P_f^{-1} & Z_s P_s^{-1} - Z_f P_f^{-1} (I_{n_1} - A_{11})^{-1} (A_{12} + B_1 Z_s P_s^{-1}) \end{bmatrix},$$

which concludes the proof. ■

B.2 Proof of Proposition 1

The proof is an extension of [Yur04] to the switched systems case. First, notice that if the stability conditions of Theorem 9 hold, there exists a common quadratic Lyapunov function $V(x(t)) = x_f(t)' P_f x_f(t) > 0$ and matrices $Q_f^i \succ 0$, $i \in \mathcal{I}$, such that $\dot{V}(x_f(t)) = x_f(t)'(\varepsilon^{-1} M_{11}^{\sigma(t)'} P_f + \varepsilon^{-1} P_f M_{11}^{\sigma(t)}) x_f(t) \leq -x_f(t)' \varepsilon^{-1} Q_f^{\sigma(t)} x_f(t)$. Let us define $\lambda_{min}^{Q_f} = min\{\lambda_{min}(Q_f^i),\ i \in \mathcal{I}\}$ and $\lambda_{max}^{Q_s} = max\{\lambda_{max}(Q_s^i),\ i \in \mathcal{I}\}$, for all $t \geq t_0$. Consider the inequalities

$$\lambda_{min}(P_f) \|x_f(t)\|^2 \leq V(x_f(t)) \leq \lambda_{max}(P_f) \|x_f(t)\|^2 \tag{B.10}$$

and

$$\dot{V}(x_f(t)) \leq -\varepsilon^{-1}\lambda_{min}^{Q_f}\|x_f(t)\|^2 \leq -\frac{\lambda_{min}^{Q_f}}{\varepsilon\lambda_{max}(P_f)}V(x_f(t)). \tag{B.11}$$

Integrating (B.11), we obtain

$$\int_{t_0}^{t}\frac{dV(x_f(t))}{V(x_f(t))} = ln\left(\frac{V(x_f(t))}{V(x_f(t_0))}\right) \leq -\frac{\lambda_{min}^{Q_f}}{\varepsilon\lambda_{max}(P_f)}t,$$

and then:

$$V(x_f(t)) = V(x_f(t_0))exp\left(-\frac{\lambda_{min}^{Q_f}}{\varepsilon\lambda_{max}(P_f)}t\right).$$

Using (B.10), we get an upper bound for the norm of the state variables corresponding to the fast dynamics:

$$\|x_f(t)\| \leq \left(\frac{\lambda_{max}(P_f)}{\lambda_{min}(P_f)}\right)^{\frac{1}{2}}\|x_f(t_0)\|exp\left(-\frac{\lambda_{min}^{Q_f}}{2\varepsilon\lambda_{max}(P_f)}t\right). \tag{B.12}$$

A similar procedure yields a lower bound for the norm of the state variables corresponding to the slow dynamics:

$$\|x_s(t)\| \geq \left(\frac{\lambda_{min}(P_s)}{\lambda_{max}(P_s)}\right)^{\frac{1}{2}}\|x_s(t_0)\|exp\left(-\frac{\lambda_{max}^{Q_s}}{2\lambda_{min}(P_s)}t\right). \tag{B.13}$$

Finally, the ratio of the exponents in (B.12) and (B.13) is

$$\eta = \frac{\lambda_{min}(P_s)\lambda_{min}^{Q_f}}{\varepsilon\lambda_{max}(P_f)\lambda_{max}^{Q_s}}.$$

■

B.3 Proof Theorem 10

Let us assume

$$P(\varepsilon) = \begin{bmatrix} P_1(\varepsilon) & P_2(\varepsilon) \\ P_2(\varepsilon)' & P_3(\varepsilon) \end{bmatrix} \succ 0, \tag{B.14}$$

$$Z^i(\varepsilon) = \begin{bmatrix} Z_1^i(\varepsilon) & Z_2^i(\varepsilon) \end{bmatrix}, \tag{B.15}$$

$$Q^i(\varepsilon) = \begin{bmatrix} Q_1^i(\varepsilon) & Q_2^i(\varepsilon) \\ Q_2^i(\varepsilon)' & Q_3^i(\varepsilon) \end{bmatrix} \succ 0, \tag{B.16}$$

with

$$\begin{aligned} P_1(\varepsilon) &= P_f + \varepsilon P_2 P_s^{-1} P_2', \\ P_2(\varepsilon) &= \varepsilon P_2 = -\varepsilon\sum_{h=1}^{N} {M_{11}^h}^{-1}(M_{12}^h P_s + N_1^h Z_s^h), \\ P_3(\varepsilon) &= \varepsilon P_s, \end{aligned} \tag{B.17}$$

$$Z_1^i(\varepsilon) = Z_f^i + \varepsilon Z_s^i P_s^{-1} P_2', \quad Z_2^i(\varepsilon) = \varepsilon(Z_s^i + Z_f^i P_f^{-1} Y^i), \tag{B.18}$$

$$\begin{aligned} Q_1^i(\varepsilon) &= \varepsilon^{-1} Q_f^i, \quad Q_2^i(\varepsilon) = -((M_{11}^i + N_1^i Z_f^i P_f^{-1}) Y^i + P_f {M_{21}^i}' + Z_f^{i\prime} N_2^{i\prime}), \\ Q_3^i(\varepsilon) &= \varepsilon(Q_s^i - (M_{21}^i + N_2^i Z_f^i P_f^{-1}) Y^i - Y^{i\prime}({M_{21}^i}' + P_f^{-1} Z_f^{i\prime} N_2^{i\prime})), \end{aligned} \tag{B.19}$$

and

$$Y^i = -\sum_{h=1, h\neq i}^{N} {M_{11}^h}^{-1} (M_{12}^h P_s + N_1^h Z_s^h). \tag{B.20}$$

Substituting (3.30) and (B.14)-(B.16) in (3.36), we have:

$$\begin{bmatrix} X_1^i(\varepsilon) & X_2^i(\varepsilon) \\ X_2^i(\varepsilon)' & X_3^i(\varepsilon) \end{bmatrix} \prec 0 \tag{B.21}$$

with

$$\begin{aligned} X_1^i(\varepsilon) = \varepsilon^{-1}(&M_{11}^i P_1(\varepsilon) + P_1(\varepsilon) {M_{11}^i}' + M_{12}^i P_2(\varepsilon)' + \\ &P_2(\varepsilon) {M_{12}^i}' + N_1^i Z_1^i(\varepsilon) + Z_1^i(\varepsilon)' N_1^{i\prime} + Q_1^i(\varepsilon)), \\ X_2^i(\varepsilon) = \varepsilon^{-1}&M_{11}^i P_2(\varepsilon) + \varepsilon^{-1} M_{12}^i P_3(\varepsilon) + P_1(\varepsilon) {M_{21}^i}' + \\ &P_2(\varepsilon)' {M_{22}^i}' + \varepsilon^{-1} N_1^i Z_2^i(\varepsilon) + Z_1^i(\varepsilon)' N_2^{i\prime} + Q_2^i(\varepsilon), \\ X_3^i(\varepsilon) = &M_{22}^i P_3(\varepsilon) + P_3(\varepsilon) {M_{22}^i}' + M_{21}^i P_2(\varepsilon) + P_2(\varepsilon)' {M_{21}^i}' + \\ &N_2^i Z_2^i(\varepsilon) + Z_2^i(\varepsilon)' N_2^{i\prime} + Q_3(\varepsilon). \end{aligned}$$

Replacing the values of $P(\varepsilon), Z^i(\varepsilon), Q^i(\varepsilon)$ and the equations (3.33), (B.17)-(B.20), we obtain:

$$\begin{aligned} X_1^i(\varepsilon) = &\ \varepsilon^{-1}(M_{11}^i P_f + P_f {M_{11}^i}' + N_1^i Z_f^i + Z_f^{i\prime} N_1^{i\prime} + Q_f^i + O(\varepsilon)) = \varepsilon^{-1}(X_f^i + O(\varepsilon)), \\ X_2^i(\varepsilon) = &\ \varepsilon(P_2' {M_{22}^i}' + O(\varepsilon)) = \varepsilon(X_2^i + O(\varepsilon)), \\ X_3^i(\varepsilon) = &\ \varepsilon(M_s^i P_s + P_s {M_s^i}' + N_s^i Z_s^i + Z_s^{i\prime} N_s^{i\prime} + Q_s^i + O(\varepsilon)) = \varepsilon(X_s^i + O(\varepsilon)). \end{aligned}$$

The inequality (B.21) can be written as

$$\begin{bmatrix} \varepsilon^{-1}(X_f^i + O(\varepsilon)) & \varepsilon(X_2^i + O(\varepsilon)) \\ (\star)' & \varepsilon(X_s^i + O(\varepsilon)) \end{bmatrix} \prec 0.$$

Satisfying the conditions (3.37) and (3.38) implies that $X_f^i \prec 0$ and $X_s^i \prec 0$. This means that there exists a scalar $\varepsilon_{max} > 0$ such that $X_s^i + O(\varepsilon) \prec 0$ and $X_f^i - \varepsilon^2 X_2^i {X_s^i}^{-1} X_2^{i\prime} + O(\varepsilon) \prec 0$, $\forall\, i \in \mathcal{I}$ and $\forall \varepsilon \in (0, \varepsilon_{max}]$. Hence, using the Schur complement, the LMI (3.36) is verified. Since $P_f \succ 0$ and $P_s \succ 0$, (B.14) holds. Furthermore, substituting (B.19) in (B.16), we obtain

$$\begin{aligned} Q^i(\varepsilon) = &\begin{bmatrix} \varepsilon^{-1} I_{n_1} & 0 \\ 0 & I_{n_2} \end{bmatrix} \times \\ &\begin{bmatrix} Q_f^i & -((M_{11}^i + N_1^i Z_f^i P_f^{-1}) Y^i + P_f {M_{21}^i}' + Z_f^{i\prime} N_2^{i\prime}) \\ (\star)' & Q_s^i - (M_{21}^i + N_2^i Z_f^i P_f^{-1}) Y^i - Y^{i\prime}({M_{21}^i}' + P_f^{-1} Z_f^{i\prime} N_2^{i\prime}) \end{bmatrix} \times \\ &\begin{bmatrix} I_{n_1} & 0 \\ 0 & \varepsilon I_{n_2} \end{bmatrix} \succ 0 \end{aligned}$$

which, using the Schur complement, holds if and only if

$$\begin{bmatrix} Q_f^i + N_1^i Z_f^i P_f^{-1} Z_f^{i\prime} N_1^{i\prime} & H^i & N_1^i Z_f^i & 0 \\ (\star)' & L^i & Y^{i\prime} & N_2^i Z_f^i + Y^{i\prime} \\ (\star)' & (\star)' & P_f & 0 \\ (\star)' & (\star)' & (\star)' & P_f \end{bmatrix} \succ 0, \tag{B.22}$$

with $H^i = -(M_{11}^i Y^i + P_f M_{21}^{i\prime} + Z_f^{i\prime} N_2^{i\prime})$ and $L^i = Q_s^i - M_{21}^i Y^i - Y^{i\prime} M_{21}^{i\prime} + N_2^i Z_f^i P_f^{-1} Z_f^{i\prime} N_2^{i\prime} + Y^{i\prime} P_f^{-1} Y^i$. (3.39) is non negative definite. This implies that the constraint (B.22) holds $\forall\, i \in \mathcal{I}$.

In order to find K^i, consider $u_s(t) = K_s^i x_s(t) = Z_s^i P_s^{-1} x_s(t)$ and $u_f(t) = K_f^i x_f(t) = Z_f^i P_f^{-1} x_f(t)$. The composite controller is given by $u_c(t) = u_s(t) + u_f(t) = K_s^i x_s(t) + K_f^i x_f(t)$. Letting $x_s(t) = x_2(t)$ and $x_f(t) = x_1(t) + {M_{11}^i}^{-1}(M_{12}^i x_s(t) + N_1^i u_s(t)) = x_1(t) + {M_{11}^i}^{-1}(M_{12}^i + N_1^i K_s^i) x_s(t)$, we have:

$$u_c(t) = Z_s^i P_s^{-1} x_2(t) + Z_f^i P_f^{-1} x_1(t) + Z_f^i P_f^{-1} {M_{11}^i}^{-1}(M_{12}^i + N_1^i Z_s^i P_s^{-1}) x_2(t). \tag{B.23}$$

When $\varepsilon \to 0$, substituting (B.14) and (B.15) in $K^i(\varepsilon) = Z^i(\varepsilon) P(\varepsilon)^{-1}$ and applying the formula of the inverse of block matrix given in Appendix A.2 we find (B.23), which concludes the proof. ■

B.4 Proof Theorem 12

Let us assume

$$P^i(\varepsilon) = \begin{bmatrix} P_1^i(\varepsilon) & P_2^i(\varepsilon) \\ P_2^i(\varepsilon)' & P_3(\varepsilon) \end{bmatrix} \succ 0, \tag{B.24}$$

$$Z^i(\varepsilon) = \begin{bmatrix} Z_1^i(\varepsilon) & Z_2^i(\varepsilon) \end{bmatrix}, \tag{B.25}$$

$$Q^{ij}(\varepsilon) = \begin{bmatrix} Q_1^i & Q_2^{ij}(\varepsilon) \\ Q_2^{ij}(\varepsilon)' & Q_3^i(\varepsilon) \end{bmatrix} \succ 0, \tag{B.26}$$

$$S^i(\varepsilon) = P^i(\varepsilon)^{-1} = \begin{bmatrix} S_1^i(\varepsilon) & S_2^i(\varepsilon) \\ S_2^i(\varepsilon)' & S_3^i(\varepsilon) \end{bmatrix} \succ 0, \tag{B.27}$$

with

$$\begin{aligned} P_1^i(\varepsilon) &= P_f^i + \varepsilon P_2^i P_s^{-1} P_2^{i\prime}, \\ P_2^i(\varepsilon) &= \varepsilon P_2^i = \varepsilon (I_{n_1} - A_{11}^i)^{-1}(A_{12}^i P_s + B_1^i Z_s^i), \\ P_3(\varepsilon) &= \varepsilon P_s, \end{aligned} \tag{B.28}$$

$$Z_1^i(\varepsilon) = Z_f^i + \varepsilon Z_s^i P_s^{-1} P_2^{i\prime}, \quad Z_2^i(\varepsilon) = \varepsilon Z_s^i, \tag{B.29}$$

$$
\begin{aligned}
&Q_1^i = Q_f^i, \quad Q_2^{ij}(\varepsilon) = \varepsilon(P_2^j - P_2^i - (A_{11}^i P_f^i + B_1^i Z_f^i) P_f^{i^{-1}} (A_{21}^i P_f^i + B_2^i Z_f^i)'),\\
&Q_3^i(\varepsilon) = \varepsilon^2(Q_s^i - (A_{21}^i P_f^i + B_2^i Z_f^i) P_f^{i^{-1}} (A_{21}^i P_f^i + B_2^i Z_f^i)'),
\end{aligned} \tag{B.30}
$$

$$
\begin{aligned}
&S_1^i(\varepsilon) = (P_1^i(\varepsilon) - P_2^i(\varepsilon) P_3(\varepsilon)^{-1} P_2^i(\varepsilon)')^{-1}, \quad S_2^i(\varepsilon) = -S_1^i(\varepsilon) P_2^i(\varepsilon) P_3(\varepsilon)^{-1},\\
&S_3^i(\varepsilon) = P_3(\varepsilon)^{-1} + P_3(\varepsilon)^{-1} P_2^i(\varepsilon)' S_1^i(\varepsilon) P_2^i(\varepsilon) P_3(\varepsilon)^{-1}.
\end{aligned} \tag{B.31}
$$

Substituting (3.58), (B.24)-(B.27) in (3.64), we have:

$$
\begin{bmatrix} X_1^{ij}(\varepsilon) & X_2^{ij}(\varepsilon) \\ X_2^{ij}(\varepsilon)' & X_3^i(\varepsilon) \end{bmatrix} \prec 0 \tag{B.32}
$$

with:

$$
\begin{aligned}
X_1^{ij}(\varepsilon) =& A_{11}^i P_1^i(\varepsilon) A_{11}^{i\,\prime} + A_{12}^i P_2^i(\varepsilon)' A_{11}^{i\,\prime} + A_{11}^i P_2^i(\varepsilon) A_{12}^{i\,\prime} + A_{12}^i P_3(\varepsilon) A_{12}^{i\,\prime} +\\
& A_{11}^i Z_1^i(\varepsilon)' B_1^{i\prime} + A_{12}^i Z_2^i(\varepsilon)' B_1^{i\prime} + B_1^i Z_1^i(\varepsilon) A_{11}^{i\,\prime} + B_1^i Z_2^i(\varepsilon) A_{12}^{i\,\prime} +\\
& B_1^i (Z_1^i(\varepsilon) S_1^i(\varepsilon) Z_1^i(\varepsilon)' + Z_2^i(\varepsilon) S_2^i(\varepsilon)' Z_1^i(\varepsilon)' + Z_1^i(\varepsilon) S_2^i(\varepsilon) Z_2^i(\varepsilon)' +\\
& Z_2^i(\varepsilon) S_3^i(\varepsilon) Z_2^i(\varepsilon)') B_1^{i\prime} - P_1^j(\varepsilon) + Q_1^i,
\end{aligned}
$$

$$
\begin{aligned}
X_2^{ij}(\varepsilon) =& A_{11}^i P_1^i(\varepsilon) A_{21}^{i\,\prime}\varepsilon + A_{12}^i P_2^i(\varepsilon)' A_{21}^{i\,\prime}\varepsilon + A_{11}^i P_2^i(\varepsilon)(I_{n_2} + \varepsilon A_{22}^i)' + A_{12}^i P_3^i(\varepsilon) \times\\
& (I_{n_2} + \varepsilon A_{22}^i)' + A_{11}^i Z_1^i(\varepsilon)' B_2^{i\prime}\varepsilon + A_{12}^i Z_2^i(\varepsilon)' B_2^{i\prime}\varepsilon + B_1^i Z_1^i(\varepsilon)\varepsilon A_{21}^{i\,\prime} +\\
& B_1^i Z_2^i(\varepsilon)(I_{n_2} + \varepsilon A_{22}^i)' + B_1^i (Z_1^i(\varepsilon) S_1^i(\varepsilon) Z_1^i(\varepsilon)' + Z_2^i(\varepsilon) S_2^i(\varepsilon)' Z_1^i(\varepsilon)' +\\
& Z_1^i(\varepsilon) S_2^i(\varepsilon) Z_2^i(\varepsilon)' + Z_2^i(\varepsilon) S_3^i(\varepsilon) Z_2^i(\varepsilon)') B_2^{i\prime}\varepsilon - P_2^j(\varepsilon) + Q_2^{ij}(\varepsilon),
\end{aligned}
$$

$$
\begin{aligned}
X_3^i(\varepsilon) =& \varepsilon A_{21}^i P_1^i(\varepsilon) A_{21}^{i\,\prime}\varepsilon + \varepsilon A_{21}^i P_2^i(\varepsilon)(I_{n_2} + \varepsilon A_{22}^i)' + (I_{n_2} + \varepsilon A_{22}^i) P_2^{i\prime}(\varepsilon) A_{21}^{i\,\prime}\varepsilon +\\
& (I_{n_2} + \varepsilon A_{22}^i) P_3(\varepsilon)(I_{n_2} + \varepsilon A_{22}^i)' + \varepsilon A_{21}^i Z_1^i(\varepsilon)' B_2^{i\prime}\varepsilon + (I_{n_2} + \varepsilon A_{22}^i) \times\\
& Z_2^i(\varepsilon)' B_2^{i\prime}\varepsilon + \varepsilon B_2^i Z_1^i(\varepsilon) A_{21}^{i\,\prime}\varepsilon + \varepsilon B_2^i Z_2^i(\varepsilon)(I_{n_2} + \varepsilon A_{22}^i)' + \varepsilon B_2^i (Z_1^i(\varepsilon) \times\\
& S_1^i(\varepsilon) Z_1^i(\varepsilon)' + Z_2^i(\varepsilon) S_2^i(\varepsilon)' Z_1^i(\varepsilon)' + Z_1^i(\varepsilon) S_2^i(\varepsilon) Z_2^i(\varepsilon)' +\\
& Z_2^i(\varepsilon) S_3^i(\varepsilon) Z_2^i(\varepsilon)') B_2^{i\prime}\varepsilon - P_3(\varepsilon) + Q_3(\varepsilon).
\end{aligned}
$$

Replacing the values of $P^i(\varepsilon), Z^i(\varepsilon), Q^{ij}(\varepsilon),\ S^i(\varepsilon)$ and the equations (3.61), (B.28)-(B.31), we obtain:

$$
\begin{aligned}
X_1^{ij}(\varepsilon) =& A_{11}^i P_f^i A_{11}^{i\,\prime} + A_{11}^i Z_f^{i\,\prime} B_1^{i\prime} + B_1^i Z_f^i A_{11}^{i\,\prime} +\\
& B_1^i Z_f^i P_f^{i^{-1}} Z_f^{i\,\prime} B_1^{i\prime} - P_f^j + Q_f^i + O(\varepsilon) = X_1^{ij} + O(\varepsilon),
\end{aligned}
$$

$$
\begin{aligned}
X_2^{ij}(\varepsilon) =& \varepsilon^2 (A_{12}^i P_2^{i\prime} A_{21}^{i\,\prime} + A_{11}^i P_2^i A_{22}^{i\,\prime} + A_{12}^i Z_s^{i\prime} B_2^{i\prime} + B_1^i Z_s^i A_{22}^{i\,\prime} +\\
& B_1^i (-Z_s^i P_s^{-1\prime} P_2^{i\prime} P_f^{i^{-1\prime}} Z_f^{i\prime} - Z_f^i P_f^{i^{-1}} P_2^i P_s^{-1} Z_s^{i\prime} + Z_s^i P_s^{-1} Z_s^{i\prime}) B_2^{i\prime} + O(\varepsilon)) =\\
& \varepsilon^2 (X_2^i + O(\varepsilon)),
\end{aligned}
$$

$$
X_3^i(\varepsilon) = \varepsilon^2 (A_s^i P_s + P_s A_s^{i\prime} + B_s^i Z_s + Z_s' B_s^{i\prime} + Q_s^i + O(\varepsilon)) = \varepsilon^2 (X_3^i + O(\varepsilon)).
$$

The inequality (B.32) can be written as

$$\begin{bmatrix} X_1^{ij} + O(\varepsilon) & \varepsilon^2(X_2^i + O(\varepsilon)) \\ (\star)' & \varepsilon^2(X_3^i + O(\varepsilon)) \end{bmatrix} \prec 0.$$

Satisfying the conditions (3.65) and (3.66) implies that $X_1^{ij} \prec 0$ and $X_3^i \prec 0$. This means that there exists a scalar $\varepsilon_{max} > 0$ such that $X_3^i + O(\varepsilon) \prec 0$ and $X_1^{ij} - \varepsilon^2 X_2^i {X_3^i}^{-1} {X_2^i}' + O(\varepsilon) \prec 0$, $\forall (i,j) \in \mathcal{I} \times \mathcal{I}$ and $\forall\, \varepsilon \in (0, \varepsilon_{max}]$. Hence, using the Schur complement, the inequality (3.64) is verified. Since $P_f^i \succ 0$ and $P_s \succ 0$, (B.24) holds. Furthermore, substituting (B.30) in (B.26), we obtain:

$$Q^{ij}(\varepsilon) = \begin{bmatrix} I_{n_1} & 0 \\ 0 & \varepsilon I_{n_2} \end{bmatrix} \begin{bmatrix} Q_f^i & P_2^j - P_2^i - (A_{11}^i P_f^i + B_1^i Z_f^i) {P_f^i}^{-1} (A_{21}^i P_f^i + B_2^i Z_f^i)' \\ (\star)' & Q_s^i - (A_{21}^i P_f^i + B_2^i Z_f^i) {P_f^i}^{-1} (A_{21}^i P_f^i + B_2^i Z_f^i)' \end{bmatrix} \times \begin{bmatrix} I_{n_1} & 0 \\ 0 & \varepsilon I_{n_2} \end{bmatrix} \succ 0$$

which, using the Schur complement, holds if and only if

$$\begin{bmatrix} Q_f^i + (A_{11}^i P_f^i + B_1^i Z_f^i) {P_f^i}^{-1} (A_{11}^i P_f^i + B_1^i Z_f^i)' & P_2^j - P_2^i & A_{11}^i P_f^i + B_1^i Z_f^i \\ (\star)' & Q_s^i & A_{21}^i P_f^i + B_2^i Z_f^i \\ (\star)' & (\star)' & P_f^i \end{bmatrix} \succ 0. \tag{B.33}$$

(3.67) is non negative definite. This implies that the constraint (B.33) holds $\forall\, (i,j) \in \mathcal{I} \times \mathcal{I}$.

In order to find K^i, consider $u_s(k) = K_s^i x_s(k) = Z_s^i P_s^{-1} x_s(k)$ and $u_f(k) = K_f^i x_f(k) = Z_f^i {P_f^i}^{-1} x_f(k)$. The composite controller is given by $u_c(k) = u_s(k) + u_f(k) = K_s^i x_s(k) + K_f^i x_f(k)$. Letting $x_s(k) = x_2(k)$ and $x_f(k) = x_1(k) - (I_{n_1} - A_{11}^i)^{-1}(A_{12}^i x_s(k) + B_1^i u_s(k)) = x_1(k) - (I_{n_1} - A_{11}^i)^{-1}(A_{12}^i + B_1^i K_s^i) x_s(k)$, we have

$$\begin{aligned} u_c(k) = {} & Z_s^i P_s^{-1} x_2(k) + Z_f^i {P_f^i}^{-1} x_1(k) - \\ & Z_f^i {P_f^i}^{-1} (I_{n_1} - A_{11}^i)^{-1} (A_{12}^i + B_1^i Z_s^i P_s^{-1}) x_2(k) \end{aligned} \tag{B.34}$$

When $\varepsilon \to 0$, substituting (B.24) and (B.25) in $K^i(\varepsilon) = Z^i(\varepsilon) {P^i(\varepsilon)}^{-1}$ and applying the formula of the inverse of block matrix given in Appendix A.2 we find (B.34), which concludes the proof. ■

B.5 Construction of the augmented state matrix

From Theorem 13, when the bumpless transfer controller is on we have:

$$u^{bt,i}(k) = Q^i(k) \begin{bmatrix} x(k) \\ \tilde{u}^i(k) \\ g^i(k+1) \end{bmatrix} \tag{B.35}$$

where

$$\tilde{u}^i(k) = \begin{cases} \tilde{u}^{i,0}(k) + (k - t_i + 1)p^i(k) & if \quad t_i \leq k < t_i + \tau_i^M \\ 0 & otherwise, \end{cases} \tag{B.36}$$

with

$$\tilde{u}^{i,0}(k) = K^j x(t_i - 1) \tag{B.37}$$

and

$$p^i(k) = \frac{1}{\tau_i^M}(K^i x(t_i) - K^j x(t_i - 1)). \tag{B.38}$$

Let $\tau_k^i = k - t_i + 1$. The evolution of the signal g^i in (B.35) is given by (4.16), which can be rewritten as

$$g^i(\tau_k^i) = G^{i,u}(\tau_k^i)\tilde{u}^{i,0}(\tau_k^i) + G^{i,p}(\tau_k^i)p^i(\tau_k^i) \tag{B.39}$$

where

$$G^{i,u}(\tau_k^i) = -\sum_{\eta=0}^{\tau_i^M - \tau_k^i} \left(\prod_{\zeta=\tau_k^i+1}^{\tau_i^M+1-\eta} M^i(\zeta) \right) \Pi^i(\tau_k^i + 1 - \eta)B^i,$$

$$G^{i,p}(\tau_k^i) = -\sum_{\eta=0}^{\tau_i^M - \tau_k^i} \left(\prod_{\zeta=\tau_k^i+1}^{\tau_i^M+1-\eta} M^i(\zeta) \right) \Pi^i(\tau_k^i + 1 - \eta)B^i(\tau^M - \eta)$$

and

$$M^i(\tau_k^i) = A^{i'}(I - \Pi^i(\tau_k^i)\tilde{B}^i)^{-1},$$

with Π^i and $\tilde{B}^i$ defined in equations (4.15) and (4.17), respectively. The closed form (B.39) allows to express equation (4.16) as a function of $\tilde{u}^{i,0}$ and p^i. Hence, for $t_i \leq k < t_i + \tau_i^M$, the closed loop system (4.2)-(4.4) becomes:

$$\begin{aligned} x(k+1) =& \bar{A}^i(\tau_k^i + 1)x(k) + (\bar{B}^i(\tau_k^i + 1) - B^i\tilde{N}^i(\tau_k^i + 1)G^{i,u}(\tau_k^i + 1))\tilde{u}^{i,0}(\tau_k^i) + \\ & (\tau_k^i\bar{B}^i(\tau_k^i + 1) - B^i\tilde{N}^i(\tau_k^i + 1)G^{i,p}(\tau_k^i + 1))p^i(\tau_k^i), \end{aligned}$$

with

$$\bar{A}^i(\tau_k^i) = (I_n + B^i\tilde{N}^i(\tau_k^i)\Pi^i(\tau_k^i))A^i,$$

$$\bar{B}^i(\tau_k^i) = B^i(I_r + \tilde{N}^i(\tau_k^i)\Pi^i(\tau_k^i)B^i)$$

and $\tilde{N}^i$ defined in equation (4.14). $\tilde{u}^{i,0}(\tau_k^i)$ and $p^i(\tau_k^i)$ are initialized as function of $x(k)$ and $x(k-1)$ at the switching time ($k = t_i$, $\tau_k^i = 1$). Using (B.37) and (B.38), we find

$$Y^i(j, \tau_k^i)|_{\tau_k^i=1} = \begin{bmatrix} \bar{H}^i(\tau_k^i + 1) & \bar{L}^{ji}(\tau_k^i + 1) & 0_{n\times r} & 0_{n\times r} \\ I_n & 0_{n\times n} & 0_{n\times r} & 0_{n\times r} \\ 0_{r\times n} & K^j & 0_{r\times r} & 0_{r\times r} \\ \frac{1}{\tau_i^M}K^i & -\frac{1}{\tau_i^M}K^j & 0_{r\times r} & 0_{r\times r} \end{bmatrix}$$

with

$$\bar{H}^i(\tau_k^i) = \bar{A}^i(\tau_k^i) + \frac{1}{\tau_i^M}(\bar{B}^i(\tau_k^i) - B^i\tilde{N}^i(\tau_k^i)G^{i,p}(\tau_k^i))K^i$$

and

$$\bar{L}^{ji}(\tau_k^i) = (\bar{B}^i(\tau_k^i) - B^i\tilde{N}^i(\tau_k^i)G^{i,u}(\tau_k^i))K^j - \frac{1}{\tau_i^M}(\bar{B}^i(\tau_k^i) - B^i\tilde{N}^i(\tau_k^i)G^{i,p}(\tau_k^i))K^j.$$

$\tilde{u}^{i,0}(\tau_k^i)$ and $p^i(\tau_k^i)$ remain constant for $2 \leq \tau_k^i \leq \tau_i^M$. We have

$$Y^i(j,\tau_k^i)|_{2\leq\tau_k^i\leq\tau_i^M} = \begin{bmatrix} \bar{A}^i(\tau_k^i+1) & 0_{n\times n} & \bar{U}^i(\tau_k^i+1) & \bar{P}^i(\tau_k^i+1) \\ I_n & 0_{n\times n} & 0_{n\times r} & 0_{n\times r} \\ 0_{r\times n} & 0_{r\times n} & I_r & 0_{r\times r} \\ 0_{r\times n} & 0_{r\times n} & 0_{r\times r} & I_r \end{bmatrix}$$

with

$$\bar{U}^i(\tau_k^i) = \bar{B}^i(\tau_k^i) - B^i\tilde{N}^i(\tau_k^i)G^{i,u}(\tau_k^i)$$

and

$$\bar{P}^i(\tau_k^i) = \tau_k^i\bar{B}^i(\tau_k^i) - B^i\tilde{N}^i(\tau_k^i)G^{i,p}(\tau_k^i).$$

When the bumpless transfer controller is off $u^{bt,i}(k) = 0$, then we get:

$$Y^i(j,\tau_k^i)|_{\tau_k^i>\tau_i^M} = Y_s^i = \begin{bmatrix} A^i + B^iK^i & 0_{n\times(n+2r)} \\ I & 0_{n\times(n+2r)} \\ 0_{2r\times n} & 0_{2r\times(n+2r)} \end{bmatrix},$$

which is constant for any $(i,j) \in \mathcal{I}\times\mathcal{I}$. ■

Appendix C

Robust Steering Control Toolbox

The objective of this appendix is to present *RSCT* (*Robust Steering Control Toolbox*), a *MATLAB* toolbox which implements the algorithms necessary to the HSM robust steering control design [MDI+ar], [MDI+09e]. *RSCT* has been written in *MATLAB R14SP1* (*Release 14* with *Service Pack 1*) and tested on *Windows XP* and *Windows VISTA* Operating Systems. A *GUI* (Graphical User Interface) is provided. A LMI solver is required to compute the controllers. To interface *MATLAB* to the most popular solvers, the free *MATLAB* toolbox *YALMIP* is used [Lö4]. We tested two solvers: *SeDuMi*, that is available free of charge under *GNU/GPL* open source license [Stu99], and *LMILAB*, that can be found in the *MATLAB-Robust Control Toolbox* [GNLC95].

To install *RSCT*, remove any old version, unzip the file *RSCT.rar* and add the directory *"\RSCT\software_RSCT"* to your *MATLAB* paths. This operation may be directly done by the main *MATLAB* toolbar choosing *File→Set Path...→Add with Subfolders....* *SeDuMi* and *YALMIP* may be installed following a similar procedure.

To run *RSCT*, tape "RSCT" on the *MATLAB* Command Window. The Main *GUI* shown in Fig. C.1 will appear.

C.1 Main *GUI*

The Main *GUI* allows to compute the controllers, export the results to files, check the stability of the closed loop system and reach the other *GUIs* from the *File toolbar* (*Create a new family GUI*, *HSM simulator GUI*, *A3S GUI*). First, the number of stands $n \in \{5, 6, 7\}$ must be set using the corresponding checkboxes. Thus a database of products must be loaded in order to compute a new controller. To this aim, go to *File toolbar→Load Database*. Choose the *.txt* file which contains the desired database bounds, and then the path of the products database. The *.txt* file, called *database_bounds.txt*, may be created using the specific *GUI* described in section C.2. Each product of the database

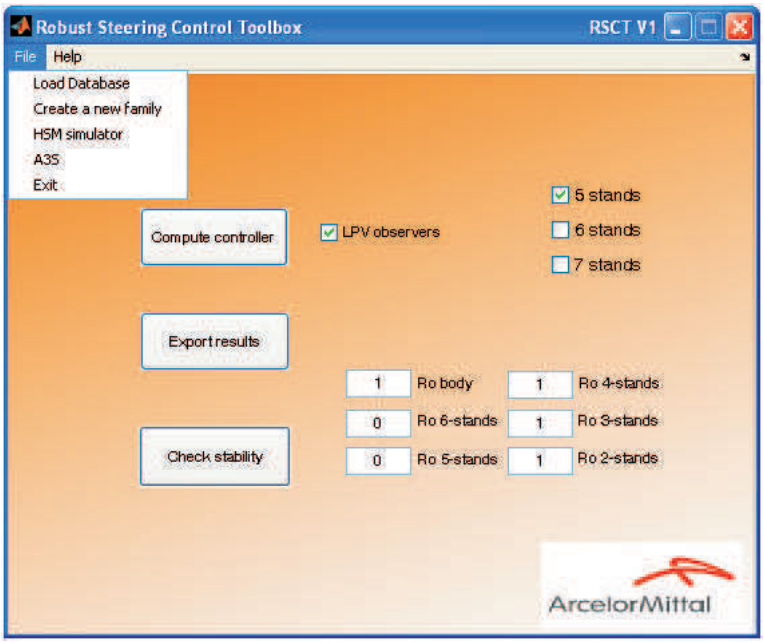

Figure C.1: Main *GUI*

is represented by a *.mat* file containing its characteristics and the corresponding HSM setting. The database may be created through the *A3S GUI* described in section C.4, or provided by the plants.

The tuning of the default control system weighting matrices is done by modifying the R_0 boxes of the *GUI*. We obtain $R = R_0 D_{qu'} D_{qu}$, where D_{qu} is the weighting matrix given in chapter 5.Hence, the bottom *Compute controller* calls the method which computes a different observer based state-feedback H_2 robust controller for each subsystem. If the checkbox *LPV observers* is active, a specific observer is designed for each vertex product, in addition to the average observer designed by default. These observers may be used to implement a linear parameter varying (LPV) strategy in order to take into account the different physical parameters of the rolled products during the observation of the state variables. If the LMI solver does not find a solution, *RSCT* shows a warning, as in Fig. C.2. The bottom *Export results* saves the controller information on the path: \RSCT\controller_data\Matrices_n_stands_*database_bounds*_Rx*Ro*\, where n is the number of stands, *database_bounds* corresponds to the name of the *database_ bounds.txt* file and R_0 is the numerical value of the R_0 *body* box. $3(n-1)+2$ **.txt* files are generated ($5(n-1)+2$ if the checkbox *LPV observers* is active). The syntax is coherent with the controller files used on the Eisenhüttenstadt plant.

Once loaded a database of products and a controller, the bottom *Check stability* yields the results of the posteriori stability test for each subsystem and for the full tail end switched system [MDI+09e]. If the LMI solver does not find a solution, *RSCT* shows a warning.

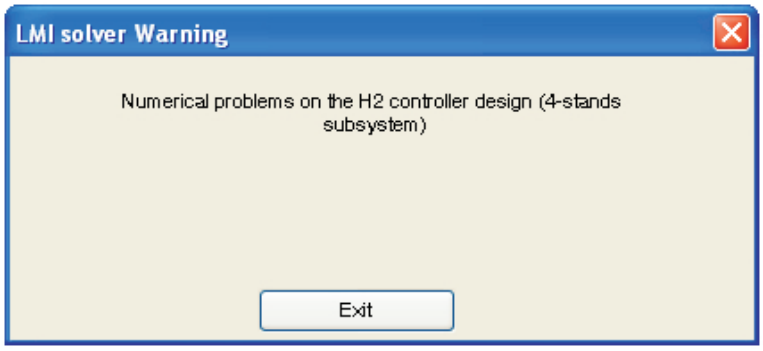

Figure C.2: Warning : LMI not feasible

C.2 Create a new family *GUI*

This *GUI* allows to compute the convex hull vertices of a new family of products. First, the name and the convex hull bounds of the family must be set on the specific boxes (Fig. C.3). The bounds concern the set $\mathcal{U}^m = \{w,\ h,\ \sigma_{in},\ \sigma_{out}\}$, where w is the strip width, h is the output thickness of the strip in the last stand and σ_{in} and σ_{out} are the hardness of the strip in the first and in the last stand, respectively. Hence, a database of products (represented by a **.mat* file) must be loaded from

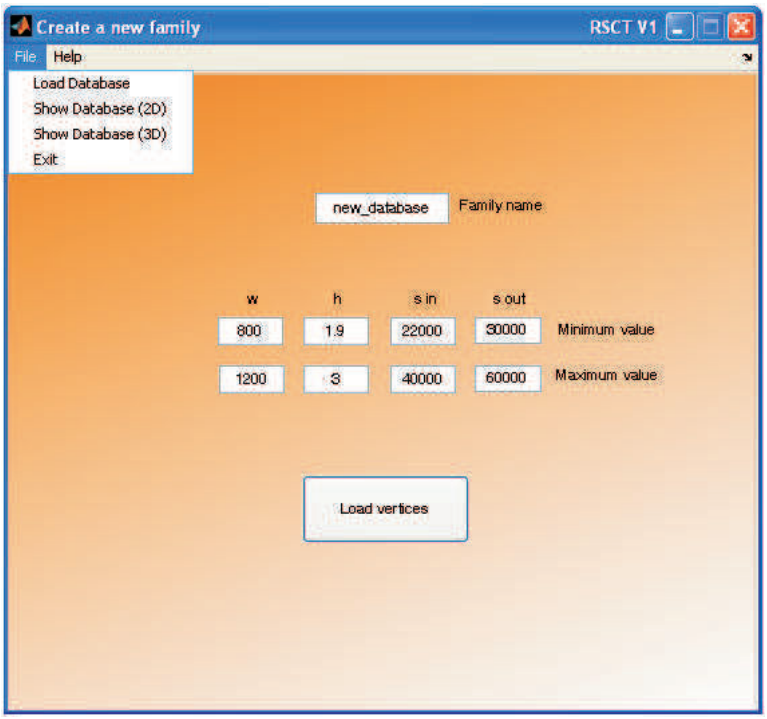

Figure C.3: New family *GUI*

the *File toolbar*. As in the Main *GUI*, it suffices to indicate the database path. Finally, the coordinates of the 16 convex hull vertices must be set. This operation

is semi-manual because of the extremely various shapes that the database can have. To start, push the bottom *Load vertices*. A *2D* projection of the database will appear (Fig. C.4). The four cartesian coordinates of the convex hull vertices corresponding to the given projection can be set using the left bottom of the mouse. Thus, push *Enter* to change projection, for a total of three projections. The coordinates of the vertices on the last three *2D* projections are computed automatically and then the file $\backslash RSCT\backslash database\_bound\backslash new\_family\_name.txt$ is created. Two first rows contain the family bounds set by the *GUI*. This file is composed by a matrix $\in \mathbb{R}^{18\times 4}$. Last 16 rows represent the coordinates of the convex hull vertices corresponding to the family.

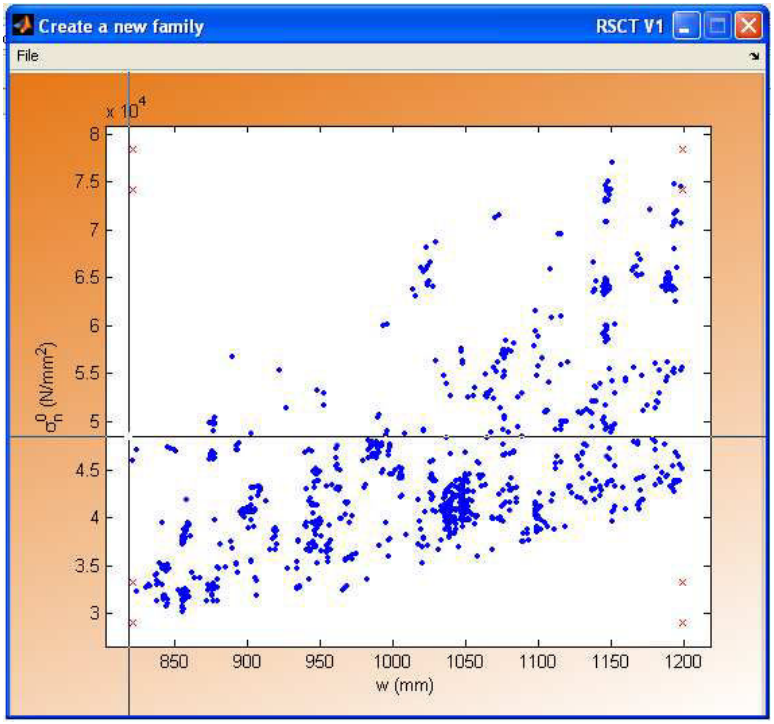

Figure C.4: Vertices setting: An example

$2D$ and $3D$ projections of the convex hull are available by the *File toolbar*. The red x represent the convex hull vertices and the blue points represent the database products which belong to the family. An example is shown in Fig. C.5 and C.6.

C.3 HSM Simulator *GUI*

This *GUI* allows to simulate the open and closed loop system behavior through the *MATLAB-Simulink* nonlinear system model presented in chapter 1. First, a product must be loaded from the *File toolbar*. Each product is described by a *.mat* file, available by the database, and by a *.txt* file, which contains the *IBA Analyzer* output (the coilbox perturbation and the tail end switching instants).

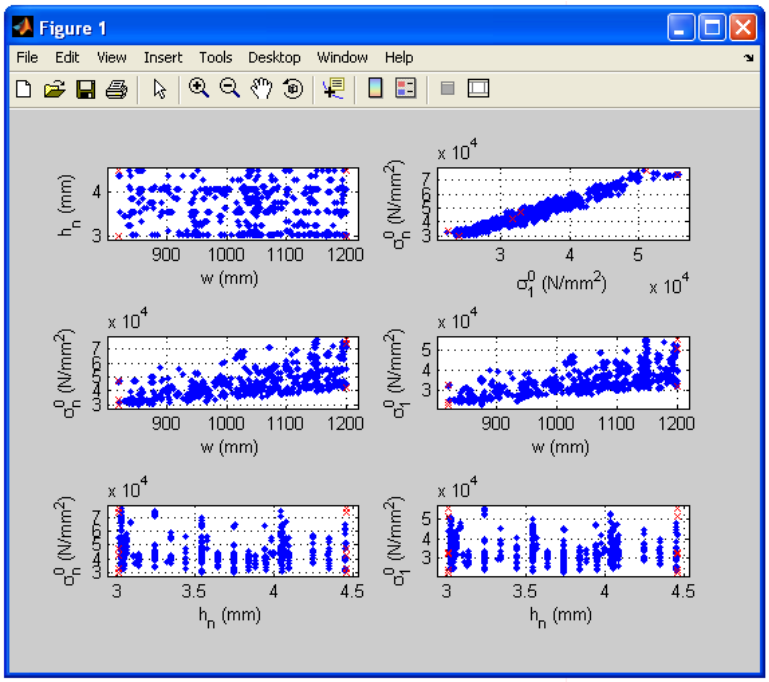

Figure C.5: $2D$ database projections: An example

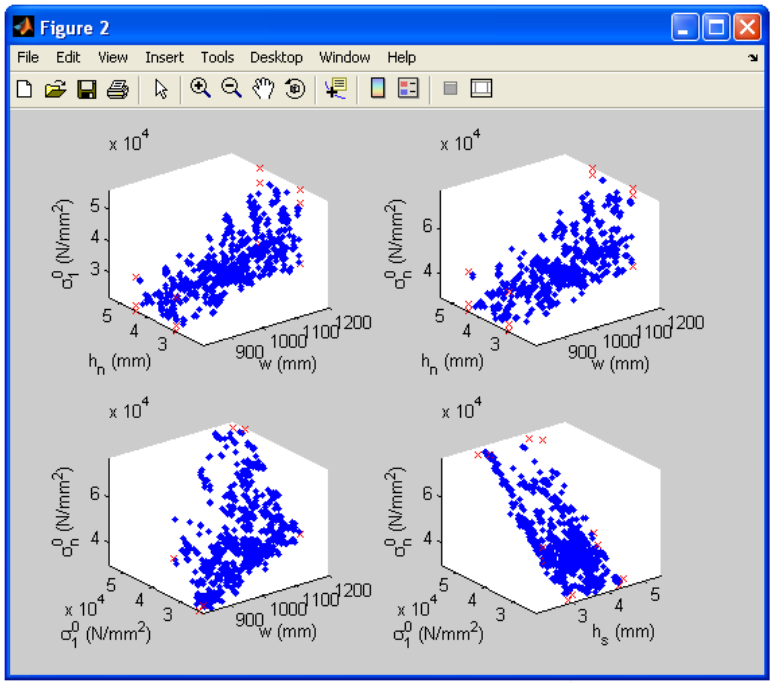

Figure C.6: $3D$ database projections: An example

Hence, a controller must be loaded by the *File toolbar*. It suffices to indicate the controller path. If the syntax of the *.txt* controller files is not the same of the output generated by the command *Export results* of the Main *GUI*, an error

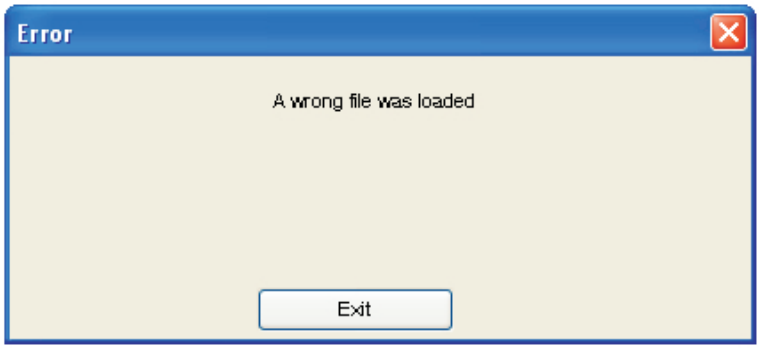

Figure C.7: Error : A wrong file was loaded

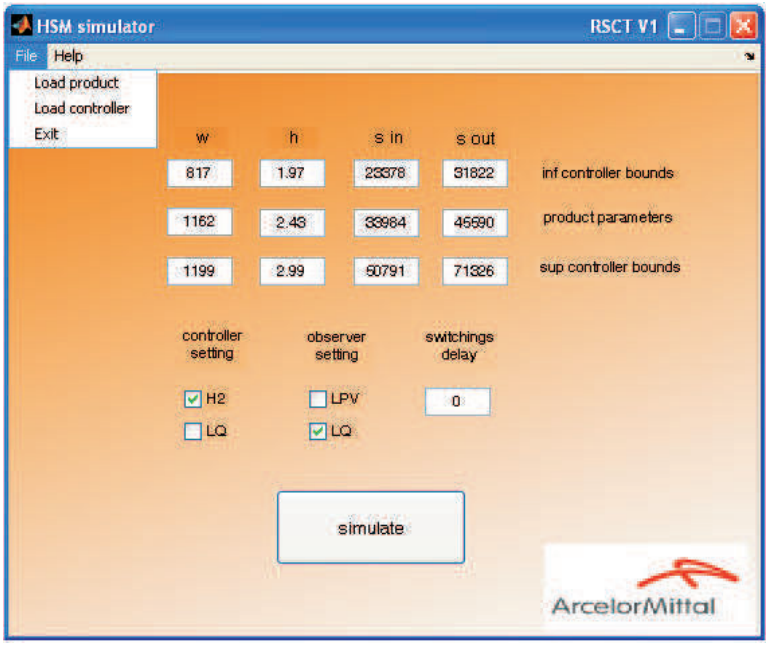

Figure C.8: HSM simulator *GUI*

message will be show (Fig. C.7).

The main physical parameters concerning the product and the controller are summarized on the *GUI* boxes (Fig. C.8). The closed loop system may be simulated using two different kind of controllers (H_2 or average LQ) and observers (LPV or average LQ). A checkbox consents to add a delay on the controller switchings.

C.4 *A3S GUI*

A3S is a software developed by *ArcelorMittal* researchers in a *Visual Basic* ambiance. It computes the **.mat* files representing the products through a manual procedure stand by stand. To integrate this functionality in *RSCT*, we rewrote

the *A3S* numerical algorithms in *MATLAB* code and we implemented an automatic procedure to create m consecutive products. The new *A3S GUI* is shown in Fig. C.9. The *A3S* input is represented by a *.txt* file which contains the phys-

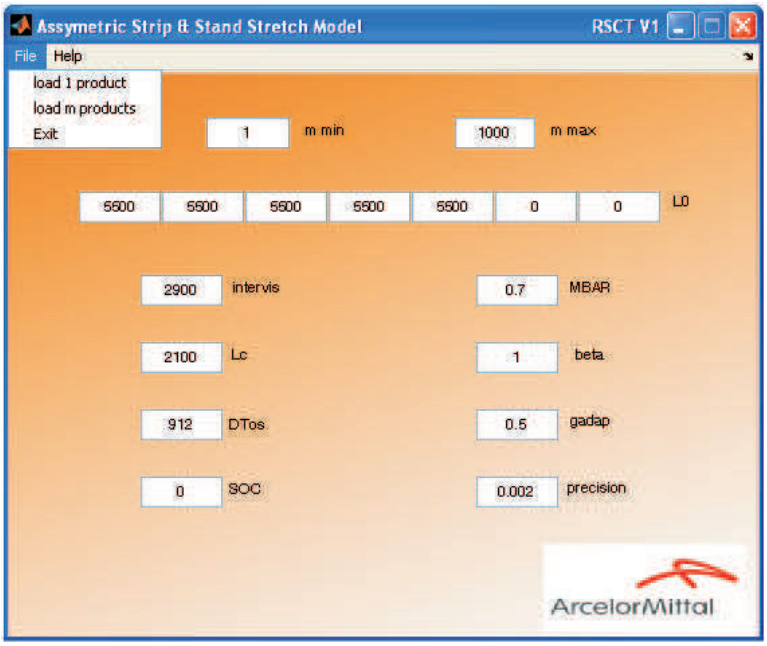

Figure C.9: *A3S GUI*

ical characteristics of a product (*DT, DS, ET, ES, Fwo, Fwm, Fmes, LARTOL, epe, eps, Temp, VITCYL, TRACTE, TRACTS*). These data must be provided by the plants.

From the *GUI* boxes, the setup of the HSM parameters (L0, intervis, Lc DTos, SOC) and of the numerical algorithm (mbar, beta, gadap, precision) can be modified. From the *File toolbar*, we can load a single product, or m consecutive products. The boxes m_{min} and m_{max} allow to choose the serial number of the first and the last product that will be load. If we load m products, the input **.txt* files must respect the syntax: *"optional_ text_ 1, serial_ number, optional_ text_ 2, .txt"*, where th strings *"optional_ text_ 1"* and *"optional_ text_ 2"* cannot contain numerical characters.

Notice that a convergence problem arises for about the 1% of the products. In this case, the algorithm of *A3S* cannot reach the stop criterion and loops infinitely. For obtain a solution with this kind of products, you must stop the routine (*CTRL+C*), modify the strip width *LARTOL* of some millimeters in the input file, and load once more the file.

C.5 Options setting

Only the sampling time, the *LMI* solver flags and the tuning parameters of the HSM simulator, which are different for each plant, must be set from the file

\RSCT\software_RSCT\default_setting_n_stands.m, where n is the number of stands. All the other parameters may be directly set by the *GUIs*.

Bibliography

[ALI08] M. Alwan, X. Liu, and B. Ingalls. Exponential stability of singularly perturbed switched systems with time delay. *Nonlinear Analysis: Hybrid Systems*, 2(3):913–921, 2008.

[AM89] B.D.O. Anderson and J.B. Moore. *Optimal control: linear quadratic methods*. Prentice-Hall, 1989.

[And93] B.D.O. Anderson. Controller design: Moving from theory to practice. *IEEE Control Systems Magazine*, 13(4):16–25, 1993.

[AW96] A.B. Arehart and W.A. Wolovich. Bumpless switching controllers. In *Conference on Decision and Control*, 1996.

[BGFB94] S. Boyd, L.E. Ghaoui, E. Feron, and V. Balakrishnan. *Linear Matrix Inequalities in system and control theory*. Society for Industrial and Applied Mathematics, 1994.

[BH75] A.E. Bryson and Y.C. Ho. *Applied optimal control*. John Wiley, 1975.

[BKG02] B. Bulut, M.R. Katebi, and M.J. Grimble. Co-ordinated control of profile and shape in hot strip finishing mills with nonlinear dynamics. *IEE Proceedings - Control Theory and Applications*, 149(5):471–480, 2002.

[Bla81] G. Blankenship. Singularly perturbed difference equations in optimal control problems. *IEEE Transactions on Automatic Control*, 26(4):911– 917, 1981.

[BMS07] F. Blanchini, S. Miani, and C. Savorgnan. Stability results for linear parameter varying and switching systems. *Automatica*, 43(10):1817–1823, 2007.

[Bra98] S. Branicky. Multiple Lyapunov function and other analysis tools for switched and hybrid systems. *IEEE Transactions on Automatic Control*, 43(4):475–482, 1998.

[CRCF08] I.S. Choi, J. A. Rossiter, J.S. Chung, and P.J. Fleming. An MPC strategy for hot rolling mills and applications to strip threading control problems. In *IFAC world congress*, 2008.

[CRF07] I.S. Choi, J.A. Rossiter, and P.J. Fleming. Looper and tension control in hot rolling mills: A survey. *Journal of Process Control*, 17(6):509–521, 2007.

[CS08] S.Y. Cheong and M.G. Safonov. Bumpless transfer for adaptive switching controls. In *IFAC World Congress*, 2008.

[DBI+08] J. Daafouz, R. Bonidal, C. Iung, P. Szczepanski, N. Naumann, and U. Koschack. New steering control at EKO Stahl finishing mill. In *The Iron & Steel Technology Conference and Exposition*, 2008.

[DM99] W.P. Dayawansa and C.F. Martin. A converse Lyapunov theorem for a class of dynamical systems which undergo switching. *IEEE Transactions on Automatic Control*, 44(4):751–760, 1999.

[DRI02] J. Daafouz, P. Riedinger, and C. Iung. Stability analysis and control synthesis for switched systems: a switched Lyapunov function approach. *IEEE Transactions on Automatic Control*, 47(11):1883–1887, 2002.

[DW06] K. Dong and F. Wu. Online switching control design of LFT systems. In *Conference on Decision and Control*, 2006.

[EP98] C. Edwards and I. Postlethwaite. Anti-windup bumpless transfer schemes. *Automatica*, 34(2):199–210, 1998.

[FFT92] Y. Furukawa, S. Fujii, and H. Taoka. Application of steering control in hot strip mill. *Tetsu-to-Hagane (Journal of the Iron and Steel Institute of Japan)*, 78(8):141–144, 1992.

[FLMR95] M. Fliess, J. Lévine, P. Martin, and P. Rouchon. Flatness and defect of non-linear systems: Introductory theory and examples. *International journal of control*, 61(6):1327–1361, 1995.

[GA96] S.F. Graebe and A. Ahlen. *The control handbook*. CRC press, 1996.

[GC06a] J.C. Geromel and P. Colaneri. Stability and stabilization of continuous-time switched linear systems. *SIAM Journal on Control and Optimization*, 45(5):1915–1930, 2006.

[GC06b] J.C. Geromel and P. Colaneri. Stability and stabilization of discrete time switched systems. *International Journal of Control*, 79(7):719–728, 2006.

[GDB98] G. Garcia, J. Daafouz, and J. Bernussou. H_2 guaranteed cost control for singularly perturbeduncertain systems. *IEEE Transactions on Automatic Control*, 43(9):1323–1329, 1998.

[GDB02] G. Garcia, J. Daafouz, and J. Bernussou. The infinite time near optimal decentralized regulator problem for singularly perturbed systems: A convex optimization approach. *Automatica*, 38(8):1397–1406, 2002.

[GF82] M. Grimble and J. Fotakis. The design of strip shape control systems for Sendzimir mills. *IEEE Transactions on Automatic Control*, 27(3):656– 666, 1982.

[GNLC95] P. Gahinet, A. Nemirovski, A.J. Laub, and M. Chilali. LMI *Control Toolbox User's Guide*. The Math Works Inc., 1995.

[GP98] E.J.M Geddes and I. Postlethwaite. Improvements in product quality in tandem cold rolling using robust multivariable control. *IEEE Transactions on Control Systems Technology*, 6(2):257–269, 1998.

[Han88] R. Hanus. Anti-windup and bumpless transfer: A survey. In *12th IMACS world congress*, 1988.

[HDI06] L. Hetel, J. Daafouz, and C. Iung. Robust stability analysis and control design for switched uncertain polytopic systems. In *5th IFAC Workshop on Robust Control*, 2006.

[HKH87] R. Hanus, M. Kinnaert, and J. Henrotte. Conditioning technique, a general anti-windup and bumpless transfer method. *Automatica*, 23(6):729–739, 1987.

[HM99] J. Hespanha and A.S. Morse. Stability of switched systems with average dwell-time. In *IEEE Conference on Decision and Control*, 1999.

[KCMN94] M.V. Kothare, P.J. Campo, M. Morari, and C.N. Nett. A unified framework for study of anti-windup designs. *Automatica*, 30(12):1869–1883, 1994.

[Kha02] H.K. Khalil. *Nonlinear Systems*. Prentice-Hall, Inc., NJ, 2002.

[KI83] H. Kando and T. Iwazumi. Sub-optimal control of discrete regulator problems via time-scale decomposition. *International Journal of Control*, 37(6):1323–1347, 1983.

[KI86] H. Kando and T. Iwazumi. Multirate digital control design of an optimal regulator via singular perturbation theory. *International Journal of Control*, 44(6):1555–1578, 1986.

[KKO86] P. Kokotovic, H.K. Khalil, and J. O'Reilly. *Singular perturbation methods in control: Analysis and design*. Academic Press, 1986.

[Kok75] P. Kokotovic. A Riccati equation for block-diagonalization of ill-conditioned systems. *IEEE Transactions on Automatic Control*, 20(6):812– 814, 1975.

[KS68] P. Kokotovic and P. Sannuti. Singular perturbation method for reducing the model order in optimal control design. *IEEE Transactions on Automatic Control*, 13(4):377–384, 1968.

[KT83] T. Kimura and M. Tagawa. Automatic steering control of strip rolling mills. *The Hitachi Review*, 65(2):25–30, 1983.

[KT86] H. Kuwano and N. Takahashi. Sensor-type automatic steering control system for rolling mill -1^{st} report. *Ishikawajima-Harima Engineering Review*, 26(1):35–40, 1986.

[LÖ4] J. Löefberg. YALMIP : A toolbox for modeling and optimization in MATLAB. In *IEEE international symposium on computer aided control systems design*, 2004.

[LA07] H. Lin and P.J. Antsaklis. Switching stabilizability for continuous-time uncertain switched linear systems. *IEEE Transactions on Automatic Control*, 52(4):633–646, 2007.

[LA09] H. Lin and P.J. Antsaklis. Stability and stabilizability of switched linear systems: A survey of recent results. *IEEE Transactions on Automatic Control*, 54(2):308–322, 2009.

[LHM99] D. Liberzon, J. Hespanha, and A.S. Morse. Stability of switched systems: a Lie-algebraic condition. *Systems Control letters*, 37(3):117–122, 1999.

[Lib03] D. Liberzon. *Switching in systems and control*. Birkhäuser, 2003.

[LK84] B. Litkouhi and H. Khalil. Infinite-time regulators for singularly perturbed difference equations. *International Journal of Control*, 39(3):587–598, 1984.

[LM99] D. Liberzon and A.S. Morse. Basic problems in stability and design of switched systems. *IEEE Control Systems Magazine*, 19(5):59–70, 1999.

[LSZ03] X. Liu, X. Shen, and Y. Zhang. Exponential stability of singularly perturbed systems with time delay. *Applicable Analysis*, 82(2):117–130, 2003.

[MBS+08] I. Malloci, R. Bonidal, P. Szczepanski, J. Daafouz, and C. Iung. *Robust Steering Control Toolbox*. Internal Rapport ArcelorMittal, 2008.

[MDI09a] I. Malloci, J. Daafouz, and C. Iung. Stability and stabilization of two-time scale switched linear systems under arbitrary switching rules. *Internal Rapport*, 2009.

[MDI09b] I. Malloci, J. Daafouz, and C. Iung. Stabilization of continuous-time singularly perturbed switched systems. In *IEEE Conference on Decision and Control*, 2009.

[MDI+09c] I. Malloci, J. Daafouz, C. Iung, R. Bonidal, and P. Szczepanski. Contrôle robuste d'un laminoir à chaud. In *Journées Doctorales et Nationales du GDR MACS*, 2009.

[MDI+09d] I. Malloci, J. Daafouz, C. Iung, R. Bonidal, and P. Szczepanski. Robust steering control of hot strip mill. In *European Control Conference*, 2009.

[MDI+09e] I. Malloci, J. Daafouz, C. Iung, R. Bonidal, and P. Szczepanski. Switched system modeling and robust steering control of the tail end phase in a hot strip mill. *Nonlinear Analysis: Hybrid Systems*, 3(3):239–250, 2009.

[MDIB09] I. Malloci, J. Daafouz, C. Iung, and R. Bonidal. A LMI solution to the LQ problem for discrete time singularly perturbed systems. In *European Control Conference*, 2009.

[MDI+ar] I. Malloci, J. Daafouz, C. Iung, R. Bonidal, and P. Szczepanski. Robust steering control of hot strip mill. *IEEE Transactions on Control Systems Technology*, To appear.

[MDIS09] I. Malloci, J. Daafouz, C. Iung, and P. Szczepanski. Switched system modeling and robust steering control of the tail end phase in a hot strip mill. In *IFAC Conference on Analysis and Design of Hybrid Systems*, 2009.

[MHD+08] I. Malloci, L. Hetel, J. Daafouz, C. Iung, and R. Bonidal. Une approche pour maîtriser les discontinuités de la commande pour les sysèmes linéaires à commutation en temps discret. In *Conférence International Francophone d'Automatique*, 2008.

[MHD+09] I. Malloci, L. Hetel, J. Daafouz, C. Iung, and R. Bonidal. Bumpless transfer for discrete-time switched systems. In *American Control Conference*, 2009.

[MIYS01] Y. Marushita, H. Ikeda, K. Yano, and S. Shindo. Advanced control method of steering on the hot rolling mill. In *5th IFAC Automation in Mining, Mineral, and Metal Processing*, 2001.

[MK97] Y. Mori and Y. Kuroe. A solution to the common Lyapunov function problem for continuous-time systems. In *Conference on decision and control*, 1997.

[MN80] H. Matsumoto and K. Nakajima. Automatic side-walk control in hot strip mill. In *Japanese joint conf. for the technology of plastic*, 1980.

[Mor96] A.S. Morse. Supervisory control of families of linear set-point controllers - part 1: Exact matching. *IEEE Transactions on Automatic Control*, 41:1413–1431, 1996.

[MP89] A.P. Molchanov and Y.S. Pyatnitskiy. Criteria of asymptotic stability of differential and difference inclusions encountered in control theory. *Systems & Control Letters*, 13(1):59–64, 1989.

[Nai88] D.S. Naidu. *Singular perturbation methodology in control systems.* Peter Peregrinus Limited, 1988.

[Nai02] D.S. Naidu. Singular perturbations and time scales in control theory and applications: An overview. *Dynamics of Continuous, Discrete & Impulsive Systems. Series B. Applications & Algorithms*, 9(2):233–278, 2002.

[NKK+80] K. Nakajima, T. Kajiwara, T. Kimura, T. Kikuma, H. Matsumoto, and M. Tagawa. Automatic side-walk control in hoy strip mill. In *Japanese spring conf. for the technology of plasticity*, 1980.

[NN94] Y.E. Nesterov and A. Nemirovsky. *Interior Point Polynomial Methods in Convex Programming.* SIAM, 1994.

[OH97] Y. Okamura and I. Hoshino. State feedback control of the strip steering for aluminum hot rolling mill. *Control Engineering Practice*, 5(8):1035–1042, 1997.

[OIGH93] Y. Ohta, H. Imanishi, L. Gong, and H. Haneda. Computer generated Lyapunov functions for a class of nonlinear systems. *IEEE Transactions on Circuits and Systems I: Fundamental Theory and Applications*, 40(5):343–354, 1993.

[Oka03] N. Okada. *Method and device of plate steering control on rolling mill.* KAWASAKI STEEL CORP. Patent: P2003-275812A, 2003.

[OMAH05] M. Okada, K. Murayama, Y. Anabuki, and Y. Hayashi. VSS control of strip steering for hot rolling mills. In *IFAC world congress*, 2005.

[PD91] P. Peleties and R.A. DeCarlo. Asymptotic stability of m-switched systems using Lyapunov-like functions. In *American Control Conference*, 1991.

[PG94] P.L.D. Peres and J.C. Geromel. An alternate numerical solution to the linear quadratic problem. *IEEE Transactions on Automatic Control*, 39(1):198–202, 1994.

[PS08] J. Pittner and M.A. Simaan. Control of a continuous tandem cold metal rolling process. *Control Engineering Practice*, 16(11):1379–1390, 2008.

[RN82] A.K. Rao and D.S. Naidu. Singular perturbation method applied to the open-loop discrete optimal control problem. *Optimal Control Applications and Methods*, 3(2):121–131, 1982.

[San68] P. Sannuti. *Singular perturbation method in the theory of optimal control*. PhD Thesis, University of Illinois, Urbana-Champaign, 1968.

[SCGB06] C. Seatzu, D. Corona, A. Giua, and A. Bemporad. Optimal control of continuous-time switched affine systems. *IEEE Transactions on Automatic Control*, 51(5):726–741, 2006.

[SESP99] E. Skafidas, R.J. Evans, A.V. Savkin, and I.R. Petersen. Stability results for switched controller systems. *Automatica*, 35(4):553–564, 1999.

[SK69] P. Sannuti and P. Kokotovic. Near-optimum design of linear systems by a singular perturbation method. *IEEE Transactions on Automatic Control*, 14(1):15–22, 1969.

[SN02] R.N. Shorten and K.S. Narendra. Necessary and sufficient conditions for the existence of a common quadratic Lyapunov function for a finite number of stable second order linear time-invariant systems. *International Journal of Adaptive Control and Signal Processing*, 16(10):709–728, 2002.

[SN03] R.N. Shorten and K.S. Narendra. On common quadratic Lyapunov functions for pairs of stable LTI systems whose system matrices are in companion form. *IEEE Transactions on Automatic Control*, 48(4):618–621, 2003.

[SP98] M.J. Steeper and G.D. Park. Development of steering control system for reversing hot mills. *Iron and steel engineer*, 75(11):21–24, 1998.

[SS92] H. Saitoh and T. Sakimoto. Development of advanced steering control of hot strip mill in steel production process. 1992.

[Stu99] J.F. Sturm. Using SeDuMi 1.02, a Matlab Toolbox for optimisation over symmetric cones. *Optimization Methods and Software*, 11-12:625–653, 1999.

[SWM+07] R.N. Shorten, F. Wirth, O. Mason, K. Wulff, and C. King. Stability criteria for switched and hybrid systems. *SIAM Review*, 49(4):545–592, 2007.

[TAB+06] M.C. Turner, N. Aouf, D.G. Bates, I. Postlethwaite, and B. Boulet. Switched control of a vertical/short take-off land aircraft: an application of linear quadratic bumpless transfers. *Journal of Systems and Control Engineering*, 220(3):157–170, 2006.

[Tak01] R. Takahashi. State of the art in hot rolling process control. *Control Engineering Practice*, 9(9):987–993, 2001.

[Tik48] A. Tikhonov. On the dependence of the solutions of differential equations on a small parameter. *Matematicheskii Sbornik*, 22(64):193–204, 1948.

[TK97] A.R. Teel and N. Kapoor. The $\mathcal{L}_2$ anti-windup problem: Its definition and solution. In *European Control Conference*, 1997.

[TW99] M.C. Turner and D.J. Walker. Modified linear quadratic bumpless transfer. In *American Control Conference*, 1999.

[TW00] M.C. Turner and D.J. Walker. Linear quadratic bumpless transfer. *Automatica*, 36:1089–1101, 2000.

[Utk92] V.I. Utkin. *Sliding modes in control and optimization.* Springer-Verlag, 1992.

[Vas63] A.B. Vasil'eva. Asymptotic behaviour of solutions to certain problems involving non-linear differential equations containing a small parameter multiplying the highest derivatives. *Russian Mathematical Surveys*, 18(3):13–81, 1963.

[VFBO07] J.G. VanAntwerp, A.P. Featherstoneb, R.D. Braatzc, and B.A. Ogunnaiked. Cross-directional control of sheet and film processes. *Automatica*, 43(2):191–211, 2007.

[YHF08] S.K. Yildiz, B. Huang, and J.F. Forbes. Dynamics and variance control of hot mill loopers. *Control Engineering Practice*, 16(1):89–100, 2008.

[Yur04] V.D. Yurkevich. *Design of nonlinear control systems with the highest derivative in feedback.* World Scientific, 2004.

[ZB09] K. Zheng and J. Bentsman. Input/output structure of the infinite horizon LQ bumpless transfer and its implications for transfer operator synthesis. *International Journal of Robust and Nonlinear Control*, page DOI:10.1002/rnc.1484, 2009.

[ZHYM01] G. Zhai, B. Hu, K. Yasuda, and A.N. Michel. Stability analysis of switched systems with stable and unstable subsystems: An average dwell time approach. *International Journal of Systems Science*, 32(8):1055 –1061, 2001.

[ZLBT06] K. Zheng, A.H. Lee, J. Bentsman, and C.W. Taft. Steady-state bumpless transfer under controller uncertainty using the state/output feedback topology. *IEEE Transactions on Control Systems Technology*, 14(1):3–17, 2006.

[ZLW+04] L. Zaccarian, Y. Li, E. Weyer, M. Cantoni, and A. R. Teel. Anti-windup for marginally stable plants applied to open water channels. In *Asian Control Conference*, 2004.

[ZT02] L. Zaccarian and A.R. Teel. A common framework for anti-windup, bumpless transfer and reliable designs. *Automatica*, 38(10):1735–1744, 2002.

[ZT05] L. Zaccarian and A.R. Teel. The $\mathcal{L}_2(l_2)$ bumpless transfer problem for linear plants: Its definition and solution. *Automatica*, 41(7):1273–1280, 2005.

Titre : Sur les systèmes à commutation à deux échelles de temps: Une application au contrôle de guidage de bande dans un laminoir à chaud.

Résumé : Dans cette thèse, on s'est attaché à résoudre un certain nombre de problèmes qui apparaissent lorsqu'on traite des problèmes concrets de contrôle: phénomènes à plusieurs échelles de temps, discontinuités de la commande lors du basculement d'un correcteur à un autre, nécessité de concevoir un nombre limité de correcteurs différents malgré une gamme très importante des produits traités. Pour illustrer concrètement les résultats obtenus, nous nous sommes appuyés sur un exemple industriel concret, le contrôle de guidage de bande durant le processus de laminage dans un laminoir à chaud. D'abord, nous proposons une solution convexe au problème de commande optimale linéaire quadratique pour les systèmes linéaires à deux échelles de temps en temps discret. Ensuite, nous établissons des conditions suffisantes, formulées sous la forme d'inégalités matricielles linéaires, qui permettent de vérifier la stabilité d'un système à commutation à deux échelles de temps et de synthétiser des correcteurs stabilisants. Nous proposons aussi dans ce travail une méthode pour minimiser les discontinuités sur la commande dans le cadre des systèmes à commutation. Dans le contexte du contrôle de guidage de bande pour un laminoir à chaud, nous ne pouvons pas négliger l'influence des paramètres incertains, qui sont dus principalement au fait que ce genre de système traite une gamme de produits très large. Donc, dans la synthèse du correcteur, nous prenons en compte ces variations en divisant l'ensemble des produits en plusieurs familles et en synthétisant un correcteur différent pour chaque famille.

Mots-clés : Contrôle de guidage de bande, Laminoir à chaud, Systèmes à commutation, Perturbations singulières, Robustesse.

Title : Two time scale switched systems: An application to steering control in hot strip mills.

Abstract: This Ph.D. thesis deals with a certain number of problems arising in practical implementation of control systems: multi time scale phenomena, sudden modifications on the system dynamics, discontinuities on the control signal due to controller switchings, the need of design a limited number of controllers in spite of a wide variation on the physical parameters. In order to illustrate the validity of the obtained results, we resort to a real problem concerning the steel production framework, the robust steering control of a hot strip finishing mill. First, a convex solution of the linear quadratic control design for discrete two time scale systems is proposed. Hence, we address the stability problem of two time scale switched systems. We show that stability of the slow and fast switched subsystems under arbitrary switching rules does not imply the stability of the corresponding two time scale switched system in the singular perturbation form. An additional constraint, independent of the value of the singular parameter and of the switching rule, is provided in terms of linear matrix inequalities. We also introduce a bumpless transfer method for switched systems aiming at reducing the discontinuities on the control signal. Dwell time conditions assessing the asymptotic stability of the closed loop switched system are established. The practical contribution of this thesis, the robust steering control design, exploits most of previous results. The objective is to guarantee the stability of the hot strip mill system and improve the quality of the rolled products.

Keywords: Steering control, Hot strip mill, Switched systems, Singular perturbation, Robustness.

INSTITUT NATIONAL
POLYTECHNIQUE
DE LORRAINE

AUTORISATION DE SOUTENANCE DE THESE
DU DOCTORAT DE L'INSTITUT NATIONAL
POLYTECHNIQUE DE LORRAINE

o0o

VU LES RAPPORTS ETABLIS PAR :
Monsieur Germain GARCIA, Professeur, LAAS, CNRS, Toulouse

Monsieur Jean LEVINE, Professeur, CAS, ENSMP, Fontainebleau

Le Président de l'Institut National Polytechnique de Lorraine, autorise :

Monsieur MALLOCI Ivan

NANCY BRABOIS
2, AVENUE DE LA
FORET-DE-HAYE
BOITE POSTALE 3
F - 54501
VANDŒUVRE CEDEX

à soutenir devant un jury de l'INSTITUT NATIONAL POLYTECHNIQUE DE LORRAINE, une thèse intitulée :

"Sur les systèmes à commutation à deux échelles de temps. Une application au contrôle de guidage de bande dans un laminoir à chaud"

en vue de l'obtention du titre de :

DOCTEUR DE L'INSTITUT NATIONAL POLYTECHNIQUE DE LORRAINE

Spécialité : « **Automatique et Traitement du Signal** »

Fait à Vandoeuvre, le 29 octobre 2009
Le Président de l'I.N.P.L.,
F. LAURENT

TEL. 33/03.83.59.59.59
FAX. 33/03.83.59.59.55